ISSN 1346-1192

Annual Report of the National Astronomical Observatory of Japan

Volume 14 Fiscal 2011

Cover Caption

Most distant and ancient supernovae discovered by the Subaru Telescope. In the image, which show the Subaru Deep Field, numerous supernovae related to white dwarfs were found, and ten of them had exploded more than ten billion years ago. This discovery gives an important clue to study how the heavy elements created in the ancient universe (Graur et al. MNRAS, 417, 916, 2011).

Postscript

Editor Publications Committee

HANAOKA, Yoichiro
UEDA, Akitoshi
OE, Masafumi
SÔMA, Mitsuru
NISHIKAWA, Jun
MIYOSHI, Makoto
YOSHIDA, Haruo

Publisher National Institutes of Natural Sciences

National Astronomical Observatory of Japan

2-21-1 Osawa, Mitaka-shi, Tokyo 181-8588, Japan
TEL: +81-422-34-3600
FAX: +81-422-34-3960
http://www.nao.ac.jp/

Printer **SANREI Printing Co., Ltd**

2-32-1, Kanda-Jinbocho, Chiyoda-ku, Tokyo 101-0051, Japan
TEX: +81-3-5276-0811
FAX: +81-3-5276-0812

Annual Report of the National Astronomical Observatory of Japan
Fiscal **2011**

T A B L E O F C O N T E N T S

Annual Report of the
National Astronomical Observatory of Japan
Fiscal 2011

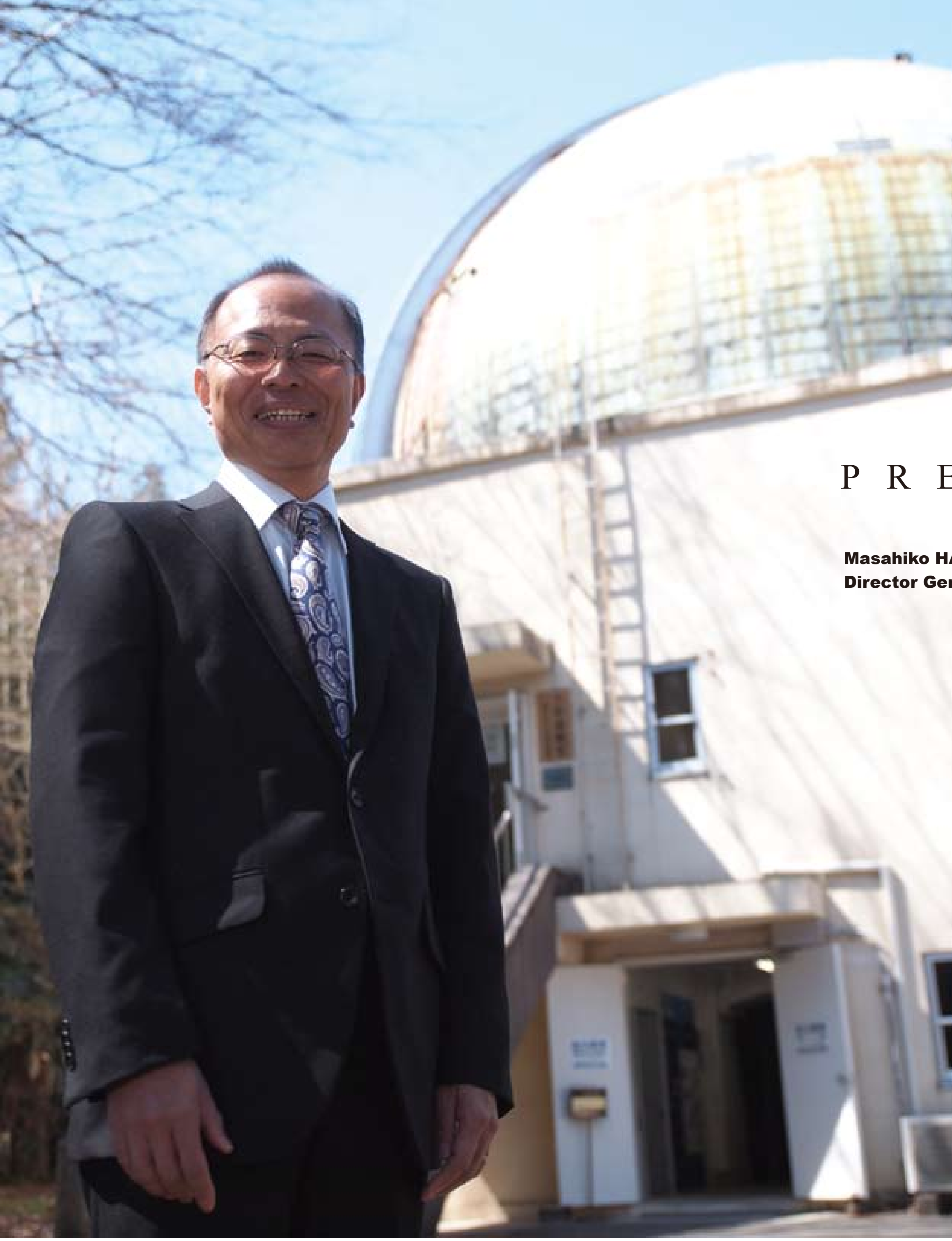

PREFACE

Masahiko HAYASHI
Director General of NAOJ

It is my pleasure to present the Annual Report of the National Astronomical Observatory of Japan (NAOJ) for the fiscal year 2011 (FY2011).

The FY2011 began in the aftermath of the East Japan Earthquake. Although the earthquake caused significant damage to two antennas at the Mizusawa VLBI Observatory in Tohoku – including a 20-metre VLBI Earth Rotation Astrometry (VERA) antenna – and a further two VLBI antennas located in Takahagi and Hitachi, they have all been restored and are fully operational. It is also worth noting that the supercomputer at the Mitaka headquarters was in fallback operations during the 2011 summer season in order to reduce energy consumption.

On July 2, there was a coolant leak from the prime focus of the Subaru Telescope. As a result, we were forced to temporarily stop the operation of the telescope as the primary mirror and observing instruments, including

Suprime-Cam, were inoperative. We apologize to Subaru users and other persons concerned for the inconvenience caused by this interruption. Corrective measures were taken immediately, by cleaning the primary mirror and repairing the damaged instruments. Furthermore, a special committee was established to investigate the cause of the leak in order to prevent a future recurrence.

The ALMA project is making steady progress at the Atacama plateau in Chile. Currently, 16 antennas out of 66 are available for observations. The Joint ALMA Observatory announced the call for proposals for Cycle 0 – a preliminary open-use period, with 16 antennas this year. By the end of June 2011, more than 900 proposals were submitted from all over the world, revealing extraordinarily high levels of interest from the global scientific community in ALMA. About 150 proposals were submitted to Cycle 0 from Japan, the second largest number of submissions among the ALMA member countries. The Cycle 0 observation began in October 2011 and we expect some exciting results from ALMA observations to be released to the public in the near future.

Meanwhile, the Subaru Telescope continues to be productive, despite the accident mentioned above. More than 120 scientific papers are published per year, which means about one research paper every three days. Many of the papers published in the FY2011 are categorized into two areas: the first is distant galaxies, clusters of galaxies and dark matter; the second is exoplanets and disks around young stars. These are the main streams of modern astronomy, where the Subaru Telescope plays an important role. In fact, the Subaru Telescope has made remarkable contribution to the advancement of evolutionary studies of distant galaxies and clusters of galaxies.

The most impressive feature of the Subaru Telescope is its wide-field capability. Now we have developed a 900-megapixel Hyper Suprime-Cam at the NAOJ Advanced Technology Center in Mitaka. It will provide a field of view several times larger than the current Suprime-Cam. Furthermore, new corrector optics will provide sharp and undistorted stellar images over the entire CCD area.

The Subaru Telescope has successfully imaged gaseous giant exoplanets, but imaging Earth-like rocky planets is impossible. We need a larger light collecting area, sharper imaging resolution, and higher contrast. This will be achieved by the Thirty Meter Telescope (TMT), which will be constructed on Mauna Kea, at a slightly lower elevation than Subaru. Representatives from the prospective partners – Japan, USA (California and NSF), Canada, India and China – are busy coordinating the construction of TMT, which is expected to begin in the spring of 2014. Japan plans to assume the construction of the telescope structure and part of the primary mirror.

There are also growing aspirations for Solar-C, a next generation space-based solar observatory that will succeed Hinode. Recently, the solar activity appears to be slipping out of phase from its long sustained 11-year period, which has been attracting global attention because it might eventually cause significant environmental changes. The NAOJ recognizes the importance of such research and is always committed to fulfilling its societal responsibilities.

The FY2012 will mark the completion of ALMA and the 30th anniversary of the Nobeyama Radio Observatory, which has produced some astounding scientific achievements. Astronomy is always rapidly changing, with new telescopes being planned and realized, while those that were once at the frontier of science eventually become obsolete. It is the mission of the NAOJ to respond to these changes and to provide advanced facilities that attract top researchers from around the world so that we can return important scientific results to society.

Masahiko HAYASHI
Director General of NAOJ

I Scientific Highlights

(April 2011 – March 2012)

Complex Scattered Radiation Fields and Multiple Magnetic Fields in the Protostellar Cluster in NGC 2264

KWON, Jungmi, TAMURA, Motohide
(Graduate University for Advanced Studies / NAOJ)

KANDORI, Ryo, KUSAKABE, Nobuhiko, HASHIMOTO, Jun, NAKAJIMA, Yasushi
(NAOJ)

NAKAMURA, Fumitaka
(Graduate University for Advanced Studies / NAOJ)

NAGAYAMA, Takahiro
(Nagoya University)

NAGATA, Tetsuya
(Kyoto University)

HOUGH, James H.
(University of Hertfordshire)

WERNER, Michael W.
(Jet Propulsion Laboratory)

TEIXEIRA, Paula S.
(European Southern Observatory)

Near-infrared imaging polarimetry in the *J*, *H*, and *Ks* bands has been carried out for the protostellar cluster region around NGC 2264 IRS 2 in the Monoceros OB1 molecular cloud. Various infrared reflection nebula clusters (IRNCs) associated with NGC 2264 IRS 2 and the IRAS 12 S1 core, as well as local infrared reflection nebulae (IRNe), were detected. The illuminating sources of the IRNe were identified with known or new near- and mid-infrared sources. In addition, 314 point-like sources were detected in all three bands and their aperture polarimetry was studied. Using a color-color diagram, reddened field stars and diskless pre-main-sequence stars were selected to trace the magnetic field (MF) structure of the molecular cloud. The mean polarization position angle of the point-like sources is 81° ± 29° in the cluster core, and 58° ± 24° in the perimeter of the cluster core, which is interpreted as the projected direction on the sky of the MF in the observed region of the cloud. The Chandrasekhar-Fermi method gives a rough estimate of the MF strength to be about 100 μG. A comparison with recent numerical simulations of the cluster formation implies that the cloud dynamics is controlled by the relatively strong MF. The local MF direction is well associated with that of CO outflow for IRAS 12 S1 and consistent with that inferred from submillimeter polarimetry. In contrast, the local MF direction runs roughly perpendicular to the Galactic MF direction [1].

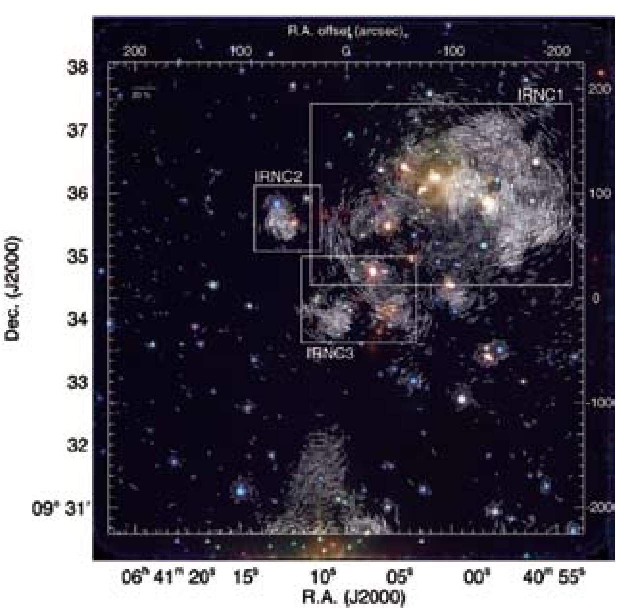

Figure 1: *H* polarization vector map superposed on the color composite image in the IRSF/SIRPOL *JHKs* (blue), Spitzer/IRAC 5.8 μm and Spitzer/MIPS 24 μm (red) bands. The length of the vectors is proportional to the degree of polarization. Shown in the upper left corner is a 20% vector. The vectors were made by 6 × 6 pixel smoothing (twice the seeing size), and the vectors were shown every 6 pixels with intensities greater than 3σ above the mean sky level, where is the standard deviation of sky brightness. Three IRNCs are labeled.

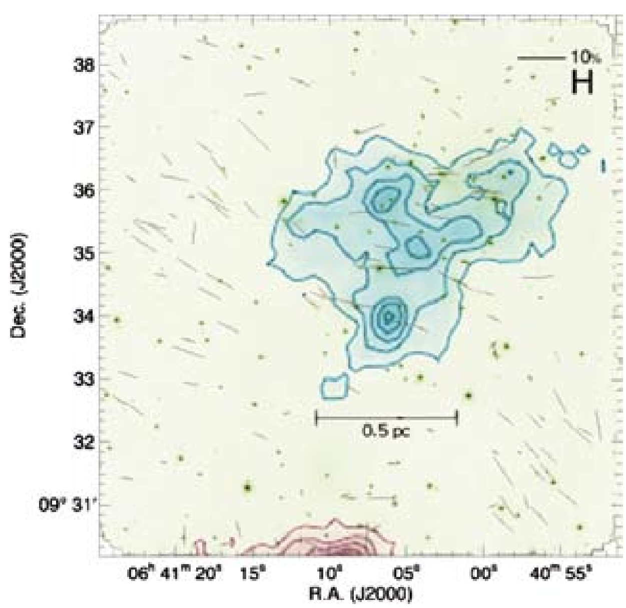

Figure 2: Stokes *I* image of the *H* band with contours of 870 μm continuum emission [2]. Con- tours are at 0.5, 1.0, 1.5, 2.0, and 2.5 Jy beam^{-1}. Red con- tours: dense cluster of the IRS 1 region. Blue contours: dense cluster of the IRS 2 region.

References

[1] Kwon, J., et al.: 2011, *ApJ*, **741**, 35.
[2] Williams, J., Garland, C.: 2002, *ApJ*, **568**, 259.

Potential Members of Stellar Kinematic Groups within 30 pc of the Sun

NAKAJIMA, Tadashi, MORINO, Jun-Ichi
(NAOJ)

Age dating of individual stars in general is a very difficult task. Usually groups of stars or stellar clusters provide us with age-controlled sample of stars. For instance, a globular cluster is considered to be the source of an old sample of coeval stars in the halo with rather uniform metallicity. On the other hand, an open cluster provides us with a relatively young sample of stars with a similar age in the Galactic disk.

Some open clusters are located closer to the Sun than the nearest-by star-forming regions, such as Taurus and Chamaeleon dark clouds located at about 140 pc of the Sun. Due to the proximity, spatial localization alone is not a stringent criterion for the membership for these clusters. At least the proper motion and mean radial velocity have been used to define a kinematic group. Nearby streams of stars identified this way are called “stellar kinematic groups (SKGs)”. At least eleven SKGs are known to date [1]. Owing to the success of *Hipparcos* in measuring parallaxes and proper motions of stars in the solar neighborhood, and to ground-based observational efforts to obtain radial velocities of nearby stars, three-dimentional velocity information is available for a set of nearby stars brighter than about $V = 11$ measured by *Hipparcos* within about 40 pc of the Sun.

A sample of age-controlled young stars in the very solar neighborhood has a wide range of applications. For instance, the direct detection of sub-stellar companions and planets is possible only around these young stars with the present-day technology, since brown dwarfs and planets shine only by the release of their gravitational energy. For instance, Gl 229A, the main star of Gl 229B, was selected as a target for the brown dwarf search, based on its kinematic youth as a young disk star [2,3]. However, the age of Gl 229AB system is not known precisely enough to estimate the mass of Gl 229B. Since the luminosity of a brown dwarf or a planet depends on both its mass and age, the knowledge of the age is essential in obtaining the mass from its luminosity. Other than that, age controlled samples are useful for the studies of stellar properties such as chromospheric and coronal activities, magnetic field strength, rotation, and the presence of circumstellar disks around them.

We analyze the kinematic histories of stars within 30 pc of the Sun, for which three-dimensional spatial coordinates and three-dimensional velocity vectors, are available. From this sample, we extract members of stellar kinematic groups (SKGs) in the following manner. First, we consider in the three-dimensional velocity space centered on the local standard of rest, a sphere with a radius of 8 km s^{-1} centered on the mean velocity vector of a particular SKG. Around each SKG velocity center, we have found significant excess of stars compared to background field stars. For each candidate, in the three-dimensional spatial coordinate space, its trajectory is traced back in time by the age of the relevant SKG, to obtain the estimated distance from the SKG center at the time of the SKG’s birth by the epicyclic approximation and harmonic vertical motion. It often happens that a star is a candidate member of multiple SKGs. Then we rank the candidacy to multiple SKGs based on the smallness of distance separations. This way, we have kinematically selected 238 candidates. Then we further impose at least one of the following qualitative criteria to be a member: spectral type A or B, variability, or EUV and X-ray emission. We have finally selected 137 candidate members of SKGs out of a sample of 966 stars [4].

SKG	Age (Myr)	# of members
TW Hydra	8	13
η Cha	8	6
Cha-Near	10	7
β Pic	12	8
Tuc-Hor	30	7
IC 2391	45	17
AB Dor	50	18
Pleiades	120	0
Castor	200	19
Ursa Major	300	33
Hyades	600	9

References

[1] Zuckerman, B., Song, I.: 2004, *ARA&A*, **42**, 685.
[2] Nakajima, T., Oppenheimer, B. R., Kulkarni, S. R., Golimowski, D. A., Durrance, S. T.: 1995, *Nature*, **378**, 463.
[3] Leggett, S. K.: 1992, *ApJS*, **82**, 351.
[4] Nakajima, T., Morino, J-I.: 2012, *AJ*, **143**, 2.

Beryllium Abundances of Solar-Analog Stars

TAKEDA, Yoichi, TAJITSU, Akito, KAWANOMOTO, Satoshi, ANDO, Hiroyasu, SAKURAI, Takashi
(NAOJ)

HONDA, Satoshi
(Kyoto University)

The surface Li abundances (A_{Li}) in solar-analog stars (i,e., early G-type main-sequence stars like our Sun) show a remarkably large diversity amounting to more than ~2 dex. Why such a large difference is produced for stars with similar parameter values? We previously found in statistical study on 118 selected solar-analogs based on the OAO/HIDES spectra that A_{Li} depends upon the rotational velocity (see [1]). This finding was further corroborated from the viewpoint of stellar activity (controlled by rotation via a dynamo) estimated from the core flux of the Ca II 8542 line [2].

Then, why slow rotation leads to an efficient Li depletion? Interestingly, according to Bouvier's recent theoretical simulation [3], slow rotators develop a high degree of differential rotation between the radiative core and the convective envelope, which eventually promotes lithium depletion by enhanced mixing, while such core–envelope decoupling does not evolve in faster rotators. Then, the key to understanding the mixing process lies in "the bottom of the convection zone" (i.e., "tachocline"), where the condition may be probed by examining the abundance of Be along with Li (each having different burning temperatures). (See Figure 1 showing the structure of the solar envelope model taken from [4].)

Accordingly, we conducted an extensive beryllium abundance analysis for the same sample of 118 solar analogs (based on the high-dispersion UV spectra obtained with Subaru/HDS in 2009–2010) by applying the spectrum synthesis technique to the near-UV region comprising the Be II line at 3131.066 Å, in an attempt to investigate how and whether Be suffers any depletion such as the case of Li showing a large diversity.

Our findings are as follows (cf. Figure 2):

—In marked contrast to Li, most (~96%) of the solar analogs are superficially similar in terms of their A_{Be}.

—However, 4 out of 118 stars turned out strikingly Be-deficient (by >~2 dex) and these 4 stars have the lowest $v_{\mathrm{e}} \sin i$, the lowest stellar activity, and depleted A_{Li}.

—Moreover, even for the other majority showing an apparent similarity in Be, we can recognize a tendency that A(Be) gradually increases with an increase in $v_{\mathrm{e}} \sin i$.

These results suggest that any solar analog star (including the Sun) generally suffers some kind of rotation-dependent Be depletion, for which we suspect two kinds of mechanisms may operate: The "strong" process should work only in limited cases under special conditions but depletes surface Be very efficiently once triggered, whereas the "weak" process acts on most stars and slowly reduce Be in the outer envelope. Contributions of theoreticians are awaited toward developing a reasonable model accounting for these observational facts.

See [5] for more details of this study.

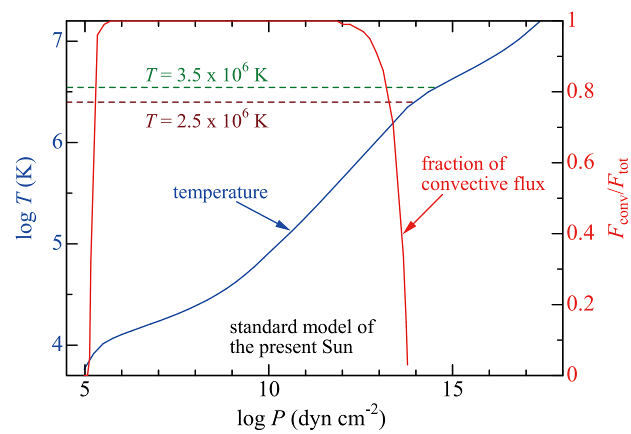

Figure 1: Physical structure of the envelope of the Sun.

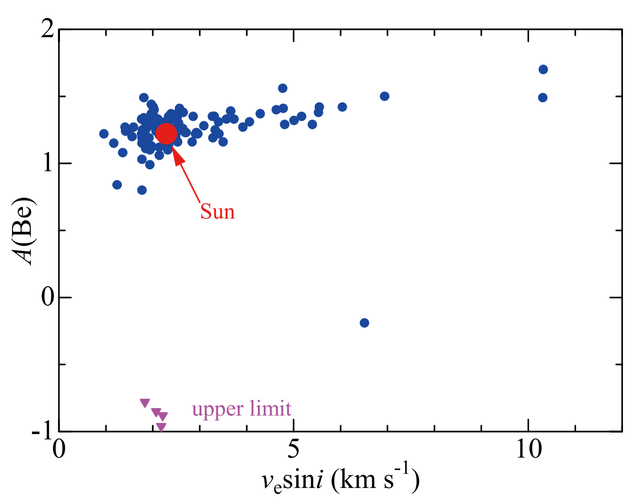

Figure 2: Be abundances plotted against the projected rotational velocity.

References

[1] Takeda, Y., Kawanomoto, S., Honda, S., Ando, H., Sakurai, T.: 2007, *A&A*, **468**, 663.
[2] Takeda, Y., Honda, S., Kawanomoto, S., Ando, H., Sakurai, T.: 2010, *A&A*, **515**, A93.
[3] Boubier, J.: 2008, *A&A*, **489**, L53.
[4] Stix, M.: 2002, The Sun, 2nd ed. (Berlin: Springer), ch.6.
[5] Takeda, Y., Tajitsu, A., Honda, S., Kawanomoto, S., Ando, H., Sakurai, T.: 2011, *PASJ*, **63**, 697.

Infrared 18μm High-Spatial-Resolution Imaging of nearby Luminous Infrared Galaxies Using Subaru and Gemini South Telescopes

IMANISHI, Masatoshi (NAOJ)
IMASE, Keisuke, OI, Nagisa (GUAS/NAOJ)
ICHIKAWA, Kohei (Kyoto University)

Luminous infrared galaxies (LIRGs) radiate very large infrared luminosities with $L_{IR} > 10^{11} L_{\odot}$, and so must possess luminous energy sources hidden behind dust, which absorbs the bulk of the primary energetic radiation, is heated, and produces strong thermal infrared radiation. The dust-obscured hidden energy sources can be either starburst (energy release by nuclear fusion reaction inside stars) and/or AGN activity (release of gravitational energy by a mass accreting active supermassive black-hole). We have previously performed systematic infrared 2.5–40 μm low-resolution spectroscopy of LIRGs, to investigate the relative energetic roles of starburst and AGN activity [1,2]. Based on the strengths of polycyclic aromatic hydrocarbon emission and dust absorption features detected in infrared spectra, AGNs with hard primary energetic radiation and more centrally-concentrated energy source geometry than dust, can be differentiated from normal starbursts which emit soft energetic radiation and have mixed energy sources and dust geometry. Although AGNs and normal starbursts are distinguishable, an **extreme** starburst, consisting of HII-regions only and showing an exceptionally centrally-concentrated energy source geometry, can produce similar infrared spectral shapes to AGNs, and so cannot be ruled out based on infrared spectroscopy alone.

It is shown, both theoretically and observationally, that there is an upper limit for the emission surface brightness of starburst activity with ~$10^{13} L_{\odot}$ kpc^{-2} [3,4], because the radiative energy generation efficiency of nuclear fusion inside stars is modest (0.7 % of Mc^2). It is very difficult even for an extreme starburst to exceed this threshold by a large factor, as long as the extreme starburst is powered by nuclear fusion. On the other hand, an AGN can produce much higher emission surface brightness, because the efficiency of a mass accreting supermassive blackhole can be 6–42 % of Mc^2. Thus, a very high emission surface brightness energy source, if detected, must be an AGN, rather than an extreme starburst.

We performed infrared 18 μm high-spatial-resolution imaging of nearby luminous infrared galaxies using Subaru 8.2 m and Gemini South 8.1 m telescopes (Figure 1). Infrared 18 μm observations can probe the dominant dust emission components of luminous infrared galaxies, and the point spread function (PSF) is stable at 18 μm, due to the reduction of Earth's atmospheric turbulence, making reliable discussion of intrinsic emission's spatial extent possible. Since we can constrain the emission size more strongly, and obtain a more stringent lower limit of emission surface brightness using ground-based large 8–10 m telescopes than space-based satellites with small apertures, our ground-based data play a crucial role. We found that many LIRGs with AGN signatures in previously-taken infrared spectra show emission surface brightnesses much higher than the maximum value set by a starburst phenomenon, supporting the AGN scenario for these galaxies, rather than the extreme starburst picture [5].

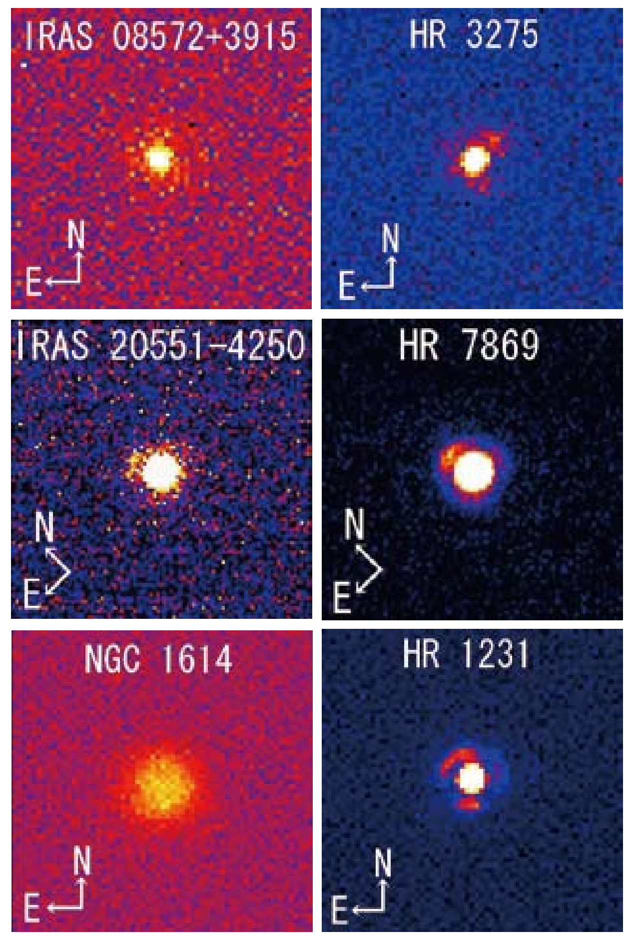

Figure 1: Infrared 18 μm images taken with Subaru (Top and bottom; 5″×5″) and Gemini South telescope (Middle; 8″×8″). (Left) : galaxies. (Right) : corresponding PSF reference stars. North and East directions are indicated. (Top and middle): Infrared emission from galaxies is compact and its spatial extent is indistinguishable from PSF stars. The observed very high emission surface brightnesses suggest AGNs. (Bottom): Galaxy infrared emission is spatially extended, and can be explained by a normal starburst.

References

[1] Imanishi, M., et al.: 2007, *ApJS*, **171**, 72.
[2] Imanishi, M., et al.: 2010, *ApJ*, **721**, 1233.
[3] Thompson, T. A., et al.: 2005, *ApJ*, **630**, 167.
[4] Soifer, B. T., et al.: 2000, *AJ*, **119**, 509.
[5] Imanishi, M., et al.: 2011, *AJ*, **141**, 156.

The Inner Structure of Collisionless Magnetic Reconnection

ZENITANI, Seiji
(NAOJ)

Magnetic reconnection is a driving engine of solar flares, stellar flares, and quite probably bursty events in high-energy astrophysical sites. The reconnection process is driven by a small-scale “dissipation region” surrounding the reconnection point (X-point), at which a plasma ideal condition breaks down. Recently, kinetic particle-in-cell (PIC) simulations have revealed that the electron ideal condition is violated in many locations in collisionless reconnection: i.e., the nonidealness cannot locate the dissipation region. To overcome this problem, we have proposed an electron-frame dissipation measure as a new marker of the dissipation region [1],

$$D_e = \gamma_e[\vec{j}\cdot(\vec{E}+\vec{v}_e\times\vec{B}) - \rho_c(\vec{v}_e\cdot\vec{E})] \qquad (1)$$

where $\gamma_e = [1-(v_e/c)^2]^{-1/2}$ is the Lorentz factor for the electron bulk velocity and ρ_c is the charge density. This stands for the nonideal energy conversion in the MHD framework as well as the energy transfer in the moving frame of electron’s bulk flow.

The measure gives us a new perspective to understand the structure of magnetic reconnection. Figure 1 shows magnetic field lines and key physical quantities in a $2\text{-}\frac{1}{2}$ dimensional PIC simulation with antiparallel symmetric fields [2]. Kinetic reconnection exhibits a highly-modulated field-line structure due to Hall effects. One can recognize a well-known quadruple pattern of the out-of-plane magnetic field B_y in the rear panel. In such a complicated geometry, the previous measure (the electron frozen-in) falsely detects an elongated nondissipative region. In contrast, our new measure D_e successfully distinguishes a compact and narrow dissipation region around the X-point (the central red region in the front panel). Series of PIC simulations suggest that the size of the dissipation region is controlled by electron physics. The dissipation region is typically ~$O(1)d_e^{loc}$ thick and ~$O(10)d_e^{loc}$ long, where d_e^{loc} is a local electron inertial length. More work is necessary for better prediction. We have also discussed structures surrounding the dissipation region, such as a narrow fast electron jet and a shock-like jet front. Our understanding is summarized in a unified picture in Ref. [2].

It is important to verify the new theory in the real world. Efforts are in progress to probe the dissipation region by laboratory experiments or by satellite observations in the terrestrial magnetosphere. Hopefully NASA’s upcoming magnetospheric multiscale (MMS) mission [3] will observe reconnection sites at electron-scale spatial and temporal resolutions after 2014. We hope that MMS will find an unambiguous evidence for the dissipation region.

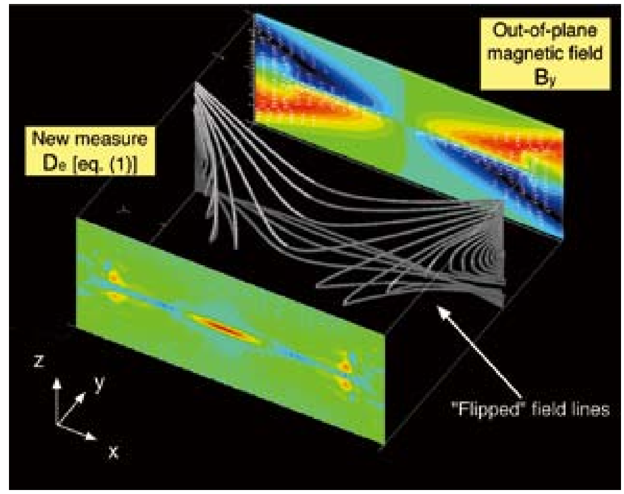

Figure 1: Magnetic field lines, the dissipation measure D_e (Eq. 1), and the out-of-plane magnetic field B_y from run 1A in Ref. [2].

References

[1] Zenitani, S., et al.: 2011, *Phys. Rev. Lett.*, **106**, 195003.
[2] Zenitani, S., et al.: 2011, *Phys. Plasmas*, **18**, 122108.
[3] http://mms.gsfc.nasa.gov/.

Clustered Star Formation in Magnetic Clouds: Properties of Dense Cores Formed in Outflow-Driven Turbulence

NAKAMURA, Fumitaka (NAOJ)
LI, Zhi-Yun (University of Virginia)

Millimeter and submillimeter observations of dense cores in nearby parsec-scale cluster-forming clumps have shown that the core mass function (CMF) resembles the stellar initial mass function (IMF). This suggests that the observed dense cores may be the direct progenitors of individual stars and the bulk of the stellar IMF may be at least partly determined by cloud fragmentation in the parsec-scale dense clumps. Thus, understanding the formation process of dense cores is a key step towards a full understanding of how stars form.

In this study, we investigate the physical properties of dense cores formed in turbulent, magnetized, parsec-scale clumps of molecular clouds, using three-dimensional numerical simulations that include protostellar outflow feedback. In a cluster-forming clump, protostellar outflow feedback can play an important role in turbulence regeneration. In our previous studies, we demonstrated that protostellar outflows can resupply the supersonic turbulence, keeping the clumps near a quasi-virial equilibrium state for a relatively long time [1,2].

Figure 1 compares the column density distributions along the y-axis for the three models with different initial magnetic field strengths, at a stage when the star formation efficiency has reached 16 %. Figure 1 indicates that the global density distribution depends on the initial magnetic field strength. In the presence of a moderatelystrong magnetic field, the cloud material condenses preferentially along the magnetic field lines into a large-scale filamentary structure that is nearly perpendicular to the initial magnetic field direction. The dense cores are distributed primarily along the main filament.

Then, we identified dense cores using the CLUMPFIND algorithm and found the following.

1. Dense cores do not follow Larson's linewidth-size relation. We find that the velocity dispersions of dense cores show little correlation with core radius, irrespective of the strength of the magnetic field and outflow feedback. In the absence of a magnetic field, the majority of the cores have supersonic velocity dispersions, whereas in the presence of a moderately-strong magnetic field, the cores tend to be subsonic or at most transonic.

2. We find that most of the cores are out of virial equilibrium, with the external pressure due to ambient turbulence dominating the self-gravity. The core formation and evolution is largely controlled by the dynamical compression due to outflow-driven turbulence. Such a situation is contrast to the strongly-magnetized (magnetically subcritical) case, where the self-gravity plays a more important role in the core dynamics, particularly for massive cores.

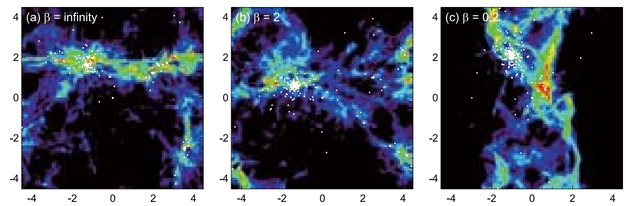

Figure 1: Column density snapshots on the x-z plane for (a) model N1 ($t = 4.6t_{\mathrm{ff,c}} \sim 0.9$ Myr), (b) W1 ($t = 6.5t_{\mathrm{ff,c}} \sim 1.2$ Myr), and (c) S1 ($t = 7.4t_{\mathrm{ff,c}} \sim 1.4$ Myr) at the stage when 16 % of the total mass has been converted into stars. The positions of the formed stars are overlaid with the dots. The units of length are the central Jeans length $L_J = (\pi c_s^2/G\rho_0)^{1/2} \simeq 0.17(T/20\mathrm{K})^{1/2}(n_{\mathrm{H_2},0}/2.69 \times 10^4\,\mathrm{cm^{-3}})^{-1/2}$ pc.

3. Even an initially-weak magnetic field can retard star formation significantly, because the field is amplified by supersonic turbulence to an equipartition strength. In such an initially weak field, the distorted field component dominates the uniform one. In contrast, for a moderately-strong field, the uniform component remains dominant. Such a difference in the magnetic structure can be observed in simulated polarization maps of dust thermal emission. Recent polarization measurements show that the field lines in nearby cluster-forming clumps are spatially well-ordered, indicative of a moderately-strong, dynamically-important, field.

Our simulations indicate that in clustered star formation moderately strong magnetic field is needed to reproduce the physical properties of dense cores [3].

References

[1] Nakamura, F., Li, Z.-Y.: 2007, *ApJ*, **662**, 395.
[2] Wang, P., Li, Z.-Y., Abel, T., Nakamura, F.: 2010, *ApJ*, **709**, 27.
[3] Nakamura, F., Li, Z.-Y.: 2011, *ApJ*, **740**, 36.

Molecular Outflows From the Protocluster, Serpens South

NAKAMURA, Fumitaka[1], SUGITANI, Koji[2], SHIMAJIRI, Yoshito[1], TSUKAGOSHI, Takashi[3]
HIGUCHI, Aya[1], NISHIYAMA, Shogo[4], KAWABE, Ryohei[1], TAKAMI, Michiriro[5]
KARR, Jennifer L.[5], GUTERMUTH, Robert A.[6], WILSON, Grant[6]

1: NAOJ, 2: Nagoya City University, 3: University of Tokyo, 4: Kyoto University, 5: ASIAA, 6: University of Massachusetts

Most stars form in clusters. Therefore, understanding the formation process of star clusters is a key step towards a full understanding of how stars form. Recent observations have revealed that star clusters form in turbulent, magnetized, parsec-scale dense clumps of molecular clouds. These clumps contain masses of 10^2–$10^3\,M_\odot$, fragmenting into an assembly of cores that collapse to produce stars. In cluster-forming clumps, stellar feedback such as protostellar outflows, stellar winds, and radiation rapidly start to shape the surroundings. Because of the short separations between forming stars and cores, these feedback mechanisms are expected to control subsequent star formation. However, the roles of the stellar feedback on cluster formation remain poorly understood observationally.

In this study, we carried out molecular outflow survey toward a young embedded cluster, Serpens South, in CO (3–2) using the ASTE 10 m telescope, and attemped to reveal the role of molecular outflows in star formation in this cluster-forming region. Serpens South is a nearby embedded cluster, recently discovered by Guthermuth et al. (2008) using the Spitzer Space telescope.

An interesting characteristic of the cluster is its extremely-high fraction of protostars. In the central region, the number fraction of protostars (Class I) relative to the YSOs detected by the Spitzer telescope (Class I/II) reaches about 80 %. This fraction is largest among the cluster-forming regions known within the nearest 400 pc. This suggests that Serpens South is in the very early phase of cluster formation.

The main results are summarized as follows.

1. We found that many outflow components concentrate in the dense part where the protocluster resides. Most of these outflow components appear to move away from the dense part.

2. We estimated the global physical quantities of the outflows. The total outflow mass, momentum, and energy seem smaller than those of the Serpens Cloud Core, a nearby typical parsec-scale cluster-forming clump, located about 3° north of Serpens South. However, the characteristic outflow speed appears somewhat larger than that of the Serpens Cloud Core. This may imply that the YSO populations of Serpens South are younger than those of the Serpens Cloud Core.

3. The outflow energy injection rate is likely to be somewhat larger than the energy dissipation rate of the supersonic turbulence, suggesting that the outflow feedback can significantly contribute to the generation of the supersonic turbulence in the dense clump. Assuming the median stellar mass of $0.5\,M_\odot$, the mean outflow momentum per unit stellar mass is estimated to be about 4 km s^{-1}, under the assumption of optically-thin gas.

4. The total outflow energy appears significantly smaller than the global gravitational energy of the dense part where the protocluster is located. In other words, it may be difficult to destroy the cluster-forming clump by the current outflow activity. This may be inconsistent with the dynamical model of cluster formation, for which the outflow feedback due to the initial star burst is envisioned to disperse the dense gas from the cluster-forming clump [1].

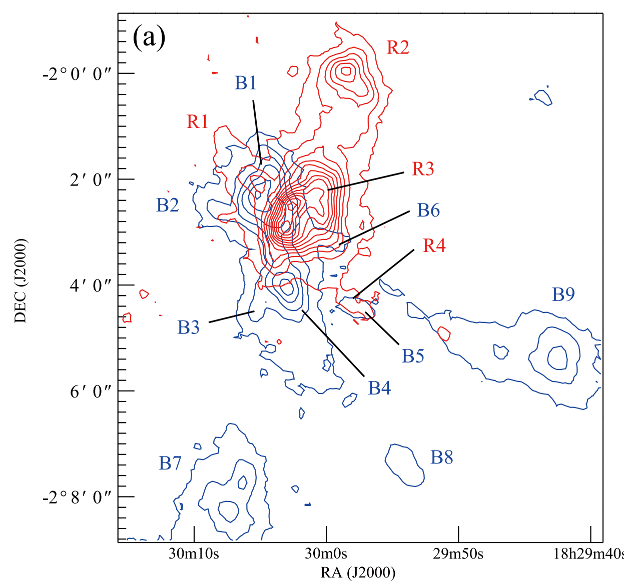

Figure 1: Molecular outflow lobes identified from CO (J = 3–2) emission toward the Serpens South protocluster. The blue contours represent blueshifted ^{12}CO gas and red contours represent redshifted ^{12}CO gas. The blue and red contour levels go up in 6 K km s^{-1} step, starting from 3 K km s^{-1}. The integration ranges are −9.75 to 3.75 km s^{-1} for blueshifted gas and 11.25 to 29.25 km s^{-1} for redshifted gas.

Reference

[1] Nakamura, F., Sugitani, K., Shimajiri, Y., et al.: 2011, *ApJ*, **737**, 56.

Evidence For Cloud-Cloud Collision and Parsec-Scale Stellar Feedback Within the L1641-N Region

NAKAMURA, Fumitaka[1], MIURA, Tomoya[2], KITAMURA, Yoshimi[3], SHIMAJIRI, Yoshito[1]
KAWABE, Ryohei[1], AKASHI, Toshiya[4], IKEDA, Norio[3], TSUKAGOSHI, Takashi[5]
MOMOSE, Munetake[6], NISHI, Ryoichi[2], LI, Zhi-Yun[7]

1: NAOJ, 2: Niigata University, 3: JAXA, 4: Tokyo Tech. University, 5: University of Tokyo, 6: Ibaraki University, 7: University of Virginia

Most stars form in GMCs. In GMCs, various environmental effects such as large-scale flows, supernovae, and stellar feedback from young stars (winds, radiation, and outflows) often shape the cloud structure and dynamics, triggering and suppressing the formation of the next-generation stars. Fingerprints of these environmental effects have been found in some star-forming regions, However, the roles of the environmental effects in star formation remain poorly understood observationally. This is partly because wide-field, high spatial and/or spectral resolution observations, which are needed to resolve the cloud structure and kinematics in detail, are still limited. In particular, stellar feedbacks such as winds or outflows are often extended to parsec-scale. Wide-field observations of the cloud structure and kinematics are needed to unveil such environmental effects. At the same time, it is necessary to resolve the cloud structure at a scale of "dense cores", which are the basic units of individual star formation (≈ 0.1 pc ~ one arcmin at a distance of 400 pc), in order to uncover a link between individual star formation and the environmental effects.

In this study, to understand how the environmental effects influence the internal structure and kinematics in star-forming molecular clouds, we present the results of wide-field ^{12}CO ($J = 1$–0) mapping observations toward the L1641-N region, a nearby active star-forming region in the Orion A giant molecular cloud complex, using the Nobeyama 45 m radio telescope. Our data have high angular (≈ 21″) resolution, allowing us to resolve spatial structures at a scale of 0.04 pc at a distance of 400 pc.

The main results are summarized as follows.

The ^{12}CO ($J = 1$–0) velocity channel maps suggest that the blueshifted ($V_{LSR} < 6\,\mathrm{km\,s^{-1}}$) and redshifted ($V_{LSR} > 7\,\mathrm{km\,s^{-1}}$) components are interacting with each other. Since the two components appear to overlap toward the dust filaments identified by the AzTEC/ASTE observations (Shimajri et al. 2010) on the plane of the sky, the collision between the two components may have occurred almost along the line of sight.

We found several parsec-scale shells in the ^{12}CO ($J = 1$–0) data cube. Some of the shells appear to be spatially well-ordered and homocentric. The centers of the shells are close to either the L 1641-N or V 380 Ori cluster centers, implying that the star formation activity in the clusters may be responsible for the formation and evolution of the shells.

The molecular gas distribution and kinematical structure of this region led us to the following scenario. On the large scale of at least about 1–10 pc, a cloud-cloud collision may have occurred almost along the line of sight in this region, contributing to the formation of several dense filaments. The cloud-cloud collision have triggered the formation of the L1641-N cluster. Multiple protostellar winds and outflows from the cluster member YSOs created large expanding bubbles that can be recognized in the ^{12}CO and ^{13}CO maps. Here, we call these YSO winds as "protocluster winds". The shell surrounding V 380 Ori also has two different velocity components both in the ^{12}CO and ^{13}CO maps. Both the cloud-cloud collision and the protocluster winds are likely to have created the complicated cloud morphology and kinematics.

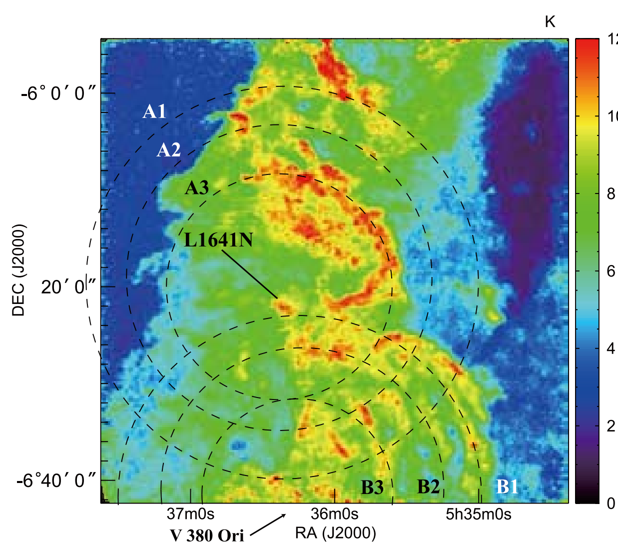

Figure 1: CO (1–0) peak intensity map twoard the L1641-N region in Orion A. The image indicates that several prominent shells shape the cloud structure in this region. We propose that these shells were created by protostellar winds, stellar feedback from forming star clusters. See [1] for more detail.

Reference

[1] Nakamura, F., Miura, T., Shimajiri, Y., et al.: 2012, *ApJ*, **746**, 25.

Hα Emission from Magellanic Stream

YAGI, Masafumi, KOMIYAMA, Yutaka (NAOJ)
YOSHIDA, Michitoshi (Hiroshima University)

Magellanic Stream is a long and narrow filament of neutral hydrogen gas which extends more than 180 degree around our Galaxy. It is thought to be a stripped gas from both of or one of the Magellanic clouds by their interaction. Most of the stream is observed as a neutral hydrogen gas [1], and no stars have been detected in it. Nevertheless, Hα emission is observed from some part of the stream [2,3], and the ionizing mechanism has been in debate.

We can expect that an optical intermediate-dispersion spectroscopic observation with a wide spectral coverage would be helpful to investigate the ionization sources. For example, as one of the hyposethes for the ionization, "shock cascade" model predicted a high Hβ/Hα ratio [4]. If we could measure the ratio from an observation, the models would be verified. The difficulty was, however, that the previous Hα observations used Fabry-Pérot spectrographs and the spatial information were averaged out. The spatial resolution was about 7 arcmin at most. The resolution is not enough for long-slit spectroscopy or multi object spectroscopy.

Aiming for breakthrough, we observed a 50 arcmin square region around one of the previous Hα detection in Hα narrowband and R-band filter using 2kCCD camera at the Kiso Observatory of the University of Tokyo in September and November in 2011 [5]. The exposure time corrected for the weather dimming was about 5 hours in total, and the limiting surface brightness was about 24 mag per square arcseconds as 1σ. We detected three parallel filamentary structures of Hα excess which lie a short distance away from a previous study (Fig. 1). The filaments are 2 arcminutes wide and 6–30 arcminutes long with 12 arcminutes intervals. Their position overlaps the neutral hydrogen stucture of the Magellanic Stream, but it also overlaps a nearby structure of hydrogen gas (Fig. 2).

If the Hα comes from a part of Magellanic Stream, it is qualitatively consistent with the shock cascade model; the surface of an upstream cloud is stripped by the interaction with the halo gas and then heated up by the collision with the following cloud at the downstream. If it is a nearby object, on the otherhand, it is difficult to make such a long, narrow and straight ionized gas structure. A possible explanation would be that several Fossil Strömgren Trails [6], a traveling white dwarf left its Strömgren sphere, were somehow created at the same direction from us. We will try to determine the recession velocity of the emission by spectroscopy and to answer whether they belong to Magellanic Stream ($v \sim -200$ km/s) or near by gas ($v \sim -40$ km/s).

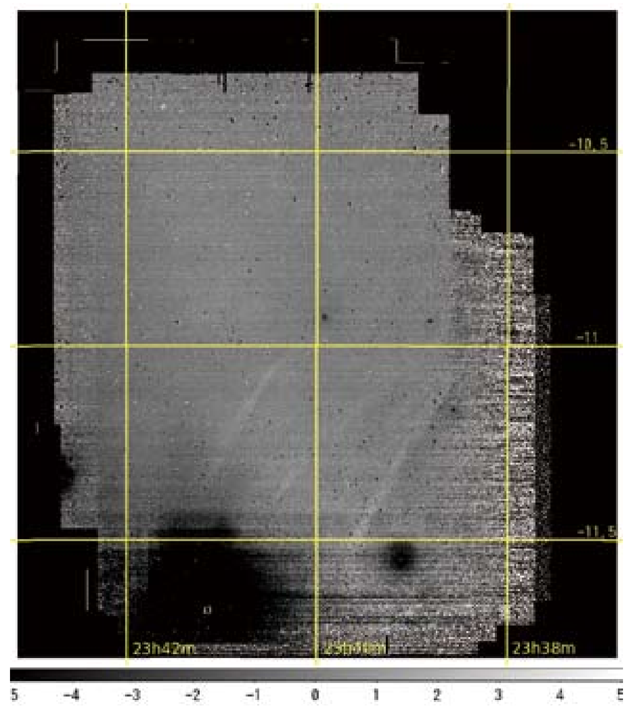

Figure 1: R-band subtracted N657 (Hα) image. Around the center, three parallel filamentary structures running from the top right to the bottom left direction are recognized.

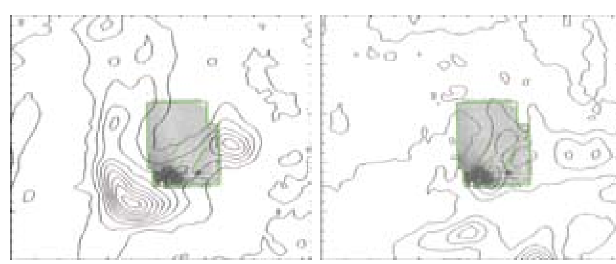

Figure 2: Hα emission overlaied on the contour of neutral hydrogen gas [7,8]. The left is the gas of Magellanic Stream, and the right is nearby Galactic gas.

References

[1] Mathewson, D. S., et al.: 1974, *ApJ*, **190**, 291.
[2] Weiner, B. J., Williams, T. B.: 1996, *AJ*, **111**, 1156.
[3] Putman, M. E., et al.: 2003, *ApJ*, **586**, 170.
[4] Bland-Hawthorn, J., et al.: 2007, *ApJ*, **670**, L109.
[5] Yagi, M., Komiyama, Y., Yoshida, M.: 2012, *ApJ*, **749**, L2.
[6] McCullough, P. R., Benjamin, R. A.: 2001, *AJ*, **122**, 1500.
[7] McClure-Griffiths, N. M., et al.: 2009, *ApJS*, **181**, 398.
[8] Kalberla, P. M. W., et al.: 2010, *A&A*, **512**, A14.

Three Classical Cepheid Variable Stars in the Nuclear Bulge of the Milky Way

MATSUNAGA, Noriyuki, KOBAYASHI, Naoto
(University of Tokyo)

KAWADU, Takahiro, NAGATA, Tetsuya
(Kyoto University)

NISHIYAMA, Shogo, TAMURA, Motohide
(NAOJ)

NAGAYAMA, Takahiro
(Nagoya University)

BONO, Giuseppe
(Universita di Roma Tor Vergata)

FEAST, Michael W.
(University of Cape Town)

The star formation history and the triggering process for star formation of the nuclear bulge of our Galaxy remain to be resolved. Classical Cepheid variable stars have pulsation periods that decrease with increasing age, so it is possible to probe the star-formation history. We have reported the presence of three classical Cepheids in the nuclear bulge with pulsation periods of approximately 20 days [1]. No Cepheids with longer or shorter periods were found. We infer that there was a period about 25 Myr ago, and possibly lasting until recently, in which star formation increased relative to the period of 30–70 Myr ago.

We conducted a near-infrared survey for the 0°.33 by 0°.5 area around the Galactic center [2], where no classical Cepheids were known before. The data were taken with the Infrared Survey Facility (IRSF) 1.4-m telescope and the SIRIUS near-infrared camera located at the South African Astronomical Observatory. Approximately 90 time-series images were collected in each of the J, H and K_S bands during eight years between 2001 and 2008, and three classical Cepheids were discovered on the basis of their light curves (Fig. 1).

All of our classical Cepheids have periods close to 20 days, suggesting their ages of 25 ± 5 Myr. We can estimate the star-formation rate at about 25 Myr ago by assuming an initial mass function and the lifetime spent by the Cepheid inside the instability strip, and find that the star-formation rate was $0.075^{+0.15}_{-0.05}\ M_{\odot}\,\mathrm{yr}^{-1}$ in the entire nuclear bulge 20–30 Myr ago. On the other hand, the absence of shorter-period Cepheids leads to $0.02\ M_{\odot}\,\mathrm{yr}^{-1}$ as a 1σ upper limit on the star-formation rate for 30–70 Myr ago. Thus we find the change in the star-formation rate between 20 and 70 Myr ago in the nuclear bulge.

A recent investigation suggested that the star formation rate was low a few tens of millions of years ago and then increased to a peak at about 0.1 Myr ago, followed by a decline in very recent times [3]. However, the tracers used give only a rough timescale for the range 1–100 Myr ago. Our estimates have much higher time resolution for the 20–70 Myr range and indicate an increase in star-formation rate within this period.

It is of interest to consider how and why such time variations in star formation occurred. Episodic star formation has been suggested in some of the so-called pseudobulges, the central regions of a few barred spiral galaxies, possibly growing with bar-driven gas inflow. Our result suggests that episodic star formation on a short timescale of about 25 Myr occurred in the nuclear bulge, which some authors claim to be a pseudobulge [4]. The timescale is comparable with that of the cyclic gas accumulation predicted for the central part of the Milky Way [5].

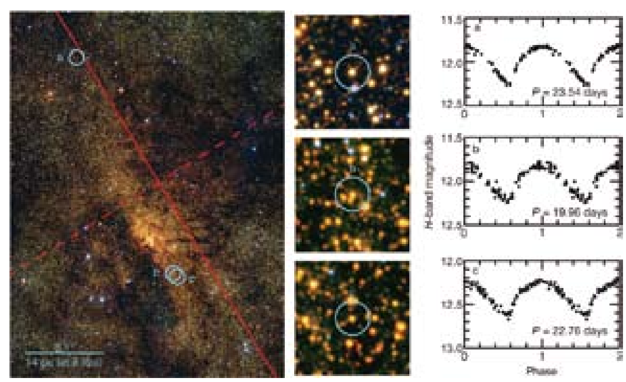

Figure 1: The classical Cepheids discovered in the Nuclear Bulge. The near-infrared false-color image (left), close-ups around the Cepheids (middle), and the H-band light curves are shown. The positions of the Cepheids are shown by blue circles.

References

[1] Matsunaga, N., et al.: 2011, *Nature*, **477**, 188.
[2] Matsunaga, N., et al.: 2009, *MNRAS*, **399**, 1709.
[3] Yusef-Zadeh, F., et al.: 2009, *ApJ*, **702**, 178.
[4] Binney, J., et al.: 2009, *IAUS*, **254**, 145.
[5] Stark, A. A., et al.: 2004, *ApJ*, **614**, L41.

Near-Infrared Imaging Polarimetry toward Serpens South: Revealing the Importance of the Magnetic Field

SUGITANI, Koji
(Nagoya City University)

NAKAMURA, Fumitaka, TAMURA, Motohide, NISHIYAMA, Shogo, KANDORI, Ryo, KAWABE, Ryohei
(NAOJ)

WATANABE, Makoto
(Hokkaido University)

NAGAYAMA, Takahiro, SATO, Shuji
(Nagoya University)

NAGATA, Tetsuya
(Kyoto University)

GUTERMUTH, Robert A., WILSON, Grant W.
(University of Massachusetts)

It is now widely accepted that stars form predominantly within clusters inside dense clumps of molecular clouds (MCs) that are turbulent and magnetized. However, how clusters form in such dense clumps remains poorly understood. Recent numerical simulations suggest that a moderately strong magnetic field (MF) is needed to impede star formation in MCs for the simulated star formation rates to match observed values (e.g., [1]). In contrast, weak MF (a few μG) is claimed in MCs where turbulent compression largely controls the structural formation of MCs on scales of a few to several parsecs [2]. In the later case, the MFs associated with cluster-forming clumps are expected to be distorted significantly by supersonic turbulent flows.

To characterize the MF structure of cluster-forming clumps, it is important to uncover the global MF structures associated with cluster-forming clumps. So we carried out near-infrared polarization observations of filamentary clouds in the Serpens South embedded cluster [3], which is believed to be in a very early stage of cluster formation. Although some small deviation is seen, the MF is roughly perpendicular to the main filament elongated toward the NW and SE direction (Fig. 1, here the polarization vectors are assumed to be the directions of the local MF). This ordered MF configuration suggests that the MF is strong enough to regulate the entire structure of the main filament and, therefore, that the formation of the main filament has proceeded under the influence of the MF.

In contrast to the main filament, sub-filaments that converge on the central part of the cluster or intersect the main filament, appears to be nearly parallel to the MF direction. They could be outflows from the cluster or inflow toward the main filament. Recent CO observations toward Serpens South suggest that CO outflow lobes are anti-correlated with the sub-filaments [4], reinforcing the inflow view of the sub-filaments.

In addition, the global MF appears to be curved in the southern part of the observed region. This curved morphology suggests that the global MF is distorted by gravitational contraction along the main filament toward the northern part, where the mass of the cloud seems to be mostly concentrated. Using the Chandrasekhar-Fermi method, the MF strength is roughly estimated to be a few $\times 100\,\mu$G in two zones along the main filament.

All the above results show that the MF appears to significantly influence the dynamics of the Serpens South cloud. This does not appear to support the weak MF models of MC evolution/cluster formation, at least not for the Serpens South cloud

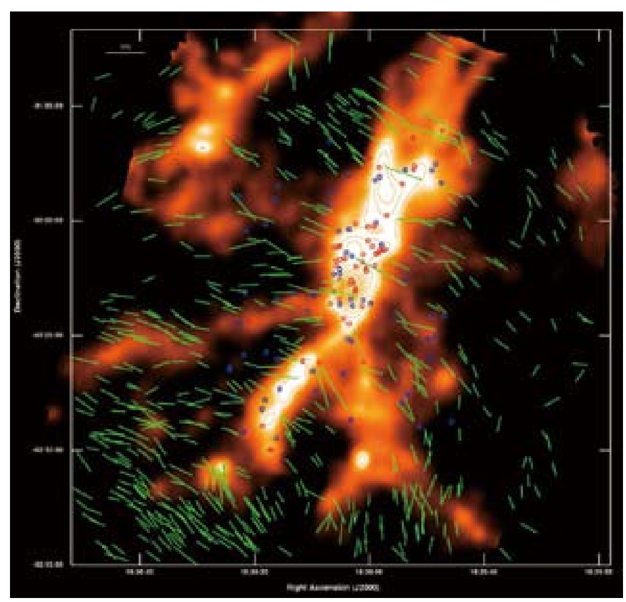

Figure 1: *H*-band polarization vector map toward Serpens South for point sources, superposed on the 1.1-mm dust-continuum image. YSOs are indicated by red (class 0/I) and blue (class II) open circles.

References

[1] Li, Z.-Y., Nakamura, F.: 2006, *ApJ*, **640**, L187.
[2] Padoan, P., et al.: 2001, *ApJ*, **553**, 227.
[3] Sugitani, K., et al.: 2011, *ApJ*, **734**, 63.
[4] Nakamura, F., et al.: 2011, *ApJ*, **737**, 56.

Oscillation Phenomena in the Disk around the Massive Black Hole Sagittarius A*

MIYOSHI, Makoto (NAOJ)   SHEN, Zhi-Qiang (SHAO)

OYAMA, Tomoaki (NAOJ)   TAKAHASHI, Rohta (TNCT)   KATO, Yoshiaki (NAOJ)

The existence of black holes has been definitely established while zooming-in the relativistic region is still in difficulty though promising in near future. Sagittarius A* (Sgr A*), the most convincing massive black hole at the Galactic center, shows short time flares with quasiperiodic oscillations (QPO) with P = 17, 22, & 33 min in near-infrared and X-ray regions originated from near the central black hole.

Here we report the detection of radio QPOs with structure changes using the Very Long Baseline Array (VLBA) at 43 GHz [1]. We found conspicuous patterned changes of the structure with P = 16.8, 22.2, 31.4, &56.4 min, roughly in a 3 : 4 : 6 : 10 ratio. The first two periods show a rotating one-arm structure, while the P = 31.4 min shows a rotating 3-arm structure, as if viewed edgeon. At the central 50 μas the P = 56.4 min period shows a double amplitude variation of those in its surroundings. Spatial distributions of the oscillation periods indicate that the disk of Sgr A* is presumably almost edge-on, rotating around an axis with $PA = -10°$. The observed VLBI images of Sgr A* remain several features of the black hole accretion disk of Sgr A* in spite of being obscured and broadened by scattering of surrounding plasma.

If the QPOs originate in a strong gravity field where the relativistic effect plays an important role, the periods of QPOs should depend on the mass and the spin of a massive black hole. Recent theories of disk seismology predict that peak frequencies of QPOs can be scaled by a mass of central black holes as an analogy to QPOs in black hole X-ray binaries (BXB). For example, in GRO J1655-40, a peak frequency of high frequency QPOs is about $3 \times 10^2 (6.0{-}6.6\, M_\odot / M_{\rm BH})$ Hz (where $M_\odot$ is a solar mass), with the result that a corresponding peak frequency using the mass of Sgr A* derived from the orbital motions of surrounding stars ($3.6 \pm 0.3 \times 10^6 M_\odot$) is about 5.1×10^{-4} Hz (P = 32 min), which is one of our findings. Detailed analysis with the obtained four QPO periods and wave-warp resonant oscillation model predicts the spin of Sgr A* to be 0.44 ± 0.08 and the black hole mass to be $(4.2 \pm 0.4) \times 10^6 M_\odot$ [2].

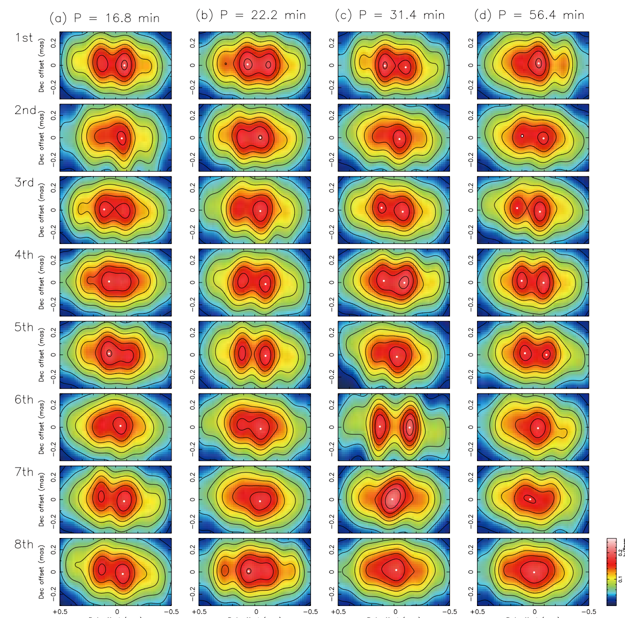

Figure 1: The slit-modulation-imaging (SMI) [3] maps with the 4 periods P = 16.8(a), 22.2(b), 31.4(c), *and* 56.4 min (d). The 8 maps show the images in phase frame series with respective periods. The white filled circles mark the intensity peak position in each map. In P = 31.4 & 56.4 min, second peaks are also marked with circles. Total amplitudes of respective periods are 22 mJy (P = 16.8 min), 24 mJy (P = 22.2 min), 24 mJy (P = 31.4 min), and 20 mJy (P = 56.4 min), which obtained by Fourier transform.

References

[1] Miyoshi, M., Shen, Z.-Q., Oyama, T., Takahashi, R., Kato, Y.: 2011, *PASJ*, **63**, 1093-1116.

[2] Kato, Y., Miyoshi, M., Takahashi, R., Negoro, H., Matsumoto, R.: 2010, *MNRAS*, **402**, L74-L78.

[3] Miyoshi, M.: 2008, *PASJ*, 60, 1371-1386.

Observational Identification of First Cores: Non-LTE Radiative Transfer Simulation

TOMISAKA, Kohji, TOMIDA, Kengo
(NAOJ)

A first core is a first hydrostatic object formed in the course of dynamical contraction of a molecular cloud core. Since the inflow pattern changes drastically before and after the first core formation, it is regarded as a milestone in the star formation process. Although the first core was predicted by Larson in 1969 [1], this has not been confirmed by observation yet. In order to identify the first core from a mapping observation, the features expected for the first core are studied for CS rotation transitions at radio wavelengths [2]. The non-LTE radiation transfer is calculated for the results of radiation magnetohydrodynamical simulations of the contraction of the magnetized molecular cloud core in rotation [3]. Figure 1 indicates the structure at the age of $\tau = 6.45 \times 10^2$ yr after the first core formation.

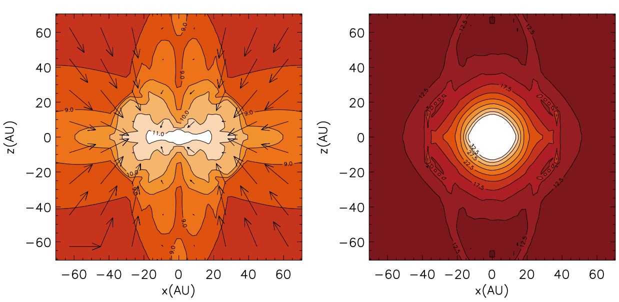

Figure 1: Density and velocity (left) and temperature (right) distributions. This 140-AU scale map shows that a first core warms the surrounding gas and an outflow is ejected vertically by the effect of rotation and magnetic field. Inflowing gas is essentially isothermal with a temperature of $T \simeq 10$ K, while the first core has higher temperature.

We use the Monte-Carlo method to solve the non-LTE radiation transfer in a nested grid hierarchy. Balance equation between radiative excitaion, induced emission, spontaneous deexcitaion, collisional excitation and deexcitation is solved, coupled with the radiation transfer equation. Denoting the number density of the J level (energy level $E(J)$) as n_J , we can write the balance equation as $n_J \sum_{J' \neq J} R_{JJ'} = \sum_{J' \neq J} n_{J'} R_{J'J}$ (J = 0, 1, ⋯, $J_{\max}$), where $R_{JJ'}$ represents the transition probability from J to J'

$$\text{as } R_{JJ'} \begin{cases} = A_{JJ'} + B_{JJ'}\mathcal{J}_{\nu JJ'} + nC_{JJ'} & \text{for } J > J', \\ = B_{JJ'}\mathcal{J}_{\nu JJ'} + nC_{JJ'} & \text{for } J < J', \end{cases}$$

where $A_{JJ'}$ and $B_{JJ'}$ represent Einstein's coefficients, the former being the coefficient for spontaneous emission and the latter the coefficient for absorption ($J < J'$) and induced emission ($J > J'$). $C_{JJ'}$ is the collisional transition rate from J to J' for collisions with H_2 molecules whose density is denoted by n. The average intensity of radiation with a frequency of $\nu = [E(J') - E(J)]/\mathrm{h}$ is written as $\mathcal{J}_{\nu JJ'}$, where h is the Plank constant.

In the first core phase, an outflow arises from the vicinity of the first core due to the twisted magnetic field amplified by the rotation motion of the contracting gas disk.

The disk and outflow system has several characteristic observational features (Fig. 2): (i) relatively opaque lines indicate asymmetry in the emission lines in which the blue side is stronger than the red side (an infall signature of the envelope); (ii) in the edge-on view, the disk has a signature of simultaneous rotation and infall, i.e., the integrated intensity of the approaching side is brighter than that of the receding side and the gradient in the intensity-weighted velocity is larger in the approaching side; (iii) the observed outflow indicates rotation around the rotation axis. The size of the outflow gives the approximate age after the first core is formed, since the outflow is not expected for the earlier runaway isothermal collapse phase.

The reason why the mirror symmetry is broken in the rotating infall disk is understood as follows. This assymmetry arises due to the self-absorption. Since the temperature decreases outwardly, the emission from the portion near the tangential point is absorbed by foreground rotating inflow gas. In this configuration, velocity difference between gases which contribute emission and absorption is larger for approating side rather than receding side of rotation.

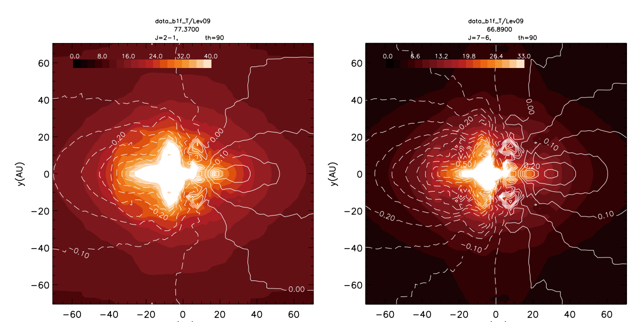

Figure 2: Expected distribution of the integrated intensity of the CS J = 2−1 (left) and J = 7−6 (right) emissions. The integrated intensities are shown with false color and intensityweighted mean velocity (first moment) is shown in white contour lines. This shows the edge-on view.

References

[1] Larson, R. B.: 1969, *MNRAS*, **145**, 271.
[2] Tomisaka, K., Tomida, K.: 2011, *PASJ*, **63**, 1151.
[3] Tomida, K., Tomisaka, K., Matsumoto, T., Ohsuga, K., Machida, M. N., Saigo, K.: 2010, *ApJ*, **714**, L58.

A discovery of Red Star Forming Galaxies in Groups at $z = 0.4$

KOYAMA, Yusei (NAOJ / University of Tokyo)
KODAMA, Tadayuki, NAKATA, Fumiaki (NAOJ)
SHIMASAKU, Kazuhiro, OKAMURA, Sadanori (University of Tokyo)

In the present-day Universe, galaxy properties are strongly correlated with the environment where the galaxies reside. For example, high-density environment such as clusters are dominated by red ellipticals and S0s, while general field environments are dominated by blue star-forming spirals or irregulars [1]. In order to study the origin of this environmental dependence of galaxy properties, the most direct and useful approach is to observe distant clusters of galaxies, because distant clusters are the young stage of present-day clusters where we can see active assembly of galaxies in the past Universe. In particular, wide-field observations of distant clusters enable us to unveil filamentary large-scale structures around the clusters [2], and to investigate the galaxy properties in such intermediate-density environment. Some previous studies with Subaru Telescope have shown that galaxy colours are strongly changing from blue to red in such cluster surrounding environment, and suggested that the cluster surrounding structures are key for understanding galaxy evolution (but not yet fully cultivated) [3,4,5]. Therefore, in order to study galaxy activities in such key environment more in detail, we heve carried out an Hα-based star-forming galaxy survey of the CL0939+4713 cluster (Abell 851) at $z = 0.41$ [6].

The Abell 851 cluster was studied with the Prime Focus Camera on Subaru (Suprime-Cam) [3], and a huge structure over ~10 Mpc has been identified around the cluster. Fortunately, the Hα line (rest-frame 6563 Å) from this cluster can be neatly captured by the narrowband filter NB921 (λ_c =9180 Å) on Suprime-Cam. Combining the available broad-band data (*BVRIz′*), we have identified more than 400 Hα emitting galaxies with star formation rates of >0.3 $M_\odot$/yr along the large-scale structure (Fig. 1). An intriguing finding from this survey is the colours of the Hα emitters: the majority of them show blue colours reflecting their young stellar population (as expected), while we find a non-negligible fraction of them show red colours with $B - I > 2$. Such red Hα emitters are expected to be dust-reddened star forming galaxies (dusty starbursts), and they are probably in the transitional stage from blue star forming population to red quiescent one. We find that the red Hα emitters are very rare in the cluster central region (within ~1 Mpc from the cluster centre), while as can be seen in Fig. 1 they are most strongly concentrated in group-scale environment which are located far from the cluster (we find that ~30 % of star forming galaxies in groups show red colours). This result shows that dusty starbursts are triggered in the group-scale environment (rather than highest-density cluster core), and suggests that this strong activity is related to the acceleration of galaxy evolution in distant group environment. We finally stress that this study provides us with an important clue on cluster galaxy evolution, and this is a great achievement of Subaru Telescope with wide-field of view.

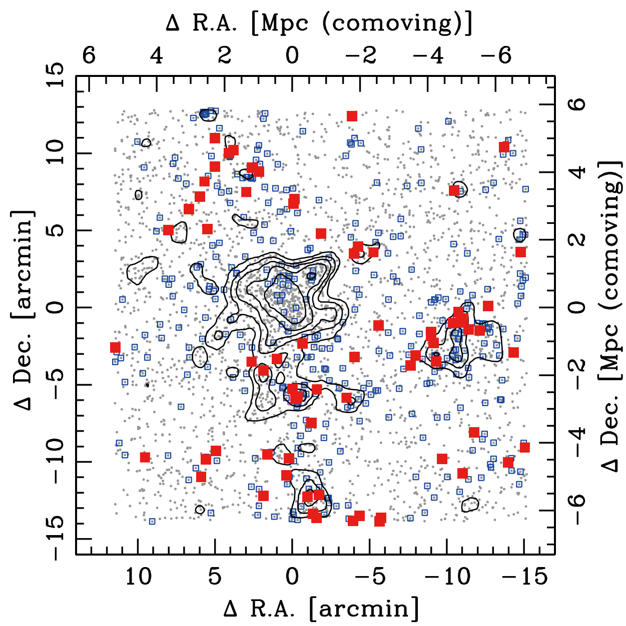

Figure 1: The large-scale structure around the Abell 851 cluster at $z = 0.41$, revealed by Suprime-Cam imaging. The grey dots show the photo-z selected members and the contours are drawn based on the surface number density of member galaxies. The red and blue squares indicate the red and blue Hα emitters, respectively. It is clear that the "red emitters" are preferentially found in the group-scale environment located far away from the cluster core.

References

[1] Dressler, A.: 1980, *ApJ*, **236**, 351.
[2] Kodama, T., et al.: 2005, *PASJ*, **57**, 309.
[3] Kodama, T., et al.: 2001, *ApJ*, **562**, 9.
[4] Tanaka, M., et al.: 2005, *MNRAS*, **362**, 268.
[5] Koyama, Y., et al.: 2008, *MNRAS*, **391**, 1758.
[6] Koyama, Y., et al.: 2011, *ApJ*, **734**, 66.

Subaru Measurements of Spin-Orbit Alignment Angles of Exoplanets

NARITA, Norio (NAOJ)
HIRANO, Teruyuki (MIT / University of Tokyo)
SATO, Bun'ei (Tokyo Institute of Technology)
AOKI, Wako, TAMURA, Motohide (NAOJ)

Since the discovery of the first exoplanet in 1995, scientists have identified more than 700 exoplanets, planets outside of our solar system, nearly all of which are giant planets. Most of these giant exoplanets closely orbit their host stars, unlike our solar system's giant planets, like Jupiter, that orbit the Sun from a distance. Accepted theories propose that these giant planets originally formed from abundant planet-forming materials far from their host stars and then migrated to their current close locations. Different migration processes have been suggested to explain close-in giant exoplanets.

Disk-planet interaction models of migration focus on interactions between the planet and its protoplanetary disk, the disk from which it originally formed. Sometimes these interactions between the protoplanetary disk and the forming planet result in forces that make the planet fall toward the central star. This model predicts that the spin axis of the star and the orbital axis of the planet will be in alignment with each other. Planet-planet interaction models of migration have focused on mutual scatterings among giant planets. Migration can occur from planet scattering, when multiple planets scatter during the creation of two or more giant planets within the protoplanetary disk. While some of the planets scatter from the system, the innermost one may establish a final orbit very close to the central star. Another planet-planet interaction scenario, Kozai migration, postulates that the long-term gravitational interaction between an inner giant planet and another celestial object such as a companion star or an outer giant planet over time may alter the planet's orbit, moving an inner planet closer to the central star. Few-body interactions, including planetplanet scattering and Kozai migration, could produce an inclined orbit between the planet and the stellar axis.

Overall, the inclination of the orbital axes of close-in planets relative to the host stars' spin axes emerges as a very important observational basis for supporting or refuting migration models upon which theories of orbital evolution center. For this reason, we have conducted observations with the Subaru Telescope to measure the Rossiter-McLaughlin (hereafter, RM) effect of transiting planetary systems so as to investigate these inclinations.

The RM effect refers to apparent irregularities in the radial velocity or speed of a celestial object in the observer's line of sight during planetary transits. Unlike the spectral lines that are generally symmetrical in measures of radial velocity, those with the RM effect deviate into an asymmetrical pattern. Such apparent variation in radial velocity during a transit reveals the sky-projected angle between the stellar spin axis and planetary orbital axis [1]. Subaru Telescope has participated in previous measurements of the RM effect, which we have investigated for over ten exoplanetary systems. In 2011, we newly found that XO-2b has a well-aligned orbit [2], whereas XO-3b has highly inclined orbits (Figure 1) [3].

The latest observational results about the RM effect, including those obtained independently of the findings reported here, suggest that about one-third of the observed hot Jupiter systems have highly inclined planetary orbits. Also, it has now turned out that the latest distribution of the spin-orbit alignment angles have dependences on stellar temperature and age [4,5].

We plan to extend our targets to smaller planets in the future aiming to uncover the whole picture of planetary migration mechanisms.

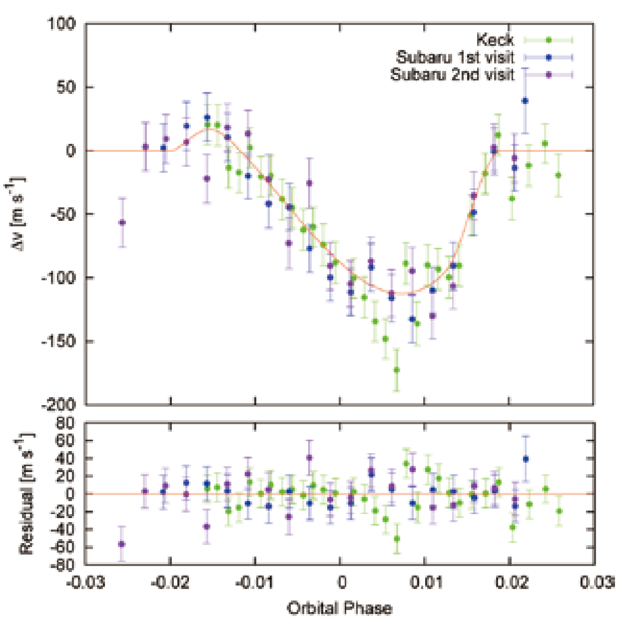

Figure 1: The Rossiter-McLaughlin effect of XO-3b taken with the Subaru HDS (purple and blue points). Also plotted are the Keck HIRES data (green) which cover a partial transit.

References

[1] Hirano, T., et al.: 2011, *PASJ*, **63**, S531-S536.
[2] Narita, N., et al.: 2011, *PASJ*, **63**, L67-L71.
[3] Hirano, T., et al.: 2011, *ApJ*, **742**, 69.
[4] Winn, J. N., et al.: 2010, *ApJ*, **718**, L145-L149.
[5] Triaud, A. M. D., et al.: 2011, *A&A*, **534**, L6.

The Standard IMF in the Outskirts of M83

KODA, Jin (Stony Brook University)
YAGI, Masafumi (NAOJ)
BOISSIER, Samuel (Laboratoire d'Astrophysique de Marseille)
GIL DE PAZ, Armando (Universidad Complutense de Madrid)
IMANISHI, Masatoshi (NAOJ)
DONOVAN MEYER, Jennifer (Stony Brook University)
MADORE, Barry F. (Carnegie Institution of Washington)
THILKER, David A. (The Johns Hopkins University)

The initial mass function (IMF) is of crucial importance to developing models of star formation and galaxy evolution. Most observations are consistent with a universal IMF [1]; however, recently, a non-universal IMF has been inferred [2]. The IMF in low-density environments could be truncated (or steeper) at its high-mass end. Fewer high-mass stars appear to form in dwarf and low surface brightness galaxies [3].

The Galaxy Evolution Explorer (GALEX) ultraviolet (UV) satellite has revealed tantalizing evidence for star formation far beyond the optical edge of galactic disks. These extended UV (XUV) disks are providing a new opportunity for studying the mode of star formation in extremely low-density, low star-forming environments. By capitalizing on the exceedingly high sensitivity and wide field-of-view of the Suprime-Cam, we observe the whole extension of the large XUV disk of the nearby galaxy M83 (Figure 1). GALEX UV images are sensitive to both O and B stars but cannot distinguish between them, while Subaru Hα images are sensitive almost exclusively to O stars since only O stars produce appreciable HII regions. Therefore, the combination of Subaru and GALEX can determine the high-mass end of the IMF. Suprime-Cam with the Hα filter (i.e., NA659) detects every HII region around a single O star at the distance of M83.

Our new observations enable the first complete census of very young stellar clusters over the entire XUV disk. Combining Subaru and GALEX data with a stellar population synthesis model, we find that (1) the standard, but stochastically-sampled, IMF is preferred over the truncated (or steeper) IMF, because there are low mass stellar clusters ($10^{2-3}\,M_{\odot}$) that host massive O stars, which should not exist under the truncated IMF; that (2) the standard Salpeter IMF and a simple aging effect explain the counts of FUV-bright and Hα-bright clusters with masses $> 10^3\,M_{\odot}$; and that (3) the Hα to FUV flux ratio over the XUV disk supports the standard IMF. To reach conclusion (2), we assumed instantaneous cluster formation and a constant cluster formation rate over the XUV disk.

Suprime-Cam covers a large area even outside the XUV disk − far beyond the detection limit of the HI gas. This permits us to statistically separate the stellar clusters in the disk from background contamination. The new data, model, and previous spectroscopic studies provide overall consistent results with respect to the internal dust extinction ($A_V \sim 0.1$ mag) and low metallicity ($\sim 0.2\,Z_{\odot}$) using the dust extinction curve of the Small Magellanic Cloud. The background subtraction and extinction correction have been the major issues in studies of the IMF in external galaxies. This result is published in [4].

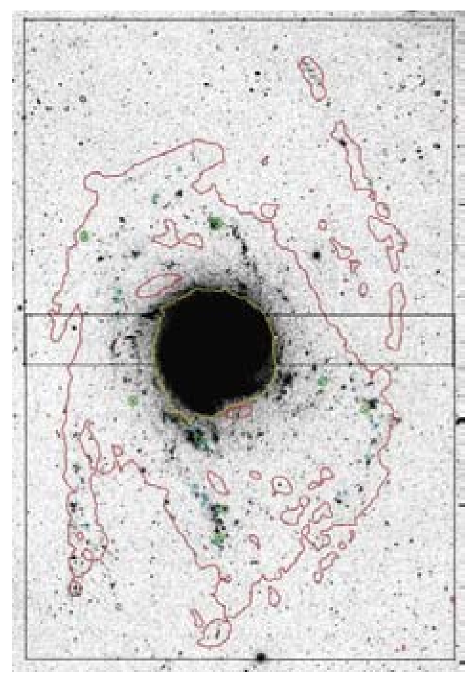

Figure 1: Suprime-Cam coverage of the XUV disk of M83. The background is a GALEX far-UV (FUV) image. Solid overlapping rectangles are two Suprime-Cam pointings. The inner (yellow) contour is roughly at the traditional edge of the optical disk. The outer (red) counter is at an HI surface density of 1.5×10^{20} cm^{-2} [5]. The Hα-bright clusters (NA659 − $R_c < -1$ mag) are also plotted: green for clusters with $> 10^3\,M_{\odot}$ and cyan for the ones with $< 10^3\,M_{\odot}$.

References

[1] Kroupa, P.: 2002, *Science*, **295**, 82.
[2] Bastian, N., Covey, K. R., Meyer, M. R.: 2010, *ARA&A*, **48**, 339.
[3] Meurer, G., Wong, O. I., Kim, J. H., et al.: 2009, *ApJ*, **695**, 765.
[4] Koda, J., Yagi, M., Boissier, S., et al.: 2012, *ApJ*, **749**, 20.
[5] Miller, E. D., Bregman, J. N., Wakker, B. P.: 2009, *ApJ*, **692**, 470.

Photometric Observations of 107P/Wilson-Harrington

URAKAWA, Seitaro, OKUMURA, Shin-ichiro, NISHIYAMA, Kota, SAKAMOTO, TsuyoshI, TAKAHASHI, Noritsugu
(Japan Spaceguard Association)

ABE, Shiunsuke (National Central University)
ISHIGURO, Masateru (Seoul University)
KITAZATO, Kohei (Aizu University)

OHTA, Kouji (Kyoto University)
KAWAI, Nobuyuki (Tokyo Institute of Technology)

KURODA, Daisuke, SHIMIZU, Yasuhiro, NAGAYAMA, Shogo, YANAGISAWA, Kenshi
(NAOJ)

YOSHIDA, Michitoshi (Hiroshima University)
HASEGAWA, Sunao, YOSHIKAWA, Makoto (JAXA)

Introduction: Main-belt comets (MBCs) are objects that display cometary activities in the main-belt asteroid (MBA) region [1]. The mechanism of the cometary activity is controversial: i.e. impact collisions or ice sublimations. The discovery of MBCs indicates that objects in the outer-MBA region have enough volatile materials, as suggested by the Nice model [2]. Furthermore, some outer-MBAs would migrate to the orbit of near-earth objects (NEOs). A part of such volatile rich objects would impact with the Earth in the earliest stage of the Solar System. The study of objects in which cometary activity is shown provides keys to the origin of Earth's water and life.

107P/Wilson-Harrington: 107P/Wilson-Harrington (also know as 4015 Wilson-Harrington, hereafter, 107P) was discovered accompanied by a faint cometary tail in 1949 [3]. Despite a devoted search, no cometary activity has been detected since the initial observation [4]. A numerical simulation mentions that there is a 65 % chance that 107P has an origin in the outer-MBAs region [5]. Thus, 107P might include much volatile material like MBCs. Moreover, if the cometary activity of 107P is driven by impact collisions, the collision would affect the rotation of 107P. In that case, the lightcurve of 107P shows the multi-periodicity. Besides, 107P is a promising target by an advanced asteroid probe. Clarification of the rotational states of 107P is important to design the future sample return mission.

Results: We had conducted the photometric observations of 107P in 2009-2010 apparition. The lightcurve had showed a periodicity of 0.2979 day (7.15 h) and 0.0993 day (2.38 h), which has a commensurability of 3:1 (Fig. 1) [6]. We suggest the following four possibilities for the interpretation. 1) 107P is a tumbling object with a sidereal rotation period of 0.2979 day and a precession period of 0.0993 day. 2-A) 107P is not a tumbler. The sidereal rotation period is 0.2979 day. The period of 0.0993 day represents the roughly symmetrical hexagonal shape. 2-B) 107P is not a tumbler. The sidereal rotation period is 0.2979 day. The period of 0.0993 day comes from the binary eclipse. 2-C) The observations were conducted at the phase angle of around 50 √? √£. Therefore, the shade by topography would provide the period of 0.0993 day. In that case, 107P is not a tumbler. The sidereal rotation period is 0.1490 day (a half period of 0.2970 day). Tumbling, binary aster oid, and the topographical effect imply that the cometary activity of 107P results from the impact collisions.

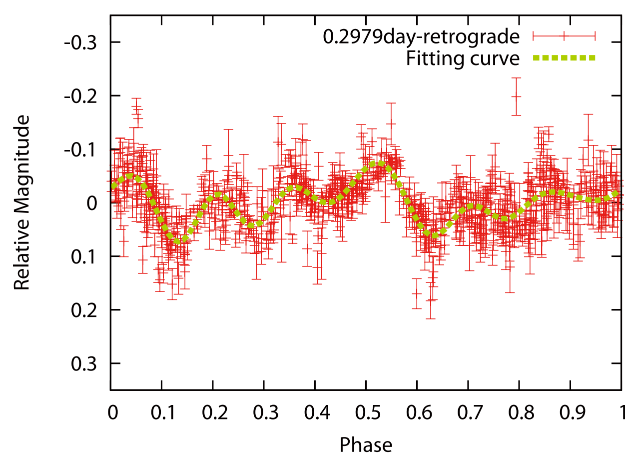

Figure 1: Lightcurve of 107P.

References

[1] Hsieh, H. H., Jewitt, D.: 2006, *Science*, **312**, 561.
[2] Levison, H., et al.: 2009, *Nature*, **460**, 364.
[3] Fernandez, Y. R., et al.: 1997, *Icarus*, **128**, 114.
[4] Ishiguro, M., et al.: 2011, *ApJ*, **726**, 101.
[5] Bottke, W. F., et al.: 2002, *Icarus*, **156**, 399.
[6] Urakawa, S., et al.: 2011, *Icarus*, **215**, 17.

Images of the Extended Outer Regions of the Debris Ring around HR 4796 A*

THALMANN, Christian[1], DOMINIK, Carsten[1], JANSON, Markus[2], BUENZLI, Esther[3], WISNIEWSKI, John[4]
BRANDT, Timothy[5], KNAPP, Gillian[5], TURNER, Edwin[5], MORO-MARTIN, Amaya[6], SCHNEIDER, Glenn[7]
USUDA, Tomonori[8], EGNER, Sebastian[8], TERADA, Hiroshi[8], TOMONO, Daigo[8], TAKAMI, Hideki[8]
GOLOTA, Taras[8], GUYON, Olivier[8], HAYANO, Yutaka[8], HAYASHI, Masahiko[8], HAYASHI, Saeko[8], ISHII, Miki[8]
NISHIMURA, Tetsuo[8], PYO, Tae-Soo[8], TAKATO, Naruhisa[8], KUDO, Tomoyuki[8], CARSON, Joseph[9]
MCELWAIN, Michael[10], GRADY, Carol[10], ABE, Lyu[11], GOTO, Miwa[12], HENNING, Thomas[12], BRANDER, Wolfgang[12]
FELDT, Markus[12], HODDAP, Klaus[13], SERABYN, Eugene[14], TAKAMI, Michihiro[15], FUKUE, Tsubasa[8]
HASHIMOTO, Jun[8], IYE, Masanori[8], KANDORI, Ryo[8], KUSAKABE, Nobuhiko[8], MATSUO, Taro[8]
MIYAMA, Syoken[8], MORINO, Jun-ichi[8], SUZUKI, Ryuji[8], SUTO, Hirohi[8], TAMURA, Motohide[8]
KUZUHARA, Masayuki[16], TAKAHASHI, Yasuhiro[16], WATANABE, Makoto[17], YAMADA, Toru[18]

1: University of Amsterdam, 2: University of Toronto, 3: Institute for Astronomy, 4: University of Washington, 5: Princeton University, 6: CAB-CSIC/INTA, 7: The University of Arizona, 8: NAOJ, 9: College of Charleston, 10: Goddard Space Flight Center, 11: University of Nice, 12: Max Planck Institute for Astronomy, 13: University of Hawaii, 14: Jet Propulsion Laboratory, 15: Institute of Astronomy and Astrophysics, 16: Univesity of Tokyo, 17: Hokkaido University, 18: Tohoku University

Vega-type debris disks were first identified by infrared (IR) excesses around nearby main sequence stars [1]. The dust content of these second-generation disk systems is believed to be continuously replenished via collisional breakup of remnant planetesimals [2]. Since the imaging of the β Pic system [3], nearly two dozen nearby debris disks have been spatially resoved. The morphological appearance of resolved debris disks is predicted by several mechanisms, e.g., interactions between dust in the disk and nearby planets [4].

We present high-contrast images of HR 4796A taken with Subaru/HiCIAO in H-band, resolving the debris disk in scattered light[4]. HR 4796A is a young (~8–10 Myr; [5]), nearby (72.8 ± 1.7 pc; [6]), A0V-type star first identified as a debris disk system from an IR excess observed with IRAS [7]. The application of specialized angular differential imaging methods (ADI) allows us to trace the inner edge of the disk with high precision, and reveals a pair of "streamers" extending radially outwards from the ansae. Using a simple disk model with a power-law surface brightness profile, we demonstrate that the observed streamers can be understood as part of the smoothly tapered outer boundary of the debris disk, which is most visible at the ansae. Our observations are consistent with the expected result of a narrow planetesimal ring being ground up in a collisional .Based on data collected at the Subaru Telescope, which is operated by the National Astronomical Observatory of Japan. cascade, yielding dust with a wide range of grain sizes. Radiation forces leave large grains in the ring and push smaller grains onto elliptical, or even hyperbolic trajectories. We measure and characterize the disks surface brightness profile, and confirm the previously suspected offset of the disks center from the stars position along the rings major axis. Furthermore, we present first evidence for an offset along the minor axis. Such offsets are commonly viewed as signposts for the presence of unseen planets within a disks cavity. Our images also offer new constraints on the presence of companions down to the planetary mass regime (~9 M_{Jup} at 0″.5, ~3 M_{Jup} at 1″).

* Based on data collected at the Subaru Telescope, which is operated by the National Astronomical Observatory of Japan.

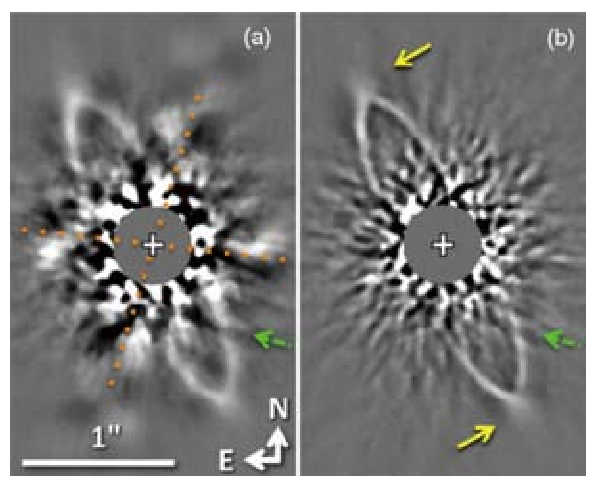

Figure 1: High-contrast images of the HR 4796 A debris disk. White plussigns mark the star's location. The saturated central area is masked in gray. (a) Subaru HiCIAO H-band data after reduction with simple ADI (subtraction of a median background) and median smoothing on a scale of 5 pixels (=48 mas ~1 λ/D). Orange dotted lines mark the mean of the spider diffraction pattern. The stretch is linear between $\pm 3 \times 10^{-5}$ times the stellar peak flux. (b) The same after ADI reduction with the LOCI algorithm, using conservative settings (optimization region area of 10,000 PSF footprints). Note the "streamers" extending radially out from the ansae (yellow arrows). Linear stretch of $\pm 1.5 \times 10^{-5}$.

References

[1] Aumann, H. H., et al.: 1984, *ApJ*, **278**, L23.
[2] Wyatt, M. C., et al.: 2008, *ARA&A*, **46**, 339.
[3] Smith, B. A., et al.: 1984, *Science*, **226**, 1421.
[4] Thalmann, C., et al.: 2011, *ApJ*, **743**, L6.
[5] Stauffer, J. R., et al.: 1995, *ApJ*, **454**, 910.
[6] van Leeuwen, F.: 2007, *A&A*, **474**, 653.
[7] Jura, M.: 1991, *ApJ*, **383**, L79.

Development of the Ultra-Low Loss Mirrors for Gravitational Wave Detector

TATSUMI, Daisuke, UEDA, Akitoshi
(NAOJ)

At long last construction of the next generation gravitational wave (GW) detector KAGRA has begun. Because the detector consists of a 100Watt class high power laser and complex optical cavities, high quality mirrors are key items to obtain its designed performance. Not only optical properties but also mechanical one need to be high quality. Therefore, the mirror developments for KAGRA detector are very complex and difficult.

Our group is in charge of the ultra low loss and high reflectivity mirror developments and of the high damage threshold mirror for the high power laser. The research is collaborated with the University of Tokyo, the University of electro-communications, and several Japanese optics companies. Storing large number of photons in an optical cavity is effective to improve the sensitivity of not only GW detectors but also of general precise measurements using laser interferometers. To realize this situation, the cavity should have high finesse which corresponds to a number of bounces of photons in the cavity. High reflection mirrors are necessary for this reason. If we need very high reflectivity of more than 99.99 %, its optical loss becomes important. In general easy-obtainable mirrors have a untolerable loss of 100 ppm level. Because no transmitted light is available, such cavity cannot be used for precise measurements. Therefore, it is our immediate target to develop mirrors which are compatible with high reflectivity of more than 99.99 % and low loss of less than 10 ppm. At the time TAMA detector was constructed, it was succeeded to achieve ultra low loss of 1.5 ppm [1]. Unfortunately the optics company which was collaborated with our group withdrew. Now we collaborate with several companies to recover the mirror quality. Final target is to break our world lowest loss record.

As the first step, a scatter meter was constructed in TAMA experimental hall which has been used for the GW observation experiments. Figure 1 shows an experimental setup on a table. To obtain extremely good sensitivity, the following efforts are undertaken: 1) a pinhole filter is applied to obtain ideal Gaussian beam profile, 2) the lock-in detection method is applied to obtain good signal-to-noise ratio for the scattering light power measurement, 3) an acousto-optical modulator is applied to reduce the scattering noises at the modulator such as the mechanical chopper, and 4) a low-scattering beam dumper for the transmitted light of the objective mirror is developed.

Figure 2 shows a histogram of two dimensional scan results for a fused silica plate which is polished with a micro-roughness of less than 0.75 Å. An averaged scattering of 1.5 ppm was obtained. Theoretically the relationship between micro-roughness and scattering is represented by Eq. (1).

$$\mathrm{TIS} = \left(\frac{4\pi\delta}{\lambda}\right)^2 \tag{1}$$

Here λ is the wavelength of the laser and δ is micro-roughness. In our case, the wavelength is at 1064 nm and micro-roughness is 0.75 Å, and hence the scattering (Total Integrated Scatter) is expected to be 1 ppm. This value is consistent with our measured one [2].

By using this system, a lot of trial mirrors are being evaluated to obtain high reflectivity and low loss mirrors.

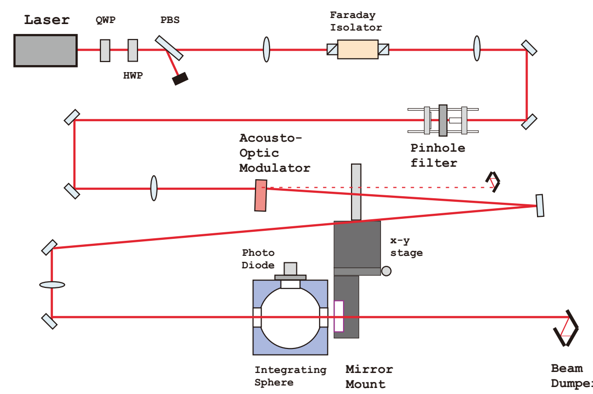

Figure 1: An experimental setup for the scatter mater.

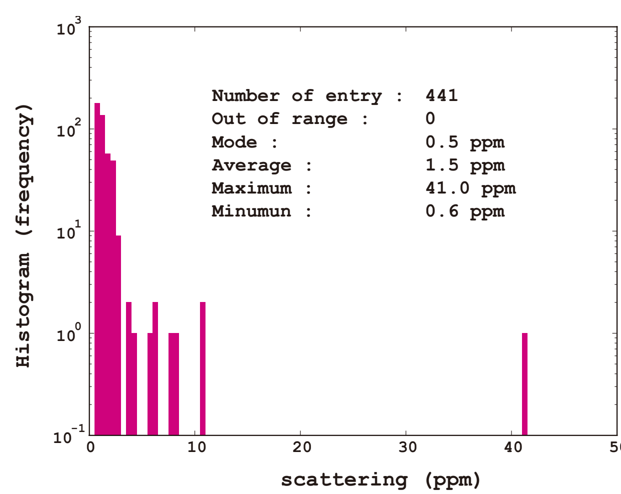

Figure 2: A histogram for a fused silica plate. An averaged scattering of 1.5 ppm was obtained.

References

[1] Ueda, A., et al.: 1996, *Opt. Rev.*, **3**, 369.
[2] Tatsumi, D.: 2012, Talk presented at annual meeting (spring) of Japan Astronomical Society, V249a.

Astrometry of 6.7 GHz Methanol Maser toward W3(OH) with Japanese VLBI Network

MATSUMOTO, Naoko, HONMA, Mareki
(The Graduate University for Advanced Studies / NAOJ)
ISONO, Yasuko
(Nagoya University)
UJIHARA, Hideki
(NICT)
KIMURA, Kimihiro, MATSUMOTO, Kouhei
(Osaka Prefecture University)
SAWADA-SATOH, Satoko
(NAOJ)
DOI, Akihiro
(ISAS)
FUJISAWA, Kenta
(Yamaguchi Univerisity)
UENO, Yuji
(NAOJ)

We present the results of multi-epoch VLBI observations for 6.7 GHz methanol maser emission toward the UC HII region of W3(OH) with Japanese VLBI Network (JVN) [1]. Based on phase-referencing VLBI astrometry, we derived the trigonometric annual parallax to be 0.598 ± 0.067 mas, corresponding to a distance of $1.67^{+0.21}_{-0.17}$ kpc. This is the first detection of parallax for a 6.7 GHz methanol maser source with JVN, following European VLBI Network [2], and demonstrates that JVN/VERA is capable of conducting VLBI astrometry for 6.7 GHz methanol maser sources within a few kpc from the Sun. Based on in-beam mapping of the W3(OH) methanol maser, we also measured the internal proper motions of its 6.7 GHz methanol maser for the first time. The internal proper motions basically show north-south expansion with a velocity of few km s^{-1}, being similar to OH masers. The spatial distribution and the internal proper motions of 6.7 GHz methanol masers suggest a rotating and expanding torus structure surrounding the UC HII region.

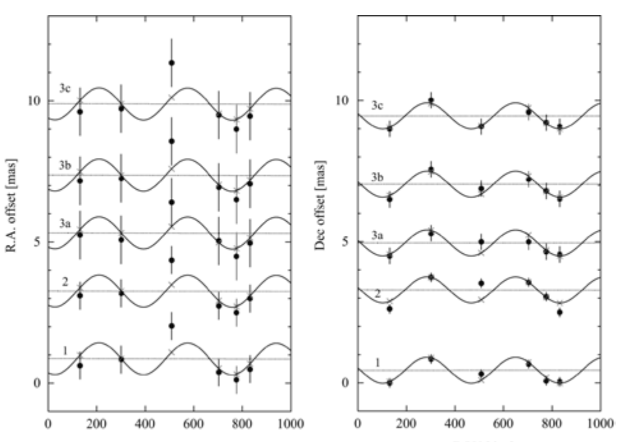

Figure 1: Results of positional offsets variation for the maser components of $v_{LSR} = -43.10$ (1), -43.80 (2), -45.91 (3a), -45.20 (3b), and -45.60 (3c) km s^{-1} after subtracting the best-fit proper motions. The first day corresponds to New Year's day 2008.

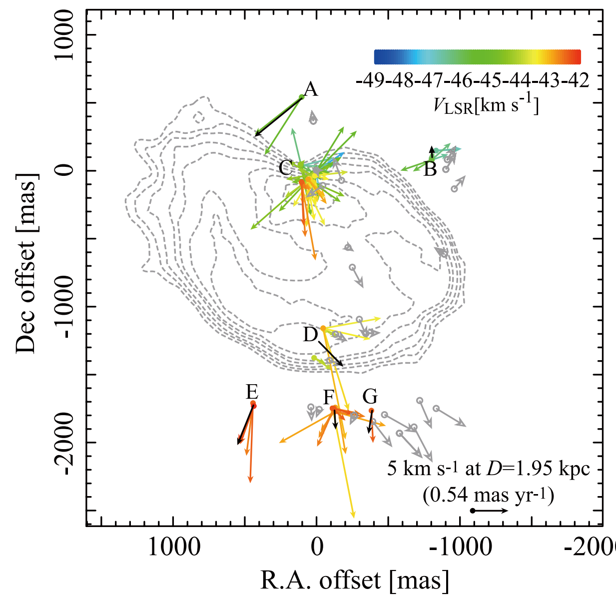

Figure 2: Internal proper motion for 6.7 GHz methanol maser components toward W3(OH). Color-codes represent the LSR velocity. The colored vectors show the directions and amplitudes of the relative proper motions on the sky plane to the reference component with the −45.4 km s^{-1} LSR velocity. The thick black vectors show the averaged relative proper motion at each cluster of A, B, and D-G to the C cluster around the origin. The proper motion vectors of 1665 MHz OH maser (gray vectors) and the contour map of 15 GHz radio continuum emission of the UCHII region (broken lines) are taken from Bloemhof, Reid, and Moran [3].

References

[1] Matsumoto, N., et al.: 2011, *PASJ*, **63**, 1345.
[2] Rygl, K. L. J., et al.: 2010, *A&A*, **511**, A2.
[3] Bloemhof, E. E., Reid, M. J., Moran, J. M.: 1992, *ApJ*, **397**, 500.

Statistical Study of Flux Emergences on the Sun

OTSUJI, Kenichi (NAOJ)
KITAI, Reizaburo, ICHIMOTO, Kiyoshi, SHIBATA, Kazunari (Kyoto University)

Since *Hinode* has been launched in 2006, it has revealed new aspects of the sun. We carried out the statistical study of flux emergences on the solar surface observed with *Hinode* Solar Optical Telescope (SOT), which clarified that the total flux of one emerging flux region controls its spatial size and the timescale of emergence [1].

The solar activities such as flares occur according to the release of magnetic energy transported from the convective zone. Emerging flux regions are where the flux tubes from the convective zone emerge onto the solar surface, and take important role in the studies on the solar activities like flares, coronal mass ejections and their effects on the earth.

The result of this study showed the power-law relation between the total flux and the mean flux growth rate of emerging flux regions. This implies that one can estimate the final emerged flux amount of a region from its mean flux growth rate of the initial phase, which can be used for the space weather forecasting.

Hinode SOT observed 101 flux emergence events in between November 2006 and August 2010 with magnetogram. Figure 1 shows the example of a flux emergence event observed on December 30, 2009. From the observed data, physical parameters of emerging flux regions were measured with respect to the spatial size (d_{max}), emerged total flux amount (Φ_{max}) and the mean flux growth rate ($\langle d\Phi/dt \rangle$). As the result, we obtained the power-law relations as shown in Figure 2.

$$d_{max} \propto \Phi_{max}^{0.27} \quad (1)$$

$$\left\langle \frac{d\Phi}{dt} \right\rangle \propto \Phi_{max}^{0.57} \quad (2)$$

These results give the observational support to the flux tube evolution and emergence model at the convective zone. Further investigation with comparing to the simulation for revealing more realistic picture of the solar interior is required.

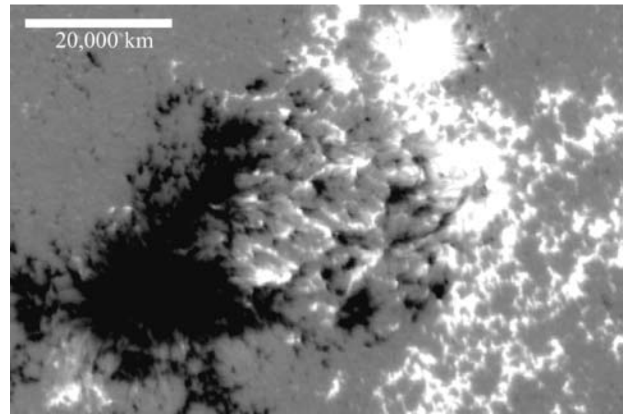

Figure 1: Magnetic field of the emerging flux region observed on December 30, 2009 by *Hinode* SOT. Between the large black and white area corresponding to sunspots, the flux emergence occurs.

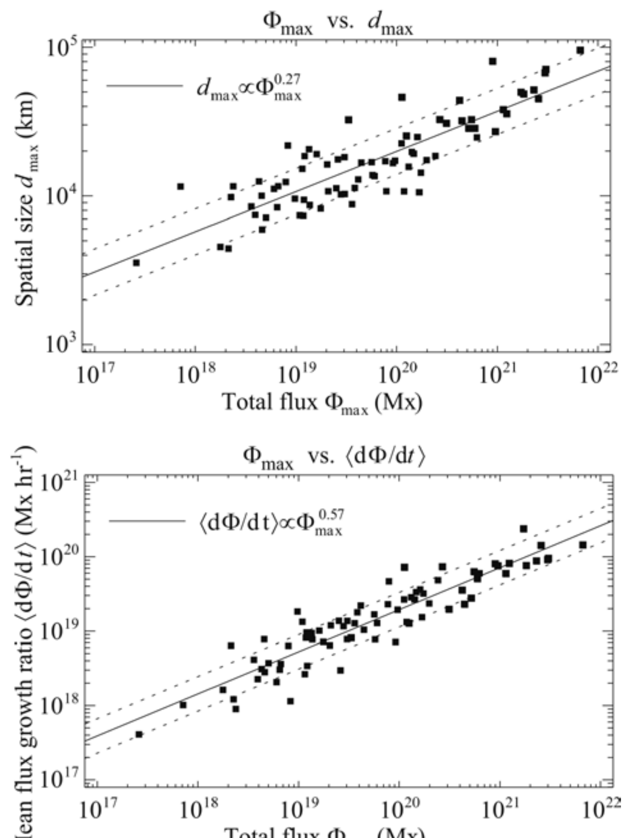

Figure 2: The scatterplots of the total flux (Φ_{max}), spatial size (d) and mean flux growth rate ($\langle d\Phi/dt \rangle$) of the emerging flux regions.

Reference

[1] Otsuji, K., Kitai, R., Ichimoto, K., Shibata, K.: 2011, *PASJ*, **63**, 1047.

Properties of Star-Forming Galaxies in a Cluster and Its Surrounding Structure at $z = 1.46$

HAYASHI, Masao, KODAMA, Tadayuki, KOYAMA, Yusei, TANAKA, Ichi
(NAOJ)
TADAKI, Ken-ichi
(University of Tokyo)

Galaxies in the local Universe have properties dependent on environments as galaxy clusters tend to be dominated by massive, passively evolving galaxies with an elliptical morphology [1]. Galaxy clusters at high redshift (z) provide important clues to understanding galaxy formation and evolution, since going back to as high redshift as possible enables us to approach the epoch when galaxy clusters were formed. Indeed, recent surveys suggest that there are a lot of active, star-forming galaxies even in clusters or proto-clusters at $z \gtrsim 1.5$ and the prominent sequence of red galaxies in color–magnitude diagram, which is peculiar to galaxy clusters at $z \lesssim 1$, seems to be formed during $z \sim 1$–3 [2].

XMMXCS J2215.9-1738 cluster at $z = 1.46$ is one of the most massive galaxy clusters at $z > 1$ [3]. We conducted a wide-field [OII] emission line survey in and around this high-z cluster with Suprime-Cam on the Subaru Telescope, and selected 380 [OII] emitting galaxies in the region of 32×23 arcmin^2. Among them, 16 [OII] emitters in the central region of the cluster were confirmed by near-infrared spectroscopy with MOIRCS on the Subaru Telescope. Thanks to the wide-field coverage, we found that [OII] emitters are distributed along filamentary large-scale structures around the cluster for the first time (Figure 1), which are among the largest structures of star-forming galaxies ever identified at $1.3 \lesssim z \lesssim 3.0$. We defined several environments such as cluster core, outskirts, filament, and field as shown in Figure 1, and investigated the environmental dependence of properties of star-forming galaxies at $z = 1.46$.

The colour–magnitude diagram of $z' - K$ vs. K for the [OII] emitting galaxies shows that a significantly higher fraction of [OII] emitters with red $z' - K$ colours is seen in the cluster core than in other environments. It seems that the environment which hosts such red star-forming galaxies shifts from the core region at $z = 1.46$ to the outskirts of clusters at lower redshifts. The multi-colour analysis of the red emitters indicates that these galaxies are more like nearly passively evolving galaxies which host [OII] emitting AGNs, rather than dust-reddened star-forming [OII] emitters. We also find that the cluster has experienced high star formation activities at rates comparable to that in the field at $z = 1.46$ in contrast to lower redshift clusters, and that star formation activity in galaxy clusters on average increases with redshift up to $z = 1.46$. In addition, line ratios of [NII]/Hα and [OIII]/Hβ indicate that a mass–metallicity relation exists in the cluster at $z = 1.46$, which is similar to that of star-forming galaxies in the field at $z \sim 2$.

In summary, we have found that star formation activity of galaxies at $z = 1.46$ is not yet strongly dependent on environments, and that even the cluster core is experiencing high star forming activity comparable to those in other lower-density regions [4].

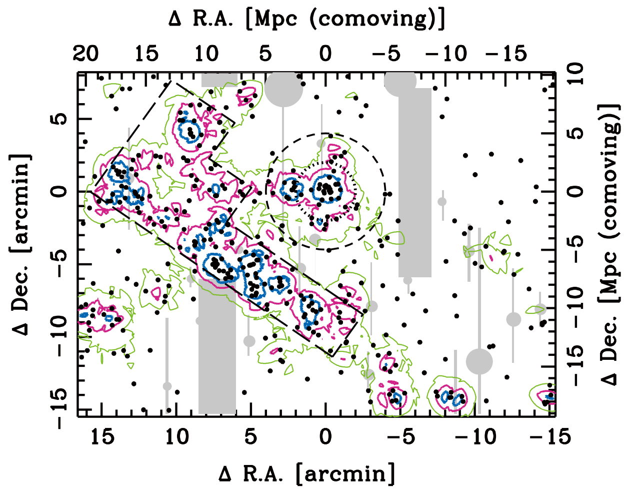

Figure 1: Distribution of 380 [OII] emitters at $z = 1.46$ in and around the cluster. North is up, and east is to the left. The axes show relative coordinates from the cluster centre. Black dots show the [OII] emitters. Cluster core, outskirts, and filament regions are defined by a dotted-line circle, broken-line circle, and long-dashed lines, respectively. The rest of the area is defined as the field. Blue, magenta and green contours show the local density of [OII] emitters.

References

[1] Dressler, A., et al.: 1997, *ApJ*, **490**, 577.
[2] Kodama, T., et al.: 2007, *MNRAS*, **377**, 1717.
[3] Stanford, S. A., et al.: 2006, *ApJ*, **646**, L13.
[4] Hayashi, M., et al.: 2011, *MNRAS*, **415**, 2670.

Practical Method to Derive Non-Linear Response Functions of Cameras for Scientific Imaging

HANAOKA, Yoichiro, SUZUKI, Isao, SAKURAI, Takashi
(NAOJ)

We developed a practical method to derive response functions which convert the amount of incident light to the A/D counts of cameras for scientific imaging [1]. Some cameras do show non-linear responses, and we have to know them to carry out photometric analysis with the data taken by such cameras. We applied this method for an InGaAs near-infrared camera, XEVA-CL-640 (XENICS), and succeeded to derive a response function, even though it was complicated non-linear one. In principle, such response functions can be derived from the output A/D counts, S, measured at various incident light levels, I, which are accurately controlled over the whole dynamic range. However, it is not easy to actually do such measurements with high accuracy. Then we developed a new practical method to derive non-linear response functions. In this method, we need a mechanism to accurately control the amount of incident light into cameras just within a limited dynamic range and at a limited number of steps (relative light level T, which may be exposure time, transparency, etc.). A variable brightness light source (brightness B), which supplies the incident light into cameras, is also necessary, but we do not need to know its accurate brightness.

Figure 1(a) shows the raw results measured under such conditions; output A/D values, S, are measured at several T's under various unknown B's (the brightness of the incident light, I, is written as $I = BT$). It seems that without knowing B's, it is difficult to derive the relation between I and S from the results shown in Figure 1(a). However, we can derive IdS/dI, because the relation $dI = BdT$ based on $I = BT$ brings $dS/dT = BdS/dI$, and this means $TdS/dT = TBdS/dI = IdS/dI$. The value TdS/dT can be derived from the known values, T and S, and therefore, without knowing B, we can derive a unique relation between T and $TdS/dT(= IdS/dI)$ as shown in Figure 1(b). The relation seen in Figure 1(b) can be converted to the relation between I and S through the numerical integration. Figure 1(c) shows the derived relation between I and S, namely the response function of the camera. Obviously the function is non-linear. Figure 1(d) shows a close-up of the low-light level portion of Figure 1(c), and we can find a complex non-linear behavior.

We are using a XEVA camera for the polarimetry of the infrared solar light, which requires high accuracy measurements. Compensation of the non-linearity based on the derived function works well, and we have quantitatively high-quality observational data.

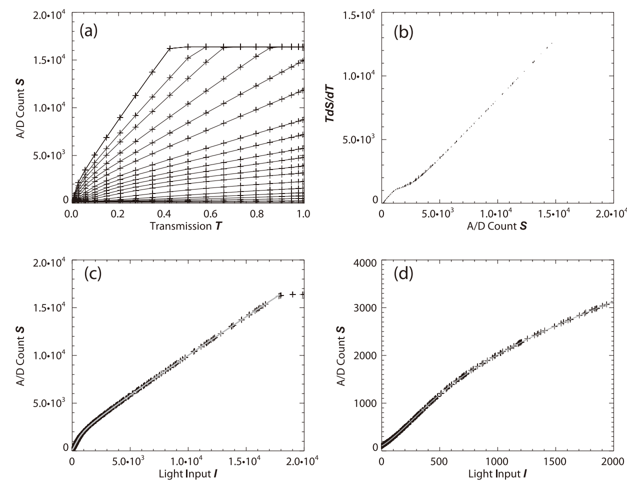

Figure 1: (a) Measured A/D counts S at various values T are shown with plus signs. Each line represents the measurements carried out under the same brightness B of the light source. (b) Relation between the measured A/D count, S, and the TdS/dT value. All the measured points are on a unique curve, regardless of the values of B. (c) Calculated non-linear response function between the amount of light input, I, and the output A/D count, S, is shown with a solid grey line. The measured points shown in Figure 1(a) are also plotted with plus signs. (d) Enlargement of the low-I range of panel (c).

Reference

[1] Hanaoka, Y., Suzuki, I., Sakurai, T.: 2011, *App. Opt.*, **50,** 2401-2407.

Substellar Objects in nearby Young Clusters (SONYC). IV. A Census of Very Low Mass Objects in NGC 1333

SCHOLZ, Alexander (Dublin Institute for Advanced Studies)
MUZIC, Koraljka (University of Toronto)
GEERS, Vincent C. (ETH Zurich)
BONAVITA, Mariangela (University of Toronto)
JAYAWARDHANA, Ray (University of Toronto / NAOJ)
TAMURA, Motohide (NAOJ)

SONYC (Substellar Objects in Nearby Young Clusters) is a program to investigate the frequency and properties of young substellar objects with masses down to a few times that of Jupiter [1]. Here we present a census of very low mass objects in the ~1 Myr old cluster NGC 1333. We analyze nearinfrared spectra taken with Fiber Multi-Object Spectrograph/ Subaru for 100 candidates from our deep, widefield survey and find 10 new likely brown dwarfs with spectral types of M6 or later. Among them, there are three with later than M9 and one with early L spectral type, corresponding to masses of 0.006 to 0.02 $M_\odot$, so far the lowest mass objects identified in this cluster.

The combination of survey depth, spatial coverage, and extensive spectroscopic follow-up makes NGC 1333 one of the most comprehensively surveyed clusters for substellar objects. In total, there are now 51 objects with spectral type M5 or later and/or effective temperature of 3200 K or cooler identified in NGC 1333; 30–40 of them are likely to be substellar. NGC 1333 harbors about half as many brown dwarfs as stars, which is significantly more than in other well-studied star-forming regions (Fig. 1), thus raising the possibility of environmental differences in the formation of substellar objects. The brown dwarfs in NGC 1333 are spatially strongly clustered within a radius of less than 1 pc (Fig. 2), mirroring the distribution of the stars. The disk fraction in the substellar regime is 66 %, lower than for the total population (83 %) but comparable to the brown dwarf disk fraction in other 2–3 Myr old regions [2].

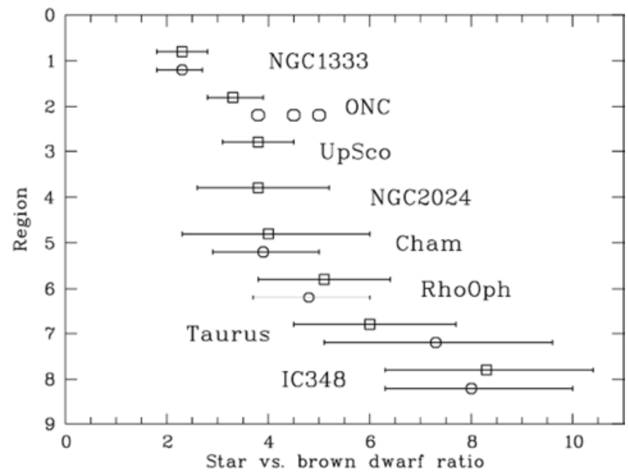

Figure 1: Star vs. brown dwarf ratios for various starforming regions. Squares are values with 0.08–1.0 $M_\odot$ as stellar and 0.03–0.08 $M_\odot$ as brown dwarfs, while circles are 0.08 –10 $M_\odot$ as stellar and 0.02–0.08 $M_\odot$ as brown dwarfs.

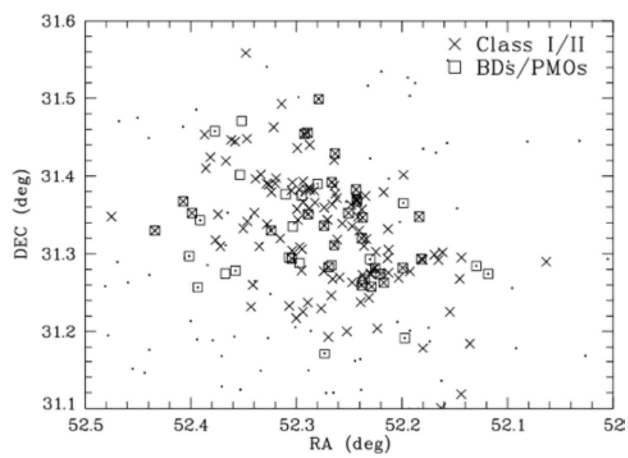

Figure 2: Spatial distribution of NGC 1333 members. Crosses are all 137 objects with Spitzer excess and squares are all confirmed brown dwarfs. Objects with spectroscopy for which we can exclude that they are substellar members are shown with dots.

References

[1] Tamura, M., et al.: 1998, *Science*, **282**, 1095.
[2] Scholz, A., et al.: 2012, *ApJ*, **744**, 6.

Star Formation Activity in the Galactic HII Complex S255-S257

OJHA, D. K.[1], SAMAL, M. R.[2], PANDEY, A. K.[2], BHATT, B. C.[3], GHOSH, S. K.[1], SHARMA, S.[2]
TAMURA, M.[4], MOHAN, V.[5], ZINCHENKO, I.[6]

1: Tata Institute of Fundamental Research, India, 2: Aryabhatta Research Institute, India, 3: Indian Institute of Astrophysics, 4: NAOJ, 5: Inter-University Centre for Astronomy and Astrophysics, India, 6: Russian Academy of Sciences

We present results on the star formation activity of an optically obscured region containing an embedded cluster (S255-IR) and molecular gas between two evolved HII regions, S255 and S257. We have studied the complex using optical and near-infrared (NIR) imaging, optical spectroscopy, and radio continuum mapping at 15 GHz, along with Spitzer-IRAC results. We found that the main exciting sources of the evolved HII regions S255 and S257 and the compact HII regions associated with S255-IR are of O9.5−B3 V nature, consistent with previous observations. Our NIR observations reveal 109 likely young stellar object (YSO) candidates in an area of about 4.9 arcmin × 4.9 arcmin centered on S255-IR, which include 69 new YSO candidates (see Fig. 1). To see the global star formation, we constructed the V-I/V diagram for 51 optically identified IRAC YSOs in an area of about 13 arcmin × 13 armin centered on S255-IR. We suggest that these YSOs have an approximate age between 0.1 and 4 Myr, indicating a non-coeval star formation. Using spectral energy distribution models, we constrained physical properties and evolutionary status of 31 and 16 YSO candidates outside and inside the gas ridge, respectively. The models suggest that the sources associated with the gas ridge are younger (mean age about 1.2 Myr) than the sources outside the gas ridge (mean age about 2.5 Myr). The positions of the young sources inside the gas ridge at the interface of the HII regions S255 and S257 favor a site of induced star formation (Fig. 2) [1].

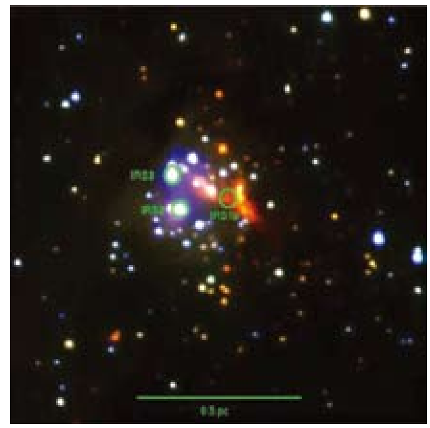

Figure 1: JHKs color-composite image of the S255-IR SFR (J, blue; H, green; and Ks, red). Only the central 1.5 arcmin × 1.5 arcmin is shown here. The ionizing sources of the compact and UC HII regions S255-2a, S255-2b, and S255-2c (marked with circles) are labeled IRS3, IRS2, and IRS1b, respectively. North is up and east is to the left.

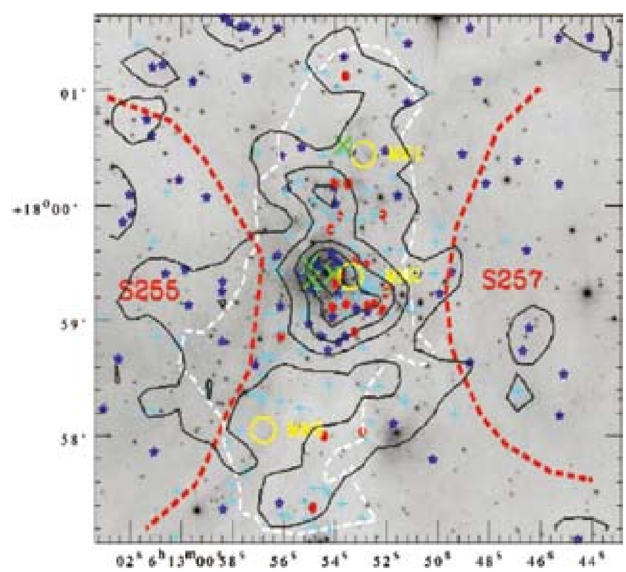

Figure 2: Spatial distributions of YSOs identified using the NIR CC diagram (asterisks), sources detected only in the H and Ks bands (filled circles), and sources detected only in the Ks band (plus symbols), overlaid on Ks-band image. The white dashed line shows the outer periphery of the dust continuum emission at 870 μm. The yellow circles are the positions of 1.2 mm continuum cores in the gas ridge. The red dashed lines are the demarcation of the outer boundaries of the S255 and S257. The large crosses represent the positions of the radio continuum sources. The YSO density contours are shown by black lines.

Reference

[1] Ojha, D. K., et al.: 2011, *ApJ*, **738**, 156.

Scaling Law of Relativistic Sweet-Parker Type Magnetic Reconnection

TAKAHASHI, Hiroyuki, KUDOH, Takahiro (NAOJ)
MASADA, Youhei (Kobe University)
MATSUMOTO, Jin (Kyoto University)

Magnetic reconnection is one of the most important subjects in the studies of space, laboratory, and astrophysical plasmas. It plays an essential role in the understanding of energy conversion processes in high energy plasmas that characterize astrophysical compact objects.

While issues concerning the physical mechanisms and properties of magnetic reconnection remain unsettled in the relativistic regime, a few theoretical studies of relativistic effects have been made. Lyutikov & Uzdensky studied relativistic Sweet.Parker type reconnection within the framework of magnetohydrodynamics (MHD). They found that the reconnection-driven outflow can have an ultra-relativistic speed (Lorentz factor $\gamma \gg 1$) when the magnetic energy is preferentially converted to kinetic energy [1]. They concluded that the reconnection rate would be enhanced in the relativistic regime due to Lorentz contraction. In contrast, Lyubarsky concluded that the outflow cannot be accelerated to a relativistic speed ($\gamma \simeq 1$) because the magnetic energy should be converted into thermal energy [2]. The effect of the Lorentz contraction is then negligible and the reconnection rate would not be enhanced.

We performed the two-dimensional Relativistic Resistive Magnetohydrodynamic (R2MHD) simulations to determine the energy conversion rate of the Sweet-Parker type magnetic reconnection in the relativistic regime [3]. Figure 1 shows the numerical results of the R2MHD simulations. At the initial state, we give a small perturbation around the origin. Then, the magnetic field lines start to reconnect around the origin. The plasma inflowing in to the current sheet is evacuated in the ± y-direction (formation of the reconnection outflow). We can see that the plasma is heated up inside the current sheet. The magnetic energy is liberated in the diffusion region by the Ohmic dissipation. Most of the magnetic energy is converted not into the kinetic, but into the thermal energy. Then, the enhancement of the thermal energy density, which is larger than the rest mass energy density, contributes to the plasma inertia due to the relativistic effects. The increase in the plasma inertia leads to the slow outflow (Lorentz factor $\simeq 1$). This indicates the relativistic effects such as the Lorentz contraction on the energy conversion rate cannot be expected.

Next, we evaluate the reconnection rate $\mathcal{R}$, which characterizes the energy conversion rate. We confirmed that the reconnection rate relates with the magnetic Reynolds number $R_M = 4\pi L v_A / \eta$, where L, v_A, and η are the length of the current sheet, Alfvén velocity and electric resistivity, respectively. The reconnection rate in the relativistic reconnection is well fitted by $\mathcal{R} = R_M^{-0.5}$ as well as that in the non-relativistic plasma. Also we found that the reconnection rate is almost independent of the initial magnetic field strength. Thus, we conclude that the Sweet-Parker type magnetic reconnection is the slow process for the energy conversion not only in the nonrelativistic regime but also in the relativistic regime.

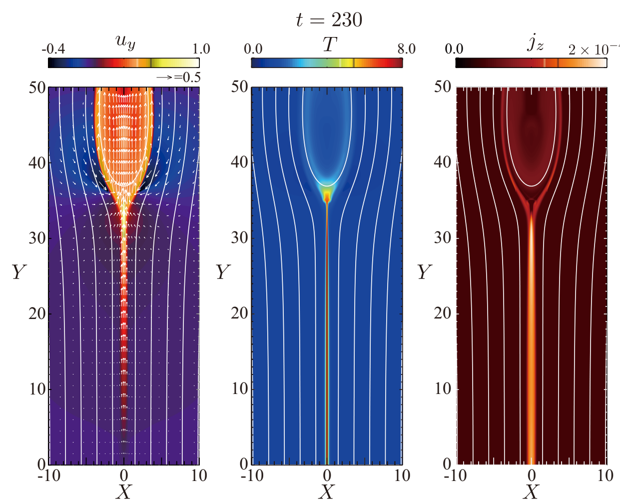

Figure 1: Numerical results of R2MHD simulations. Color shows the outflow (y-direction) four velocity, gas temperature, and the current density from left to right, respectively. Curves and arrows denote for the magnetic field lines and the velocity fields.

References

[1] Lyubarsky, Y. E.: 2005, *MNRAS*, **358**, 113.
[2] Lyutikov, M., Uzdensky, D.: 2003, *ApJ*, **589**, 893.
[3] Takahashi, H. R., Kudoh, T., Masada, Y., Matsumoto, J.: 2011, *ApJ*, **739**, L53.

Size Distribution of Main-Belt Asteroids with High Inclination

TERAI, Tsuyoshi (NAOJ)
ITOH, Yoichi (University of Hyogo)

Asteroids in the main-belt region between the Mars and Jupiter orbits have been fractions of the remnant planetesimals. Main-belt asteroids (MBAs) undergo collisions and disruption with each other. Their size distribution is primary determined by the impact strength (critical specic energy per unit mass required to catastrophically disrupt the target) [1]. The impact strength increases with size, and the degree of the increase affects a slope of the size distribution in the size of observable asteroids (larger than sub km).

In the early Solar system, MBAs' orbital eccentricities and inclinations are pumped up via dynamical excitation due to the planetary perturbation [2]. They cause higher relative velocities than the present. It has been indicated that the size-impact strength relation depends on impact velocity [3]. MBAs possibly have a different collisional evolution under collisions with impact velocities much higher than the present mean value (~4 km sec^{-1}).

We investigate the size distribution of high-inclination MBAs which collide with an asteroid at high velocity (~10 km sec^{-1}). The size distribution of small MBAs around 1 km in diameter with high inclination remains unknown. We performed a wide-field observation for them using Subaru telescope with Suprime-Cam on high ecliptic latitude region of $\beta \sim +25°$. The archival data of Suprime-Cam was also used. We obtained the dataset of 9.0 square-degree in total.

As the result of data reduction for moving objects, more than 600 candidates of MBAs were detected. Using the sample of uniform detection probability, the cumulative size distributions (CSDs) are measured from the two groups: one includes asteroids with inclination lower than 15° and the other includes asteroids higher than 15°. We found that the latter has a shallower CSD. Furthermore, we provided continuous CSD from 0.7 km to 50 km in diameter using the Asteroid Orbital Elements Database (ASTORB) and Sloan Digital Sky Survey Moving Object Catalog (SDSS MOC). CSD is generally written as a power-law of $N(>D) \propto D^{-b}$, where D is diameter. The obtained CSDs show $b = 1.79 \pm 0.05$ for the low-inclination sample and $b = 1.62 \pm 0.07$ for the high-inclination sample. We conrmed that CSD of high-inclination MBAs has a shallower slope than that of low-inclination MBAs [4].

This result indicates the fact that large asteroids is more resistant to destruction under hypervelocity collisions. Massive bodies could have been more dominant in the main belt region during the dynamical excitation phase at the early Solar system.

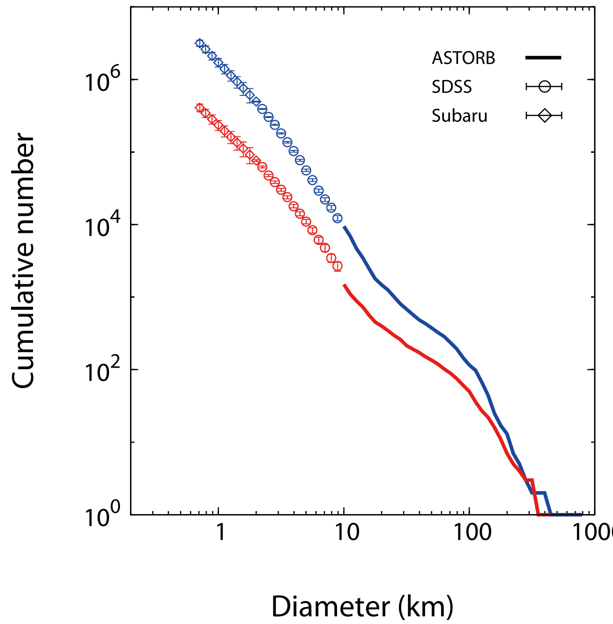

Figure 1: Cumulative size distributions of main-belt asteroid populations with inclination lower than 15° (blue) and higher than 15° (red) using the data from Asteroid Orbital Elements Database (solid lines), Sloan Digital Sky Survey Moving Object Catalog (open circles), and this study (diamonds).

References

[1] O'Brien, D. P., Greenberg, R.: 2003, *Icarus*, **164**, 334.
[2] Bottke, W. F., et al.: 2005, *Icarus*, **179**, 63.
[3] Jutzi, M., Michel, P., Benz, W., Richardson, D. C.: 2010, *Icarus*, **207**, 54.
[4] Terai, T., Itoh, Y.: 2011, *PASJ*, **63**, 335.

Orion IRc2, Radiated by the Scattering of Emission from Source I

OKUMURA, Shin-ichiro (Japan Spaceguard Association)
YAMASHITA, Takuya (NAOJ)
SAKO, Shigeyuki, MIYATA, Takashi (University of Tokyo)
HONDA, Mitsuhiko (Kanagawa University)
KATAZA, Hirokazu (JAXA/ISAS)
OKAMOTO, Yoshiko K. (Ibaraki University)

After the discovery of BN and KL in the Orion Molec- ular Cloud, following infrared observations revealed that the KL nebula splits up into a number of compact “IRc” sources. The most luminous of these, IRc2, was thought to be the dominant energy source for the KL complex. Then, radio continuum point source “I” was found at 1″ south of IRc2 [1,2], and many radio observations have showed evidence of the existence of a young stellar object (YSO) embedded in source I. However, the infrared counterpart of source I have not detected at any wavelength, and the relationship of source I to IRc2 also still remains ambiguous. A direct linkage between IRc2 and source I was revealed with a detailed analysis of the SUBARU/COMICS mid-infrared data [3]. It also shows what IRc2 really is.

Figure 1 shows the mid-infrared images of the BN/KL region obtained with COMICS. The 9.7m optical depth and the 7.8 μm/12.4 μm color temperature distribution are presented in Figure 2. For IRc2, a morphological correlation is seen between the near-infrared image [4] and the optical depth distribution, and the optical depth peak roughly coincides with the 3.8 μm peak position, IRc2-A [4]. The color temperature peak coincides with the position of source I, and no dominant temperature peak is seen at IRc2.

The spectral energy distribution (SED) of IRc2 can be reproduced by a two-temperature model; a 400 K component and a 150 K component. It resembles the SED of a YSO, BN. However, it is plausible that no dominant energy source is embedded because there is no temperature peak in IRc2. It is surprising that the shorter wavelength emission exhibits its intensity peak at the local absorption peak position, when the 3.8 μm emission arises from self-luminous objects embedded in IRc2-A. In addition, considering the polarimetric results [4], the near-infrared emission from IRc2 is most likely to be scattered radiation. Whereas, the distribution of the 400K component resembles with that of near-infrared emission, and the mid-infrared polarimetric study of IRc2 shows the possibility of the mid-infrared emission to be scattered [5]. Therefore, the mid-infrared 400 K component emission from IRc2 is due to the same source with near-infrared emission. The near-infrared emission from IRc2 is reproduced by the scattering of radiation from source I, and so is the mid-infrared emission.

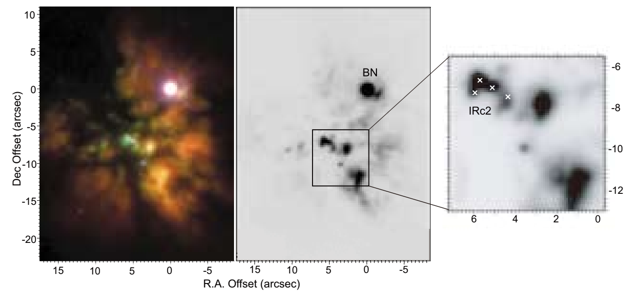

Figure 1: Mid-infrared images of the BN/KL region. Three-color composite image (8.7 μm(blue), 12.4 μm(green), 18.5 μm (red)) (left), 12.4 μm image (center), and the close-up around IRc2 (right). Coordinates are centered on the BN. Crosses show the positions of the 3.8 μm peaks [4].

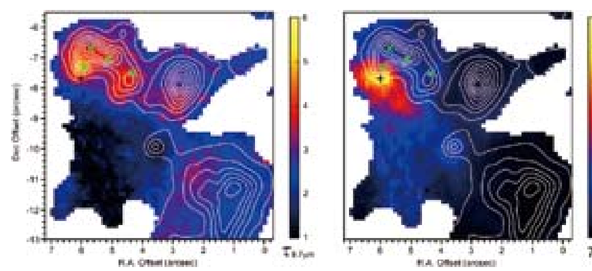

Figure 2: 9.7 μm color-coded optical depth image (left) and the 7.8 μm/12.4 μm color temperature distribution image (right) of the 7.5″ × 7.5″ field around IRc2. The overlaid contour shows the 12.4 μm surface brightness. Crosses show the positions of the 3.8 μm peaks [4], and a plus shows the position of source I.

References

[1] Garay, G., Moran, J. M., Reid, M. J.: 1987, *ApJ*, **314**, 535.
[2] Churchwell, E., et al.: 1987, *ApJ*, **321**, 516.
[3] Okumura, S., et al.: 2011, *PASJ*, **63**, 823.
[4] Dougados, C., et al.: 1993, *ApJ*, **406**, 112.
[5] Smith, C. H., et al.: 2000, *MNRAS*, **312**, 327.

Properties of Weak Measurements through Exact Evaluations

NAKAMURA, Kouji (NAOJ)
NISHIZAWA, Atsushi (Kyoto University)
FUJIMOTO, Masa-Katsu (NAOJ)

Current gravitational wave (GW) detectors have "standard quantum limit" (SQL) due to the uncertainty in quantum mechanics and GW detectors in near future needs to beat this SQL. So, quantum non-demolition measurements are researched in the GW research community and some techniques have been proposed to beat SQL. On the other hand, in quantum information, "quantum measurement theory" is developing and its experiments are carried out. Unfortunately, this development has been almost independent of GW researches. For this reason, we have been exploring applicabilities of techniques in quantum information to GW detectors.

We focused on the "weak measurement" (WM) proposed by Aharonov et al. [1] in 1988. Many experiments of WM are recently carried out and their properties look similar to current GW detectors. Then, we expect that WMs are applicable to GW detectors.

In the usual "measurement" in quantum mechanics, we treat two quantum systems which are called "system" (S) and "detector" (D). We want to measure the observable $\mathbf{A}$ associated with S and D measures $\mathbf{A}$ interacting with S. As a model of D, an one-dimensional quantum system is considered, whose canonical variables are (q, p) ($[q, p] = i$, $\hbar = 1$), and the initial state of D is assumed to be zero-mean Gaussian. The interaction is given by $H = g\delta(t - t_0)p\mathbf{A}$. The state of S before the measurement is $|S_i\rangle = \sum_k \alpha_k|a_k\rangle$, where $\{|a_k\rangle\}$ are eigenstates of $\mathbf{A}$ with eigenvalues $\{a_k\}$. After the interaction at $t = t_0$, the total system is entangled. The measurement outcome of q in D of this state becomes ga_k with the probability $|a_k|^2$. If we know the coupling constant g and if we perform this measurement for many ensemble, we obtain the expectation value $\langle S_i|\mathbf{A}|S_i\rangle$.

On the other hand, in WM, after the interaction between S and D, we concentrate only on the subensemble in which the final state S is $|S_f\rangle$. Then, the expectation value of q in D becomes $g\mathrm{Re}A_w$ within the accuracy of $O(g)$. Here, A_w is called "weak value" defined by $A_w := \langle S_f|\mathbf{A}|S_i\rangle/\langle S_f|S_i\rangle$. From this definition, when $\langle S_f|S_i\rangle \sim 0$, A_w may become large. This result is within $O(g)$ and it implies that the interaction between S and D should be sufficiently weak and g should be small enough. In other words, when we want to measure this small g, it can be measured as an amplified value $g\mathrm{Re}A_w$. This is called the "weak value amplification" (WVA). Aharonov et al. applied this WVA to the sequence of Stern-Gerlach experiments. They claimed that the neutron spin can be measured as 100.

We re-examined the scenario of WMs and concentrated only on the case of measurements of $\mathbf{A}$ with the property $\mathbf{A}^2 = 1$. This property is satisfied in many experimental setups including GW detectors. Then, we have derived the exact expectation value of q of D after the WM as

$$\frac{\langle q\rangle'}{g} = \frac{\mathrm{Re}\langle\mathbf{A}\rangle_w}{1 + \frac{1}{2}\left(1 - |\langle\mathbf{A}\rangle_w|^2\right)(e^{-s} - 1)} \qquad (1)$$

through the all-order evaluation of g [2]. Here, $s := 2g^2\langle p^2\rangle$ is the measurement strength and $\langle p^2\rangle$ is the initial variance of p in D. According to Eq. (1), for a fixed s, there is an optimal overlap $\langle S_f|S_i\rangle$ in which the amplification of the outcome is maximal. The application of Eq. (1) to the sequence of Stern-Gerlach experiments proposed by Aharonov et al. is depicted in Fig. 1.

A recent experiment suggests that Eq. (1) is also experimentally correct [3]. Based on the understanding of WMs which we have obtained, we are now discussing the applicability of WMs to GW detectors.

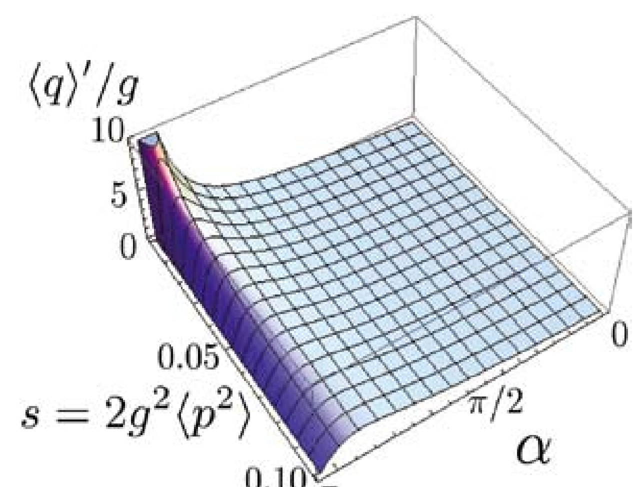

Figure 1: The application of Eq. (1) to the experiments proposed by Aharonov et al. $\alpha \to \pi$ corresponds to $\langle S_f|S_i\rangle \to 0$.

References

[1] Aharonov, Y., Albert, D. Z., Vaidman, L.: 1988, *Phys. Rev. Lett.*, **60**, 1351.
[2] Nakamura, K., Nishizawa, A., Fujimoto, M.-K.: 2012, *Phys. Rev. A*, **85**, 012113.
[3] Iinuma, M., et al.: 2011, *New J. Phys.*, **13**, 033041.

Efficient Parallel Computation of All-Pairs *N*-body Acceleration by Do Loop Folding

FUKUSHIMA, Toshio
(NAOJ)

In the Newtonian celestial mechanics, the all-pairs Nbody acceleration vectors are expressed in the form of double summation as $\mathbf{a}_j = \sum_{k=1,k\neq j}^{N} \mathbf{a}_{jk}$ where the index j runs $1 \leq j \leq N$. In the ordinary serial computation, the anti-symmetric nature of the mutual accelerations, $\mu_j \mathbf{a}_{jk} + \mu_k \mathbf{a}_{kj} = 0$, is used to halve the total computational amount from $N(N-1)$ to $N(N-1)/2$.

In the parallel computation, however, this property is not always utilized. This means that the total amount of computation is almost doubled. Indeed Figure 1 shows that the speed-up factor of the simple parallelization for various PCs suffers this defects.

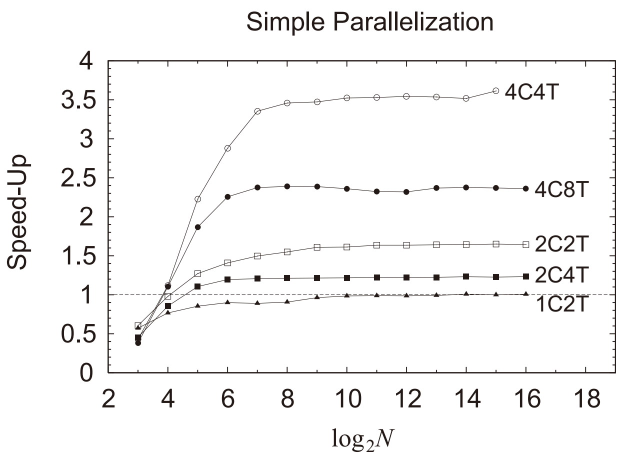

Figure 1: Size Dependence of Speed-Up Factor: Simple Parallelization.

In fact, the observed value is 1.0 for a single-core two-thread processor (1C2T), 1.7 for a dual-core twothread processor (2C2T), 1.2 for a dual-core four-thread processor (2C4T), 3.5 a quad-core four-thread processor (4C4T), and 2.4 for a quad-core 8-thread processor (4C8T), respectively. Meanwhile the ideal value is 1.0 for 1C2T, 2.0 for 2C2T and 2C4T, and 4.0 for 4C4T and 4C8T, respectively. In order to overcome this situation, we apply the idea of folding the outer do loop [1] to the computation of *N*-body acceleration [2].

Consider a do loop of the form

```
do j=1,L {task(j)}
```

where we assume that the task inside the loop is another do loop the length of which is linearly changing with the outer loop index as

```
do k=j+1,L {subtask(j,k)}
```

where the sub task is of an equal computational amount independently on the indices.

Then, we transform this double do loop such that the inner loops contain an equally balanced load as

```
do j=1,(L+1)/2 {task(j);
  if(L+1-j!=j){task(L+1-j)}}
```

As a result, we mostly recover the speed loss in the simple parallel computation of the all-pairs Newtonian *N*-body acceleration vectors as shown in Fig. 2.

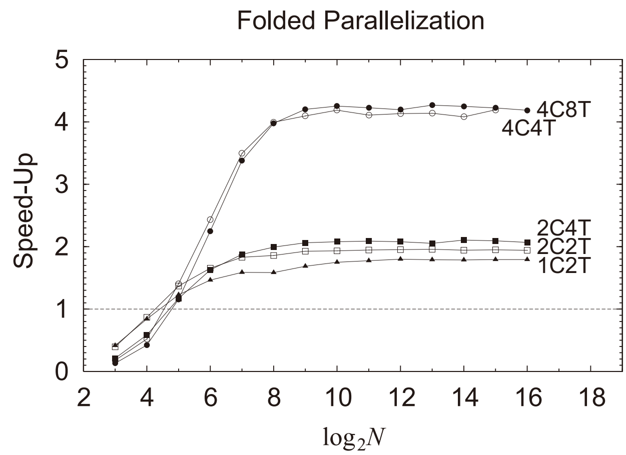

Figure 2: Size Dependence of Speed-Up Factor: Folded Parallelization.

At a consumer PC with a quad-core 8-thread processor for sufficiently large number of *N*, the new program achieves an acceleration factor of 4.5 in the single, 4.2 in the double, and 4.9 in the quadruple precision environments, respectively. This is an interesting result if considering that 4 is the theoretical value for a quad-core processor. We consider that this is due to Intel's Hyper-Threading Technology, which tries to utilize all available computational resource. In general, the present formulation will be applicable to many other computational problems.

References

[1] Ito, T., Fukushima, T.: 1997, *AJ*, **114**, 1260.
[2] Fukushima, T.: 2011, *AJ*, **142**, 18.

Detection of Proper Motion of the Sub-Parsec-Scale Jet in 3C 66B

SUDOU, Hiroshi (Gifu University)
IGUCHI, Satoru (NAOJ)

3C 66B, a giant elliptical galaxy with a redshift (z) of 0.0213, is known as an FR I radio galaxy and it has a prominent core–jet structure that extend to about 100 kpc. High-resolution imaging using very long baseline interferometry (VLBI) at 5 GHz has revealed the presence of a faint counterjet within a distance of 2 mas from the core [1]. The intensity ratio between the jet and counterjet was estimated to be approximately 10, indicating possible acceleration of the jet outflow on a sub-parsec scale. In order to search for motion of the inner jet, we carried out multi-epoch imaging of 3C 66B using VLBA [2].

From images of 3C 66B at 8.4 GHz, we found three knots at 0.7, 1.5, and 2.5 mas (0.3, 0.7, and 1.1 pc) from the core (Fig. 1). Using weighted least-squares fitting, we estimated the proper motion of the inner three knots during 1.3 years to be 0.21±0.03, 0.36±0.04, and 0.63±0.18 mas year^{-1}, which corresponds to β_{app}= 0.30±0.04, 0.49±0.06, and 0.87±0.24 (Fig. 2).

3C 66B showed that the apparent jet speed increases with a distance from the core within 3 mas (1.3 pc). This result is consistent with the fact that the sub-parsec scale counterjet was found within a distance of 2 mas from the core.

According to the relativistic beaming model, assuming that the jet accelerates with a constant viewing angle of 4.9 degrees [3], the jet speed accelerates from 0.78 c to 0.91 c, corresponding to the bulk Lorentz factor Γ from 1.60 to 2.46. Assuming the other interpretation, that is, a change in the viewing angle with a constant jet velocity of 0.78 c [3], the angle varies from 4.9 to 16.2 degrees. To reveal the kinematics and geometry of the jet in 3C 66B, further monitoring with higher dynamic-range is required over a longer period at 8.4 GHz or higher.

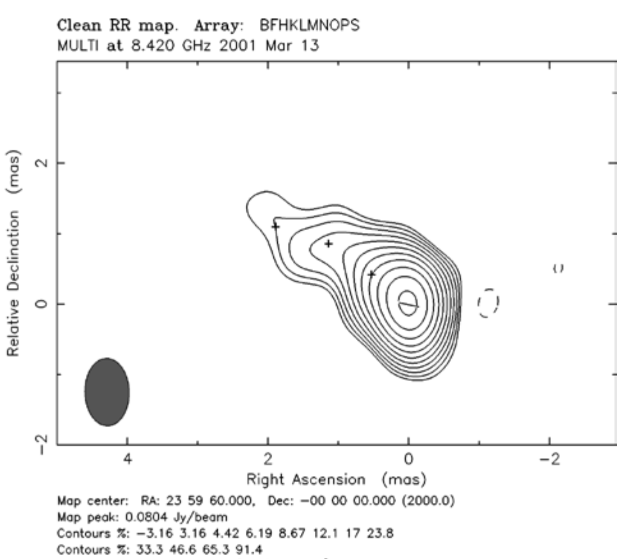

Figure 1: An 8.4 GHz image of 3C 66B observed at 2001.20. Contours are drawn at 3-σ × (1, $\sqrt{2}$, 2, 2$\sqrt{2}$, ...), the 3-σ level in this image is 0.8 mJy beam^{-1}. The synthesized beam is shown at the bottom-left of the image. The cross marks indicate the fitted position of knots using delta functionin. The Gaussian component of the core position is also shown.

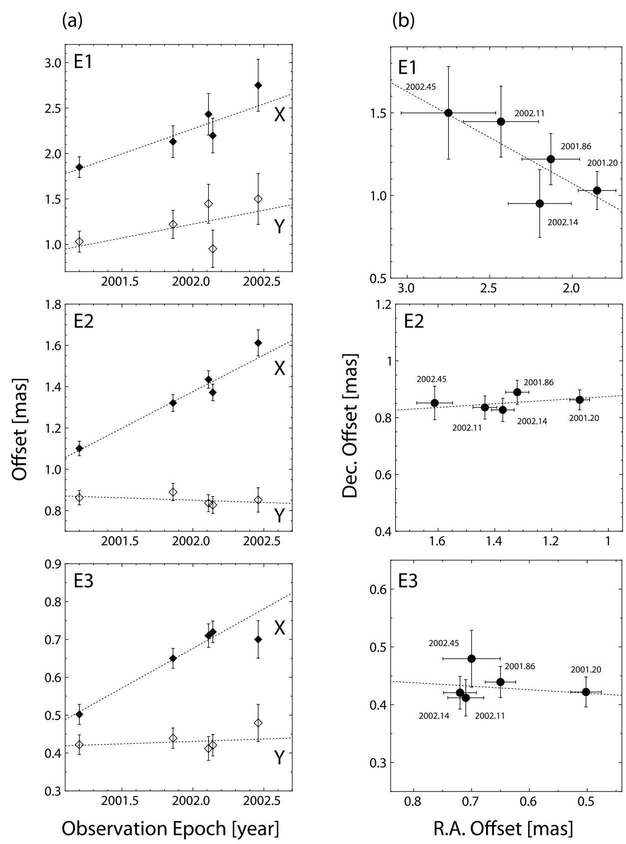

Figure 2: Linear fitting of the relative position shift of the three knots (E1, E2, and E3) at 8.4 GHz. (a) time evolution and (b) spatial distribution. A filled lozenge means the R.A. direction (X), and an open lozenge means the Dec. direction (Y). Dotted lines indicate the best fit.

References

[1] Giovannini, G., et al.: 2001, *ApJ*, **552**, 508.
[2] Sudou, H., Iguchi, S.: 2011, *AJ*, **142**, 49.
[3] Iguchi, S., Okuda, T., Sudou, H.: 2010, *ApJ*, **724**, L166.

The Millimeter Sky Transparency Imager (MiSTI)

TAMURA, Yoichi*, KOHNO, Kotaro, FUKUHARA, Masayuki, KUBOI, Akihito
(University of Tokyo)

KAWABE, Ryohei, EZAWA, Hajime, KAMAZAKI, Takeshi, OKADA, Norio
(NAOJ)

MOMOSE, Munetake, NAKAGAWA, Yuki
(Ibaraki University)

SEKIGUCHI, Tomohiko
(Hokkaido University of Education)

VILA-VILARÓ, Baltasar
(Joint ALMA Observatory)

The Millimeter Sky Transparency Imager (*MiSTI*) [1] is a small millimeter-wave scanning telescope with a 25-cm diameter dish operating at 183 GHz (Figure 1). MiSTI is installed at the ASTE site, Atacama, Chile, and it measures emission from atmospheric water vapor and its fluctuations to estimate atmospheric absorption in the millimeter to submillimeter. MiSTI observes the water vapor distribution at a spatial resolution of 0.5°, and it is sensitive enough to detect an excess path length of ≥ 0.05 mm for an integration time of 1 s. By comparing the MiSTI measurements with those by a 220 GHz tipper, we validate that the 183 GHz measurements of MiSTI are correct, down to the level of any residual systematic errors in the 220 GHz measurements.

Since 2008, MiSTI has provided real-time (every 1 hr) monitoring of the all-sky opacity distribution (Figure 2) and atmospheric transmission curves in the (sub)millimeter through the internet, allowing to know the (sub)millimeter sky conditions in Atacama.

The 183 GHz monitor is available at
http://www2.nao.ac.jp/~misti/opacity.html.

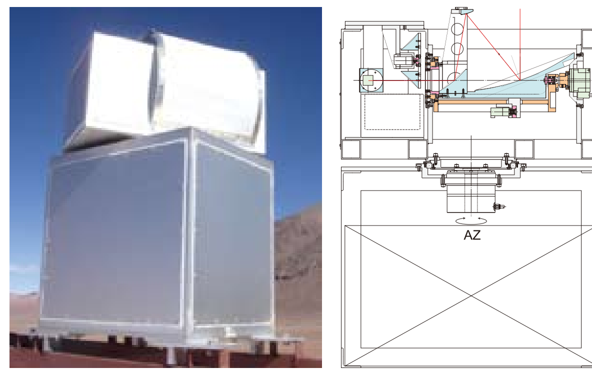

Figure 1: (*left*) A picture of the Millimeter Sky Transparent Imager (MiSTI) installed at the ASTE site. (*right*) Schematic drawing of MiSTI. The membrane and its support structures are not shown. The positions of the azimuth and elevation axes are noted by “AZ” and “EL”, respectively.

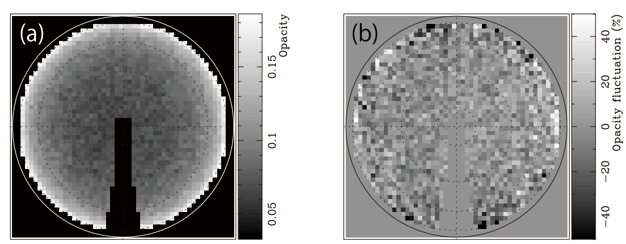

Figure 2: An example of the all-sky opacity image taken with MiSTI on 2010 July 1. (a) All-sky opacity map at 183 GHz in the fish-eye lens view. The sky hemisphere is orthographically projected to the plane of the paper. The north is top and the east is left. The solid and dotted circles indicate the horizon (El = 0°), El = 20, 40, 60, and 80°. (b) The fluctuations of the all-sky opacity map, $\delta\tau$ (Az, El).

Reference

[1] Tamura, Y., Kawabe, R., Kohno, K., et al.: 2011, *PASJ*, **63**, 347.

* The author is at NAOJ when the paper [1] was submitted.

SDSS J1334+3315: A Resolved Lensed Quasar with Separation 0″.8

RUSU, Cristian E.[1], OGURI, Masamune[2,3], INADA, Naohisa[4], KAYO, Issha[5], IYE, Masanori[1,3,6]
HAYANO, Yutaka[3], OYA, Shin[3], HATTORI, Masayuki[3], SAITO, Yoshihiko[7], ITO, Meguru[8], MINOWA, Yosuke[3]
PYO, Tae-Soo[3], TERADA, Hiroshi[3], TAKAMI, Hideki[3], WATANABE, Makoto[9]

1: University of Tokyo, 2: IPMU, 3: NAOJ, 4: Nara National College of Technology, 5: Toho University, 6: The Graduate University for Advanced Studies, 7: Tokyo Institute of Technology, 8: Victoria University, 9: Hokkaido University

We have observed the newly discovered SDSS Quasar Lens Search (SQLS) [1,2,3,4,5,6] gravitationally lensed quasar candidate pair SDSS J1334+3315 in the J, H and K' bands, using the Subaru Telescope adaptive optics system with laser guide star (LGSAO188) [7,8]. The quasar pair has a redshift of $z = 2.426$, and a separation of 0″.833. We were successful in achieving a clear detection of the lensing galaxy located in between the two quasars, thus proving that this is one gravitationally lensed quasar. In Figure 1, we show the improvement obtained in resolution due to the use of AO. We estimate the redshift of the lensing galaxy to be 0.557 based on absorption lines in the quasar spectra as well as the color of the galaxy. Our gravitational lens mass modeling with improved astrometry implies that a nearby bright galaxy ~4″ apart from the lensing galaxy is likely to affect the lens potential (Figure 2). The bright nearby galaxy is clearly revealed to be a spiral in the LGSAO188 observations.

This is the first in a campaign of Subaru Telescope adaptive optics observations of the SQLS lensed quasars, and demonstrates the usefulness of the LGSAO188 imaging for studying small-separation strong lens systems.

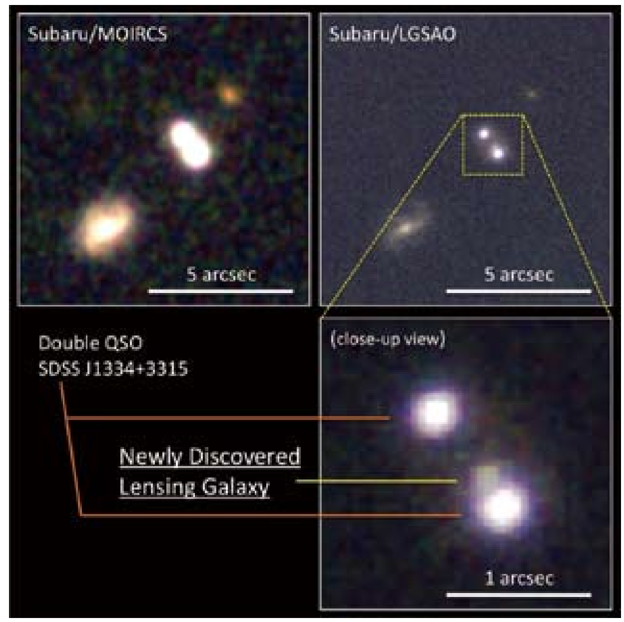

Figure 1: J, H, K' band SDSS J1334+3315 imaged without (upper left) and with adaptive optics (upper right). The lower panel, enlarged five times, shows for the first time the resolved lensing galaxy located in between the two quasar images.

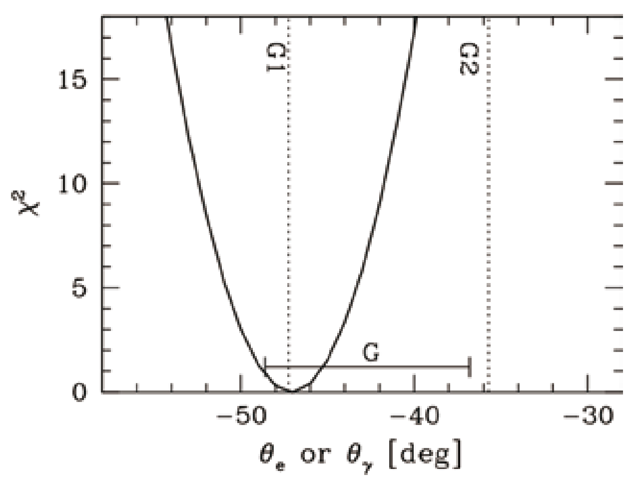

Figure 2: Best-fit χ^2 for the mass model, as a function of the position angle of the singular isothermal sphere with shear (SIS+γ) model (or alternatively, singular isothermal ellipsoid). The horizontal line indicates the 1σ range of the measured position angle of the lensing galaxy G. The vertical dotted lines show directions of the external shear corresponding to the location of nearby galaxies G1 (the bright spiral) and G2, strongly suggesting the influence of G1.

References

[1] Oguri, M., et al.: 2006, *AJ*, **132**, 999.
[2] Oguri, M., et al.: 2008, *AJ*, **135**, 512.
[3] Oguri, M., et al.: 2012, *AJ*, **143**, 120.
[4] Inada, M., et al.: 2008, *AJ*, **135**, 496.
[5] Inada, M., et al.: 2010, *AJ*, **140**, 403.
[6] Inada, M., et al.: 2012, *AJ*, **143**, 119.
[7] Hayano, Y., et al.: 2010, *SPIE*, **7736**, 21.
[8] Minowa, Y., et al.: 2010, *SPIE*, **7736**, 122.

Completing the Census of Lyα Emitters at the Reionization Epoch

KASHIKAWA, Nobunari[1,2], SHIMASAKU, Kazuhiro[3], MATSUDA, Yuichi[4], EGAMI, Eiichi[5], JIANG, Linhua[5]
NAGAO, Tohru[6], OUCHI, Masami[7], MALKAN, Matthew A.[8], HATTORI, Takashi[1], OTA, Kazuaki[7]
TANIGUCHI, Yoshiaki[6], OKAMURA, Sadanori[3], LY, Chun[9], IYE, Masanori[1], FURUSAWA, Hisanori[1]
SHIOYA, Yasuhiro[6], SHIBUYA, Takatoshi[2], ISHIZAKI, Yoshifumi[2], TOSHIKAWA, Jun[2]

1: NAOJ, 2: The Graduate University for Advanced Studies, 3: University of Tokyo, 4: Durham University, 5: University of Arizona, 6: Ehime University, 7: ICRR, Tokyo University, 8: University of Calfornia, 9: STScI

We carried out extended spectroscopic confirmations of Lyα emitters (LAEs) at z = 6.5 and 5.7 in the Subaru Deep Field. Now, the total number of spectroscopically confirmed LAEs is 45 and 54 at z = 6.5 and 5.7, respectively, and at least 81 % (70 %) of our photometric candidates at z = 6.5 (5.7) have been spectroscopically identified as real LAEs. We made careful measurements of the Lyα luminosity, both photometrically and spectroscopically, to accurately determine the Lyα and rest-UV luminosity functions (LFs), which can constrain the cosmic reionization process. Given the large number of spectroscopic confirmations in our LAE sample, the Lyα LFs at both redshifts are more tightly constrained than those in our previous studies. The substantially improved evaluation of the Lyα LF at z = 6.5 shows an apparent deficit from z = 5.7 at least at the bright end, and a possible decline even at the faint end, though small uncertainties remain. The Lyα LF at z = 6.5 shows a 24 % decrease in the Lyα luminosity, or a 34 % decrease in the LF amplitude. The rest-UV LFs at z = 6.5 and 5.7 are in good agreement, at least at the bright end, in clear contrast to the differences seen in the Lyα LF. These results imply an increase in the neutral fraction of the intergalactic medium from z = 5.7 to 6.5. The rest-frame equivalent width (EW_0) distribution at z = 6.5 seems to be systematically smaller than z = 5.7, and it shows an extended tail toward larger EW_0. The bright end of the rest-UV LF can be reproduced from the observed Lyα LF and a reasonable EW_0–UV luminosity relation. Integrating this rest-UV LF provides the first measurement of the contribution of LAEs to the photon budget required for reionization. The derived UV LF suggests that the fractional contribution of LAEs to the photon budget among Lyman break galaxies significantly increases toward faint magnitudes. Low-luminosity LAEs could dominate the ionizing photon budget, though this inference depends strongly on the uncertain faint-end slope of the Lyα LF [1].

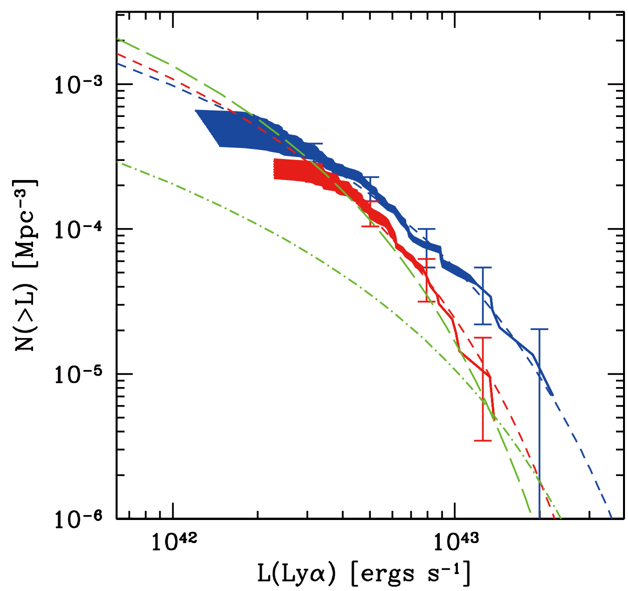

Figure 1: Comparison of the cumulative Lyα LFs of LAEs at z = 6.5 (red-shaded region) and z = 5.7 (blue-shaded region). We estimated the acceptable Lyα LF ranges as specified by the upper and lower limits. The upper limit was estimated assuming that all the uncertain photometric candidates are really LAEs, and the lower limit was estimated assuming that all the uncertain candidates are not LAEs, *i.e.*, using only the pure spectroscopically identified LAE sample. In both the upper and lower limit estimates, we corrected for the detection completeness by number weighting according to the NB magnitude. Error bars evaluated by the Poisson errors are shown in some average data points between the upper limits and lower limits. The short-dashed lines (red for z = 6.5 and blue for z = 5.7) show the fitted Schechter LFs in the case of α = −1.5. As a comparison, the green long-dashed line shows the Lyα LF at z = 6.5 from Ouchi et al. 2010, and the green dot-dashed line shows that of Hu et al. 2010.

Reference

[1] Kashikawa, N., et al.: 2011, *ApJ*, **734**, 119.

Identification of the Bursting Water Maser Features in Orion KL

HIROTA, Tomoya[1], TSUBOI, Masato[2], FUJISAWA, Kenta[3], HONMA, Mareki[1], KAWAGUCHI, Noriyuki[1]
KIM, Mi Kyoung[1], KOBAYASHI, Hideyuki[1], IMAI, Hiroshi[4], OMODAKA, Toshihiro[4], SHIBATA, Katsunori M.[1]
SHIMOIKURA, Tomomi[5], YONEKURA, Yoshinori[6]

1: Graduate University for Advanced Studies / NAOJ, 2: IRAS/JAXA, 3: Yamaguchi University, 4: Kagoshima University, 5: Tokyo Gakugei University, 6: Ibaraki University

In 2011 February, a burst event of the 22 GHz H_2O maser in Orion KL (Kleinmann-Low object) was detected. This is the third time such phenomena has been detected in Orion KL, followed by the events in 1979–1985 and 1998–1999. In spite of extensive monitoring observations with the Kagoshima 6 m single-dish telescope and VLBA during the last time burst event in 1998–1999, the origin of this maser burst is still unclear. If the current burst event would have a common origin as in the case of previous burst events, the flux density of the H_2O maser in Orion KL is expected to be $>10^6$ Jy, which will provide best opportunity to investigate the maser burst phenomenon. With this in mind, we have started monitoring observations of the bursting H_2O maser features in Orion KL with VERA since 2011 March 09 [1].

In the monitoring observations, we found that the flux density of the H_2O maser reached about 50000 Jy at the beginning of the burst event, which was three orders of magnitudes brighter than that in the quiescent phase (Figure 1), while it was still far below the previous burst events. According to the astrometric observations, the bursting maser features consisted of two spatially distinct components separated by about 5 AU at different velocities, 6.95 km s^{-1} and 7.58 km s^{-1} (Figure 2). We successfully determined the absolute positions of the bursting features for the first time ever with a submilli-arcsecond (mas) accuracy. Their positions are coincident with the shocked molecular gas called the Orion Compact Ridge. It is most likely that the protostellar outflow interacting with the Compact Ridge is a possible origin of the H_2O maser burst.

We still continue monitoring observations with VERA of the bursting masers to achieve higher astrometric accuracy. In addition, we will carry out follow-up observations with the ALAM of the submillimeter H_2O masers in Orion KL. Detailed mechanisms of the maser burst will be studied based on the multi-transition maser data.

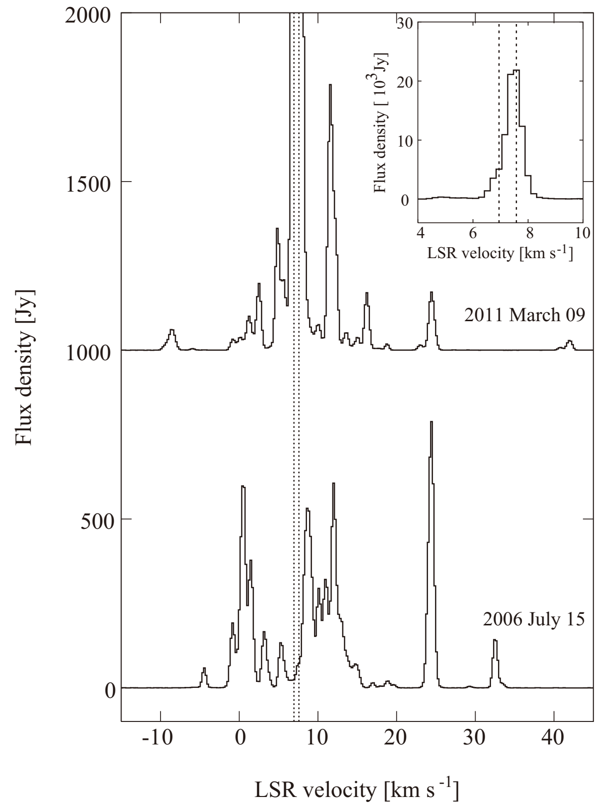

Figure 1: Cross-power spectra of the H_2O masers in the burst (upper) and the quiescent (lower) phases. Dashed lines indicate the radial velocities of the burst features. An inset shows the zoom-up of the bursting component.

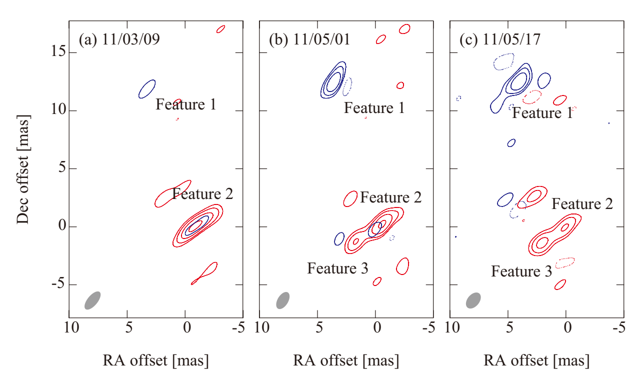

Figure 2: Channel maps of the bursting maser features on (a) 2011 March 9, (b) 2011 May 1, and (c) 2011 May 17. Red and blue contours represent the 7.58 km s^{-1} and 6.95 km s^{-1} features, respectively. The synthesized beam pattern is shown by a gray ellipse at the bottom left corner of each panel.

Reference

[1] Hirota, T., et al.: 2011, *ApJ*, **739**, L59.

Detection of Chemically Young Dark Cloud Cores in the Aquila Rift

HIROTA, Tomoya
(Graduate University for Advanced Studies / NAOJ)
SAKAI, Takeshi, SAKAI, Nami, YAMAMOTO, Satoshi
(University of Tokyo)

In the last decade, we have carried out a survey of radio spectral lines of NH_3 and carbon-chain molecules such as CCS and HC_3N with the Nobeyama 45 m radio telescope. Because carbon-chain molecules and NH_3 are expected to be abundant in the early and late stages of chemical evolution, respectively, due to different production timescales, the abundance ratio of NH_3/CCS can be used as one of the good indicators of chemical evolutionary phase of dark cloud cores.

Recently, we extensively surveyed the NH_3 and CCS lines in the Aquila Rift region, for which observational studies with molecular lines were still limited. As a result, two dense cores, CB130-3 and L673-SMM4, were detected which show remarkably intense spectra of carbon-chain molecules compared with the weak NH_3 lines [1]. According to their high NH_3/CCS ratios, they could be chemically and dynamically less evolved dense cores. Such chemically less-evolved dense cores have been found only in the Taurus Molecular Cloud and the Aquila Rift region. This implies a similarity in the physical properties and/or chemical evolutionary phases of these two molecular clouds.

We have also carried out detailed mapping observations of the CCS and NH_3 lines with the Nobeyama 45 m telescope and Effelsberg 100 m telescope of the Max Planck Institute (Figure 1), as well as a survey of other molecular lines such as DNC, $HN^{13}C$, $H^{13}CO^+$, and N_2H^+. Using these data, we compared the chemical abundances of CB130-3 and L673-SMM4 with previously known carbon-chain-rich cores in the Taurus region [1]. According to the NH_3/CCS ratios as well as the DNC/$HN^{13}C$ ratio, which is another good probe of chemical evolutionary phase of dense cores, CB130-3 and L673-SMM4 are found to be analogous to the previously known chemically young cores while their chemical evolutionary phases would be slightly older than those in the Taurus region. These two sources could be good targets to study initial conditions of protostar formation with future high-sensitivity/high-resolution studies with ALMA.

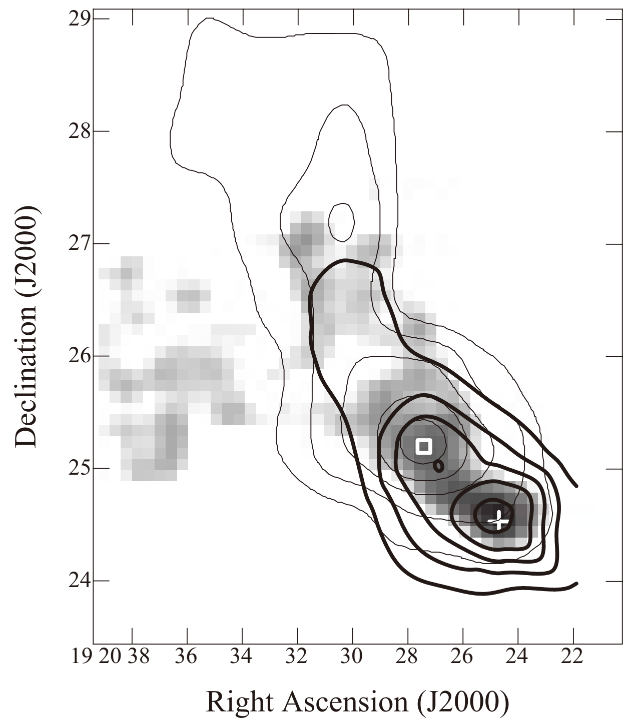

Figure 1: Distributions of CCS (thin contours) and NH_3 (bold contours) superposed on the dust continuum (gray scale) in L673-SMM4. The position offset between the NH_3 (cross) and CCS (square) peaks suggests a chemical differentiation in the core.

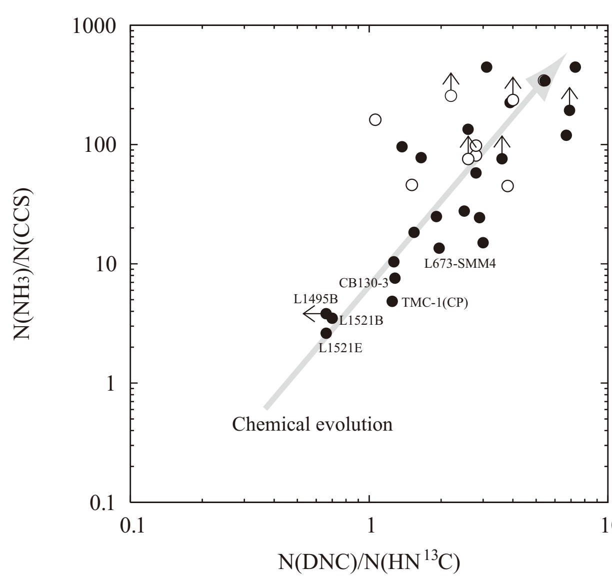

Figure 2: Relationship between NH_3/CCS and DNC/$HN^{13}C$ ratios. Filled and open symbols represent the starless and star-forming cores, respectively. Dense cores evolve from bottom-left to top-right direction (gray arrow).

Reference

[1] Hirota, T., Sakai, T., Sakai, N., Yamamoto, S.: 2011, *ApJ*, **736**, 4.

Small-JASMINE: Stray Light and Thermal Environment

YANO, Taihei, GOUDA, Naoteru, KOBAYASHI, Yukiyasu, TSUJIMOTO, Takuji, NIWA, Yoshito
(NAOJ)

YAMADA, Yoshiyuki
(Kyoto University)

YASUDA, Susumu, UTSUNOMIYA, Shin
(JAXA)

JASMINE Working Group

Small-JASMINE [1] is the astrometric satellite measuring the parallax and the proper motion with the accuracy of 10 μas level. Current status of the stray light and the thermal condition for small-JASMINE are reported.

1 Stray Light of Small-JASMINE

A lot of integration time is needed to accomplish the aim of accuracy of about 10 μas level in the Small-JASMINE mission. Accordingly, we need to observe the object until the albedo from the earth is close to the direction of 23 degrees from the observing direction. Therefore avoiding the stray light is very important task. We have investigated the baffle hood shown in Fig. 1. Inner baffle of the telescope shown in Fig. 2 is also considered.

Inner coating of the telescope using the carbon fiber developed by Energy Science Laboratories adopted by JWST is the first candidate for Small-JASMINE.

The requirement of the stray light is under 13 photons/pix/sec. It is achieved using the baffle hood and the inner baffle with the carbon fiber coating.

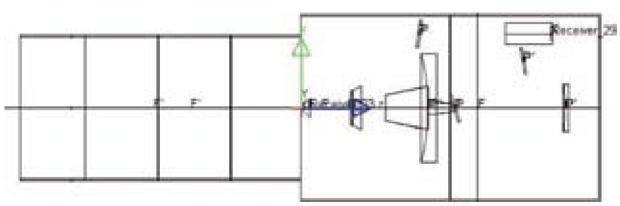

Figure 1: Baffle hood. We consider a few more baffle hoods.

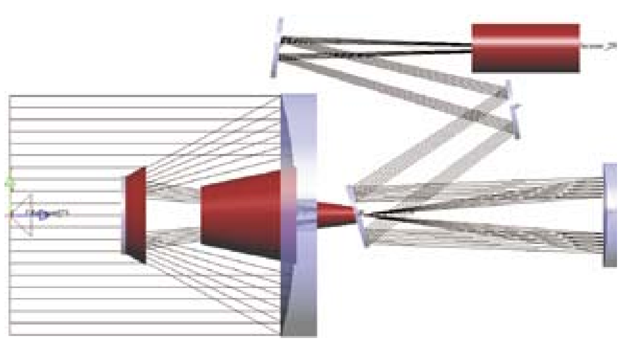

Figure 2: Inner baffle.

2 Attitude and the Thermal Condition for Small-JASMINE

The candidate of the detector of Small-JASMINE is HgCdTe detector, HAWAII-4RG-10, with 1.7 μm cut off developed by Teledyne. We need to operate the detector under 180 K. Accordingly the temperature of the telescope must be 180 K~200 K. The peltier cooling of the detector will be adopted. Then we calculate the thermal environment of the telescope under the attitude of the satellite shown in Fig. 3. We obtain that the telescope satisfies the temperature of under 190 K (See Fig. 4).

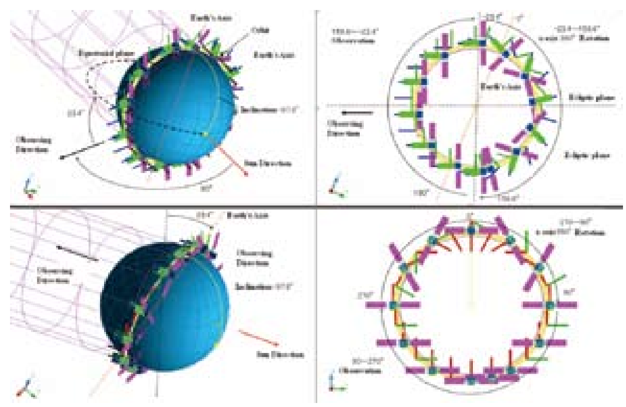

Figure 3: (Upper) attitude of the satellite in spring. (Lower) Same as upper panel but in summer.

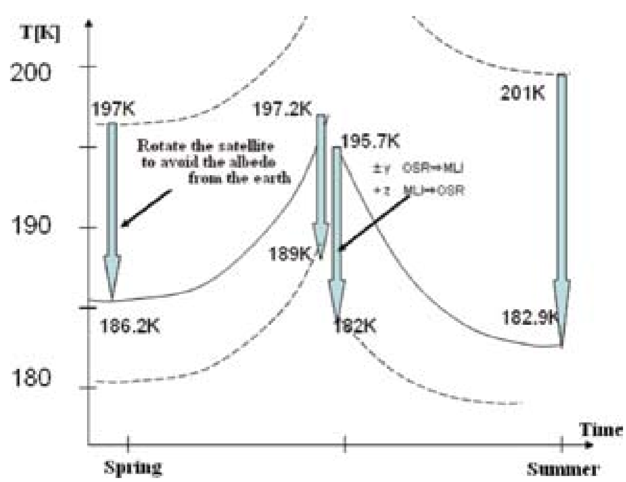

Figure 4: Tempreture of the telescope (primary mirror) against the time (season).

Reference

[1] Yano, T., et al.: 2011, *EAS Publications Series*, **45**, 449-452.

Spectroscopic Confirmation of Galaxies at $z = 6.844 - 7.213$: Demographics of Lyα Emission in $z \sim 7$ Galaxies

ONO, Yoshiaki, OUCHI, Masami (University of Tokyo)
MOBASHER, Bahram (UC Riverside)
DICKINSON, Mark (NOAO)
PENNER, Kyle (University of Arizona)
SHIMASAKU, Kazuhiro (University of Tokyo)
WEINER, Benjamin J. (Steward Observatory)
KARTALTEPE, Jeyhan S. (NOAO)
NAKAJIMA, Kimihiko (University of Tokyo)
NAYYERI, Hooshang (UC Riverside)
STERN, Daniel (JPL)
KASHIKAWA, Nobunari (NAOJ)
SPINRAD, Hyron (UC Berkeley)

One of the most outstanding questions in modern astronomy is when and how the cosmic reionization occurred. Since it requires a large number of ionizing photons, the process of reionization is closely related to an early phase of the cosmic structure formation history. Understanding the reionization process can be accomplished by studying the state of the IGM through estimates of the Lyα fraction, the fraction of Lyα emitters among dropout galaxies. Since neutral hydrogen in the IGM resonantly scatters Lyα photons, the Lyα fraction is expected to decrease at the epoch of reionization [1]. Searching for Lyα emission from samples of dropouts with available spectra at $4 < z < 6$, Stark et al. (2011) showed that the Lyα fraction does not decrease with redshift [2]. However, it is not yet clear if this trend continues at $z > 6$. To explore this, we require spectroscopy of $z \sim 7$ dropouts.

We performed Keck/DEIMOS spectroscopic observations of 11 z-dropout galaxies found in the SDF and GOODS-N fields [3,4]. An emission line is detected at 9500–10000 Å in the spectra of three objects. Since all the detected lines are singlet with a large positive weighted skewness, we conclude that the three objects are Lyα-emitting z-dropout galaxies at $z_{\rm spec} = 7.213$, 6.965, and 6.844. The $z = 7.213$ galaxy is confirmed by observations in two independent DEIMOS runs in 2010 and 2011 with three different spectroscopic configurations.

We then measure the Lyα fraction at $z \sim 7$. To reduce statistical uncertainties and possible effects of field-to-field variance, we combine our results with the z-dropout spectroscopic studies by other groups [5,6,7,8]. We find that the Lyα fraction drops from $z \sim 6$ to 7 in contrast to the reported increasing trend from $z \sim 4$ to 6. We also find that $X_{25}^{\rm Ly\alpha}$ drops more strongly in UV-faint galaxies than in UV-bright galaxies. These findings would suggest that the neutral fraction of the IGM significantly increases from $z \sim 6$ to 7, and that the increase is stronger around galaxies with fainter UV luminosities, which is consistent with inside-out reionization models where reionization proceeds from high- to low-density environments.

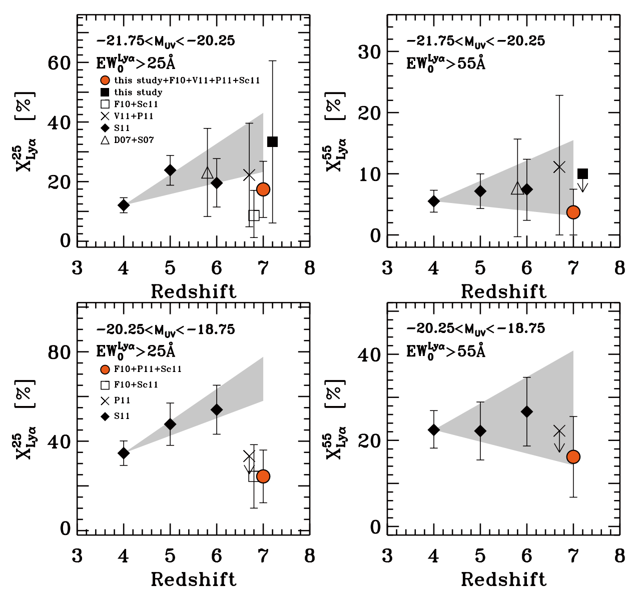

Figure 1: Evolution in the fraction of strong Lyα-emitting galaxies with $M_{\rm UV} \simeq -21.0$ (top panels) and $M_{\rm UV} \simeq -19.5$ (bottom panels) over $4 < z < 7$. The left panels show the fraction of galaxies with EW larger than 25 Å, while the right panels show the fraction of those with EW larger than 55 Å. The red filled circle is the composite result, and the shaded area is derived by extrapolating the trend seen in lower redshifts to $z \sim 7$. For details, see [4].

References

[1] Dijkstra, M., et al.: 2011, *MNRAS*, **414**, 2139.
[2] Stark, D. P., et al.: 2011, *ApJ*, **728**, L2.
[3] Ouchi, M., et al.: 2009, *ApJ*, **706**, 1136.
[4] Ono, Y., et al.: 2012, *ApJ*, **744**, 83.
[5] Fontana, A., et al.: 2010, *ApJ*, **725**, L205.
[6] Vanzella, E., et al. 2011, *ApJ*, **730**, L35.
[7] Schenker, M. A., et al.: 2012, *ApJ*, **744**, 179.
[8] Pentericci, L., et al.: 2011, *ApJ*, **743**, 132.

NRO M33 All Disk Survey of Giant Molecular Clouds (NRO MAGiC): HI to H_2 Transition

TOSAKI, Tomoka[1], KUNO, Nario[2], ONODERA, Sachiko[2], MIURA, Rie[2,3], MURAOKA, Kazuyuki[4]
SAWADA, Tsuyoshi[2], NAKANISHI, Kouichiro[2], KOMUGI, Shinya[2], HIROTA, Akihiko[2], KAWABE, Ryohei[2]
KOHNO, Kotaro[3], KANEKO, Hiroyuki[2,5], NAKANISHI, Hiroyuki[6]

1: Joetsu University of Education, 2: NAOJ, 3: Unversity of Tokyo, 4: Osaka Prefecture University, 5: The Graduate University for Advanced Studies, 6: Kagoshima University

We present the results of the Nobeyama Radio Observatory (NRO) M33 All Disk (30′ × 30′, or 7.3 kpc × 7.3 kpc) Survey of Giant Molecular Clouds (NRO MAGiC) based on ^{12}CO (J = 1−0) observations using the NRO 45-m telescope [1]. M33 is the best target to study the properties of the individual GMCs and their correlation with galactic structures such as spiral arms due to its proximity (~840 kpc) and small inclination angle. The spatial resolution of the resultant map is 19″.3 (= 81 pc) which is sufficient to identify each GMC.

We found clumpy structures with a typical spatial scale of ~100 pc, corresponding to GMCs, and no diffuse, smoothly distributed component of molecular gas at this sensitivity. The overall distribution of molecular gas roughly agrees with that of HI. However, closer inspection of the CO and HI maps suggests that not every CO emission is associated with local HI peaks, particularly in the inner portion of the disk (r < 2 kpc), although most of CO emission is located at the local HI peaks in the outer radii. We found that most uncovered GMCs are accompanied by massive star-forming regions, although the star formation rates (SFRs) vary widely from cloud to cloud.

We obtained a map of the molecular fraction, $f_{\mathrm{mol}} = \sum_{\mathrm{H_2}}/(\sum_{\mathrm{H_I}} + \sum_{\mathrm{H_2}})$, at a 100-pc resolution. This is the first f_{mol} map covering an entire galaxy with a GMC-scale resolution. We find that f_{mol} tends to be high near the center. The correlation between fmol and gas surface density shows two distinct sequences. The presence of two correlation sequences can be explained by differences in metallicity, i.e., higher (~2-fold) metallicity in the central region (r < 1.5 kpc) than in the outer parts. Alternatively, differences in scale height can also account for the two sequences, i.e., increased scale height toward the outer disk.

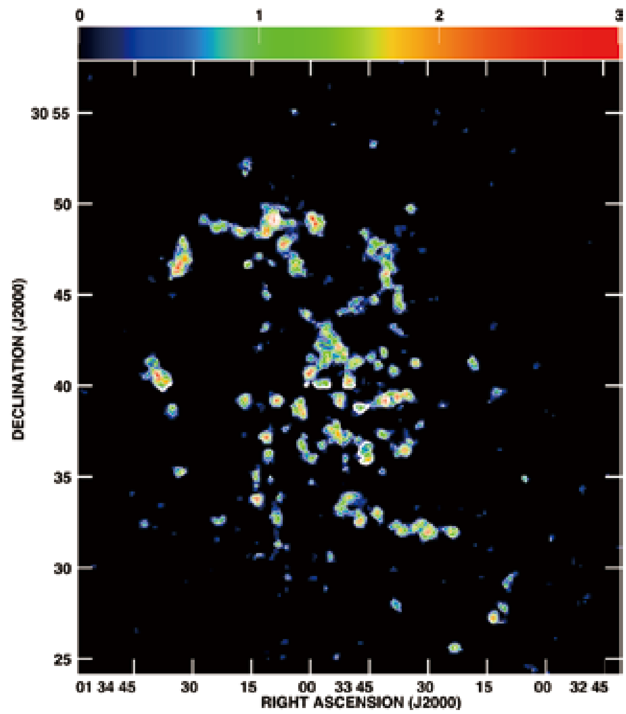

Figure 1: CO(1-0) total integrated intensity map.

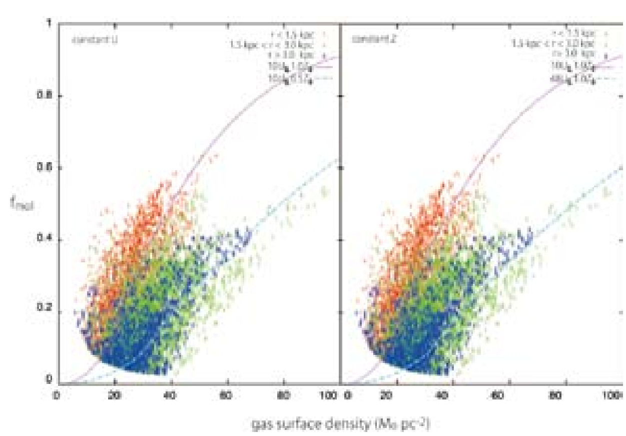

Figure 2: Correlation between gas surface density and f_{mol}. Red, blue, and green points represent data with ranges of $r \leq$ 1.5 kpc, 1.5 kpc $\leq r \leq$ 3 kpc, and $r \geq$ 3 kpc. Pink dotted and cyan dashed lines indicate correlation for $U = 10\,U_0$ at $Z = Z_0$ and $Z = 0.5\,Z_0$ (left), and for $Z = 1.0\,Z_0$ at U = 10 U_0 and $U = 48\,Z_0$ (right), respectively.

Reference

[1] Tosaki, T., et al. : 2011, *PASJ*, **63**, 1171.

Formation of a Propeller Structure by a Moonlet in a Dense Planetary Ring

MICHIKOSHI, Shugo*
(Doshisha University)

KOKUBO, Eiichiro
(NAOJ)

A moonlet embedded in a planetary ring tends to open a gap, such as Keeler or Encke gap, due to gravitational scattering [1]. Conversely, viscous diffusion of ring particles tends to close a gap. If a moonlet is sufficiently large, it will form a fully circular gap, whereas a small moonlet will form only a partial gap that consists of two azimuthally aligned lobes shaped like a propeller. Using the viscous fluid model, the formation of propellers by small moonlets was predicted. The Cassini spacecraft discovered propellers in Saturn's A ring [2,3].

The optical depth of the A ring is as high as 0.3–0.5, while that of the B ring is larger than unity. Distinct and large gravitational wakes form in rings with large optical depths [4]. Such large gravitational wakes can alter the structures around an embedded moonlet. We investigated the condition for propeller formation in a dense ring in which gravitational wakes are prevalent.

Figure 1 shows snapshots of the low and high surface density models [5]. In the low surface density model, a propeller-shaped feature is clearly visible in the weak gravitational wakes. The surface density decreases considerably in the two lobes downstream of the moonlet. They are aligned in the orbital direction and are symmetric about the moonlet. In the high surface density model, strong wake structures due to gravitational instability formed but no propeller structures are observed.

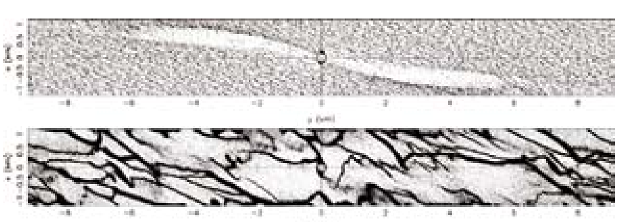

Figure 1: Snapshots of numerical simulations of low and high surface density models.

The numerical simulation results indicate that propeller formation depends on the ring surface density. The clumps in gravitational wakes typically have a mass of ~ $\Sigma\lambda^2$, where Σ is the surface density and λ is the critical wavelength of the gravitational instability. If the clump mass is greater than the moonlet mass, the gravitational wakes may not be affected by gravitational scattering due to the moonlet. Accordingly we derived the critical moonlet size that depends on the surface density around the moonlet.

We performed 25 simulations with different ring surface densities and moonlet radii so as to confirm the condition. As shown in Figure 2, we confirmed that a propeller-shaped structure is clearly observed when this condition is satisfied. If this condition is not satisfied, no distinct steady propeller structure is observed although the ring particles are affected by the moonlet to some extent.

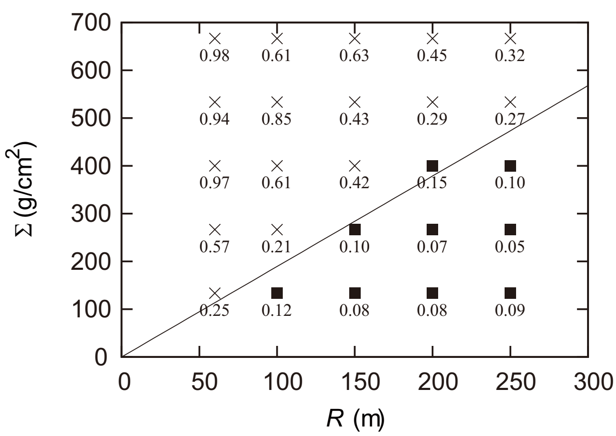

Figure 2: Condition for propeller formation in the R-Σ plane. Filled squares denote models in which clear propellers form and crosses denote models in which no propellers form. We show the ratio of the time-averaged surface density in the propeller region to the initial surface density $\bar{\Sigma}/\Sigma_0$ at each point. The solid line indicates the condition for propeller formation.

* The author is at NAOJ when the paper [5] was submitted.

References

[1] Lissauer, J. J., Shu, F. H., Cuzzi, J. N.: 1981, *Nature*, **292**, 707.
[2] Spahn, F., Sremčević, M.: 2000, *A&A*, **358**, 368.
[3] Tiscareno, M. S., et al.: 2006, *Nature*, **440**, 648.
[4] Salo, H.: 1995, *Icarus*, **117**, 287.
[5] Michikoshi, S., Kokubo, E.: 2011, *ApJ*, **732**, L23.

Secular Gravitational Instability of a Dust Layer in Shear Turbulence

MICHIKOSHI, Shugo* (Doshisha University) KOKUBO, Eiichiro (NAOJ) INUTSUKA, Shu-Ichiro (Nagoya University)

In the standard scenario of planet formation, planetesimals are the precursors of planets, the sizes of which are on the order of kilometer. Their formation process is one of the unsolved problems of the planet formation theory. From micron-sized dust grains dust particles grow to centimeter size in a protoplanetary disk by collisional agglomeration. The least understood growth phase is growth from centimeter-sized dust to kilometersized planetesimals.

One of the possible models in this stage is the gravitational instability model. A very thin and dense layer of settled dust aggregates in the mid-plane of the protoplanetary disk may be gravitationally unstable. Then the gravitational collapse of the dust layer occurs, and kilometer-sized planetesimals are formed directly. This scenario has the advantage of a very rapid formation timescale, which is on the order of the Keplerian time. However, the various hydrodynamic instabilities cause the turbulence in the protoplanetary disk. In this case, the gravitational instability may be suppressed since the dust layer can not become thin due to the turbulence [1].

We investigated the motion of dust particles in turbulent gas and derived the surface density evolution using the stochastic model [2]. We derived the advection diffusion equation with the strong coupling approximation. We solved the advection diffusion equation coupled with the Poisson equation for gravity using the linear approximation. As a result, we found that the dust layer is always unstable regardless of the turbulence strength, but its timescale becomes longer as the turbulence becomes stronger. The dust density increases monotonically because of the instability.

The physical meaning of the secular gravitational instability can be understood in terms of the responses to the density perturbation. We suppose that the density fluctuation exists. The gravitational potential is induced by the density fluctuation. Due to the resultant potential gradient, the matter moves to the local maximum point of the surface density with the terminal velocity. Therefore, the density fluctuation increases monotonically.

We applied this instability to the protoplanetary disk. This instability always occurs, but its timescale is typically very long. If the radial drift of dust particles due to gas drag is faster than the secular gravitational instability, the secular instability seems to be inefficient. In this case, the particle pileup mechanism due to the radial drift enhances the surface density of dust [3]. Thus, we should compare the timescales of the secular gravitational instability and the radial drift. Figure 1 shows the critical f_g value, where f_g is the enhancement factor of the surface density of gas, as a function of the distance from the Sun. The value J_c is the critical Richardson number. Here we assume the quasi-equilibrium shear turbulence model. If f_g is larger than the critical value, the secular gravitational instability is faster than the radial drift. When $f_g > 3$ and $J_c = 0.1$, the secular gravitational instability is faster than the radial drift in the entire disk. If this condition is satisfied, axisymmetric high-density patterns form. When the dust surface density becomes large due to this instability, the classical gravitational instability may occur finally [4]. We will investigate this process by numerical simulations in the future work.

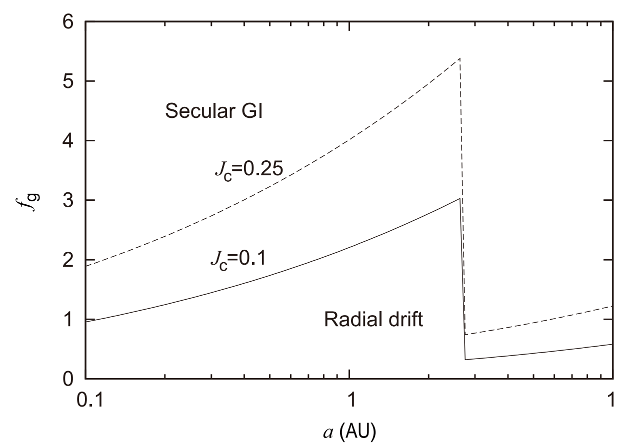

Figure 1: The critical f_g values as a function of the distance from the Sun a.

* The author is at NAOJ when the paper [2] was submitted.

References

[1] Weidenschilling, S. J.: 1980, *Icarus*, **44**, 172.
[2] Michikoshi, S., Kokubo, E., Inutsuka, S.-i.: 2012, *ApJ*, **746**, 35.
[3] Youdin, A. N., Shu, F. H.: 2002, *ApJ*, **580**, 494.
[4] Sekiya, M.: 1998, *Icarus*, **133**, 298.

Stellar Populations and Spatial Distributions of Ultra Faint Dwarf Galaxies

OKAMOTO, Sakurako (Peking University)
ARIMOTO, Nobuo, YAMADA,Yoshihiko (NAOJ)
ONODERA, Masato (Institute for Astronomy, ETH Zürich)

Dwarf spheroidal galaxies (dSphs) around the Milky Way provide us a unique opportunity to investigate galaxy formation and evolution through their resolved stars. Since 2005, extremely faint dwarf (UFD) galaxies and stellar streams are found around the Milky Way [1,2]. The newly discovered UFD galaxies are roughly 10 to 100 times fainter than the well-known “classical” dSphs, having amorphous morphology, and yet are the most dark matter (DM) dominated galaxies. Their star formation histories and detailed structural properties provide a clue to understanding of the galaxy formation at the faint-end and the Galactic tidal effects for the satellite galaxies.

We take deep images of four UFD galaxies, Canes Venatici I, II (CVn I, II), Boötes I (Boö I), and Leo IV, using the Suprime-Cam on the Subaru Telescope [3]. Color-magnitude diagrams (CMDs) extend below mainsequence turnoffs and yield measurements of the ages of stellar populations. The stellar populations of three faint UFD galaxies are estimated to be as old as the Galactic globular cluster M92. We confirm that Boö I dSph has no intrinsic color spread in the MSTO and no spatial difference in the CMD morphology, which indicates that Boö I dSph is composed of an old single stellar population. One of the brightest UFDs, CVn I dSph, shows a relatively younger age (~12.6 Gyr) with respect to fainter dSphs, and the distribution of red horizontal branch (HB) stars is more concentrated toward the center than that of blue HB stars, suggesting that the galaxy contains complex stellar populations. CVn II dSph has the smallest tidal radius of a Milky Way satellite and has a distorted shape, while Leo IV dSph shows a less concentrated spherical shape. The simple stellar population of faint UFDs indicates that the gases in their progenitors were removed more effectively than those of brighter dSphs at the occurrence of their initial star formation. This is reasonable if the progenitors of UFDs belong to less massive halos than those of brighter dSphs.

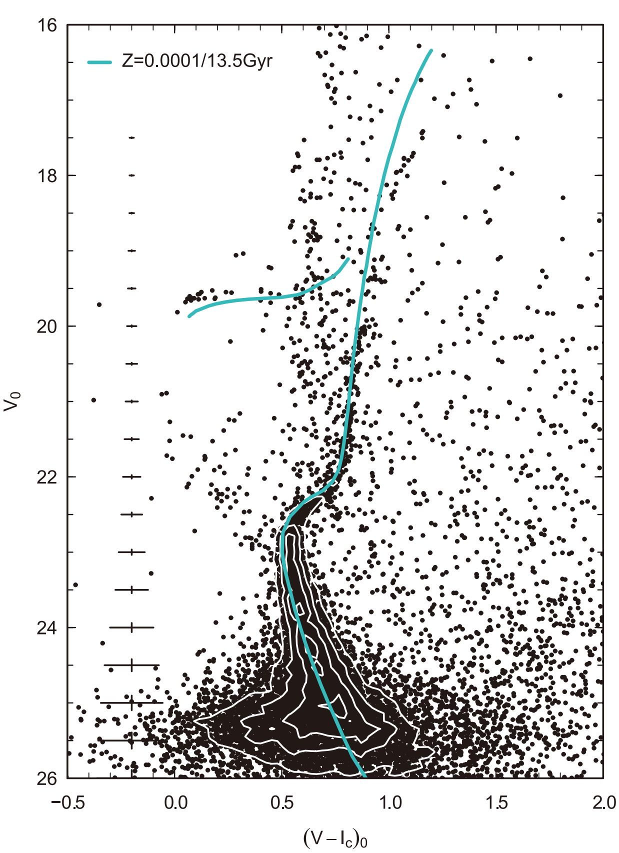

Figure 1: $(V-I_C)_0 - V_0$ CMD of whole observed region of Boötes I dSph. The theoretical Padova isochrone of Z=0.0001 and 13.7 Gyr is overlaid.

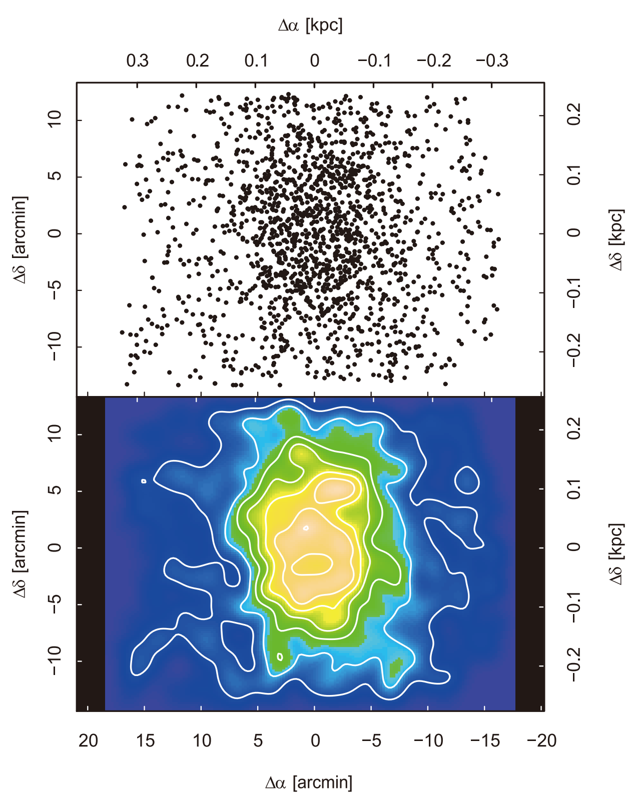

Figure 2: Spatial distribution of the member candidates selected from CMD and iso-density contour of the member candidates of Boötes I dSph.

References

[1] Willman, B., et al.: 2005, *ApJ*, **626**, 85.
[2] Belokurov, V., et al.: 2007, *ApJ*, **654**, 897.
[3] Okamoto, S., et al.: 2012, *ApJ*, **744**, 96.

The Widest-Separation Substellar Companion Candidate to a Binary T Tauri Star

KUZUHARA, Masayuki, TAMURA, Motohide, ISHII, Miki, KUDO, Tomoyuki, NISHIYAMA, Shogo, KANDORI, Ryo
(NAOJ)

Direct imaging surveys are powerful tools to search for Jupiter-mass planets around young stars, and those searchers are useful to study the theory of the formation of giant planets with wide orbits around their parent stars. Recent direct imaging surveys show that the projected separation of young planetary-mass companions (PMCs) are surprisingly wide compared with the orbital separations of planets in our solar system, extra-solar planets detected by indirect methods, and predictions of the standard core accretion model [1]. These results may suggest a diversity in the formation and evolution of PMCs. (e.g., [2]).

We present the results of the direct imaging of a PMC candidate around a *binary* T Tauri star, SR12AB (K4–M2.5), in the ρ Oph star-forming region [3]. The rst discovery of the PMC candidate, SR12 C, was made through the imaging observations carried out on 2002 using the near-infrared camera SIRIUS mounted on the 1.4-m telescope IRSF. SR12C is separated by ~8.7″, corresponding to 045 1100 AU at 125 pc (Fig. 1).

The associated members of a star-forming region share a common proper motion, and thus can be distinguished from background objects by investigating their proper motions from images obtained at multiple epochs. Two epoch images using Subaru (IRCS and CIAO), and three archive date sets (HST/NICMOS, VLT/NACO, and Gemini/QUIRC+Hokupa'a) are used for precise astrometry of the SR12 system. The separation of SR12C from SR12AB is constant from 1998 to 2008, suggesting physical relation of them. In addition, the H band spectra of SR12C shows a triangular shape, which is a characteristic feature of *young*, late-ytpe dwarfs with low surface gravity. Therefore we conclude that SR12C is a member of the ρ Oph star-forming region. In addition, the probability of a chance alignment of objects in ρ Oph, physically associated with SR12AB is very low (~1 %), indicating that SR12C is a genuine companion to SR12 AB.

Using an age-luminosity diagram, we estimate the mass of SR12 C. It has an J-band absolute brightness of 10.5 mag and infrared spectra suggesting a spectral type of M9.0 ± 0.5 and $T_{\rm eff} \approx 2400$. The bolometric luminosity of SR12C was estimated to be $\log(L = L_\odot) = -2.87 \pm 0.20$. Assuming that the age of SR12C is the same as those of YSOs in ρ Oph, the mass of SR12C was estimated as $0.013 \pm 0.007\, M_\odot$ ($14^{+7}_{-8}\, M_{\rm Jup}$) by comparing with models. Therefore SR12C is a strong PMC candidates, and the rst PMC candidate directly imaged around a *binary* T Tauri star. Considering the projected separation from SR12 AB, SR12C has the widest separation from its parent star among PMC candidates imaged so far[1]. This discovery spreads the range of distributions of the PMC candidates from ~50 to 1100 AU.

* When the manuscript was submitted, PMO candidates with the similar separations with SR12 C were reported (e.g., [4]).

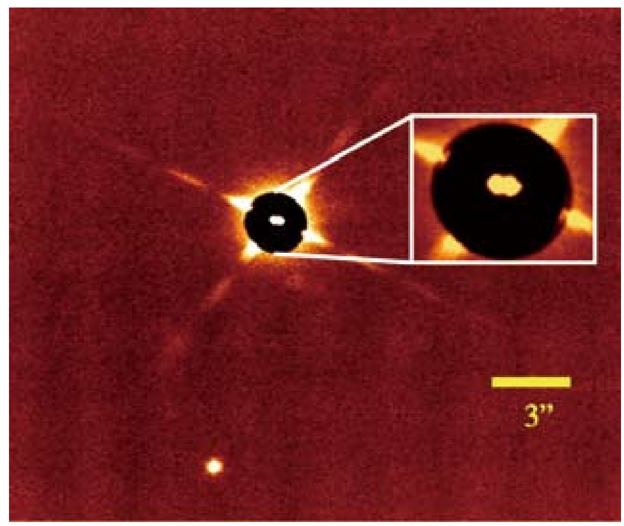

Figure 1: Subaru/CIAO K-band coronagraphic image of a binary T Tauri star SR12 AB and its planetary-mass companion candidate SR12 C. The parent binary star is blocked by the occulting mask. The companion (SR12 C) is separated by ~8.7″, corresponding to ~1100 AU at 125 pc.

References

[1] Pollack, J. B., et al.: 1996, *Icarus*, **124**, 62.
[2] Lafreniere, D., et al.: 2007, *ApJ*, **670**, 1367.
[3] Kuzuhara, M., et al.: 2011, *AJ*, **141**, 119.
[4] Burgasser, A., et al.: 2010, *ApJ*, **725**, 1405.

Astrometry of Galactic Star-Forming Region G48.61+0.02 with VERA

NAGAYAMA, Takumi, HONMA, Mareki, KOBAYASHI, Hideyuki, KAWAGUCHI, Noriyuki, UENO, Yuji
(NAOJ)

OMODAKA, Toshihiro, HANDA, Toshihiro
(Kagoshima University)

We performed the astrometry of H_2O masers in the Galactic star-forming region G48.61 + 0.02 with the VLBI Exploration of Radio Astrometry (VERA). We derived a trigonometric parallax of $199 \pm 7\,\mu$as, which corresponds to a distance of 5.03 ± 0.19 kpc. The distance to G48.61 + 0.02 is about a half of its far kinematic distance, which was often assumed previously. This distance places G48.61 + 0.02 in the Sagittarius-Carina arm and near the active star forming region and the supernova remnant W51. The obtained distance is very close to the parallactic distance of W51 Main/South, which is measured to be $5.41^{+0.31}_{-0.28}$ kpc by the H_2O maser astrometric observations with VLBA [1].

We also obtained the three dimensional motion of G48.61 + 0.02, and found that it has a large peculiar motion of $40 \pm 5\,\mathrm{km\,s^{-1}}$. The kinetic energy of the peculiar motion is estimated to be $(2 \pm 1) \times 10^{51}$ erg. What is the origin of this peculiar motion? This peculiar motion would be originated with the multiple supernovae explosions in W51, or the streaming motion across the Sagittarius-Carina arm. W51 C is the nearest SN remnant from G48.61 + 0.02. Figure 1(a) shows the position of G48.61 + 0.02 superimposed on Fermi LAT counts map in 2–10 GeV around W51 C [2]. The separation between G48.61 + 0.02 and the center of W51 C is 0.70 deg (62 pc). Figure 1(b) and (c) show the integrated intensity and the position velocity maps in the ^{13}CO $J = 1$–0 line around W51 C [3]. The explosion kinetic energy of W51 C is estimated to be $\sim 5 \times 10^{51}$ erg [2]. Considering the energetics, the SN explosion is the possible origin. G48.61 + 0.02 appears to be located on the Sagittarius-Carina arm. Therefore, the streaming motion across the spiral arm is one possible origin for the large peculiar motion of G48.61 + 0.02.

This study is published in Nagayama et al. (2011), PASJ, 63, 719.

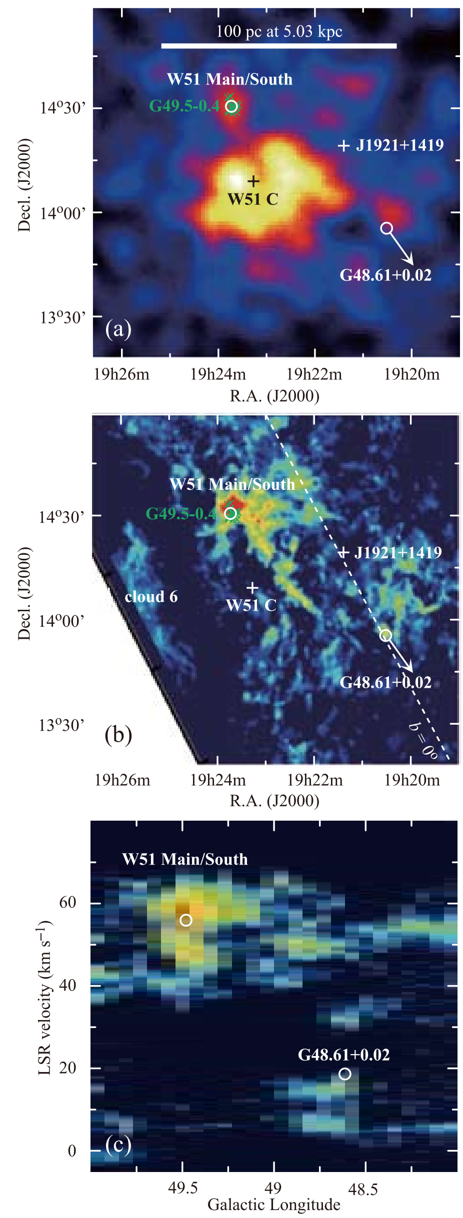

Figure 1: (a): Positions of G48.61+0.02, W51 Main/South (white circle), and OB stars in G49.5–0.4 (green cross) superimposed on *Fermi* LAT counts map in 2.10 GeV around W51 C [2]. The crosses show the center of W51 C and the position of J1921+1419. The arrow shows the motion of G48.61+0.02 relative to W51 Main/South which is obtained to be $-0.12 \pm 0.16\,\mathrm{mas\,yr^{-1}}$ ($-2.9 \pm 3.9\,\mathrm{km\,s^{-1}}$) in right ascension and $-0.17 \pm 0.19\,\mathrm{mas\,yr^{-1}}$ ($-4.1 \pm 4.6\,\mathrm{km\,s^{-1}}$) in declination. (b): same as (a), but the background shows the integrated intensity map in the ^{13}CO $J = 1$–0 line [3]. (c): Longitude-velocity map in the ^{13}CO $J = 1$–0 line [3].

References

[1] Sato, M., Reid, M. J., Brunthaler, A., Menten, K. M.: 2010, *ApJ*, **720**, 1055.
[2] Abdo, A. A., et al.: 2009, *ApJ*, **706**, L1.
[3] Jackson, J. M., et al.: 2006, *ApJS*, **163**, 145.

Particle-Particle Particle-Tree: A Direct-Tree Hybrid Scheme for Collisional N-Body Simulations

OSHINO, Shoichi (NAOJ)
FUNATO, Yoko (University of Tokyo)
MAKINO, Junichiro (Tokyo Institute of Technology)

For the time integration of collisional -body systems, such as star clusters and systems of planetesimals, the combination of direct summation for force calculation and the individual timestep algorithm has been the standard method for nearly a half century. It is not impossible to combine an individual timestep algorithm and a fast and approximate force calculation. However, it was difficult to achieve good performance on distributedmemory parallel computers for such a scheme.

Figure 1 shows the long-term variation of the relative energy error. In this case, the energy error reaches about 7.5×10^{-8} after the time integration for 10 yr (10 orbital periods), while it is 9.8×10^{-9} for 10 yr (10 periods). In other words, the energy error grows to be 10 times larger as the integration time becomes 1000 times longer. This shows that the growth of the energy error is stochastic, like a random walk. It means that the error is mainly caused by the force error of the tree scheme. The growth of the energy error is, therefore, expected to be slow, and the error is small enough even after long calculations. Figure 2 shows the calculation time per one tree timestep as a function of the total number of particles in system. We used the Intel(R) Core(TM)2 Quad CPU Q6600 (2.4 GHz). It shows that the calculation time increases as $O(N \log N)$. Therefore, we reduce the calculation cost from $O(N^2)$ to $(N \log N)$.

We have developed a new hybrid N-body simulation algorithm for simulating collisional N-body systems. This new scheme is constructed by combining the tree and direct schemes using a hybrid integrator. The results of test simulations involving the evolution of a planetesimal system show that our new scheme PPPT can drastically reduce the calculation cost, to a level comparable to the cost of a tree scheme with a constant timestep, while keeping the accuracy sufficient for realistic simulations [1].

In principle, our scheme can be used for collisional systems other than planetary systems, such as globular clusters and stars around a supermassive blackhole in the galactic center.

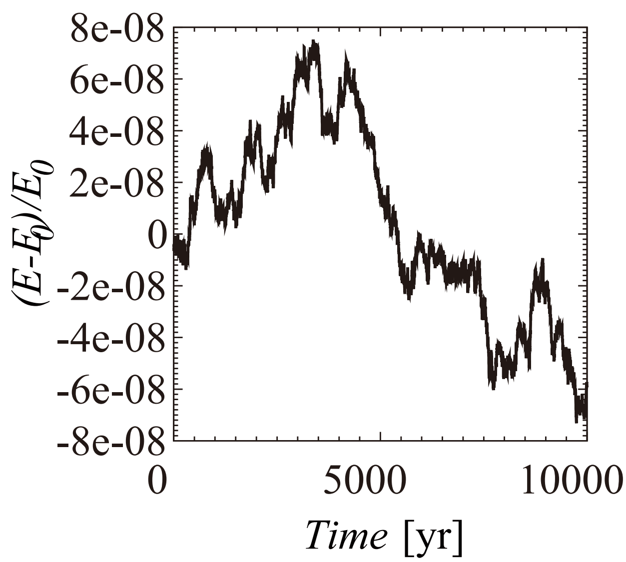

Figure 1: The relative energy error.

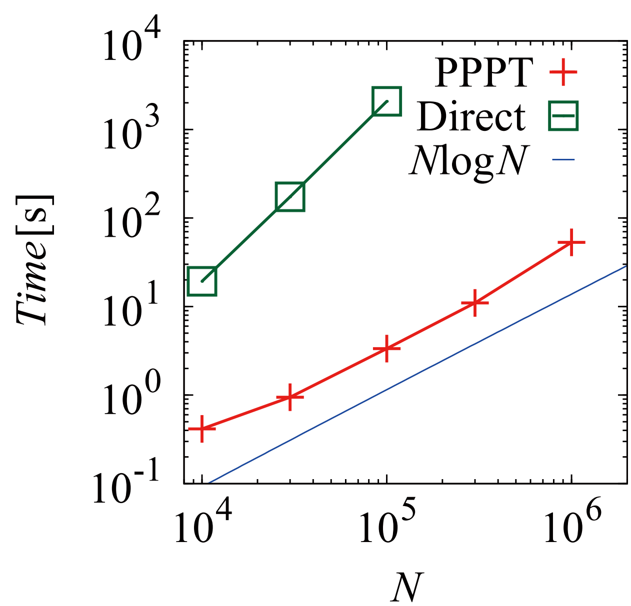

Figure 2: The calculation time plotted against a function of number of particles. The crosses and squares show the results of PPPT and fourth-order Hermite scheme, respectively.

Reference

[1] Oshino, S., Funato, Y., Makino, J.: 2011, *PASJ*, **63**, 881.

Detection of an Ultra-Bright Submillimeter Galaxy in the Subaru/XMM-Newton Deep Field Using AzTEC/ASTE

IKARASHI, Soh[1], KOHNO, Kotaro[1], MOTOHARA, Kentaro[1], TAMURA, Yoichi[1], NAKAJIMA, Kimihiko[1]
SHIMASAKU, Kazuhiro[1], TSUKAGOSHI, Takashi[1], IONO, Daisuke[2], KAWABE, Ryohei[2], EZAWA, Hajime[2]
NAKANISHI, Koichiro[2], FURUSAWA, Hisanori[2], FURUSAWA, Junko[2], TAKATA, Tadafumi[2]
HATSUKADE, Bunyo[3], MATSUHARA, Hideo[4], TAKAGI, Toshinobu[4], TANAKA, Tomohiko[5]
AGUIRRE, James E.[6], LUPU, Roxana[6], SCOTT, Kimberly S.[6], ARETXAGA, Itziar[7], HUGHES, David H.[7]
ARUMUGAM, Vinodiran[8], CIRASUOLO, Michele[8], IVISON, Rob J.[8], AUSTERMANN, Jason[9]
EARLE, Lieko[9], GLENN, Jason[9], KAMENETZKY, Julia[9], MALONEY, Philip[9], BOCK, James J.[10,11]
BRADFORD, Charles M.[10,11], ZMUIDZINAS, Jonas[10,11], MURPHY, Eric J.[11], NAYLOR, Bret J.[10]
NGUYEN, Hien[10], JOHNSON, Seth[12], WILSON, Grant W.[12], YUN, Min S.[12], MAUSKOPF, Philip D.[13]
PETERA, Thushara A.[14], WILNER, David J.[15]

1: University of Tokyo, 2: NAOJ, 3: Kyoto University, 4: Institute of Space and Astronautical Science, 5: Keio University, 6: University of Pennsylvania, 7: INAOE, 8: University of Edinburgh, 9: University of Colorado, 10: Jet Propulsion Laboratory, 11: California Institute of Technology, 12: University of Massachusetts, 13: Cardiff University, 14: Illinois Wesleyan University, 15: Harvard-Smithsonian Center for Astrophysics

We report the detection of an extremely bright (~37 mJy at 1100 μm and ~91 mJy at 880 μm) submilli-meter galaxy (SMG), AzTEC-ASTE-SXDF1100.001 (hereafter referred to as SXDF1100.001 or Orochi), discovered in 1100 μm observations of the Subaru/XMM-Newton Deep Field using AzTEC on ASTE[1]. Subsequent CARMA 1300 μm and SMA 880 μm observations successfully pinpoint the location of Orochi (Fig. 1) and suggest that it has two components, one extended (FWHM of ~4″) and one compact (unresolved). Z-Spec on CSO has also been used to obtain a wide band spectrum from 190 to 308 GHz, although no significant emission/absorption lines are found. The derived upper limit to the line-to-continuum flux ratio is 0.1–0.3 (2σ) across the Z-Spec band.

Based on the analysis of the derived spectral energy distribution from optical to radio wavelengths of possible counterparts near the SMA/CARMA peak position, we suggest that Orochi is a lensed, optically dark SMG lying at $z \sim 3.4$ behind a foreground, optically visible (but red) galaxy at $z \sim 1.4$ (Fig. 2). The deduced apparent (i.e., no correction for magnification) infrared luminosity ($L_{\rm IR}$) and star formation rate (SFR) are $6 \times 10^{13}\, L_\odot$ and 11000 $M_\odot$ yr^{-1}, respectively, assuming that the $L_{\rm IR}$ is dominated by star formation. These values suggest that Orochi will consume its gas reservoir within a short time scale (3×10^7 yr), which is indeed comparable to those in extreme starbursts like the centres of local ULIRGs.

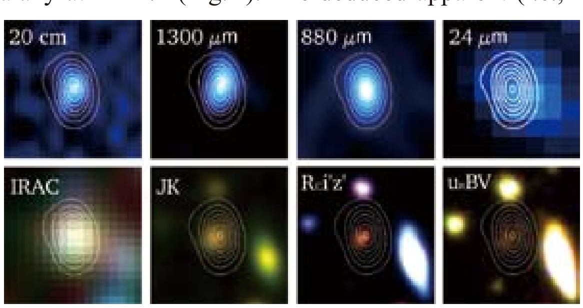

Figure 1: Multi-wavelength images of Orochi with SMA contours (3, 6, 9, 12, 15, 18, and 21 σ). The size of each image is 10″ × 10″; north is towards the top of the image and east is towards the left side of the image. From left to right and top to down: VLA 20 cm; CARMA 1300 μm; SMA 880 μm; MIPS 24 μm; rgb image of IRAC/ 3.6 μm (blue), 4.5 μm (green), 5.8 and 8 μm (red); rg image of WFCAM/ J (green) and K (red); rgb image of SuprimeCam/R, i' and z'; rgb image of SuprimeCam/u_R, B and V.

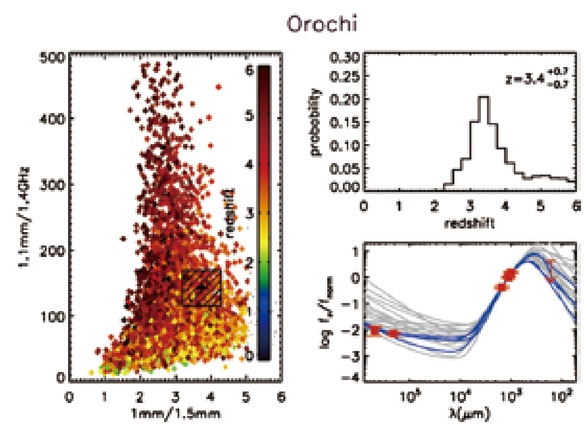

Figure 2: The left panel shows the colour-colour-redshif plot for Orochi. The flux ratios of the mock galaxies are represented as diamonds, and their redshifts are colour-coded according to the scale shown in the panel on the right. The cross represents the measured colours of Orochi, and the dashed box shows the 1σ uncertainty in each colour. The top right panel shows estimated redshift probability distribution of Orochi. In the bottom right panel, the observed SED of Orochi normalised to the flux densities at 1000 μm is shown as squares and arrows. The arrow indicates 3σ upper limits. The squares denote the detection at a level. 3σ, with 1σ error bars. The template SEDs (lines) are redshifted to $z = 3.4$. The template SEDs at this redshift compatible within 3σ error bars with the SED of Orochi are displayed as blue lines. The photometric data are shown at 1000, 1100, 1500 μm, 20 and 50 cm, and The upper limit is shown at 160 μm.

Reference

[1] Ikarashi, S., et al.: 2011, *MNRAS*, **415**, 3081.

Effects of Magnetic Fields with Log-Normal Distribution on the CMB

YAMAZAKI, Dai G. (NAOJ)
ICHIKI, Kiyotom (Nagoya University)
TAKAHASHI, Keitaro (Kumamoto University)

We research effects of a primordial magnetic field (PMF) on the temperature fluctuations and polarization anisotropies of the cosmic microwave background (CMB) [1]. We assume that spectra of a primordial magnetic field (PMF) are described by log-normal distributions (LND) to research the PMF which has a characteristic scale on the temperature fluctuations and polarization anisotropies of the CMB and constrain the parameters of the LND-PMF by the CMB observations.

Theoretical models of PMF generations on cosmological scales have been proposed by many researchers. Since such generation models are based on causal physical processes, PMFs are expected to have the model-dependent scale. If PMFs have been generated from inflation the power law model would be a good representation of the magnetic field power spectrum. On the other hand, if the PMFs was created through other mechanisms than inflation the spectrum would have a characteristic scale and may not be described as a simple power law. Furthermore, we need to understand how such PMFs cascade from smaller to larger scales to study effects of the PMFs created in the early universe on the large scale structures. Actually, we can learn behaviors of PMF cascading or inverse-cascading by simulations [2], which results, however, generally depend on cosmological parameters and models. Since such simulations generally spend too long time and have the limited dynamical range, it is not efficient to estimate distributions of the PMF by some simulations when we study cosmology and astrophysics with the PMF quantitatively.

To avoid these problems, we use a log-normal distribution (LND) in place of the power law defined as,

$$f_{\mathrm{LND}}(k; k_{\mathrm{M}}, \sigma_{\mathrm{M}}) = \frac{1}{k\sigma_{\mathrm{M}}\sqrt{2\pi}} \exp\left\{-\frac{[\ln(k) - \ln(k_{\mathrm{M}})]^2}{2\sigma_{\mathrm{M}}^2}\right\}, \quad (1)$$

where k_{M} is the characteristic scale depending on the PMF generation model, and σM is the variance. The variance σ_{M} in Eq.(1) expresses how this distribution is expanded (or concentrated) around the characteristic scale k_{M}. Therefore, the variance σ_{M} may be related to the cascading of the PMFs.

We have revealed the features of the LND-PMF effects on the CMB as follows: (1) For larger k_{M} or/and σ_{M}, the CMB spectra of TT, TE and EE from the LND-PMF are dominated by the vector mode. Meanwhile, in the opposite case, these spectra are dominated by the scalar mode. (2) The CMB spectrum of the BB polarization anisotropy for all scales and other polarization anisotropies and temperature fluctuations of the CMB for smaller scale is dominated by the vector modes. Because three parameters which characterize the LND-PMF affect the CMB power spectra differently at small and large scales we expect that tight constraints can be placed on these parameters without degeneracy. We found that the LND-PMF which generates CMB anisotropies among $1000 < \ell < 2000$ is most effectively constrainted by the current CMB data sets. For example, B_{LND} for $10^{-3}\,\mathrm{Mpc}^{-1} \leq k/h \leq 10^{-2}\,\mathrm{Mpc}^{-1}$ and $\sigma_{\mathrm{M}} = 1.0$ is limited most strongly as shown in Fig. 1.

In the near future, the tigher constraints on B_{LND} at $k_{\mathrm{M}}/h > 10^{-2}\,\mathrm{Mpc}^{-1}$ will be expected from the observations, such as *Planck*, *QUIET*, and *PolarBear* missions.

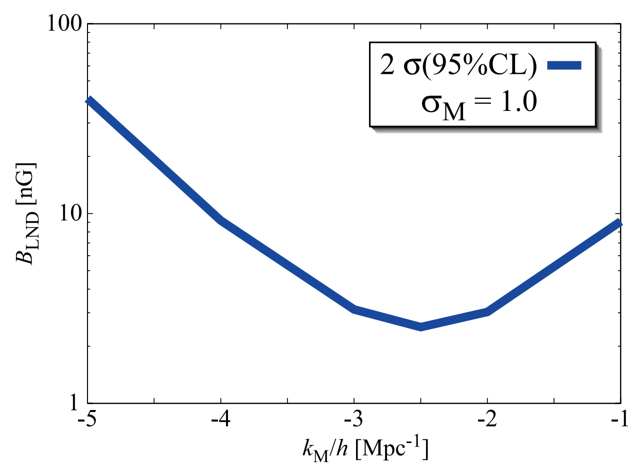

Figure 1: Constraint on the strengths of LND-PMF for $10^{-5} < k_{\mathrm{M}} < 10^{-1}$. Blue curve is the $2\,\sigma$ (95 % CL) upper limits of B_{LND} [nG]. We fix the standard cosmological parameters and use the best-fitted value from WMAP 7th + tensor mode [2].

References

[1] Yamazaki, D. G., Ichiki K., Takahashi, K: 2011, *Phys. Rev. D*, **84**, 123006.
[2] Larson D., et al.: 2011, *ApJS*, **192**, 16.

Observational Evidence for an Impact on the Main-Belt Asteroid (596) Scheila

HANAYAMA, Hidekazu (NAOJ)   ISHIGURO, Masateru (Seoul National University)   HASEGAWA, Sunao, SARUGAKU, Yuki (ISAS)

WATANABE, Jun-Ichi, FUJIWARA, Hideaki, TERADA, Hiroshi (NAOJ)   HSIEH, Henry H. (University of Hawaii)

VAUBAILLON, Jeremie J. (Observatoire de Paris)   KAWAI, Nobuyuki (Tokyo Institute of Technology)

YANAGISAWA, Kenshi, KURODA, Daisuke, MIYAJI, Takeshi, FUKUSHIMA, Hideo (NAOJ)   OHTA, Kouji (Kyoto University)

HAMANOWA, Hiromi (Hamanowa Astro. Obs.)   KIM, Junhan   PYO, Jeonghyun (KASI)   NAKAMURA, Akiko M. (Kobe University)

We made imaging observations of the main-belt asteroid (596) Scheila which was found to exhibit an outburst and a comet-like activity, using Murikabushi 105 cm telescope at the Ishigakijima Astronomical Observatory and Subaru 8.2 m telescope at the NAOJ Hawaii observatory.

We restricted the amount and size distribution of the dust particles with the analysis of the dust structure, and found when it exhibited the outburst, comparing the position angle of the dust tail and synchrones [1].

Then, we constructed the numerical model based on the laboratory experiment of the asteroid impact, and showed that the model reproduced the morphology of the comet-like dust structure [2].

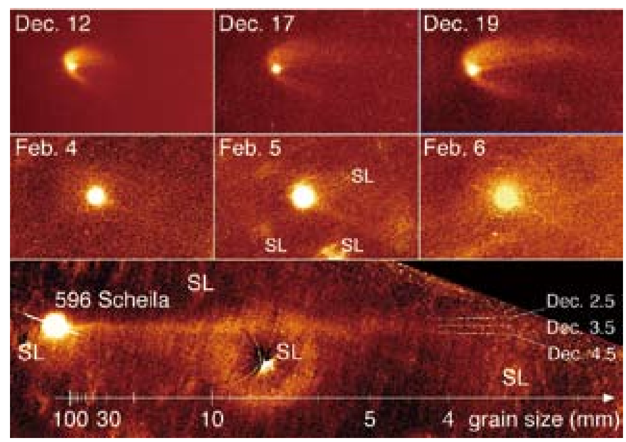

Figure 1: (596) Scheila which showed an outburst and cometlike activity. Upper and middle panels, except the middle center panel, show the dust tails observed with Murikabushi 105 cm telescope at the Ishigakijima Astronomical Observatory. The lower panel is the image of the dust tail observed with Subaru 8.2 m telescope at the NAOJ Hawaii observatory.

References

[1] Ishiguro, M., et al.: 2011, *ApJ*, **740**, L11.
[2] Ishiguro, M., et al.: 2011, *ApJ*, **741**, L24.

Multiband Optical Observation of P/2010 A2 Dust Tail

HANAYAMA, Hidekazu KIM, Junhan ISHIGURO, Masateru
(NAOJ) (Seoul National University)

HASEGAWA, Sunao, USUI, Fumihiko YANAGISAWA, Kenshi SARUGAKU, Yuki
(ISAS) (NAOJ) (ISAS)

WATANABE, Jun-ichi YOSHIDA, Michitoshi FUKUSHIMA, Hideo, MIYAJI, Takeshi
(NAOJ) (Hiroshima University) (NAOJ)

We observed the main-belt asteroid P/2010 A2 dust tail, using Murikabushi 105 cm telescope and MITSuME three-channel simultaneous imaging system at the Ishigakijima Astronomical Observatory.

The analysis of the relative reflectance of the dust tail and the type classification of the asteroid revealed that the reflectance of the P/2010 A2 dust tail resembled that of an Sq-type or C-type asteroid and the spectrum was close to ordinary chondrites [1].

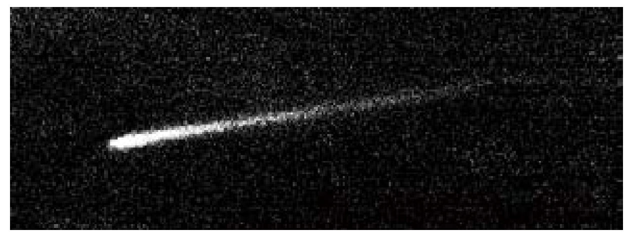

(a)

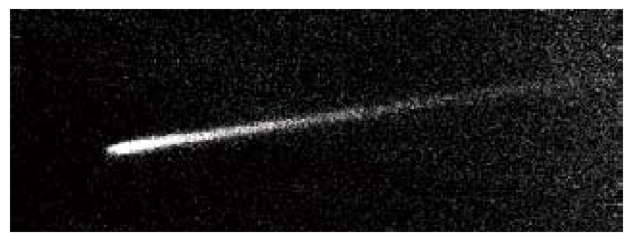

(b)

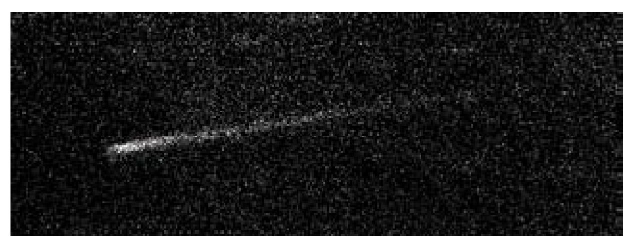

(c)

Figure 1: Images of P/2010 A2 dust trail. These are composite image in three different waveband of (a) g'-band, (b) R_c-band, and (c) I_c-band.

Reference

[1] Kim, J., et al.: 2012, *ApJ*, **746**, L11.

Expedition for Ground-Based Observation of HAYABUSA Spacecraft Re-Entry

WATANABE, Jun-ichi, OHKAWA, Takuya, SATO, Mikiya (NAOJ)
OHNISHI, Kouji (Nagano National College of Technology)
IIJIMA, Yutaka KAGAYA, Yutaka TANABE, Tsutomu (Kagaya studio)

The HAYABUSA spacecraft re-entered the Earth's atmosphere on June 13, 2010 UT., together with the capsule for the sample return. This was the first trial of the re-entry experiment as a Japanese interplanetary spacecraft. We organized an expedition to South Australia for ground-based observations, and succeeded in obtaining valuable data of various phenomena occurring at this re-entry by using 17 instruments. Our data were widely used not only for scientific analysis, but also for outreach purposes [1].

We succeeded to monitor fragmentation of the main body of HAYABUSA spacecraft at the re-entry. The fragmentation started at 13 h 52 m 5.2 s UT at 83−84 km above the sea level, and the number of fragments increased with time. The maximum number is more than a few hundreds at around 13 h 52 m 20 s, and the fragments dispersed with more than 14 km in length, and 1 km in width along the re-entry trajectory. The number decreased after the maximum, and almost ended at 13 h 52 m 31.3 s at around the height of 45 km. Under some assumptions, we derived size distribution of the fragments, which shows small power low index within a range of −1.2 and −1.4, which is similar to −1.5 of the intrinsic size distribution of assembled parts of the spacecraft. This strongly indicates that in the fragmentation phenomena the size distribution of the fragments reflects the internal structure of the parent bodies [2].

A low resolution spectroscopic observation of the capsule were also performed. The altitude at the maximal flux was ocuurred at around 56 km (13 h 52 m 19.8 s UT), and thederived blackbody temperature was 3100 ± 300 K at the altitude of 50 km, and 2400 ± 300 K at the altitude of around 40 km, respectively [3].

The brightness variation of the main body during the ablation was derived by using ghost images instead of the direct ones due to heavy saturation. Among several peaks of flare up possibly due to the rapid increase of the total cross section of fragments, the maximum brightness obtained was −13.1 ± 0.1 which is apparent magnitude at 13 h 52 m 19.8 s UT, which corresponds to the height of 57.4 km. The corresponding absolute magnitude is −13.7 ± 0.1 [4].

References

[1] Watanabe, J.-I., et al.: 2011, *PASJ*, **63**, 941-946.
[2] Watanabe, J.-I., et al.: 2011, *PASJ*, **63**, 955-960.
[3] Ohnishi, K., et al.: 2011, *PASJ*, **63**, 987-993.
[4] Ohkawa, T., et al.: 2012, *PASJ*, **64**, 11-14.

Figure 1: Image of maximal phase of the fragmentation of the HAYABUSA spacecraft at 13 h 52 m 19.8 s. Hundreds of fragments are easily recognized. Taken by OLYMPUS E-30 with a ZUIKO DIGITAL ED 35−100 mm (F 2.0) lens which was set up for sequential shooting mode of 5 frames every second. The exposure time was 1/60 second. The focal length was fixed at 100 mm, which resulted in 12.3 degrees in the diagonal field of view. The ISO was set at 3200 to achieve high sensitivity.

Global Structure of Three Distinct Accretion Flows and Outflows around Black Holes from Two-Dimensional Radiation-Magnetohydrodynamic Simulations

OHSUGA, Ken (Graduate University for Advanced Studies / NAOJ)
MINESHIGE, Shin (Kyoto University)

With a two-dimensional global Radiation-magnetohydrodynamic (RMHD) code [1], we could reproduce three distinct inflow-outflow modes around black holes. Our three models correspond to the two-dimensional RMHD version of the slim disk (supercritical flow), the standard disk, and the RIAF, all with substantial outflows (see Figure 1) [2].

We find the supercritical disk accretion flow, of which the photon luminosity exceeds the Eddington luminosity. The vertical component of the radiation force balances that of the gravity in the disk region but it largely exceeds the gravity above the disk. Our RMHD simulations reveal a new type of jet, i.e., the radiatively driven, magnetically collimated outflow, which might account for the jets of radio-loud NLS1s and microquasars [3,4]. The disk, the temperature of which is around 10^{7-8} K, is surrounded by hot outflowing matter, > 10^9 K, which would induce Compton upscattering and obscuration of the inner part of the disk. Because of the mildly collimated radiative flux, the apparent (isotropic) photon luminosity is ~$22L_E$, which is 1.5×10^{41} erg s^{-1} for the black hole of 50 $M_\odot$ in the face-on view. It implies that our supercritical model is able to explain the central engine of ULXs [5].

When the radiative cooling is effective, a cold (~10^6 K) geometrically thin disk forms and enveloped by the hot rarefied atmosphere with T_{gas} > 10^9 K, Compton upscattering the seed photons from the cold disk. The cold thermal component and the non-thermal hard component of the spectra are observed in luminous AGNs and in the high-soft state of BHBs [6,7]. The disk wind appears above the disk, which was not predicted in the framework of the standard disk model. This result seems to be consistent with the observations of the blueshifted absorption lines [8].

The simulations with low accretion rate corresponds to the RIAF. The magnetic-pressure force, together with the gas-pressure force, drives the outflows. The flow releases the energy via jets rather than via radiation. The accretion flow as well as the outflows are hot and optically thin. Thus, the spectra would resemble those of the low-luminosity AGNs and of the BHBs in their low-hard state [9].

References

[1] Ohsuga, K., et al.: 2009, *PASJ*, **61**, L7.
[2] Ohsuga, K., Mineshige, S.: 2011, *ApJ*, **736**, 2.
[3] Fender, R. P., et al.: 2004, *MNRAS*, **355**, 1105.
[4] Doi, A., et al.: 2006, *PASJ*, **58**, 829.
[5] Makishima, K., et al.: 2000, *ApJ*, **535**, 632.
[6] Brunner, H., et al.: 1997, *A&A*, **326**, 885.
[7] Kubota, A., Makishima, K.: 2004, *ApJ*, **601**, 428.
[8] Miller, J. M., et al.: 2006, *Nature*, **441**, 953.
[9] Markowitz, A., Uttley, P.: 2005, *ApJ*, **625**, L39.

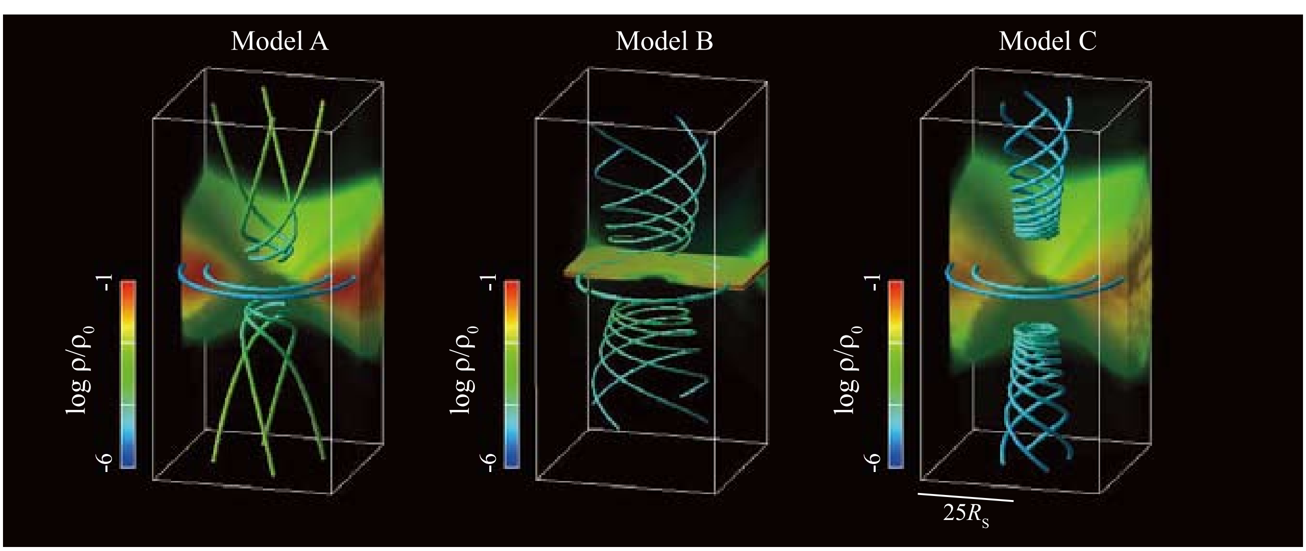

Figure 1: Simulated normalized density distributions (color) and streamlines near the black hole for three models, which correspond to the two-dimensional RMHD version of the slim disk (supercritical flow; left), the standard disk (center), and the RIAF (right).

Gravitational Wave Signatures of Magnetohydrodynamically Driven Core-collapse Supernova Explosions

TAKIWAKI, Tomoya
(NAOJ)

Core-collapse supernovae are now expected to be opening a new branch of astronomy, gravitational-wave (GW) astronomy. Currently, long baseline laser interferometers LIGO, VIRGO, GEO600, TAMA300, AIGO and KAGRA with their international networks of observatories are beginning to take data at sensitivities where astrophysical events are predicted. For these detectors, corecollapse supernovae have been proposed as one of the most plausible sources of gravitational waves.

Although the explosion mechanism of core-collapse supernovae has not been completely clarified yet, magnetohydrodynamic (MHD) explosion mechanism gathers great attention for special explosions associated with birth of magnetars instead of ordinary pulsars.

By performing a series of two-dimensional, special relativistic MHD simulations, we study signatures of gravitational waves in the MHD mechanism. The simulation code utilized here is developed at Takiwaki et al 2009 [1]. We choose to take precollapse magnetic fields less than 10^{12} G and rapid rotation based on a recent GRBoriented progenitor models. By this choice, the rotation of the central proto-neutron star amplifies magnetic fields enough strong to overwhelm the ram pressure of the accreting matter, leading to the MHD explosions. Figure 1 shows the bipolar jet generated by the magnetic field in our simulations.

We found that the total GW amplitudes show a monotonic increase after bounce for models with a strong precollapse magnetic field (10^{12} G) also with a rapid rotation imposed. Figure 2 shows the time evolution of the gravitational wave denoted above. We pointed out that this trend stems both from the kinetic contribution of MHD outflows with large radial velocities and also from the magnetic contribution dominated by the toroidal magnetic fields that predominantly trigger MHD explosions. The feature can be clearly understood with a careful analysis on the explosion dynamics. It was pointed out that the GW signals with an increasing trend, possibly visible to the next-generation detectors for a Galactic supernova, would be associated with MHD explosions exceeding 10^{51} erg. For detail, see the original paper of Takiwaki and Kotake 2011 [2].

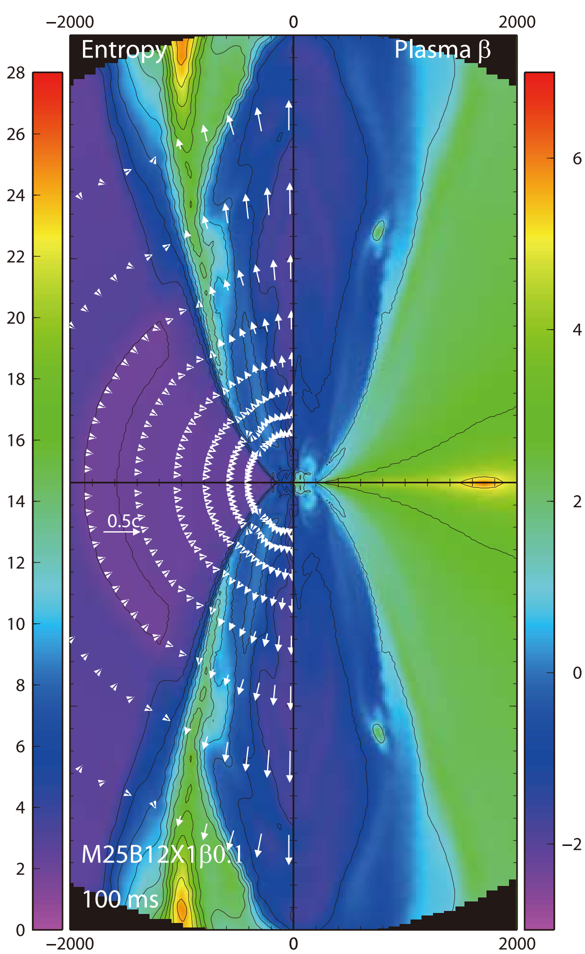

Figure 1: Time snapshot of MHD explosion: Entropy [kB] and plasma β are shown in the left and right panel, respectively.

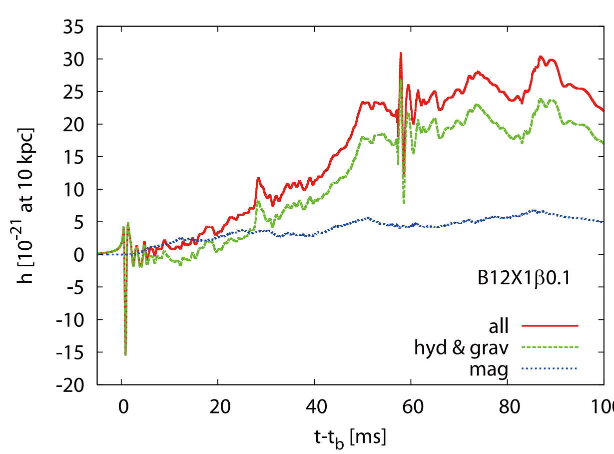

Figure 2: Amplitude of the gravitational wave as a function of time (Red line). Green and blue lines depict the contributions of hydrodynamical part and magnetic part, respectively.

References

[1] Takiwaki, T., Kotake, K., Sato, K.: 2009, *ApJ*, **691**, 1360.
[2] Takiwaki, T., Kotake, K.: 2011, *ApJ*, **743**, 30.

Cosmological Time-Dependent Quark Masses and Big Bang Nucleosynthesis

CHEOUN, Myung-Ki. (Soongsil University)
KAJINO, Toshitaka (NAOJ / University of Tokyo)
KUSAKABE, Motohiko (University of Tokyo)
MATHEWS, Grant J. (University of Notre Dame)

There has been considerable interest [1] in the use of big bang nucleosynthesis (BBN) to constrain any possible time variation of fundamental physical constants in the early universe. A time dependence of fundamental constants in an expanding universe can be a generic result [2] of theories unifying gravity and other interactions. It can be argued [3] that BBN is much more sensitive to variations in the averaged quark mass, i.e., $m_q \equiv (m_u + m_d)/2$, than other physical parameters such as variations in the fine structure constant. Hence, m_q may be the best parameter to search for evidence of time variation of fundamental constants.

We reinvestigate the constraints from BBN on a possible time-dependent quark mass [4]. The limits on such quark-mass variations are particularly sensitive to the adopted observational abundance constraints. Hence, we have adopted updated light-element abundances and uncertainties deduced from observations.

Changing m_q affects nuclear reaction rates through the dependence of the rates on nuclear binding energies and the reaction Q values. Resonant reactions of BBN were treated slightly differently than those in the previous study [1]. There are two important resonant reactions: ^{3}He(d, p)^{4}He and ^{3}H(d, n)^{4}He. We adopt an analytic reaction rate for variable nuclear binding energy [5].

For the ^{3}He(d, p)^{4}He reaction, the resonance is an excited state of the compound nucleus ^{5}Li*. For the ^{3}H(d, n)^{4}He reaction the compound nucleus is ^{5}He*. The resonance energies are related to the excitation energy in the compound nucleus and the net binding energies of the reactants. We point out that there is a consistency check on the δm_q sensitivity of the forward ^{3}He(d, p)^{4}He reaction from the reverse ^{4}He(p, d)^{3}He reaction [4]. As a test on the robustness of the constraint on $\delta m_q/m_q$ we include the variations in the resonance energy based on the parameters in this reverse channel.

In Fig. 1 we show primordial abundances as a function of variations in the quark mass $\delta m_q/m_q$ for a fixed value of baryon-to-photon ratio $\eta = 6.23 \times 10^{-10}$ from WMAP 7 data for model ΛCDM+SZ+lens. The revised constraints on ^{7}Li and ^{4}He do not confirm a concordance best fit for a positive value of $\delta m_q/m_q = 0.016 \pm 0.005$ [1]. Rather, the optimum concordance level is for much smaller values consistent with $\delta m_q/m_q = 0$. Combining limits from all nuclides (except ^{3}He), we deduce conservative concordance limits of $-0.005 \lesssim \delta m_q/m_q \lesssim 0.007$.

Since ^{4}He and D abundances mainly determine the concordance region, we present analytic formulas for the dependence of the ^{4}He and D abundances with quark mass [4]. ^{6}Li production in standard BBN occurs via the ^{4}He(d, γ)^{6}Li reaction, and some consequence of a varying quark mass on its abundance exists. Nevertheless, we show that effects of a varying quark mass on the resonant ^{4}He(d, γ)^{6}Li reaction can be safely neglected [4].

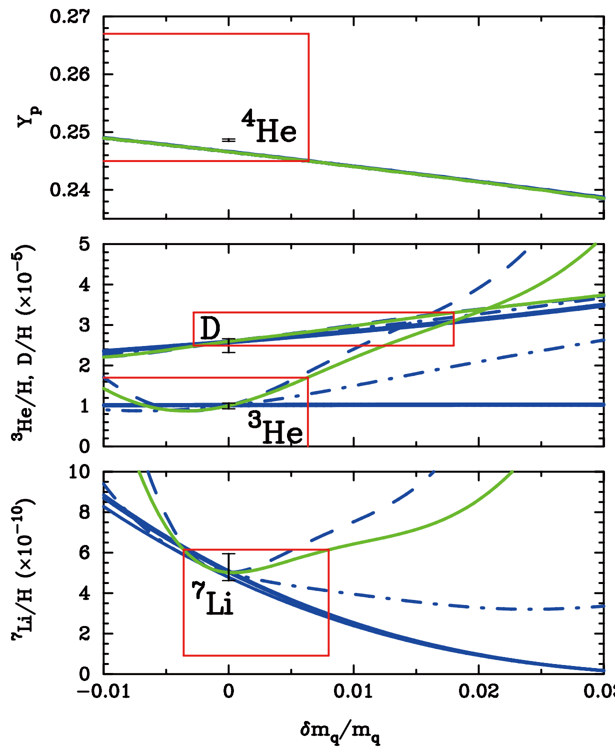

Figure 1: Calculated light-element abundances as a function of variations in the quark mass $\delta m_q/m_q$. The blue solid lines are for the case of no shifts in the resonance energies [1]. The dashed line corresponds to the resonances being shifted the same energy as the ground state. The dot-dashed line corresponds to an averaged value of the resonance sensitivity in the forward direction. The solid green curve is new to the present study. It derives from considering the reverse reaction for the determining the variation of the resonance energy. The red boxes show the allowed parameter regions for the case of the reverse reaction determined using our adopted observational constraints. Error bars at $\delta m_q/m_q = 0$ show theoretical uncertainties in standard BBN [6]. This is reprinted from [4].

References

[1] Berengut, J. C., et al.: 2010, *Phys. Lett. B*, **683**, 114.
[2] Flambaum, V. V.: 2008, *Eur. Phys. JST*, **163**, 159.
[3] Flambaum, V. V., et al.: 2007, *Phys. Rev. C*, **76**, 054002.
[4] Cheoun, M. K., et al.: 2011, *Phys. Rev. D*, **84**, 043001.
[5] Cyburt, R. H.: 2004, *Phys. Rev. D*, **70**, 023505.
[6] Cyburt, R. H., et al.: 2004, *Phys. Rev. C*, **78**, 064614.

Gamow-Teller Strengths in Ni Isotopes and Electron Capture in Gravitational Core-Collapse of Massive Stars

SUZUKI, Toshio (Nihon University / NAOJ)
HONMA, Michio (University of Aizu)
KAJINO, Toshitaka (NAOJ / University of Tokyo)
OTSUKA, Takaharu (University of Tokyo)

Electron capture reactions play the most essential roles in the core-collapse processes at the end of the life-cycle of massive stars. Accurate evaluations of the electron capture rates at high densities and temperatures are important to determine the initial conditions for the nucleosynthesis in supernova explosions [1].

Gamow-Teller (GT) transition strengths in Ni isotopes are studied by shell model calculations with the use of a new Hamiltonian in *fp*-shell, GXPF1J [2]. The GT strengths obtained are used to evaluate electron capture rates at stellar environments [1]. Calculated GT strength for ^{58}Ni and ^{60}Ni as well as the experimental data[3,4] are shown in Fig. 1. Calculated sum of the GT strengths obtained by GXPF1J is in fair agreement with observation for both ^{58}Ni and ^{60}Ni. Calculated electron capture rates for ^{58}Ni and ^{60}Ni are shown in Figs. 2.

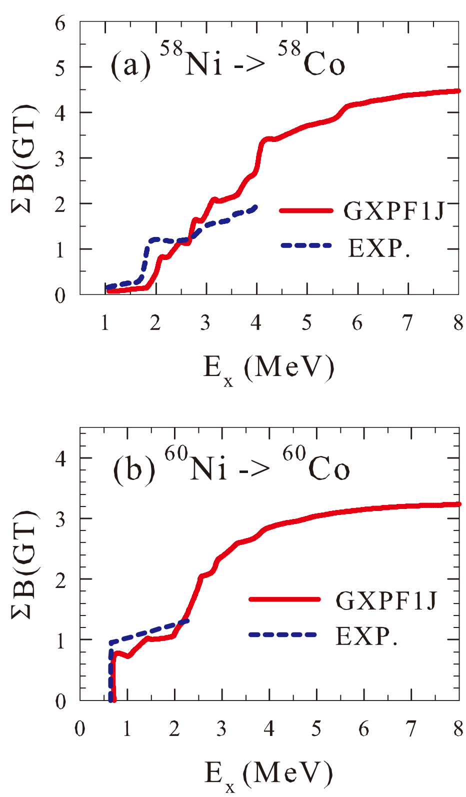

Figure 1: The sum of GT strengths in (a) ^{58}Ni and (b) ^{60}Ni up to the excitation energies (E_x) of ^{58}Co and ^{60}Co. Experimental data are taken from Refs. [3,4].

The calculated capture rates in ^{58}Ni and ^{60}Ni are found to reproduce well the rates obtained by using the experimental GT strengths [3,4]. Better evaluations of the capture rates have been obtained compared with previous calculations [3,4] as well as those by KB3G [5].

The capture rates for ^{56}Ni, and neutron-rich ^{62}Ni and ^{64}Ni isotopes as well as Co and Mn isotopes are also investigated [6]. The GT strengths for GXPF1J are generally more fragmented compared to those of conventional Hamiltonians such as KB3G. The GT distribution in ^{56}Ni obtained by GXPF1 is found to reproduce the recent (p, n) reaction data [7].

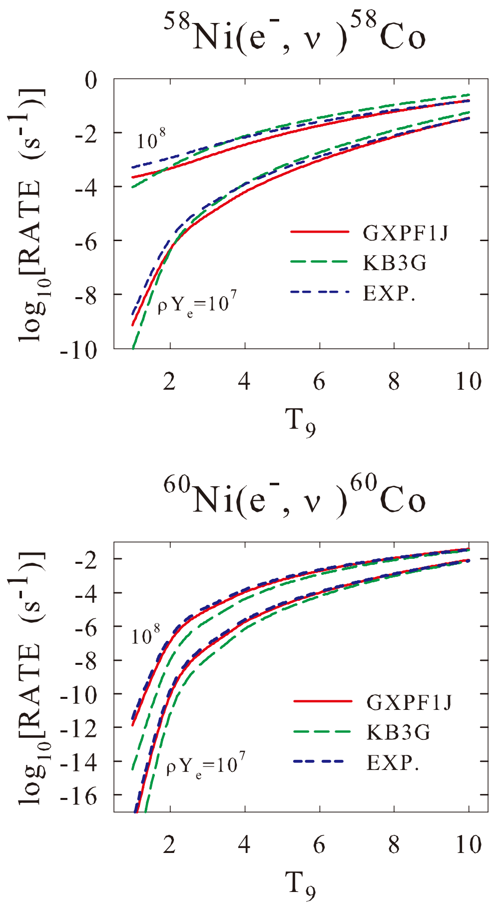

Figure 2: Electron capture rates on ^{58}Ni and ^{60}Ni obtained for GXPF1J and KB3G [5] as well as those obtained by experimental GT strength [3,4].

References

[1] Suzuki, et al.: 2011, *Phys. Rev. C*, **83**, 044619.
[2] Honma, et al.: 2005, *J. Phys. Conf. Ser.*, **20**, 7; 2002, *Phys. Rev. C*, **65**, 061301(R); 2004, **69**, 034335.
[3] Hagemann, et al.: 2004, *Phys. Lett. B*, **579**, 251.
[4] Anantaraman, et al.: 2008, *Phys. Rev. C*, **78**, 065803.
[5] Caurier, et al.: 2005, *Rev. Mod. Phys.*, **77**, 427.
[6] Suzuki, et al.: 2011, *Prog. Part. Nucl. Phys.*, **66**, 385.
[7] Sasano, et al.: 2011, *Phys. Rev. Lett.*, **107**, 202501.

Role of β-Decays of $N = 126$ Isotones in Supernova R-Process Nucleosynthesis

SUZUKI, Toshio (Nihon University / NAOJ)
YOSHIDA, Takashi (University of Tokyo)
KAJINO, Toshitaka (NAOJ / University of Tokyo)
OTSUKA, Takaharu (University of Tokyo)

The r-process is the promising nuclear process for the synthesis of about a half of heavy elements beyond iron [1,2]. Study of the r-process element synthesis has been done by considering neutrino-driven winds in supernova explosions [3] as well as ONeMg supernovae [4] and neutron-star meregers [5].

The evaluation of β-decay rates, particularly at the waiting point nuclei, is one of the important issues of the nucleosynthesis through the r-process. Investigations on the β-decays of isotones with neutron magic number of $N=82$ have been done by various methods including shell model [6], QRPA/FRDM [7] as well as CQRPA [8] etc., which lead to results consistent to one another.

For the β-decays at $N=126$ isotones, however, half-lives obtained by various calculations differ to one another [9]. First-forbidden (FF) transitions become important for these nuclei in addition to the Gamow-Teller (GT) transitions in contrast to the case of $N=82$. Beta decays of the isotones with $N=126$ are studied by shell model calculations taking into account both the Gamow- Teller (GT) and first-forbidden (FF) transitions. The FF transitions are found to be important to reduce the half-lives, by nearly twice to several times, from those by the GT contributions only as shown in Fig. 1 [1].

The present half-lives of the shell model calculations are shorter than those of the standard values of ref. [7] by 2.3 ~ 8.3 for even Z and by 1.4 ~ 2.0 for odd Z (except for $Z=71$), respectively. They increase monotonically as Z increases showing no odd-even staggering found in FRDM's. The present half-lives are longer than those of Ref. [8] by about 1.1 ~ 1.3 (1.5) for $Z=64$ ~ 67 (68) and by twice for $Z=69$ and 70, respectively.

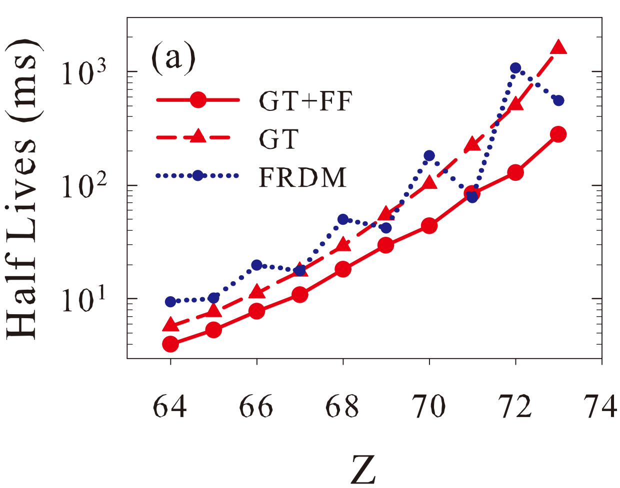

Figure 1: (a) Calculated half-lives for the $N=126$ isotones. Results of the present shell model calculations with GT and with GT+FF transitions are denoted by dashed and solid curves, respectively. Half-lives of Ref. [7] denoted as FRDM are shown by a dotted curve.

Possible implications of the short half-lives of the waiting point nuclei on the r-process nucleosynthesis during the supernova explosions are investigated. We use an analytic model for neutrino-driven winds [10] for the time evolution of thermal profiles. The third peak of the abundance of the elements in the r-process has been found to be shifted toward higher mass region as shown in Fig. 2. Although the magnitude of the shift is rather modest, it is found to be a robust effect independent of the present astrophysical conditions for the r-process as well as the quenching factors of g_A and g_V adopted in the shell model calculations [1].

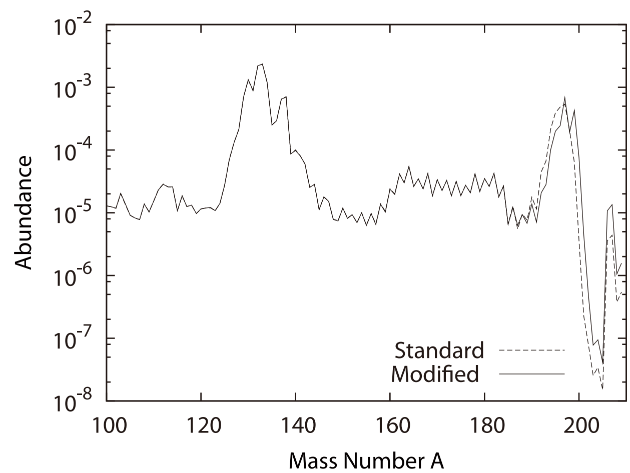

Figure 2: The abundances of elements in the r-process nucleosynthesis obtained by using the present β-decay half-lives for the $N=126$ isotones (denoted as 'modified') and standard half-lives of ref. [7] (denoted as 'standard').

References

[1] Suzuki, T., et al.: 2012, *Phys. Rev. C*, **85**, 015802.
[2] Burbridge, et al.: 1957, *Rev. Mod. Phys.*, **29**, 547; Cowan, et al.: 1991, *Phys. Rep.*, **208**, 267; Kratz, et al.: 1993, *ApJ*, **216**.
[3] Meyer, et al.: 1992, *ApJ*, **393**, 656; Woosley, et al.: 1994, *ApJ*, **433**, 229.
[4] Wanajo, et al.: 2006, *Nucl. Phys. A*, **777**, 676.
[5] Freiburghaus, et al.: 1999, *ApJ*, **525**, L121.
[6] Martinez-Pinedo, et al.: 2003, *Phys. Rev. Lett.*, **75**, 818.
[7] Moller, et al.: 1997, *At. Data Nucl. Data Tables*, **66**, 131; 2003, *Phys. Rev. C*, **67**, 055802.
[8] Borzov, et al.: 2003, *Phys. Rev. C*, **67**, 025802,
[9] Langanke, et al.: 2003, *Rev. Mod. Phys.*, **75**, 818; Grawe, et al.: 2007, *Rev. Part. Phys.*, **70**, 1525.
[10] Takahashi, et al.: 1997, Origin of Matter and Evolution of Galaxies, eds. T. Kajino, S. Kubono, Y. Yoshii (Singapore: World Scientific), 213.
[11] Nishimura, et al.: 2011, *Phys. Rev. Lett.*, **106**, 052501.

Asymmetric Neutrino Reaction from Magnetized Proto-Neutron Stars in Fully Relativistic Framework

MARUYAMA, Tomoyuki (Nihon University)
KAJINO, Toshitaka (NAOJ / University of Tokyo)
HIDAKA, Jun (NAOJ)
YASUTAKE, Nobutoshi (Chiba Institute of Technology)
CHEOUN, Myung-Ki, RYU, Chung-Yeol (Soongsil University)
MATHEWS, Grant J. (University of Notre Dame)

Various phases of the hot and dense hadronic matter are interesting topics in nuclear, particle and astro physics. The neutron star is the most possible target to realize these dense matter. Furthermore a new type of neutron stars, called "magnetars", with a super strong magnetic field have been discovered [1]. In this study only the neutrino emission is the observable information; it also gives us an interesting question as for the dense matter. Neutrino emission as well as GW is the unique observable that provides signals of the change of internal structure of the neutron star [2]. Then, we have calculated scattered and absorbed neutrinos in the hot and dense hadrons with hyperons under strong magnetic field.

Here we assume that there is uniform magnetic field along z-direction as $\vec{B} = B\hat{z}$. Even astronomically strong magnetic field is still weaker than the strong interaction order: $\sqrt{eB} \ll \mu_a$, where μ_a is the chemical potential of the particle a. We therefore treat the magnetic field in the perturbative way, ignore the contribution from the convective current, and thus consider only the spin interaction. In this approximation the cross-section is given as

$$\sigma = \sigma^0 + \Delta\sigma \qquad (1)$$

where σ^0 is independent of B, and $\Delta\sigma$ is proportional to B.

Figure 1 shows $\Delta\sigma$ of the neutrino scattering ($\nu_e \to \nu_e$) and absorption ($\nu_e \to e^-$) in the upper and lower panels, respectively, as a function of the incident neutrino angle θ_i, where the magnetic field is set to be $B = 2 \times 10^{17}$ G, and the initial neutrino energy is taken to be the chemical potential. We found that the scattering cross sections is maximum at $\theta_i = 0°$, and that the absorption cross section is minimum at $\theta_i = 0°$. In addition these results are opposite at $\theta_i = 180°$. These results lead to a very interesting phenomena that in the strong poloidal magnetic field, the neutrinos are strongly absorpted in the antarctic areas of the proto neutron-stars. This result implies that the strong magnetic field could influence the pulser-kick of proto neutron stars.

As the next step, we applied the above results to calculations of pulsar-kick in core-collapse supernovae of the proto neutron-star. In these calculations we solved the Boltzmann equation using a one-dimensional attenuation method. Then, we obtain the kick velocity of about 600 km/s for the $M_{NS} = 1.68\,M_\odot$ isothermal model with $T = 20$ MeV when the magnetic field is uniformly poloidal, with its strength $B = 2 \times 10^{17}$ G.

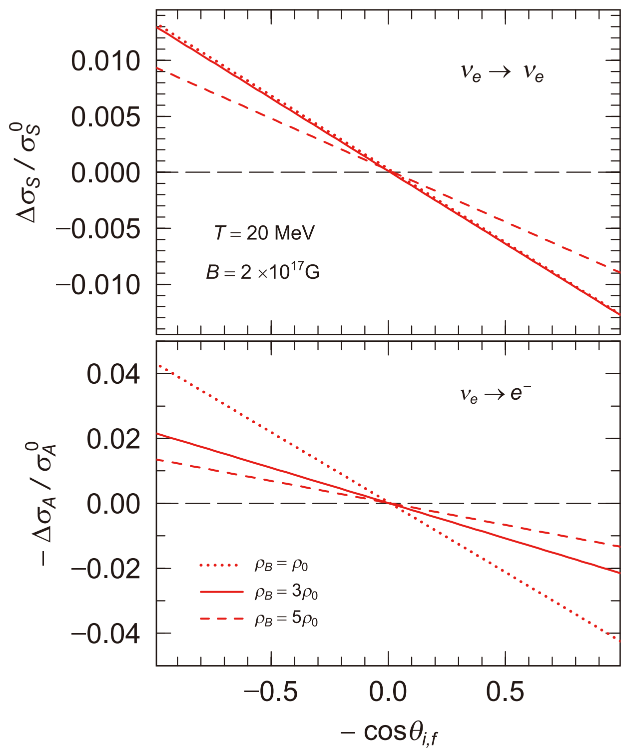

Figure 1: (Color online) Ratios of the magnetic part of the scattering cross-sections $\Delta\sigma_S$ and those of the absorption cross-sections $\Delta\sigma_A$ for $B = 2 \times 10^{17}$ G, to the cross-sections without a magnetic-field $\sigma^0_{S,A}$ at $T = 20$ MeV. Dotted, dashed and solid lines represent the results for densities of $\rho_B = \rho_0$, $3\rho_0$ and $5\rho_0$, respectively.

References

[1] Reddy, S., Prakash, M., Lattimer, J. M.: 1998, *Phys. Rev. D*, **58**, 013009.
[2] Arras, P., Lai, D.: 1999, *Phys. Rev. D*, **60**, 043001.
[3] Maruyama, T., et al.: 2011, *Phys. Rev. D*, **83**, 081303(R).

Nonlinear Neutrino Oscillations in Astronomy

PEHLIVAN, Y. (Mimar Sinan University)
BALANTEKIN, A. B. (University of Wisconsin, Madison)
KAJINO, Toshitaka (NAOJ / University of Tokyo)
YOSHIDA, Takashi (University of Tokyo)

Nonlinear neutrino flavor conversion is investigated by neutrino-neutrino scatterings in the presence of a strong neutrino background and plays an important role in some astronomical sites such as the type II supernovae, the early Universe, and possibly the sites of the gamma ray bursts [1]. In particular, the *forward scattering* and the *flavor exchange* diagrams shown in Fig. 1 play a central role because they undergo coherent superposition and therefore have a dominant contribution [2]. These terms also couple the evolutions of neutrinos with different energies and turn the flavor conversion of neutrinos into a nonlinear many-body problem.

We investigate the flavor evolution of neutrinos undergoing vacuum oscillations and self interactions in an isotropic and homogeneous environment in the absence of a net leptonic background [3]. Assuming a two neutrino mixing scenario, we point out that the resulting flavor evolution has the same dynamics and the same symmetries as i) spins in a system with spin-spin interactions and ii) pair occupation numbers in a system with BCS type pairing [3]. All three of these systems are described by an effective Hamiltonian in the form

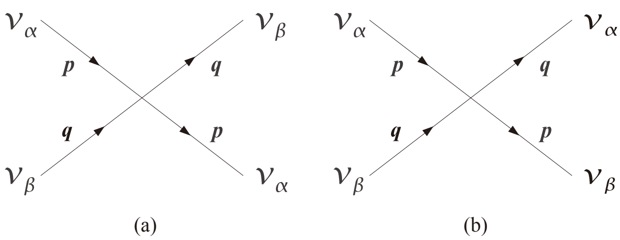

Figure 1: $\nu-\nu$ scattering diagrams corresponding to (a) forward scattering (b) and flavor exchange.

$$H = -\sum_{\omega} \omega \mathcal{J}_{\omega}^{z} + \mu \vec{\mathcal{J}} \cdot \vec{\mathcal{J}} \,. \tag{1}$$

In the case of neutrinos, the fundamental degree of freedom is the neutrino *isospin* $\vec{\mathcal{J}}$ which is defined in terms of a multiplet of neutrino states [4]. Other relevant quantities and the corresponding physical degrees of freedom are summarized in the following table:

	Neutrino Flavor Evolution	Interacting Spin System	BCS Pairing
$\vec{\mathcal{J}}$	Neutrino isospin	Spin	Pair quasispin
ω	Vacuum oscillation frequency	Gyromagnetic ratio	Single particle energy level
μ	Neutrino density	Spin-spin coupling	Pairing strength

Based on these observations, we point out that the neutrino flavor evolution possesses hidden dynamical symmetries which manifest themselves in terms of the following set of conserved quantities [3,5]:

$$h_{\omega} = \vec{B} \cdot \vec{J}_{\omega} + 2\mu \sum_{\omega'(\neq\omega)} \frac{\vec{J}_{\omega} \cdot \vec{J}_{\omega'}}{\omega - \omega'} \,. \tag{2}$$

The existence of these conserved quantities make the system completely integrable and we can write the exact eigenstates and eigenvalues using the method of Bethe ansatz [3]. Such invariants always simplify the analysis of complex systems. Here we neglected leptonic asymmetry in comparison to the neutrino background which can only be justified in the early Universe. But even when the assumptions which guarantee the existence of constants of motion (including the homogeneity and isotropy of the space) are broken, they can still provide a convenient set of variables which behave in a relatively simple manner depending on how drastic the symmetry breaking is.

The symmetries of the Hamiltonian lead to various collective flavor oscillation modes such as the synchronized oscillations and spectral splits [1,3,6] which may be manifest in a future supernova signal. For example, the analogy between self interacting neutrinos and the BCS pairing system offers an intuitive description of neutrino spectral splits in terms of the conserved quantities. Namely, the method of Bogoliubov transformation borrowed from BCS theory can describe the neutrinos in terms of noninteracting quasi-particle degrees of freedom whose adiabatic evolution from a high density region into the vacuum (like the neutrinos emanated from a supernova) results in the splits of neutrino spectra [3]. A full survey of the symmetries and the associated constants of motion of self interacting neutrinos from the point of view of the emergent collective flavor oscillation modes remains to be an open problem for future research.

References

[1] Duan, H., et al.: 2010, *Annu. Rev. Nucl. Part. Sci.*, **60**, 569.
[2] Pantaleone, J. T.: 1992, *Phys. Lett. B*, **287**, 128.
[3] Pehlivan, Y., et al.: 2011, *Phys. Rev. D*, **84**, 065008.
[4] Balantekin, A. B., Pehlivan, Y.: 2007, *J. Phys. G*, **34**, 47.
[5] Gaudin, M.: 1976, *J. Physique*, **37**, 1087.
[6] Raffelt, G. G., Smirnov, A. Y.: 2007, *Phys. Rev. D*, **76**, 125008.

Properties of the Proto-Neutron Star with Smeared Trapped Neutrinos

RYU, Chung-Yeol, CHEOUN, Myung-Ki (Soongsil University)
KAJINO, Toshitaka (NAOJ / University of Tokyo)
MARUYAMA, T. (Nihon University)

We investigate the structure of a proto-neutron star (PNS) with trapped neutrinos by using quantum hadrodynamics (QHD). Ratios of the trapped neutrinos and corresponding leptons to the baryons are usually assumed as a constant. But relevant reactions associated to the beta equilibrium could be sensitive to the given density and temperature. By adopting a phenomenological lepton density which is smeared near the surface, we calculate and discuss populations of baryons and leptons, equations of state and the mass-radius relation of a PNS in isentropic process ($S = 2$).

Calculation for a neutron star is usually constrained by three conditions, baryon number conservation, charge neutrality and beta equilibrium. But for a PNS with trapped neutrinos, the beta equilibrium has to be modified with trapped neutrinos μ_ν,

$$\mu_n \quad = \quad \mu_p + \mu_e - \mu_\nu. \tag{1}$$

In the beta equilibrium, the matter becomes symmetric matter if $\mu_e = \mu_\nu$. By considering that the neutrino propagation and the beta equilibrium may depend on density and temperature, density of electron neutrinos, ρ_{ν_e}, is assumed to be related as $\rho_{\nu_e} = x(\rho)\rho_e$. The condition for muon production is also taken as $\rho_{\nu_\mu} = x(\rho)\rho_\mu$ by satisfying the chemical equilibrium $\mu_e + \mu_{\nu_e} = \mu_\mu + \mu_{\nu_\mu}$. Here $x(\rho)$ may depend on baryon density and temperature. However, to make the problem simple, we assume that $x(\rho)$ depends on baryon density by using a phenomenological formula,

$$x(\rho) = x_0 \ [1 - \exp\{-\beta\,(\rho/\rho_0)^\gamma\}]\,, \tag{2}$$

where $\beta = 0.05$ and $\gamma = 2$ are used. When we ignore the mass of a electron, $x(\rho)$ is nearly $x(\rho) \approx 0.5$ for $\mu_e = \mu_\nu$ because the degeneracy factor of neutrino is 1. Since the condition, $x(\rho) > 0.5$, means proton rich matter, we take the $x(\rho)$ as $x < 0.5$ in all regions of a PNS. Thus, in this work, we use $x_0 = 0.3$. This ratio function implies smooth smearing of relevant leptons at the surface of a PNS.

With these formula and conditions, we obtained populations of neutrinos in Fig. 1. When comparing our results with the simple fixed lepton model [1], the ratio of neutrinos from our formula agrees with those from the simulation of transport theory [2,3]. We thus think our assumptions can explain the results of the simulation and give a physical insight for a PNS. Although our model does not have time evolution, it suggests a phenomenological model about the trapped neutrino which can be or might be reproduced by the realistic dynamical model.

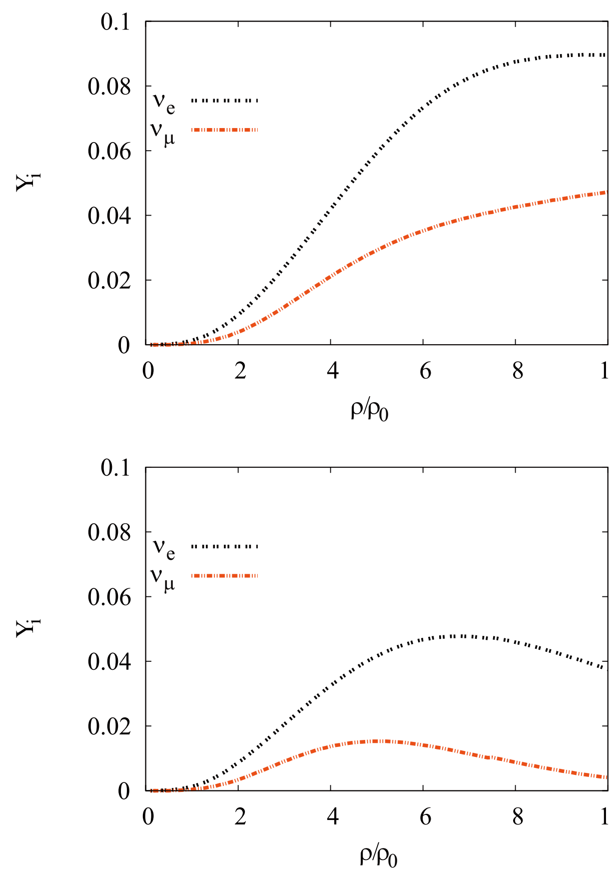

Figure 1: Population of neutrinos in nucleonic phase (*npν*) (upper) and hyperonic one (*npHν*) (lower) for density dependent Y_{L_e} model in $S = 2$ isentropic process.

References

[1] Prakash, M., et al.: 1997, *Phys. Rep.*, **280**, 1.
[2] Burrows, A., Lattimer, J. M.: 1986, *ApJ*, **307**, 178.
[3] Ryu, C. Y., et al.: 2011, *Phys. Rev. C*, **83**, 018802.

Reactions on ^{40}Ar involving solar neutrinos and neutrinos from core-collapsing supernovae

CHEOUN, Myung-Ki, HA, Eunja
(Soongsil University)
KAJINO, Toshitaka
(NAOJ / University of Tokyo)

Neutrino (ν) reactions on ^{40}Ar were of astrophysical importance because the reactions are used to detect the solar ν emitted from ^{8}B via the pp-chains in the sun through the liquid argon time projection chamber (LArTPC) in the ICARUS (Imaging of Cosmic and Rare Underground Signals) [1]. Since the maximum energy of the solar ν is thought to be about 17 MeV in the standard solar model, the ν reactions are sensitive to discrete energy states of ^{40}Ar. The Q-value for the ^{40}Ar(ν_e, e^-)^{40}K* reaction is 1.50 MeV while it is 7.48 MeV for the ^{40}Ar($\bar{\nu}_e$, e^+)^{40}Cl* reaction. Therefore, ^{40}Ar($\bar{\nu}_e$, e^+)^{40}Cl* reactions might be kinematically disfavored in the low energy ν such as solar ν's. In this respect, ^{40}Ar was claimed to effectively distinguish the ν_e and $\bar{\nu}_e$ emitted from the sun.

Recently, Ref. [1] revised previous work by focusing on the possible detection of ν oscillation of supernova (SN) ν's. The ν's from the SN explosion can give valuable information about the ν properties, because they traverse regions of dense matter in the exploding star where matter enhanced oscillations take place.

Since ν energies from the SN explosion are expected to be higher than the solar ν [2], one needs to consider the contributions from higher multi-pole transitions. Moreover $\nu(\bar{\nu})$ energies and flux emitted from the core collapsing SN explosion are believed to be peaked from a few to tens of MeV energy region [2]. Therefore, the $\nu(\bar{\nu})$-induced reactions on ^{40}Ar are sensitive to the higher excited states of the nucleus beyond nucleon thresholds, which eventually decay to lower energy states with the emission of some particles.

Here we report more advanced results [3] based on the QRPA calculation for $\nu(\bar{\nu})$-^{40}Ar reactions by solar and SN ν's, whose energy ranges are considered up to 30 and 80 MeV region, respectively. In particular, we focus on roles of higher excited states around 20 MeV although they are not verified at the experiments. Our results decrease the cross sections of ^{40}Ar(ν_e, e^-)^{40}K* reaction about 3.5 times and increase about twice those of ^{40}Ar($\bar{\nu}_e$, e^+)^{40}Cl* reaction compared to the previous calculations [1]. Consequently, the expected 12 times difference between the reactions at E_ν= 80 MeV is drastically reduced about twice, as shown in Fig. 1 [3].

Other related ν-reactions on ^{40}Ar target through charged and neutral currents are shown in Fig. 2.

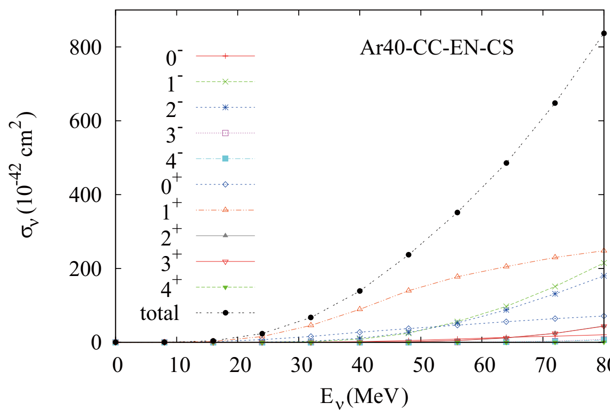

Figure 1: (Color online) Cross sections by CC current, ^{40}Ar(ν_e, e^-)^{40}K*, for solar and SN ν's.

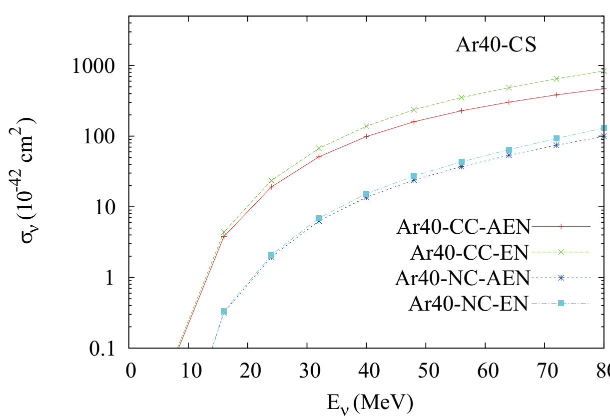

Figure 2: (Color online) Comparison of cross sections for relevant ν reactions on ^{40}Ar for SN ν's.

References

[1] Gil-Botella, I., Rubbia, A.: 2003, *J. Cosmol. Astropart. Phys.*, **10**, 009.
[2] Yoshida, T., et al.: 2008, *ApJ*, **686**, 448.
[3] Cheoun, M.-K., Ha, E., Kajino, T.: 2011, *Phys. Rev. C*, **83**, 028801.

The r-Process in Metal Poor Stars and Black Hole Formation

BOYD, R. N. (LLNL)
FAMIANO, M. A. (Western Michigan University)
MEYER, B. S. (Clemson University)
MOTIZUKI, Y. (RIKEN Nishina Center)
KAJINO, Toshitaka (NAOJ / University of Tokyo)
ROEDERER, I. U. (Carnegie Observatories)

Historically r-process studies focused on the ubiquity of the r-process, i.e., the similarity of the r-process abundances in extremely metal poor (EMP) stars to those of the Solar system. In the past decade, however, a number of EMP stars, which might have been thought to exhibit the r-process abundances, have been observed to have abundances very different from those of the standard r-process [1]. They have led to the suggestion that their abundances are produced by two classes of progenitor star r-processes.

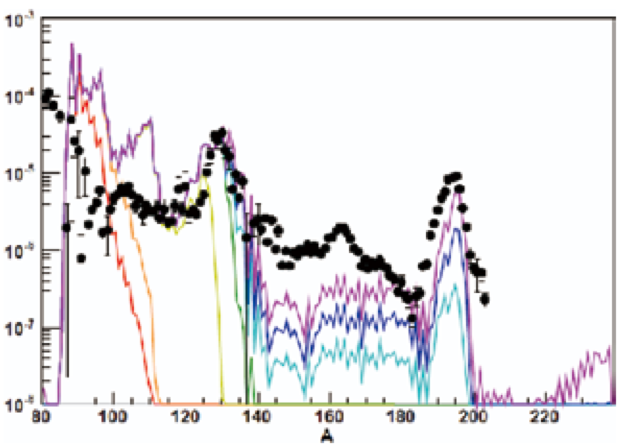

Figure 1: EMP abundance data and r-process calculations [2] using the ref. [6] trajectories, but summing results from trajectory 24 to some later trajectory. The successive curves include trajectory 24, 24–26, 24–28, 24–30, 24–31, 24–32, and 24–40. The sums to higher trajectories make both the mass 130 and 195 r-process peaks. Data are from [6].

Our papers [2,3] propose one primary site for the r-process, i.e., core-collapse supernovae. Then the r-process outliers result from progenitor stars that lie in the 25-40 solar mass range; these stars are thought to become supernovae by first collapsing to a neutron star, then having fallback onto the nascent neutron star to exceed the maximum mass for a neutron star, producing a black hole [4]. Progenitor stars more massive than 40 solar masses would collapse directly to black holes, adding no r-process material to the interstellar medium, whereas stars less massive than 25 solar masses would expel relatively large amounts to the ISM. In the 25–40 solar mass range some r-process material would be expelled to the ISM through hydrodynamic fluctuations that would produce regions with radial velocities in excess of the black hole escape velocity. The amount of material expelled would vary with the mass of the progenitor star, since the more (less) massive stars would remain as neutron stars for times that approaches zero (infinity).

We [2] applied the approach of [5], which described the r-process as occurring in the neutrino driven wind from a core-collapse supernova in 40 trajectories (thin shell wind elements), all originating within the star, but having different initial density, temperature, entropy, and electron fraction. Processing conditions for individual trajectories evolved with time and trajectory identity. Different trajectories were emitted from the star successively, but ceased when the collapse to the black hole occurred, consistent with [5] in which the total emissions of the trajectories generated a good representation of the Solar r-process abundances. Our calculations are described in more detail in [2].

Our results are shown in the Fig. 1. There it can be seen that truncating the r-process at increasing trajectory number terminates the r-process at increasingly higher mass. Note that although the curve representing trajectories 24 through 31 does reach the mass 195 u peak, the abundances in that region are nearly two orders of magnitude below that of the full r-process, which would render the higher mass nuclides difficult to observe. The abundances for that scenario would therefore appear observationally to terminate at a mass of about 140 u. The figure shows that the tr-process predictions do produce a qualitative representation of the observed abundances for the outlier stars, suggesting that all of these stars can be represented by a single r-process, provided that the truncation possibility is allowed.

References

[1] Roederer, I. U., et al.: 2010, *ApJ*, **724**, 975.
[2] Boyd, R. N., et al.: 2012, *ApJ*, **744**, L14.
[3] Boyd, R. N., et al.: 2011, *Proc. OMEG*, **11**, to be published.
[4] Heger, A., et al.: 1992, *ApJ*, **591**, 288.
[5] Woosley, et al.: 1994, *ApJ*, **433**, 229.
[6] Käppeler, F., et al.: 1989, *Rep. Prog. Phys.*, **52**, 945.

II Publications, Presentations

1. Refereed Publications

Abadie, J., et al. including **Hayama, K.**, **Izumi, K.**, **Mori, T.**: 2011, A gravitational wave observatory operating beyond the quantum shot-noise limit, *Nature Phys.*, **7**, 962-965.

Abadie, J., et al. including **Hayama, K.**, **Izumi, K., Mori, T.**: 2012, All-sky search for periodic gravitational waves in the full S5 LIGO data, *Phys. Rev. D*, **85**, 022001.

Abadie, J., et al. including **Hayama, K.**, **Kawamura, S.**: 2011, Search for Gravitational Wave Bursts from Six Magnetars, *ApJ*, **734**, L35.

Abadie, J., et al. including **Hayama, K.**, **Kawamura, S.**: 2011, Search for gravitational waves from binary black hole inspiral, merger, and ringdown, *Phys. Rev. D*, **83**, 122005.

Abadie, J., et al. including **Hayama, K.**: 2011, Directional Limits on Persistent Gravitational Waves Using LIGO S5 Science Data, *Phys. Rev. Lett.*, **107**, 271102.

Abadie, J., et al. including **Hayama, K.**: 2011, Beating the Spin-down Limit on Gravitational Wave Emission from the Vela Pulsar, *ApJ*, **737**, 93.

Abramov-Maximov, V. E., Gelfreikh, G. B., Kobanov, N. I., **Shibasaki, K.**, Chupin, S. A.: 2011, Multilevel Analysis of Oscillation Motions in Active Regions of the Sun, *Sol. Phys.*, **270**, 175-189.

Abramov-Maximov, V. E., Gelfreikh, G. B., **Shibasaki, K.**: 2011, Quasi-periodic Oscillations of Solar Active Regions in Connection with Their Flare Activity - NoRH Observations, *Sol. Phys.*, **273**, 403-412.

Abramowski, A., et al. including **Hada, K.**, **Kino, M.**, **Nagai, H.**: 2012, The 2010 Very High Energy γ-Ray Flare and 10 Years of Multi-wavelength Observations of M 87, *ApJ*, **746**, 151.

Aikawa, Y., Kamuro, D., Sakon, I., Itoh, Y., **Terada, H.**, Noble, J. A., Pontoppidan, K. M., Fraser, H. J., **Tamura, M.**, **Kandori, R.**, **Kawamura, A.**, Ueno, M.: 2012, AKARI observations of ice absorption bands towards edge-on young stellar objects, *A&A*, **538**, 57-68.

Albrecht, S., Winn, J. N., Johnson, J. A., Butler, R. P., Crane, J. D., Shectman, S. A., Thompson, I. B., **Narita, N.**, Sato, B., Hirano, T., Enya, K., Fischer, D.: 2011, Two Upper Limits on the Rossiter-McLaughlin Effect, with Differing Implications: WASP-1 has a High Obliquity and WASP-2 is Indeterminate, *ApJ*, **738**, 50.

Araki, M., **Takano, S.**, Yamabe, N., Koshikawa, H., Tsukiyama, K., Nakane, A., Okabayashi, T., Kunimatsu, A., Kuze, N.: 2012, A Search for Interstellar Carbon-Chain Alcohol HC_4OH in Star-Forming Region L1527 and Dark Cloud TMC-1, *ApJ*, **744**, 163.

Archinal, B. A., et al. including **Fukushima, T.**: 2011, Report of the IAU Working Group on Cartographic Coordinates and Rotational Elements: 2009, *Celest. Mech. Dyn. Astron.*, **109**, 101-135.

Aretxaga, I., Wilson, G. W., Aguilar, E., Alberts, S., Scott, K. S., Scoville, N., Yun, M. S., Austermann, J., Downes, T. P., **Ezawa, H.**, Hatsukade, B., Hughes, D. H., **Kawabe, R.**, Kohno, K., **Oshima, T.**, Perera, T. A., Tamura, Y., Zaballos, M.: 2011, AzTEC Millimeter Survey of the COSMOS Field – III. Source Catalog Over 0.72 sq. deg. and Plausible Boosting by Large-Scale Structure, *MNRAS*, **415**, 3831-3850.

Aspin, C., Beck, T. L., Davis, C. J., Froebrich, D., Khanzadyan, T., Magakian, T. Yu., Moriarty-Schieven, G. H., Movsessian, T. A., Mitchison, S., Nikogossian, E. G., **Pyo, T.-S.**, Smith, M. D.: 2011, CSO Bolocam 1.1 mm Continuum Mapping of the Braid Nebula Star Formation Region in Cygnus OB7, *AJ*, **141**, 139.

Barbary, K., et al. including **Hattori, T.**, **Kashikawa, N.**: 2011, The Hubble Space Telescope Cluster Supernova Survey. VI. The Volumetric Type Ia Supernova Rate, *ApJ*, **745**, 31.

Barbary, K., et al. including **Hattori, T.**, **Kashikawa, N.**: 2011, The Hubble Space Telescope Cluster Supernova Survey. II. The Type Ia Supernova Rate in High-redshift Galaxy Clusters, *ApJ*, **745**, 32.

Barker, M. K., Ferguson, A. M. N., Irwin, M. J., **Arimoto, N.**, Jablonka, P.: 2012, Quantifying the faint structure of galaxies: the late-type spiral NGC 2403, *MNRAS*, **419**, 1489-1506.

Barro, G., Perez-Gonzalez, P. G., Gallego, J., Ashby, M. L. N, Kajisawa, M., **Miyazaki, S.**, Yamada, T., Zamorono, J.: 2011, UV-to-FIR Analysis of Spitzer/IRAC Sources in the Extended Groth Strip. II. Photometric Redshifts, Stellar Masses, and Star Formation Rates, *ApJS*, **193**, 30-64.

Batista, V., et al. including **Fukui, A.**: 2011, MOA-2009-BLG-387Lb: a massive planet orbiting an M dwarf, *A&A*, **529**, A102.

Bayo, A., Barrado, D., Stauffer, J., Morales-Calderón, M., Melo, C., Huélamo, N., Bouy, H., Stelzer, B., **Tamura, M.**, Jayawardhana, R.: 2011, Spectroscopy of very low mass stars and brown dwarfs in the Lambda Orionis star forming region. I. Enlarging the census down to the planetary mass domain in Collinder 69, *A&A*, **536**, A63.

Bekki, K., **Tsujimoto, T.**: 2011, Formation of the Galactic bulge from a two-component stellar disc: explaining cylindrical rotation and a vertical metallicity gradient, *MNRAS*, **416**, L60-L64.

Bekki, K., **Tsujimoto, T.**: 2011, Origin of Chemical and Dynamical Properties of the Galactic Thick Disk, *ApJ*, **738**, 4.

Bellagamba, F., Maturi, M., **Hamana, T.**, Meneghetti, M., **Miyazaki, S.**, Moscardini, L.: 2011, Optimal filtering of optical and weak lensing data to search for galaxy clusters: application to the COSMOS field, *MNRAS*, **413**, 1145-1157.

Birn, J., Hesse, M., **Zenitani, S.**: 2011, Reconnection in compressible plasmas: Extended conversion region, *Physics of Plasmas*, **18**, 111202.

Borissova, J., et al. including **Tamura, M.**: 2011, New Galactic star clusters discovered in the VVV survey, *A&A*, **532**, A131.

Boyd, R. N., Famiano, M., Meyer, B. S., Motizuki, Y., **Kajino, T.**, Roederer, I. U.: 2011, The r-process in Metal Poor Stars, and Black Hole Formation, *ApJ*, **744**, L14.

Boyd, R. N., **Kajino, T.**, Onaka, T.: 2011, Supernovae, Neutrinos, and the Chirality of the Amino Acids, *Int. J. Mol. Sci.*, **12** , 3432-3444.

Burningham, B., Leggett, S. K., Homeier, D., Saumon, D., Lucas, P. W., Pinfield, D. J., Tinney, C. G., Allard, F., Marley, M.

S., Jones, H. R. A., Murray, D. N., **Ishii, M.**, Day-Jones, A., Gomes, J., Zhang, Z. H.: 2011, The properties of the T8.5p dwarf Ross 458C, *MNRAS*, **414**, 3590.

Carollo, D., Beers, T. C., Bovy, J., Sivarani, T., Norris, J. E., Freeman, K. C., **Aoki, W.**, Lee, Y. S., Kennedy, C. R.: 2012, Carbon-enhanced Metal-poor Stars in the Inner and Outer Halo Components of the Milky Way, *ApJ*, **744**, 195.

Cheoun, M. K., Ha, E., **Kajino, T.**: 2011, Neutrino reactions on ^{40}Ar for solar and core-collapsing supernova neutrinos, *Phys. Rev. C*, **83**, 028801.

Cheoun, M. K., **Kajino, T.**, Kusakabe, M., Mathews, G. M.: 2011, Time Dependent Quark Masses and Big Bang Nucleosynthesis Revisited, *Phys. Rev. D*, **84**, 043001.

Choi, M., Kang, M., **Tatematsu, K.**, Lee, J.-E., Park, G.: 2011, Radio Imaging of the NGC 1333 IRAS 4A Region: Envelope, Disks, and Outflows of a Protostellar Binary System, *PASJ*, **63**, 1281-1291.

Chorley, N., Foullon, C., Hnat, B., Nakariakov, V. M., **Shibasaki, K.**: 2011, Period persistence of long period oscillations in sunspots, *A&A*, **529**, A123.

Christopherson, A. J., Malik, K. A., Matravers, D. R., **Nakamura, K.**: 2011, Comparing two different formulations of metric cosmological perturbation theory, *Class. Quantum Grav.*, **28**, 225024.

Collins, M. L. M., et al. including **Arimoto, N.**: 2011, The scatter about the 'Universal' dwarf spheroidal mass profile: a kinematic study of the M31 satellites And V and And VI, *MNRAS*, **417**, 1170-1182.

Curran, S. J., Whiting, M. T., Combes, F., **Kuno, N.**, Francis, P., Nakai, N., Webb, J. K., Murphy, M. T., Wiklind, T.: 2011, On the Absence of Molecular Absorption in High Redshift Millimetre-Band Searches, *MNRAS*, **416**, 2143-2153.

Davis, C. J., Cervantes, B., Nisini, B., Giannini, T., Takami, M., Whelan, E., Smith, M. D., Ray, T. P., Chrysostomou, A., **Pyo, T.-S.**: 2011, VLT integral field spectroscopy of embedded protostars: using near-infrared emission lines as tracers of accretion and outflow, *A&A*, **528**, A3.

Deguchi, S., Sakamoto, T., Hasegawa, T.: 2012, Kinematics of Red Variables in the Solar Neighborhood I. Basic Data Obtained by an SiO Maser Survey, *PASJ*, **64**, 4.

Doi, A., **Nakanishi, K.**, **Nagai, H.**, Kohno, K., Kameno, S.: 2011, Millimeter Radio Continuum Emissions as the Activity of Supermassive Black Holes in Nearby Early-type Galaxies and Low-luminosity Active Galactic Nuclei, *AJ*, **142**, 167.

Donovan Meyer, J., Koda, J., **Momose, R.**, Fukuhara, M., Mooney, T., Towers, S., Egusa, F., Kennicutt, R., **Kuno, N.**, Carty, M., **Sawada, T.**, Scoville, N.: 2012, Resolved Measurements of Xco in NGC 6946, *ApJ*, **744**, 42.

Dowson, W. A., Wittman, D., Jee, M. J., Gee, P., Hughes, J. P., Tyson, J. A., Schmidt, S., Thrman, P., Bradac, M., **Miyazaki, S.**, Lemaux, B., **Utsumi, Y.**, Margoniner, V. E.: 2012, Discovery of a Dissociative Galaxy Cluster Merger with Large Physical Separation, *ApJ*, **747**, L42.

Ebizuka, N., Ichiyama, K., Yamada, T., Tokoku, C., Onodera, M., Hanesaka, M., Kodate, K., Katsuno, U. Y., Maruyama, M., Shimasaku, K., **Tanaka, I.**, Yoshikawa, T., **Kashikawa, N.**, **Iye, M.**, Ichikawa, T.: 2011, Cryogenic Volume-Phase Holographic Grisms for MOIRCS, *PASJ*, **63**, 605-612.

Edmonds, D., Borguet, B., Arav, N., Dunn, J. P., Penton, S., Kriss, G. A., Korista, K., Costantini, E., Steenbrugge, K., Gonzalez-Serrano, J. I., **Aoki, K.**, Bautista, M., Behar, E., Benn, C., Crenshaw, D. M., Everett, J., Gabel, J., Kaastra, J., Moe, M., Scott, J.: 2011, Galactic-scale Absorption Outflow in the Low-luminosity Quasar IRAS F04250-5718: Hubble Space Telescope/Cosmic Origins Spectrograph Observations, *ApJ*, **739**, 7.

Elmasli, A., Fossati, L., Folsom, C. P., Albayrak, B., **Izumiura, H.**: 2012, A spectroscopic study of DD Uma: Ursa Major group member and candidate for BRITE, *New Astron.*, **17**, 221-226.

Enya, K., et al. including **Yamashita, T.**, **Narita, N.**, **Matsuo, T.**, **Tamura, M.**, **Nishikawa, J.**, **Kokubo, E.**, **Hayano, Y.**, **Oya, S.**, **Guyon, O.**: 2011, The SPICA coronagraphic instrument (SCI) for the study of exoplanets, *Adv. Space Res.*, **48**, 323-333.

Espada, D., Muñoz-Mateos, J. C., Gil de Paz, A., Sabater, J., Boissier, S., Verley, S., Athanassoula, E., Bosma, A., Leon, S., Verdes-Montenegro, L., Yun, M., Sulentic, J.: 2011, Star Formation in the Extended Gaseous Disk of the Isolated Galaxy CIG 96, *ApJ*, **736**, 20.

Espada, D., Verdes-Montenegro, L., Huchtmeier, W. K., Sulentic, J., Verley, S., Leon, S., Sabater, J.: 2011, The AMIGA sample of isolated galaxies. VIII. The rate of asymmetric H I profiles in spiral galaxies, *A&A*, **532**, A117.

Folatelli, G., et al. including **Tanaka, M.**: 2012, Unburned Material in the Ejecta of Type Ia Supernovae, *ApJ*, **745**, 74.

Froebrich, D., et al. including **Pyo, T. S.**: 2011, UWISH2 - the UKIRT Widefield Infrared Survey for H_2, *MNRAS*, **413**, 480-492.

Fujii, M. S., Baba, J., Saitoh, T. R., Makino, J., **Kokubo, E.**, Wada, K.: 2011, The Dynamics of Spiral Arms in Pure Stellar Disks, *ApJ*, **730**, 109

Fujii, Y., **Kroug, M.**, **Kaneko, K.**, **Gonzalez, A.**, **Uzawa, Y.**, **Kojima, T.**, **Kuroiwa, K.**, **Miyachi, A.**, Makise, K., Wang, Z., Shan, W.: 2011, Performance of the ALMA Band 10 SIS Receiver Prototype Model, *IEEE Trans. Appl. Supercond.*, **21**, 606-611.

Fujimoto, S.-I., **Kotake, K.**, Hashimoto, M.-A., Ono, M., Ohnishi, N.: 2011, Explosive Nucleosynthesis in the Neutrino-driven Aspherical Supernova Explosion of a Non-rotating 15 $M_{\rm sun}$ Star with Solar Metallicity, *ApJ*, **738**, 61.

Fujisawa, K., Sugiyama, K., Aoki, N., **Hirota, T.**, Mochizuki, N., Doi, A., **Honma, M.**, **Kobayashi, H.**, **Kawaguchi, N.**, Ogawa, H., Omodaka, T., Yonekura, Y.: 2012, Bursting Activity in a High-Mass Star-Forming Region G33.64-0.21 Observed with the 6.7 GHz Methanol Maser, *PASJ*, **64**, 17.

Fujita, K., Yamamoto, M.-Y., Abe, S., **Ishihara, Y.**, Iiyama, O., Kakinami, Y., Hiramatsu, Y., Furumoto, M., Takayanagi, H., Suzuki, T., Yanagisawa, T., Shoemaker, M., Ueda, M., Shiba, Y., Suzuki, M.: 2011, An Overview of JAXA's Ground Observation Activities for HAYABUSA Reentry, *PASJ*, **63**, 961-969.

Fukui, A., et al. including **Narita, N.**, **Tamura, M.**: 2011, Erratam: Measurements of Transit Timing Variations for WASP-5b, *PASJ*, **63**, 473-473.

Fukui, Y., et al. including **Kawamura, A.**, **Mizuno, N.**: 2012, A Detailed Study of the Molecular and Atomic Gas toward the

γ-Ray Supernova Remnant RX J1713.7-3946: Spatial TeV γ-Ray and Interstellar Medium Gas Correspondence, *ApJ*, **746**, 82.

Fukushima, T.: 2011, Precise and Fast Computation of General Complete Elliptic Integral of Second Kind, *Math. Comp.*, **80**, 1725-1743.

Fukushima, T.: 2011, Precise and Fast Computation of General Incomplete Elliptic Integral of Second Kind by Half and Double Argument Transformations, *J. Comp. Appl. Math.*, **235**, 4140-4148.

Fukushima, T.: 2011, Efficient Parallel Computation of All-Pairs *N*-body Acceleration by Do Loop Folding, *AJ*, **142**, 18-22.

Fukushima, T.: 2011, Precise and Fast Computation of a General Incomplete Elliptic Integral of Third Kind by Half and Double Argument Transformations, *J. Comp. Appl. Math.*, **236**, 1961-1975.

Fukushima, T.: 2012, Series Expansion of Symmetric Elliptic Integrals, *Math. Comp.*, **81**, 957-990.

Fukushima, T.: 2012, Numerical Computation of Spherical Harmonics of Arbitrary Degree and Order by Extending Exponent of Floating Point Numbers, *J. Geod.*, **86**, 271-285.

Furuya, K., **Aikawa, Y.**, Sakai, N., Yamamoto, S.: 2011, Carbon Isotope and Isotopomer Fractionation in Cold Dense Cloud Cores, *ApJ*, **731**, 38.

Gallagher, A. J., Ryan, S. G., Hosford, A., García Pérez, A. E., **Aoki, W.**, Honda, S.: 2012, The barium isotopic fractions in five metal-poor stars, *A&A*, **538**, A118.

García-Marín, M., et al. including **Nishiyama, S.**: 2011, Extended Submillimeter Emission of the Galactic Center and Near-infrared/submillimeter Variability of Its Supermassive Black Hole, *ApJ*, **738**, 158.

Genda, E., **Kokubo, E.**, Ida, S.: 2012, Merging Criteria for Giant Impacts of Protoplanets, *ApJ*, **744**, 137.

Giroletti, M., et al. including **Nagai, H.**: 2012, The kinematic of HST-1 in the jet of M 87, *A&A*, **538**, 538-541.

Giroletti, M., **Hada, K.**, Giovannini, G., Casadio, C., Beilicke, M., Cesarini, A., Cheung, C. C., Doi, A., Krawczynski, H., **Kino, M.**, Lee, N. P., **Nagai, H.**: 2012, The kinematic of HST-1 in the jet of M 87, *A&A*, **538**, L10.

Giroletti, M., Paragi, Z., Bignall, H., Doi, A., Foschini, L., Gabanyi, K. E., Reynolds, C., Blanchard, J., Campbell, R. M., Colomer, F., Hong, X., Kadler, M., **Kino, M.**, van Langevelde, H. J., **Nagai, H.**, Phillips, C., Sekido, M., Szomoru, A., Tzioumis, A. K.: 2011, Global e-VLBI observations of the gamma-ray narrow line Seyfert 1 PMN J0948+0022, *A&A*, **528**, L11.

Gonzalez, A., **Uzawa, Y.**, **Fujii, Y.**, **Kaneko, K.**, **Kuroiwa, K.**: 2011, A Horn-to-Horn Power Transmission System at Terahertz Frequencies, *IEEE Trans. THz Sci. and Technol.*, **1**, 416-424.

Gonzalez, A., **Uzawa, Y.**, **Fujii, Y.**, **Kaneko, K.**, **Kuroiwa, K.**: 2011, ALMA Band 10 tertiary optics, *Infrared Phys. And Technol.*, **54**, 488-496.

Goossens, S., **Ishihara, Y.**, **Matsumoto, K.**, **Sasaki, S.**: 2011, Local lunar gravity field analysis over the South Pole-Aitken basin from SELENE farside tracking data, *J. Geophys. Res.*, **117**, E02005.

Goossens, S., **Matsumoto, K.**, Liu, Q., **Kikuchi, F.**, Sato, K., **Hanada, H.**, **Ishihara, Y.**, **Noda, H.**, Kawano, N., Namiki, N., Iwata, T., Lemoine, F. G., Rowlands, D. D., Harada, Y., Chen, M.: 2011, Lunar gravity field determination using SELENE same-beam differential VLBI tracking data, *J. Geod.*, **85**, 205-228.

Goossens, S., **Matsumoto, K.**, Rowlands, D. D., Lemoine, F. G., **Noda, H.**, **Araki, H.**: 2011, Orbit determination of the SELENE satellites using multi-satellite data types and evaluation of SELENE gravity field models, *J. Geod.*, **85**, 487-504.

Gordon, K. D., et al. including **Kawamura, A.**, **Mizuno, N.**, **Muller, E.**: 2011, Surveying the Agents of Galaxy Evolution in the Tidally Stripped, Low Metallicity Small Magellanic Cloud (SAGE-SMC). I. Overview, *AJ*, **142**, 102.

Goto, M., Carmona, A., Linz, H., Stecklum, B., Henning, Th., Meeus, G., **Usuda, T.**: 2012, Kinematics of Ionized gas at 0.01 AU of TW Hya, *ApJ*, **748**, 6.

Goto, M., **Usuda, T.**, Geballe, T. R., Indriolo, N., McCall, B. J., Henning, Th., Oka, T.: 2011, Absorption-Line Survey of H_3^+ toward the Galactic Center Sources. III. Extent of Warm and Diffuse Clouds, *PASJ*, **63**, L13-L17.

Goto, T., Arnouts, S., Malkan, M., Takagi, T., Inami, H., Pearson, C., Wada, T., Matsuhara, H., **Yamauchi, C.**, Takeuchi, T. T., Nakagawa, T., Oyabu, S., Ishihara, D., Sanders, D. B., Le Floc'h, E., Lee, H. M., Jeong, W., Serjeant, S., Sedgwick, C.: 2011, Infrared luminosity functions of AKARI Sloan Digital Sky Survey galaxies, *MNRAS*, **414**, 1903-1913.

Goto, T., **Utsumi, Y.**, **Hattori, T.**, **Miyazaki, S.**, **Yamauchi, C.**: 2011, A Gunn-Peterson test with a QSO at z=6.4, *MNRAS*, **415**, L1-L5.

Goto, T., **Utsumi, Y.**, Walsh, J. R., **Hattori, T.**, **Miyazaki, S.**, Yamauchi, C.: 2012, Spectroscopy of the spatially extended Lyα emission around a quasar at z=6.4, *MNRAS*, **421**, L77-L81.

Grossi, M., **Hwang, N.**, Corbelli, E., Giovanardi, C., Okamoto, S., **Arimoto, N.**: 2011, Stellar structures in the outer regions of M 33, *A&A*, **533**, A91.

Hada, K., Doi, A., **Kino, M.**, **Nagai, H.**, **Hagiwara, Y.**, **Kawaguchi, N.**: 2011, An origin of the radio jet in M87 at the location of the central black hole, *Nature*, **477**, 185-187.

Hagiwara, Y., Baan, W. A., Kloeckner, H. R.: 2011, Very Long Baseline Interferometry Observations of NGC 6240: Resolving the Double Nuclei and Radio Supernovae, *AJ*, **142**, 17.

Han, S. C., Mazarico, E., Rowlands, D., Lemoine, F., **Goossens, S.**: 2011, New analysis of Lunar Prospector radio tracking data brings the nearside gravity field of the Moon with an unprecedented resolution, *Icarus*, **215**, 455-459.

Hanada, H., **Araki, H.**, **Tazawa, S.**, **Tsuruta, S.**, **Noda, H.**, **Asari, K.**, **Sasaki, S.**, Funazaki, K., Sato, A., Taniguchi, H., Kikuchi, M., Takahashi, T., Yamazaki, A., Ping, J., Kawano, N., Petrova, N., **Gouda, N.**, **Yano, T.**, Yamada, Y., **Niwa, Y.**, **Kono, T.**, Iwata, T.: 2012, Development of a digital zenith telescope for advanced astrometry, *Science China (Physics, Mechanics & Astronomy)*, **55**, 723-732.

Hanaoka, Y., **Suzuki, I.**, **Sakurai, T.**: 2011, Practical method to derive nonlinear response functions of cameras for scientific imaging, *Appl. Opt.*, **50**, 2401-2407.

Hanuš, J., et al. including **Yoshida, F.**, **Ito, T.**: 2011, A study of asteroid pole-latitude distribution based on an extended set of shape models derived by the lightcurve inversion method, *A&A*,

530, A134.

Hara, H., **Watanabe, T.**, Harra, L. K., Culhane, J., Leonard, Y., Peter, R.: 2011, Plasma Motions and Heating by Magnetic Reconnection in a 2007 May 19 Flare, *ApJ*, **741**, 107.

Hatsukade, B., Kohno, K., Endo, A., **Nakanishi, K.**, Ohta, K.: 2011, CO Observations of the Host Galaxy of GRB 000418 at z=1.1, *ApJ*, **738**, 33.

Hayashi, M., **Kodama, T.**, **Koyama, Y.**, **Tadaki, K.**, **Tanaka, I.**: 2011, Properties of star-forming galaxies in a cluster and its surrounding structure at z=1.46, *MNRAS*, **415**, 2670-2687.

Hesse, M., Neukirch, T., Schindler, K., Kuznetsova, M., **Zenitani, S.**: 2011, The Diffusion Region in Collisionless Magnetic Reconnection, *Space Sci. Rev.*, **160**, 3-23.

Hibon, P., **Kashikawa, N.**, Willott, C., **Iye, M.**, **Shibuya, T.**: 2011, Search for z~7 Lyα Emitters with the Suprime-Cam at the Subaru Telescope, *ApJ*, **744**, 89.

Hirano, T., **Narita, N.**, Sato, B., Winn, J. N., **Aoki, W.**, **Tamura, M.**, Taruya, A., Sato, Y.: 2011, Further Observations of the Tilted Planet XO-3: A New Determination of Spin-Orbit Misalignment, and Limits on Differential Rotation, *PASJ*, **63**, L57-L61.

Hirano, T., Suto, Y., Winn, J. N., Taruya, A., **Narita, N.**, Albrecht, S., Sato, B.: 2011, Improved Modeling of the Rossiter-McLaughlin Effect for Transiting Exoplanets, *ApJ*, **742**, 69.

Hiroi, T., Kaiden, H., Misawa, K., Niihara, T., Kojima, H., **Sasaki, S.**: 2011, Visible and near-infrared spectral survey of Martian meteorites stored at the National Institute of Polar Research, *Polar Sci.*, **5**, 337-344.

Hirota, A., **Kuno, N.**, Sato, N., Nakanishi, H., Tosaki, T., Sorai, K.: 2011, Giant Molecular Clouds in the Arm of IC 342, *ApJ*, **737**, 40.

Hirota, T., Sakai, T., Sakai, N., Yamamoto, S.: 2011, Detection of Two Carbon-chain-rich Cores: CB130-3 and L673-SMM4, *ApJ*, **736**, 4.

Hirota, T., Tsuboi, M., Fujisawa, K., **Honma, M.**, **Kawaguchi, N.**, **Kim, M. K.**, **Kobayashi, H.**, Imai, H., Omodaka, T., **Shibata, K. M.**, Shimoikura, T., Yonekura, Y.: 2011, Identification of Bursting Water Maser Features in Orion KL, *ApJ*, **739**, L59.

Honda, S., **Aoki, W.**, **Arimoto, N.**, Sadakane, K.: 2011, Enrichment of Heavy Elements in the Red Giant S 15-19 in the Sextans Dwarf Spheroidal Galaxy, *PASJ*, **63**, 523-529.

Honda, S., **Aoki, W.**, Beers, T. C., Takada-Hidai, M.: 2011, Spectroscopic Studies of Extremely Metal-poor Stars with the Subaru High Dispersion Spectrograph. V. The Zn-enhanced Metal-poor Star BS 16920-017, *ApJ*, **730**, 77.

Hong, P. K., Sugita, S., Okamura, N., Sekine, Y., **Terada, H.**, **Takatoh, N.**, **Hayano, Y.**, Fuse, T., **Pyo, T.-S.**, Kawakita, H., Wooden, D. H., Young, E. F., Lucey, P. G., Kurosawa, K., Genda, H., Haruyama, J., Furusho, R., Kadono, T., Nakamura, R., Kamata, S., Hamura, T., Sekiguchi, T., **Sôma, M.**, Noda, H., **Watanabe, J.**: 2011, A ground-based observation of the LCROSS impact events using the Subaru Telescope, *Icarus*, **214**, 21-29.

Hori, Y., Ikoma, M.: 2011, Gas Giant Formation with Small Cores Triggered by Envelope Pollution by Icy Planetesimals, *MNRAS*, **416**, 1419-1429.

Huang, K. Y., et al. including **Kuroda, D.**, **Yanagisawa, K.**: 2012, GRB 071112C: A Case Study of Different Mechanisms in X-Ray and Optical Temporal Evolution, *ApJ*, **748**, 44.

Humphrey, A., Zeballos, M., Aretxaga, I., Hughes, D. H., Yun, M. S., Cybulski, R., Wilson, G. W., Austermann, J., **Ezawa, H.**, **Kawabe, R.**, Kohno, K., Perera, T., Scott, K., Sánchez-Arguelles, D., Gutermuth, R.: 2011, AzTEC 1.1 mm Images of 16 Radio Galaxies at 0.5<z<5.2 and a Quasar at z=6.3, *MNRAS*, **418**, 74-89.

Huynh, A. N. L., Kang, W., Pak, S., Im, M., Lee, J.-E., Ho, L. C., **Pyo, T.-S.**, Daniel, T. J.: 2011, Medium Resolution Spectral Library of Late-Type Stellar Templates in Near-Infrared Band, *J. Korean Astron. Soc.*, **44**, 125-134.

Hwang, K.-H., et al. including **Fukui, A.**: 2011, OGLE-2009-BLG-023/MOA-2009-BLG-028: characterization of a binary microlensing event based on survey data, *MNRAS*, **413**, 1244-1250.

Hwang, N., Lee, M. G., Lee, J. C., Park, W.-K., Park, H. S., Kim, S. C., Park, J.-H.: 2011, Extended Star Clusters in the Remote Halo of the Intriguing Dwarf Galaxy NGC 6822, *ApJ*, **738**, 58.

Ikarashi, S., et al. including **Ezawa, H.**, **Furusawa, H.**, **Furusawa, J.**, **Iono, D.**, **Kawabe, R.**, **Nakanishi, K.**, **Takata, T.**: 2011, Detection of an ultrabright submillimetre galaxy in the Subaru/XMM-Newton Deep Field using AzTEC/ASTE, *MNRAS*, **415**, 3081-3096.

Ikeda, N., Kitamura, Y., Takita, S., Ueno, M., Suzuki, T., **Kawamura, A.**, Kaneda, H.: 2012, Far-infrared Imaging Observations of the Chamaeleon Region, *ApJ*, **745**, 48.

Imada, S., **Hara, H.**, **Watanabe, T.**, Murakami, I., Harra, L. K., Shimizu, T., Zweibel, E. G.: 2011, One-dimensional Modeling for Temperature-dependent Upflow in the Dimming Region Observed by Hinode/EUV Imaging Spectrometer, *ApJ*, **743**, 57.

Imai, H., Omi, R., Kurayama, T., **Nagayama, T.**, **Hirota, T.**, **Miyaji, T.**, Omodaka, T.: 2011, Multiple Outflows Traced by H_2O Masers around the Ultra-Compact H II Region G 34.26+0.15, *PASJ*, **63**, 1293-1311.

Imamura, T., Toda, T., Tomiki, A., Hirahara, D., Hayashiyama, T., Mochizuki, N., Yamamoto, Z. I., Abe, T., Iwata, T., **Noda, H.**, Futaana, Y., Ando, H., Häusler, B., Pätzold, M., Nabatov, A.: 2011, Radio occultation experiment of the Venus atmosphere and ionosphere with the Venus orbiter Akatsuki, *Earth, Planets and Space*, **63**, 493-501.

Imanishi, M., **Imase, K.**, **Oi, N.**, Ichikawa, K.: 2011, Subaru and Gemini High Spatial Resolution Infrared 18 micron Imaging Observations of Nearby Luminous Infrared Galaxies, *AJ*, **141**, 156.

Ishiguro, M., et al, including **Hanayama, H.**, **Watanabe, J.**, **Fujiwara, H.**, **Terada, H.**, **Yanagisawa, K.**, **Kuroda, D.**, **Miyaji, T.**, **Fukushima, H.**: 2011, Interpretation of (596) Scheila's Triple Dust Tails, *ApJ*, **741**, L24.

Ishiguro, M., et al, including **Hanayama, H.**, **Watanabe, J.**, **Fujiwara, H.**, **Terada, H.**, **Yanagisawa, K.**, **Kuroda, D.**, **Miyaji, T.**, **Fukushima, H.**: 2011, Observational Evidence for an Impact on the Main-belt Asteroid (596) Scheila, *ApJ*, **740**, L11.

Ito, H., **Kino, M.**, Kawakatu, N., Yamada, S.: 2011, Evolution of Non-thermal Shell Emission Associated with Active Galactic Nucleus Jets, *ApJ*, **730**, 120.

Iwai, K., Miyoshi, Y., Masuda, S., **Shimojo, M.**, Shiota, D., Inoue, S., Tsuchiya, F., Morioka, A., Misawa, H.: 2012, Solar Radio Type-I Noise Storm Modulated by Coronal Mass Ejections, *ApJ*, **744**, 167.

Iwata, I., Chamaraux, P.: 2011, Is the far border of the Local Void expanding?, *A&A*, **531**, A87.

Iye, M.: 2011, Subaru studies of the cosmic dawn, *Proc. Jpn. Acad. Ser. B*, **87**, 575-586.

Izumiura, H., Ueta, T., Yamamura, I., Matsunaga, N., Ita, Y., Matsuura, M., Nakada, Y., Fukushi, H., Mito, H., Tanabe, T., Hashimoto, O.: 2012, Extended dust shell of the carbon star U Hydrae observed with AKARI, *A&A*, **528**, A29.

Jain, R., Awasthi, A. K., Chandel, B., Bharti, L., **Hanaoka, Y.**, Kiplinger, A. L.: 2011, Probing the Role of Magnetic-Field Variations in NOAA AR 8038 in Producing a Solar Flare and CME on 12 May 1997, *Sol. Phys.*, **271**, 57-74.

Jiang, L., Egami, E., **Kashikawa, N.**, Walth, G., Matsuda, Y., Shimasaku, K., Nagao, T., Ota, K., Ouchi, M.: 2011, Keck Spectroscopy of Lyman-break Galaxies and Its Implications for the UV-continuum and Lyα Luminosity Functions at $z>6$, *ApJ*, **743**, 65.

Jung, T. H., Sohn, B. W., **Kobayashi, H.**, Sasao, T., **Hirota, T.**, **Kameya, O.**, Choi, Y. K., Chung, H. S.: 2011, First Simultaneous Dual-Frequency Phase Referencing VLBI Observation with VERA, *PASJ*, **63**, 375-385.

Junhan, K., et al. including **Hanayama, H.**, **Yanagisawa, K.**, **Watanabe, J.**: 2012, Multiband Optical Observation of the P/2010 A2 Dust Tail, *ApJ*, **746**, L11.

Kamezaki, T., Nakagawa, A., Omodaka, T., Kurayama, T., Imai, H., Tafoya, D., Matsui, M., Nishida, Y., **Nagayama, T.**, **Honma, M.**, **Kobayashi, H.**, **Miyaji, T.**, Mine, T.: 2012, VLBI Astrometry of the Semiregular Variable RX Bootis, *PASJ*, **64**, 7.

Kamiński, T., Tylenda, R., **Deguchi, S.**: 2011, A Molecular Cloud Within the Light Echo of V838 Monocerotis, *A&A*, **529**, A48.

Käppeler, F., Gallino, R., Bisterzo, S., **Aoki, W.**: 2011, The s process: Nuclear physics, stellar models, and observations, *Rev. Mod. Phys.*, **83**, 157-194.

Kashikawa, N., et al. including **Hattori, T.**, **Iye, M.**, **Furusawa, H.**, **Shibuya, T.**, **Ishizaki, Y.**, **Toshikawa, J.**: 2011, Completing the Census of Lyα Emitters at the Reionization Epoch, *ApJ*, **734**, 119.

Kato, Y., Steiner, O., Steffen, M., **Suematsu, Y.**: 2011, Excitation of Slow Modes in Network Magnetic Elements Through Magnetic Pumping, *ApJ*, **730**, L24.

Kawakatu, K., **Ohsuga, K.**: 2011, New Method for Exploring Super-Eddington AGNs by Near-infrared Observations, *MNRAS*, **417**, 2562-2570.

Kawamura, S., et al. including **Agatsuma, K.**, **Akutsu, T.**, **Chen, D.**, **Fujimoto, M.-K.**, **Hayama, K.**, **Ishizaki, H.**, **Izumi, K.**, **Kotake, K.**, **Nakamura, K.**, **Ohishi, N.**, **Sotani, H.**, **Takahashi, R.**, **Torii, Y.**, **Ueda, A.**: 2011, The Japanese space gravitational wave antenna: DECIGO, *Class. Quantum Grav.*, **28**, 094011.

Kawamura, T., **Morota, T.**, Kobayashi, N., Tanaka, S.: 2011, Cratering asymmetry on the Moon: New insight from the Apollo Passive Seismic Experiment, *Geophys. Res. Lett.*, **38**, L15201.

Kawate, T., **Hanaoka, Y.**, Ichimoto, K., Miura, N.: 2011, Seeing measurements using the solar limb - I. Comparison of evaluation methods for the Differential Image Motion Monitor, *MNRAS*, **416**, 2154-2162.

Kawate, T., Nishizuka, N., Oi, A., Ohyama, M., **Nakajima, H.**: 2012, Hard X-ray and Microwave emissions from Solar Flares with Hard Spectral Indices, *ApJ*, **747**, 131.

Kim, E., Kim, M., **Hwang, N.**, Lee, M. G., Chun, M.-Y., Ann, H. B.: 2011, A wide-field survey of satellite galaxies around the spiral galaxy M106, *MNRAS*, **412**, 1881-1894.

Kim, J., Pak, S., Choi, M., Kang, W., **Kandori, R.**, **Tamura, M.**, Nagata, T., **Kwon, J.**, Kato, D., Jaffe, D. T.: 2011, Near-IR Polarimetry Around 30 Doradus: I. Separation of the Galactic Sources, *J. Korean Astron. Soc.*, **44**, 135-142.

Kim, J., Ishiguro, M., **Hanayama, H.**, Hasegawa, S., Usui, F., **Yanagisawa, K.**, Sarugaku, Y., **Watanabe, J.**, Yoshida, M.: 2012, Multiband Optical Observation of the P/2010 A2 Dust Tail, *ApJ*, **746**, L11.

Kimura, J., Kawamura, T., Morito, H., **Morota, T.**, Honda, C., Kuramoto, K., Okada, T.: 2011, Sublimation's impact on temporal change of albedo dichotomy on Iapetus, *Icarus*, **214**, 596-605.

Kominami, J. D., Makino, J., Daisaka, H.: 2011, Binary Formation in Planetesimal Disks I. Equal Mass Planetesimals, *PASJ*, **63**, 1331-1344.

Komiya, Y.: 2011, Extremely Metal-poor Stars and a Hierarchical Chemical Evolution Model, *ApJ*, **736**, 73.

Komugi, S., Tosaki, T., Kohno, K., Tsukagoshi, T., **Nakanishi, K.**, **Sawada, T.**, **Kawabe, R.**, **Ezawa, H.**, **Kuno, N.**, **Onodera, S.**, Tamura, Y., Wilson, G. M., Yun, M. S., Scott, K., Perera, T. A., Austermann, J. E., Hughes, D. H., Aretxaga, I., Tanaka, K., Muraoka, K., **Miura, R.**, Egusa, F.: 2011, Temperature Variations of the Cold Dust in the Triangulum Galaxy M33, *PASJ*, **63**, 1139-1150.

Koo, B.-C., et al. including **Tatematsu, K.-I.**, **Kawabe, R.**, **Ezawa, H.**: 2011, IRAS 15099-5856: Remarkable Mid-Infrared Source with Prominent Crystalline Silicate Emission Embedded in the Supernova Remnant MSH15-52, *ApJ*, **732**, 6.

Kotake, K., Iwakami-Nakano, W., Ohnishi, N.: 2011, Effects of Rotation on Stochasticity of Gravitational Waves in the Nonlinear Phase of Core-collapse Supernovae, *ApJ*, **736**, 124.

Koyama, Y., **Kodama, T.**, **Nakata, F.**, Shimasaku, K., Okamura, S.: 2011, Red Star-forming Galaxies and Their Environment at $z=0.3$ Revealed by Panoramic Hα Imaging, *ApJ*, **734**, 66.

Kubo, M., Ichimoto, K., Lites, B. W., Shine, R. A.: 2011, Temporal Relation Between the Disappearance of Penumbral Fine-scale Structure and Evershed Flow, *ApJ*, **731**, 84.

Kurayama, T., Nakagawa, A., **Sawada-Satoh, S.**, **Sato, K.**, **Honma, M.**, **Sunada, K.**, **Hirota, T.**, Imai, H.: 2011, Annual Parallax Measurements of an Infrared Dark Cloud, MSXDC G034.43+00.24 with VERA, *PASJ*, **63**, 513-525.

Kuzuhara, M., **Tamura, M.**, **Ishii, M.**, **Kudo, T.**, **Nishiyama, S.**, **Kandori, R.**: 2011, The Widest-separation Substellar Companion Candidate to a Binary T Tauri Star, *AJ*, **141**, 119.

Kwon, J., **Tamura, M.**, **Kandori, R.**, **Kusakabe, N.**, **Hashimoto, J.**, **Nakajima, Y.**, **Nakamura, F.**, Nagayama, T., Nagata, T., Hough, J. H., Werner, M. W., Teixeira, P. S.: 2011, Complex Scattered Radiation Fields and Multiple Magnetic Fields in the Protostellar Cluster in NGC 2264, *ApJ*, **741**, 35.

Labrosse, N., Schmieder, B., Heinzel, P., **Watanabe, T.**: 2011, EUV lines observed with EIS/Hinode in a solar prominence, *A&A*, **531**, A69.

Langford, S. V., Wyithe, J. S. B., Turner, E. L., Jenkins, E. B.,

Narita, N., Liu, X., Suto, Y., Yamada, T.: 2011, A comparison of spectroscopic methods for detecting starlight scattered by transiting hot Jupiters, with application to Subaru data for HD 209458b and HD 189733b, *MNRAS*, **415**, 673-686.

Lara, M., **Fukushima, T.**, Ferrer, S.: 2011, Ceres' Rotation Solution under the Gravitational Torque of the Sun, *MNRAS*, **415**, 461-469.

Lee, J. H., **Hwang, N.**, Lee, M. G.: 2011, H II Region Luminosity Function of the Interacting Galaxy M51, *ApJ*, **735**, 75.

Leroy, A. K., Bolatto, A., Gordon, K., Sandstrom, K., Gratier, P., Rosolowsky, E., Engelbracht, C. W., **Mizuno, N.**, Corbelli, E., Fukui, Y., **Kawamura, A.**: 2011, The CO-to-H_2 Conversion Factor from Infrared Dust Emission across the Local Group, *ApJ*, **737**, 12.

Lisenfeld, U., **Espada, D.**, Verdes-Montenegro, L., **Kuno, N.**, Leon, S., Sabater, J., Sato, N., Sulentic, J., Verley, S., Yun, M. S.: 2011, The AMIGA sample of isolated galaxies. IX. Molecular gas properties, *A&A*, **534**, A102.

Ly, C., Malkan, M. A., **Kashikawa, N.**, Ota, K., Shimasaku, K., **Iye, M.**, Currie, T.: 2012, Dust Attenuation and Hα Star Formation Rates of $z\sim0.5$ Galaxies, *ApJ*, **747**, L16.

Ly, C., Malkan, M. A., **Hayashi, M.**, Motohara, K., **Kashikawa, N.**, Shimasaku, K., Nagao, T., Grady, C.: 2011, A Census of Star-forming Galaxies at $z=1-3$ in the Subaru Deep Field, *ApJ*, **735**, 91.

Lyo, A.-R., **Ohashi, N.**, Qi, C., Wilner, D. J., Su, Y.-N.: 2011, Millimeter Observations of the Transition Disk around HD 135344B (SAO 206462), *AJ*, **142**, 151.

Maciejewski, G., Dimitrov, D., Neuhäuser, R., Tetzlaff, N., Niedzielski, A., Raetz, St., Chen, W. P., Walter, F., Marka, C., Baar, S., Krejcová, T., Budaj, J., Krushevska, V., **Tachihara, K.**, Takahashi, H., Mugrauer, M.: 2011, Transit timing variation and activity in the WASP-10 planetary system, *MNRAS*, **411**, 1204-1212.

Maciejewski, A., Przybylska, M., **Yoshida, H.**: 2012, Necessary conditions for the existence of additional first integrals for Hamiltonian systems with homogeneous potential, *Nonlinearity*, **25**, 255-277.

Makise, K., Terai, H., Takeda, M., **Uzawa, Y.**, Wang, Z.: 2011, Characterization of NbTiN Thin Films Deposited on Various Substrates, *IEEE Trans. Appl. Supercond.*, **21**, 139-142.

Maruyama, T., **Kajino, T.**, Yasutake, N., Cheoun, M. K., Ryu, C.: 2011, Asymmetric Neutrino Emission from Magnetized Proto-Neutron Stars in fully Relativistic Framework including Hyperons, *Phys. Rev. D*, **83**, 081303.

Matsuda, Y., Smail, I., Geach, J. E., Best, P. N., Sobral, D., **Tanaka, I.**, **Nakata, F.**, Ohta, K., Kurk, J., **Iwata, I.**, Bielby, R., Wardlow, J. L., Bower, R. G., Ivison, R. J., **Kodama, T.**, Yamada, T., Mawatari, K., Casali, M.: 2011, An Hα search for overdense regions at $z=2.23$, *MNRAS*, **416**, 2041-2059.

Matsui, H., Saitoh, T. R., Makino, J., Wada, K., **Tomisaka, K.**, **Kokubo, E.**, Daisaka, H., Okamoto, T., Yoshida, N.: 2012, Origin of Multiple Nuclei in Ultraluminous Infrared Galaxies, *ApJ*, **746**, 26.

Matsumoto, N., **Honma, M.**, Isono, Y., Ujihara, H., Kimura, K., Matsumoto, K., **Sawada-Satoh, S.**, Doi, A., Fujisawa, K., **Ueno, Y.**: 2011, Astrometry of 6.7 GHz Methanol Maser toward W 3(OH) with Japanese VLBI Network, *PASJ*, **63**, 1345-1356.

Matsunaga, N., Kawadu, T., **Nishiyama, S.**, Nagayama, T., Kobayashi, N., **Tamura, M.**, Bono, G., Feast, M. W., Nagata, T.: 2011, Three classical Cepheid variable stars in the nuclear bulge of the Milky Way, *Nature*, **188**, 188-190.

Matsuo, T., Fukagawa, M., Kotani, T., Itoh, Y., **Tamura, M.**, Nakagawa, T., Enya, K., SCI Team: 2011, Direct detection and spectral characterization of outer exoplanets with the SPICA coronagraph instrument (SCI), *Adv. Space Res.*, **47**, 1455-1462.

Maury, A., **Ohashi, N.**, André, P.: 2012, Subarcsecond SMA observations of the prototype Class 0 object VLA1623 at 1.3 mm: a single protostar with a structured outflow cavity?, *A&A*, **539**, A130.

Meech, K. J., et al. including **Fujiyoshi, T.**, **Furusho, R.**, **Sato, M.**, **Takato, N.**, **Watanabe, J.**, **Yamashita, T.**: 2011, EPOXI: Comet 103P/Hartley 2 Observations from a Worldwide Campaign, *ApJ*, **734**, L1.

Michikoshi, S., **Kokubo, E.**, Inutsuka, S.: 2012, Secular Gravitational Instability of a Dust Layer in Shear Turbulence, *ApJ*, **746**, 35.

Michikoshi, S., **Kokubo, E.**: 2011, Formation of a Propeller Structure by a Moonlet in a Dense Planetary Ring, *ApJ*, **732**, L23.

Mineshige, S., **Ohsuga, K.**: 2011, Supercritical accretion and ULXs - what can we achieve?, *Astron. Nachr.*, **332**, 402.

Miyoshi, M., **Asaki, Y.**, **Wada, K.**, **Imai, H.**: 2012, Analysis of H_2O masers in Sharpless 269 using VERA archival data? Effect of maser structures on astrometric accuracy, *New Astron.*, **17,** 553-564.

Miyoshi, M., Shen, Z. Q., **Oyama, T.**, Takahashi, R., **Kato, Y.**: 2011, Oscillation Phenomena in the Disk around the Massive Black Hole Sagittarius A*, *PASJ*, **63**, 1093-1116.

Mizukami, T., et al. including **Mizumoto, Y.**: 2011, CANGAROO-III Observation of TeV Gamma Rays from the Unidentified Gamma-Ray Source HESS J1614-518, *ApJ*, **740**, 78.

Moritani, Y., Nogami, D., Okazaki, A. T., **Imada, A.**, **Kambe, E.**, Honda, S., Hashimoto, O., Ichikawa, K.: 2011, Drastic Spectroscopic Variability of the Be/X-Ray Binary Ariel 0535+262/V725 Tau during and after the 2009 Giant Outburst, *PASJ*, **63**, 25-29.

Motogi, K., Sorai, K., **Honma, M.**, Minamidani, T., Takekoshi, T., **Akiyama, K.**, Tateuchi, K., Hosaka, K., Ohishi, Y., Watanabe, Y., Habe, A., **Kobayashi, H.**: 2011, Intermittent maser flare around the high-mass young stellar object G353.273+0.641 - I. Data and overview, *MNRAS*, **417**, 238-249.

Muraki, Y., et al. including **Fukui, A.**: 2011, Discovery and Mass Measurements of a Cold, 10 Earth Mass Planet and Its Host Star, *ApJ*, **741**, 22.

Muraoka, K., Tosaki, T., **Miura, R.**, **Onodera, S.**, **Kuno, N.**, **Nakanishi, K.**, **Kaneko, H.**, **Komugi, S.**: 2012, ^{13}CO($J=1-0$) On-the-fly Mapping of the Giant H II Region NGC 640: Variation in Molecular Gas Density and Temperature due to Sequential Star Formation, *PASJ*, **64**, 3.

Murray, D. N., et al. including **Tamura, M.**: 2011, Blue not brown: UKIRT Infrared Deep Sky Survey T dwarfs with suppressed K-band flux, *MNRAS*, **414**, 575-586.

Muto, T., et al. including **Hashimoto, J.**, **Ohashi, N.**, **Fukue, T.**, **Guyon, O.**, **Hayano, Y.**, **Hayashi, S.**, **Ishii, M.**, **Iye, M.**,

Kandori, R., **Kudo, T.**, **Kusakabe, N.**, **Kuzuhara, M.**, **Miyama, S.**, **Morino, J.-I.**, **Nishimura, T.**, **Pyo, T.-S.**, **Suto, H.**, **Suzuki, R.**, **Takato, N.**, **Terada, H.**, **Tomono, D.**, **Takami, H.**, **Usuda, T.**, **Tamura, M.**: 2012, Discovery of Small-scale Spiral Structures in the Disk of SAO 206462 (HD 135344B): Implications for the Physical State of the Disk from Spiral Density Wave Theory, *ApJ*, **748**, 22.

Mužić, K., Scholz, A., Geers, V., Jayawardhana, R., **Tamura, M.**: 2012, Substellar Objects in Nearby Young Clusters (SONYC). V. New Brown Dwarfs in ρ Ophiuchi, *ApJ*, **744**, 134.

Nagayama, T., Omodaka, T., Handa, T., **Honma, M.**, **Kobayashi, H.**, **Kawaguchi, N.**, **Ueno, Y.**: 2011, Astrometry of Galactic Star-Forming Region G48.61+0.02 with VERA, *PASJ*, **63**, 719-725.

Nakajima, T., **Morino, J.-I.**: 2012, Potential Members of Stellar Kinematic Groups within 30 pc of the Sun, *AJ*, **143**, 2-17.

Nakamura, F., Li, Z.-Y.: 2011, Clustered Star Formation in Magnetic Clouds: Properties of Dense Cores Formed in Outflow-driven Turbulence, *ApJ*, **740,** 36.

Nakamura, F., Miura, T., Kitamura, Y., **Shimajiri, Y.**, **Kawabe, R.**, Ikeda, N., Tsukagoshi, T., Momose, M., Nishi, R., Li, Z.-Y.: 2012, Evidence for Cloud-Cloud Collision and Parsec-Scale Stellar Feedback within the L1641-N Region, *ApJ*, **746**, 25.

Nakamura, F., Sugitani, K., **Shimajiri, Y.**, Tsukagoshi, T., **Higychi, A.**, Nishiyama, S., **Kawabe, R.**, Takami, M., Karr, J. L., Gutermuth, R. A., Wilson, G.: 2011, Molecular Outflows from the Protocluster Serpens South, *ApJ*, **737**, 56.

Nakamura, K., Nishizawa, A., **Fujimoto, M.-K.**: 2012, Evaluation of weak measurements to all orders, *Phys. Rev. A*, **85**, 012113.

Nakamura, K.: 2011, General formulation of general-relativistic higher-order gauge-invariant perturbation theory, *Class. Quantum Grav.*, **28**, 12200.

Narita, N., Hirano, T., Sato, B., Harakawa, H., **Fukui, A.**, **Aoki, W.**, **Tamura, M.**: 2011, XO-2b: a Prograde Planet with Negligible Eccentricity and an Additional Radial Velocity Variation, *PASJ*, **63**, L67-L71.

Narukage, N., Sakao, T., **Kano, R.**, **Hara, H.**, **Shimojo, M.**, **Bando, T.**, Urayama, F., Deluca, E., Golub, L., Weber, M., Grigis, P., Cirtain, J., Tsuneta, S.: 2011, Coronal-Temperature-Diagnostic Capability of the Hinode/X-Ray Telescope Based on Self-Consistent Calibration, *Sol. Phys.*, **269**, 169-236.

Naruse, M., **Sekimoto, Y.**, **Miyachi, A.**, **Uzawa, Y.**, **Nitta, T.**, **Noguchi, T.**: 2012, Development of Crystal Al MKIDs by Molecular Beam Epitaxy, *J. of Low. Temp. Phys.*, **167**, 373-378.

Neuhäuser, R., et al. including **Tachihara, K.**: 2011, The Young Exoplanet Transit Initiative (YETI), *Astron. Nachr.*, **332**, 547-561.

Nicholas, B. P., Rowell, G., Burton, M. G., Walsh, A. J., Fukui, Y., **Kawamura, A.**, Maxted, N. I.: 2012, A 7 mm line survey of the shocked and disrupted molecular gas towards the W28 field TeV gamma-ray sources, *MNRAS*, **419**, 251-266.

Niino, Y.: 2011, Revisiting the metallicity of long-duration gamma-ray burst host galaxies: the role of chemical inhomogeneity within galaxies, *MNRAS*, **417**, 567-572.

Nishizuka, N., **Hara, H.**: 2011, Spectroscopic Observations of Continuous Outflows and Propagating Waves from NOAA 10942 with Extreme Ultraviolet Imaging Spectrometer/Hinode, *ApJ*, **737**, L43.

Noguchi, T., Suzuki, T., **Tamura, T.**: 2011, Subgap tunneling current at low temperature in Nb/Al-AlN/Nb SIS junctions, *IEEE Trans. Appl. Supercond.*, **21**, 320-328.

Noguchi, T., Suzuki, T., **Tamura, T.**: 2012, SIS Junctions for Millimeter and Submillimeter Wave Mixers, *IEICE Trans. Electron.*, **95-C**(3), 320-328.

Oda, H., Machida, M., Nakamura, K. E., Matsumoto, R., Narayan, R.: 2012, Global Structure of Optically Thin, Magnetically Supported, Two-Temperature, Black Hole Accretion Disks, *PASJ*, **64**, 15.

Ogawa, Y., et al. including **Sasaki, S.**, **Morota, T.**: 2011, The widespread occurrence of high-calcium pyroxene in bright-ray craters on the Moon and implications for lunar-crust composition, *Geophys. Res. Lett.*, **38**, L17202.

Oguri M., **Hamana T.**: 2011, Detailed cluster lensing profiles at large radii and the impact on cluster weak lensing studies, *MNRAS*, **414**, 1851-1861.

Oh, S. J., Roh, D. G., Wajima, K., **Kawaguchi, N.**, Byun, D. Y., Yeom, J. H., Je, D. H., Han, S. T., **Iguchi, S.**, Kawakami, K., Ozeki, K., **Kobayashi, H.**, Sasao, T., Sohn, B. W., Kim, J. H., Miyazaki, A., **Oyama, T.**, Kurayama, T.: 2011, Design and Development of a High-Speed Data-Acquisition System for the Korean VLBI Network, *PASJ*, **63**, 1229-1242.

Ohsuga, K., Mineshige, S.: 2011, Global Structure of Three Distinct Accretion Flows and Outflows around Black Holes through Two-Dimensional Radiation-Magnetohydrodynamic Simulations, *ApJ*, **736**, 2.

Ohtsuka, K., Abe, S., **Ito, T.**, Nakamura, T., Abe, M., Yano, H., **Watanabe, J.**: 2011, Do Meteoroids Originating from Near-Earth Asteroid (25143) Itokawa Exist?, *PASJ*, **63**, L73-L77.

Ojha, D. K., Samal, M. R., Pandey, A. K., Bhatt, B. C., Ghosh, S. K., Sharma, S., **Tamura, M.**, Mohan, V., Zinchenko, I.: 2011, Star Formation Activity in the Galactic H II Complex S255-S257, *ApJ*, **738**, 156.

Okamoto, S., **Arimoto, N.**, **Yamada, Y.**, Onodera, M.: 2012, Stellar Populations and Structural Properties of Ultra Faint Dwarf Galaxies, Canes Venatici I, Boötes I, Canes Venatici II, and Leo IV, *ApJ*, **744**, 96.

Okamoto, T. J., De Pontieu, B.: 2011, Propagating Waves Along Spicules, *ApJ*, **736**, L24.

Okumura, S., **Yamashita, T.**, Sako, S., Miyata, T., Honda, M., Kataza, H., Okamoto, Y. K.: 2011, Physical Relation of Source I to IRc2 in the Orion KL Region, *PASJ*, **63**, 823-834.

Ono, Y., Ouchi, M., Mobasher, B., Dickinson, M., Penner, K., Shimasaku, K., Weiner, B. J., Kartaltepe, J. S., Nakajima, K., Nayyeri, H., Stern, D., **Kashikawa, N.**, Spinrad, H.: 2012, Spectroscopic Confirmation of Three z-dropout Galaxies at z = 6.844-7.213: Demographics of Lyα Emission in $z \sim 7$ Galaxies, *ApJ*, **744**, 83.

Orozco Suárez, D., **Katsukawa, Y.**: 2012, The Distribution of Quiet-Sun Magnetic Fields at Different Heliocentric Angles, *ApJ*, **746**, 182.

Oshino, S., Funato, Y., Makino, J.: 2011, Particle-Particle Particle-Tree: A Direct-Tree Hybrid Scheme for Collisional *N*-Body Simulations, *PASJ*, **63**, 881-892.

Otsubo, T., Kunimori, H., **Noda, H.**, **Hanada, H.**, **Araki, H.**, **Kayatama, M.**: 2011, Asymmetric dihedral angle offsets for large-size lunar laser ranging retroreflectors, *Earth, Planets and Space*, **63**, e13-e16.

Otsuji, K., Kitai, R., Ichimoto, K., Shibata, K.: 2011, Statistical Study on the Nature of Solar-Flux Emergence, *PASJ*, **63**, 1047-1057.

Palacios, A., **Parthasarathy, M.**, Bharat Kumar, Y., Jasniewicz, G.: 2012, Weak G-band stars on the H-R diagram: clues to the origin of the Li anomaly, *A&A*, **538**, A68.

Paradis, D., Paladini, R., Noriega-Crespo, A., Lagache, G., **Kawamura, A.**, Onishi, T., Fukui, Y.: 2011, Spitzer Characterization of Dust in the Ionized Medium of the Large Magellanic Cloud, *ApJ*, **735**, 6.

Pavlenko, E. P., Kato, T., Antonyuk, O. I., **Imada, A.**, **Ishioka, R.**, Maehara, H.: 2011, Features of the orbital variability in the brightness of the WZ Sge type dwarf nova V1108 Her, *Astrophysics*, **54**, 483-495.

Pehlivan, Y., Balantekin, A. B., **Kajino, T.**, Yoshida, T.: 2011, Invariants of Collective Neutrino Oscillations, *Phys. Rev. D*, **84**, 065008.

Petrov, L., **Honma, M.**, **Shibata, S. M.**: 2012, The KCAL VERA 22 GHz Calibrator Survey, *AJ*, **143**, 35.

Portas, A., Scott, T. C., Brinks, E., Bosma, A., Verdes-Montenegro, L., Heesen, V., **Espada, D.**, Verley, S., Sulentic, J., Sengupta, C., Athanassoula, E., Yun, M.: 2011, H I Asymmetries in the Isolated Galaxy CIG 292, *ApJ*, **739**, L27.

Reeves, K. K., Gibson, S. E., Kucera, T. A., Hudson, H. S., **Kano, R.**: 2012, Thermal Properties of a Solar Coronal Cavity Observed with the X-Ray Telescope on Hinode, *ApJ*, **746**, 146.

Reiter, M., Shirley, Y. L., Wu, J., Brogan, C., Wootten, A., **Tatematsu, K.-I.**: 2011, Evidence for Inflow in High-Mass Star-Forming Clumps, *ApJ*, **740**, 40.

Reiter, M., Shirley, Y. L., Wu, J., Brogan, C., Wootten, A., **Tatematsu, K.-I.**: 2011, The Physical Properties of High-Mass Star-forming Clumps: A Systematic Comparison of Molecular Tracers, *ApJS*, **195**, 1.

Reznikova, V. E., **Shibasaki, K.**, Sych, R. A., Nakariakov, V. M.: 2012, Three-minute Oscillations above Sunspot Umbra Observed with the Solar Dynamics Observatory/Atmospheric Imaging Assembly and Nobeyama Radioheliograph, *ApJ*, **746**, 119.

Rusu, C. E., **Oguri, M.**, Inada, N., Kayo, I., **Iye, M.**, **Hayano, Y.**, **Oya, S.**, **Hattori, M.**, **Saito, Y.**, **Ito, M.**, **Minowa, Y.**, **Pyo, T.-S.**, **Terada, H.**, **Takami, H.**, **Watanabe, M.**: 2011, SDSS J133401.39+331534.3: A New Subarcsecond Gravitationally Lensed Quasar, *ApJ*, **738**, 30.

Rygl, K. L. J., Brunthaler, A., Sanna, A., Menten, K. M., Reid, M. J., van Langevelde, H. J., **Honma, M.**, Torstensson, K. J. E., Fujisawa, K.: 2012, Parallaxes and proper motions of interstellar masers toward the Cygnus X star-forming complex. I. Membership of the Cygnus X region, *A&A*, **539**, A79.

Ryu, C. Y., Maruyama, T., **Kajino, T.**, Cheoun, M. K.: 2011, Properties of the proto-neutron star with smeared trapped neutrinos, *Phys. Rev. C*, **83**, 018802.

Saito, R. K., et al. including **Tamura, M.**: 2012, VVV DR1: The first data release of the Milky Way bulge and southern plane from the near-infrared ESO public survey VISTA variables in the Vía Láctea, *A&A*, **537**, A107.

Sakai, T., Sakai, N., Furuya, K., **Aikawa, Y.**, **Hirota, T.**, Yamamoto, S.: 2012, DNC/HNC Ratio of Massive Clumps in Early Evolutionary Stages of High-mass Star Formation, *ApJ*, **747**, 140.

Sakamoto, K., Mao, R.-Q., Matsushita, S., Peck, A. B., **Sawada, T.**, Wiedner, M. C.: 2011, Star-forming Cloud Complexes in the Central Molecular Zone of NGC 253, *ApJ*, **735**, 19.

Sakari, C. M., Venn, K. A., Irwin, M., **Aoki, W.**, **Arimoto, N.**, Dotter, A.: 2011, Detailed Chemical Abundances of Four Stars in the Unusual Globular Cluster Palomar 1, *ApJ*, **740**, 106.

Sakata, Y., Morokuma, T., Minezaki, T., Yoshii, Y., **Kobayashi, Y.**, Koshida, S., Sameshima, H.: 2011, Ultraviolet Continuum Color Variability of Luminous Sloan Digital Sky Survey QSOs, *ApJ*, **731**, 50.

Sarkar, G., García-Hernández, D. A., **Parthasarathy, M.**, Manchado, A., García-Lario, P., **Takeda, Y.**: 2012, High-resolution spectroscopy of the high-velocity hot post-AGB star LS III +52°24 (IRAS 22023+5249), *MNRAS*, **421**, 679-699.

Sato, M., Takada, M., **Hamana, T.**, Matsubara, T.: 2011, Simulations of Wide-field Weak-lensing Surveys. II. Covariance Matrix of Real-space Correlation Functions, *ApJ*, **731**, 76.

Scholz, A., Muzic, K., Geers, V., Bonavita, M., Jayawardhana, R., **Tamura, M.**: 2012, Substellar Objects in Nearby Young Clusters (SONYC). IV. A Census of Very Low Mass Objects in NGC 1333, *ApJ*, **744**, 6.

Selhorst, C. L., Giménez de Castro, C. G., Válio, A., Costa, J. E. R., **Shibasaki, K.**: 2011, The Behavior of the 17 GHz Solar Radius and Limb Brightening in the Spotless Minimum XXIII/XXIV, *ApJ*, **734**, 64.

Shen, Z., Li, J., Miyazaki, A., Huang, L., Sault, R. J., **Miyoshi, M.**, Tsuboi, M., Tsutsumi, T.: 2011, Intra-Day Variability of Sagittarius A* at Multi-Wavelengths, *J. Astrophys. Astron.*, **32**, 13-18.

Shibasaki, K., Alissandrakis, C. E., Pohjolainen, S.: 2011, Radio Emission of the Quiet Sun and Active Regions (Invited Review), *Sol. Phys.*, **273**, 309-337.

Shimizu, T., Ichimoto, K., **Suematsu, Y.**: 2012, Precursor of Sunspot Penumbral Formation Discovered with Hinode Solar Optical Telescope Observations, *ApJ*, **747**, L18.

Shimoikura, T., Dobashi, K., Sakurai, T., **Takano, S.**, Nishiura, S., **Hirota, T.**: 2012, Molecular Line Observations of MCLD 123.5+24.9 in the Polaris Cirrus, *ApJ*, **745**, 195.

Shin, I.-G., et al. including **Fukui, A.**: 2012, Microlensing Binaries Discovered through High-magnification Channel, *ApJ*, **746**, 127.

Shiozaki, S., Imai, H., Tafoya, D., Omodaka, T., **Hirota, T.**, **Honma, M.**, Matsui, M., **Ueno, Y.**: 2011, H_2O Maser Motions and the Distance of the Star-Forming Region G192.16-3.84, *PASJ*, **63**, 1219-1228.

Sitko, M. L., et al. including **Tamura, M.**: 2012, Variability of Disk Emission in Pre-main Sequence and Related Stars. II. Variability in the Gas and Dust Emission of the Herbig Fe Star SAO 206462, *ApJ*, **745**, 29.

Skowron, J., et al. including **Fukui, A.**: 2011, Binary Microlensing Event OGLE-2009-BLG-020 Gives Verifiable Mass, Distance, and Orbit Predictions, *ApJ*, **738**, 87.

Sofue, Y., **Nagayama, T.**, Matsui, M., Nakagawa, A.: 2011, Near-Solar-Circle Method for Determining the Galactic Constants, *PASJ*, **63**, 867-831.

Song, Q., Huang, G., **Nakajima, H.**: 2011, Co-Analysis of Solar Microwave and Hard X-Ray Spectral Evolution1. In Two Frequency and Energy Ranges, *ApJ*, **734**, 113.

Sotani, H.: 2011, Torsional oscillations in tensor-vector-scalar theory, *Phys. Rev. D*, **83**, 124030.

Sotani, H.: 2011, Constraints on Pasta Structure of Neutron Stars from Oscillations in Giant Flares, *MNRAS*, **417**, L70-L73.

Strader, J., Romanowsky, A. J., Brodie, J. P., Spitler, L. R., Beasley, M. A., Arnold, J. A., **Tamura, N.**, Sharples, R., **Arimoto, N.**: 2011, Wide-field Precision Kinematics of the M87 Globular Cluster System, *ApJS*, **197**, A33.

Suda, T., Hirschi, R., Fujimoto, M. Y.: 2011, Stellar Evolution Constraints on the Triple-α Reaction Rate, *ApJ*, **741**, 61.

Suda, T., Yamada, S., Katsuta, Y., **Komiya, Y.**, Ishizuka, C., **Aoki, W.**, Fujimoto, M. Y.: 2011, The Stellar Abundances for Galactic Archaeology (SAGA) data base - II. Implications for mixing and nucleosynthesis in extremely metal-poor stars and chemical enrichment of the Galaxy, *MNRAS*, **412**, 843-874.

Sudou, H., **Iguchi, S.**: 2011, Proper Motion of the Sub-Parsec Scale Jet in the Radio Galaxy 3C 66B, *AJ*, **142**, 49.

Sugimura, M., Yamaguchi, T., Sakai, T., **Umemoto, T.**, Sakai, N., **Takano, S.**, **Aikawa, Y.**, Hirano, N., Liu, S. Y., Millar, T. J., Nomura, H., Su, Y. N., Takakuwa, S., Yamamoto, S.: 2011, Early Results of the 3 mm Spectral Line Survey toward the Lynds 1157 B1 Shocked Region, *PASJ*, **63**, 459-472.

Sugitani, K., **Nakamura, F.**, Watanabe, M., **Tamura, M.**, **Nishiyama, S.**, Nagayama, T., **Kandori, R.**, Nagata, T., Sato, S., Gutermuth, R. A., Wilson, G. W., **Kawabe, R.**: 2011, Near-infrared-imaging Polarimetry Toward Serpens South: Revealing the Importance of the Magnetic Field, *ApJ*, **734**, 63.

Sumi, T., et al. including **Fukui, A.**: 2011, Unbound or distant planetary mass population detected by gravitational microlensing, *Nature*, **473**, 349-352.

Suwa, Y., **Kotake, K.**, **Takiwaki, T.**, Liebendörfer, M., Sato, K.: 2011, Impacts of Collective Neutrino Oscillations on Core-collapse Supernova Explosions, *ApJ*, **738**, 165.

Suzuki, K., **Nagai, H.**, **Kino, M.**, Kataoka, J., Asada, K., Doi, A., Inoue, M., Orienti, M., Giovannini, G., Giroletti, M., Lahteenmaki, A., Tornikoski, M., Leon-Tavares, J., Bach, U., Kameno, S., **Kobayashi, H.**: 2012, Exploring the Central Sub-parsec Region of the γ-Ray Bright Radio Galaxy 3C 84 with VLBA at 43 GHz in the Period of 2002-2008, *ApJ*, **746**, 140.

Suzuki, N., et al. including **Hattori, T.**, **Kashikawa, N.**: 2011, The Hubble Space Telescope Cluster Supernova Survey. V. Improving the Dark-energy Constraints above $z > 1$ and Building an Early-type-hosted Supernova Sample, *ApJ*, **746**, 85.

Suzuki, T., **Honma, M.**, Mao, H., Otsuka, T., **Kajino, T.**: 2011, Evaluation of Electron Capture Reaction Rates in Ni Isotopes in Stellar Environments, *Phys. Rev. C*, **83**, 044619.

Suzuki, T., **Honma, M.**, Yoshida, T., Mao, H., **Kajino, T.**, Otsuka, T.: 2011, Spin-dependent nuclear weak processes and nucleo-synthesis in stars, *Prog. Part. Nucl. Phys.*, **66**, 385-389.

Suzuki, T., Yoshida, T., **Kajino, T.**, Otsuka, T.: 2012, Beta Decays of Isotones with Neutron Magic Number of N=126 and R-process Nucleosynthesis, *Phys. Rev. C*, **85**, 015802.

Sych, R., Zaqarashvili, T. V., Nakariakov, V. M., Anfinogentov, S. A., **Shibasaki, K.**, Yan, Y.: 2012, Frequency drifts of 3-min oscillations in microwave and EUV emission above sunspots, *A&A*, **539**, A23.

Takahashi, R., Oguri, M., Sato, M., **Hamana, T.**: 2011, Probability Distribution Functions of Cosmological Lensing: Convergence, Shear, and Magnification, *ApJ*, **742**, 15.

Takahashi, H. R., **Kudoh, T.**, Masada, Y., Matsumoto, J.: 2011, Scaling Law of Relativistic Sweet-Parker Type Magnetic Reconnection, *ApJ*, **739**, L53.

Takahashi, J., Itoh, Y., **Takahashi, S.**: 2011, Mid-Infrared Spectroscopy of 11 Main-Belt Asteroids, *PASJ*, **63**, 499-511.

Takeda, Y., **Tajitsu, A.**, Honda, S., **Kawanomoto, S.**, **Ando, A.**, **Sakurai, T.**: 2011, Beryllium Abundances of Solar-Analog Stars, *PASJ*, **63**, 697-713.

Takeda, Y., Ueno, S.: 2011, Iodine-Cell Spectroscopy Applied to Investigating the Solar Differential Rotation, *Sol. Phys.*, **270**, 447-461.

Takeuchi, T., Muto, T., Okuzumi, S., **Ishitsu, N.**, Ida, S.: 2011, Induced Turbulence and the Density Structure of the Dust Layer in a Protoplanetary Disk, *ApJ*, **744**, 990.

Takiwaki, T., **Kotake, K.**: 2011, Gravitational Wave Signatures of Magnetohydrodynamically Driven Core-collapse Supernova Explosions, *ApJ*, **743**, 30.

Tamura, Y., **Kawabe, R.**, Kohno, K., Fukuhara, M., Momose, M., **Ezawa, H.**, Kuboi, A., **Sekiguchi, T.**, **Kamazaki, T.**, Vila-Vilaró, B., Nakagawa, Y., **Okada, N.**: 2011, The Millimeter Sky Transparency Imager (MiSTI), *PASJ*, **63**, 347-356.

Terai, T., Itoh. Y.: 2011, Size Distribution of Main-Belt Asteroids with High Inclination, *PASJ*, **63**, 335-346.

Terzo, S., Reale, F., Miceli, M., Klimchuk, J. A., **Kano, R.**, **Tsuneta, S.**: 2011, Widespread Nanoflare Variability Detected with Hinode/X-Ray Telescope in a Solar Active Region, *ApJ*, **736**, 111.

Thalmann, C., et al. including **Usuda, T.**, **Egner, S.**, **Fukue, T.**, **Golota, T.**, **Guyon, O.**, **Hashimoto, J.**, **Hayano, Y.**, **Hayashi, S.**, **Ishii, M.**, **Iye, M.**, **Kandori, R.**, **Kudo, T.**, **Kusakabe, N.**, **Kuzuhara, M.**, **Matsuo, T.**, **Miyama, S.**, **Morino, J.-I.**, **Nishimura, T.**, **Pyo, T.-S.**, **Suto, H.**, **Suzuki, R.**, **Takahashi, Y. H.**, **Takato, N.**, **Terada, H.**, **Tomono, D.**, **Takami, H.**, **Tamura, M.**: 2011, Images of the Extended Outer Regions of the Debris Ring around HR 4796 A, *ApJ*, **743**, L6.

Thalmann, C., **Usuda, T.**, Kenworthy, M., Janson, M., Mamajek, E. E., Brandner, W., Dominik, C., Goto, M., **Hayano, Y.**, Henning, T., Hinz, P. M., **Minowa, Y.**, **Tamura, M.**: 2011, Piercing the Glare: A Direct Imaging Search for Planets in the Sirius System, *ApJ*, **732**, L34.

Tomida, K., **Machida, M. N.**, **Saigo, K.**, **Tomisaka, K.**, Matsumoto, T.: 2011, Erratum: Exposed Long-lifetime First Core: A New Model of First Cores Based on Radiation Hydrodynamics, *ApJ*, **732**, 18.

Tomisaka, K., **Tomida, K.**: 2011, Observational Identification of First Cores: Non-LTE Radiative Transfer Simulation, *PASJ*, **63**, 1151-1164.

Torii, K., et al. including **Kawamura, A.**, **Mizuno, N.**: 2011, Molecular Clouds in the Trifid Nebula M20: Possible Evidence for a Cloud-Cloud Collision in Triggering the Formation of the

First Generation Stars, *ApJ*, **738**, 46.
Tosaki, T., **Kuno, N.**, **Onodera, S.**, **Miura, R.**, **Sawada, T.**, Muraoka, K., **Nakanishi, K.**, **Komugi, S.**, Nakanishi, H., **Kaneko, H.**, **Hirota, A.**, Kohno, K., **Kawabe, R.**: 2011, NRO M33 All-Disk Survey of Giant Molecular Clouds (NRO MAGiC). I. H I to H2 Transition, *PASJ*, **63**, 1171-1179.
Totani, T., Takeuchi, T. T., Nagashima, M., **Kobayashi, M. A. R.**, Makiya, R.: 2011, Infrared Spectral Energy Distribution in the AKARI All Sky Survey: Correlations with Galaxy Properties, and Their Physical Origin, *PASJ*, **63**, 1181-1206.
Toujima, H., **Nagayama, T.**, Omodaka, T., Handa, T., Koyama, Y., **Kobayashi, H.**: 2011, Propagation of Highly Efficient Star Formation in NGC 7000, *PASJ*, **63**, 1259-1272.
Tsai, M., Hwang, C.-Y., Matsushita, S., Baker, A. J., **Espada, D.**: 2012, Interferometric CO(3-2) Observations toward the Central Region of NGC 1068, *ApJ*, **746**, 129.
Tsuboi, M., Kamegai, K., Miyazaki, A., **Nakanishi, K.**, Kotani, T.: 2012, Isolated Millimeter Flares of Cyg X-3, *PASJ*, **64**, 9.
Tsujimoto, T., Bekki, K.: 2011, Implications of a non-universal IMF from C, N, and O abundances in very metal-poor Galactic stars and damped Lyα absorbers, *A&A*, **530**, A78.
Tsujimoto, T., Bekki, K.: 2012, Two-component Galactic Bulge Probed with Renewed Galactic Chemical Evolution Model, *ApJ*, **747**, 125.
Tsujimoto, T.: 2011, Chemical Signature Indicating a Lack of Massive Stars in Dwarf Galaxies, *ApJ*, **736**, 113.
Tsukamoto, Y., **Machida, N. M.**: 2011, Classification of the circumstellar disc evolution during the main accretion phase, *MNRAS*, **416**, 591-600.
Ueda, J., **Iono, D.**, Petitpas, G., Yun, M. S., Ho, P. T. P., **Kawabe, R.**, Mao, R.-Q., Martin, S., Matsushita, S., Peck, A. B., Tamura, Y., Wang, J., Wang, Z., Wilson, C. D., Zhang, Q.: 2012, Unveiling the Physical Properties and Kinematics of Molecular Gas in the Antennae Galaxies (NGC 4038/9) Through High Resolution CO ($J = 3-2$) Observations, *ApJ*, **745**, 65.
Urakawa, S., et al. including **Kuroda, D.**, **Yanagisawa, K.**, **Nagayama, S.**: 2011, Photometric observations of 107P/ Wilson-Harrington, *Icarus*, **215**, 17-26.
Usui, F., **Kuroda, D.**, Müller, T. G., Hasagawa, S., Ishiguro, M., Ootsubo, T., Ishihara, D., Kataza, H., Takita, S., Oyabu, S., Ueno, M., Matsuhara, H., Onaka, T.: 2011, Asteroid Catalog Using Akari: AKARI/IRC Mid-Infrared Asteroid Survey, *PASJ*, **63**, 1117-1138.
van Dishoeck, E. F., et al. including **Aikawa, Y.**: 2011, Water in Star-forming Regions with the Herschel Space Observatory (WISH). I. Overview of Key Program and First Results, *PASP*, **123**, 138-170.
van Putten, M., Kanda, N., Tagoshi, H., **Tatsumi, D.**, **Fujimoto, M.**, Della, M.: 2011, Prospects for true calorimetry on Kerr black holes in core-collapse supernovae and mergers, *Phys. Rev. D*, **83**, 044046.
Wada, T., **Shibata, S.**: 2011, A particle simulation for the global pulsar magnetosphere - II. The case of dipole field, *MNRAS*, **418**, 612-624.
Walsh, C., Nomura, H., Millar, T. J., **Aikawa, Y.**: 2012, Chemical Processes in Protoplanetary Disks. II. On the Importance of Photochemistry and X-Ray Ionization, *ApJ*, **747**, 114.
Wang, L., Sato, B., Zhao, G., Liu, Y.-J., **Noguchi, K.**, **Ando, H.**, **Izumiura, H.**, **Kambe, E.**, Omiya, M., Harakawa, H., Liu, F., Wu, X.-S., **Takeda, Y.**, Yoshida, M., **Kokubo, E.**: 2012, A possible substellar companion to the intermediate-mass giant HD 175679, *Res. Astron. Astrophys.*, **12**, 84-92.
Williams, C. C., Giavalisco, M., Porciani, C., Yun, M. S., Pope, A., Scott, K. S., Austermann, J. E., Aretxaga, I., Hatsukade, B., Lee, K.-S., Wilson, G. W., Cybulski, J. R., Hughes, D. H., **Kawabe, R.**, Kohno, K., Perera, T., Schloerb, F. R.: 2011, On the Clustering of Sub-Millimeter Galaxies, *ApJ*, **733**, 92.
Wong, T., et al. including **Kawamura, A.**: 2011, The Magellanic Mopra Assessment (MAGMA). I. The Molecular Cloud Population of the Large Magellanic Cloud, *ApJS*, **197**, 16.
Woo, J. H., Kim, J, H., **Imanishi, M.**, Park, D.: 2012, The Connection between 3.3 micron Polycyclic Aromatic Hydrocarbon Emission and Active Galactic Nucleus Activity, *AJ*, **143**, 49.
Yamaguchi, T., **Takano, S.**, Sakai, N., Sakai, T., Liu, S.-Y., Su, Y.-N., Hirano, N, Takakuwa, S., **Aikawa, Y.**, Nomura, H., Yamamoto, S.: 2011, Detection of Phosphorus Nitride in the Lynds 1157 B1 Shocked Region, *PASJ*, **63**, L37-L41.
Yamaguchi, T., Yoshikawa, M., **Yagi, M.**, Tholen, D. J.: 2011, Entry Dispersion Analysis for the HAYABUSA Spacecraft using Ground-Based Optical Observation, *PASJ*, **63**, 979-985.
Yamamoto, M. Y., **Ishihara, Y.**, Hiramatsu, Y., Kitamura, K., Ueda, M., Shiba, Y., Furumoto, M., Fujita, K.: 2011, Detection of Acoustic/Infrasonic/Seismic Waves Generated by Hypersonic Reentry of HAYABUSA Capsule and Fragmented Parts of Spacecraft, *PASJ*, **63**, 971-978.
Yamamoto, S., Matsunaga, T., Ogawa, Y., Nakamura, R., Yokota, Y., Ohtake, M., Haruyama, J., **Morota, T.**, Honda, C., Hiroi, T., Kodama, S.: 2011, Prefight and infight calibration of the Spectral Profiler onboard SELENE (Kaguya), *IEEE Trans. Geosci. Remote Sens.*, **49**, 4660-4676.
Yamamoto, S., Nakamura, R., Matsunaga, T., Ogawa, Y., **Ishihara, Y.**, **Morota, T.**, Hirata, N., Ohtake, M., Hiroi, T., Yokota, Y., Haruyama, J.: 2011, Olivine-rich exposures in the South Pole-Aitken Basin, *Icarus*, **218**, 331-344.
Yamauchi, C., Fujishima, S., Ikeda, N., Inada, K., Katano, M., Kataza, H., Makiuti, S., Matsuzaki, K., Takita, S., Yamamoto, Y., Yamamura, I., Ishihara, D., Oyabu, S.: 2011, AKARI-CAS—Online Service for AKARI All-Sky Catalogues, *PASP*, **123**, 852-864.
Yamauchi, C.: 2011, Development of 2MASS Catalog Server Kit, *PASP*, **123**, 1324-1333.
Yamazaki, D., Ichiki, K., Takahashi, K.: 2011, Effects of a primordial magnetic field with log-normal distribution on the cosmic microwave background, *Phys. Rev. D*, **84**, 123006.
Yan, J., **Goossens, S.**, **Matsumoto, K.**, Ping, J., Harada, Y., Iwata, T., Namiki, N., Li, F., Tang, G., Cao, J., **Hanada, H.**, Kawano, N.: 2011, CEGM02: An improved lunar gravity model using Chang'E-1 orbital tracking data, *Planet. Space Sci.*, **62**, 1-9.
Yen, H.-W., Takakuwa, S., **Ohashi, N.**: 2011, Kinematics and Physical Conditions of the Innermost Envelope in B335, *ApJ*, **742**, 57.
Yokota, Y., et al. including **Morota, T.**, **Sasaki, S.**: 2011, Lunar photometric properties at wavelengths 0.5−1.6 μm acquired by

SELENE Spectral Profiler and their dependency on local albedo and latitudinal zones, *Icarus*, **215**, 639-660.

Yoshida, T., Takamura, A., Kimura, K., Kawagoe, T., **Kajino, T.**, Yokomakura, H.: 2011, Supernova neutrino signals in liquid Argon detector and neutrino magnetic moment, *Phys. Lett. B*, **704**, 108-112.

Yun, M. S., et al. including **Ezawa, H.**, **Iono, D.**, **Kawabe, R.**: 2012, Deep 1.1 mm-Wavelength Imaging of the GOODS-South Field by AzTEC/ASTE-II. Redshift Distribution and Nature of the Submillimetre Galaxy Population, *MNRAS*, **420**, 957-985.

Yung, B. H. K., Nakashima, J., Imai, H., **Deguchi, S.**, Diamond, P. J., Kwok, S.: 2011, High Velocity Precessing Jets from the Water Fountain IRAS 18286-0959 Revealed by Very Long Baseline Array Observations, *ApJ*, **741**, 94.

Zenitani, S., Hesse, M., Klimas, A., Black, C., Kuznetsov, M.: 2011, The inner structure of collisionless magnetic reconnection: The electron-frame dissipation measure and Hall fields, *Physics of Plasmas*, **18**, 122108.

Zhao, B., Li, Z.-Y., **Nakamura, F.**, Krasnopolsky, R., Shang, H.: 2011, Magnetic Flux Expulsion in Star Formation, *ApJ*, **742**, 10.

2. Publications of the National Astronomical Observatory of Japan

Honma, M., **Hirota, T.**, **Jike, T.**, **Kameya, O.**, **Kawaguchi, N.**, **Kobayashi, H.**, Kurayama, T., **Manabe, S.**, **Miyaji, T.**, **Nagayama, T.**, **Niinuma, K.**, Omodaka, T., **Oyama, T.**, **Sato, K.**, **Shibata, K.-M.**, **Tamura, Y.**: 2011, Performance of VERA in the Phase-Referencing Astrometry, *Publ. of the National Astron. Obs. of Japan*, **13**, 57-69.

Noda, S., **Furusawa, J.**, **Furusho, R.**, **Yamada, Y.**, **Furusawa, H.**, Ozawa, T., **Takata, T.**, **Ichikawa, Y.**: 2011, PSF Analysis of 7 Years' Subaru/Suprime-Cam Data, *Publ. of the National Astron. Obs. of Japan*, **13**, 71-81.

3. Report of the National Astronomical Observatory of Japan (in Japanese)

Ishizaki, H., **Agatsuma, K.**, Majorana, E., **Takahashi, R.**: 2000, Parametric Excitation of an Inverted Pendulum Incorporated to the Seismic Attenuation System of the Gravitational Wave Interferometer, *Rep. Nat. Astron. Obs. Japan*, **14**, 1-14.

4. Conference Proceedings

Aikawa, Y., Furuya, K., Wakelam, V., Hersant, F., Matsumoto, T., Saigo, K., **Tomida, K.**, **Tomisaka, K.**, Garrod, R. T., Herbst, E.: 2011, Hydrodynamical-Chemical Models from Prestellar Cores to Protostellar Cores, Proc. IAU Symp. 280, Eds. J. Cernicharo, R. Bachiller, 33-42.

Aikawa, Y., Kamuro, D., Sakon, I., Itoh, Y., Noble, J. A., Pontoppidan, K. M., Fraser, H. J., Terada, H., **Tamura, M.**, **Kandori, R.**, **Kawamura, A.**, Ueno, M.: 2011, AKARI observations of ice absorption bands towards edge-on YSOs, ASP Conf. Ser. 439, Eds. M. R. Morris, Q. D. Wang, F. Yuan.

Aikawa, Y., Kamuro, D., Sakon, I., Itoh, Y., Noble, J. A., Pontoppidan, K. M., Fraser, H. J., Terada, H., **Tamura, M.**, **Kandori, R.**, **Kawamura, A.**, Ueno, M.: 2011, AKARI observations of ice absorption bands towards edge-on YSOs, Proc. IAU Symp. 280, Eds. J. Cernicharo, R. Bachiller, 78.

Anan, T., Ichimoto, K., Ueno, S., Kimura, G., Nakatani, Y., Kaneda, N., **Hagino, M.**, **Suzuki, I.**: 2011, Developments of the Multi-wavelength Polarimeter of the Domeless Solar Telescope at the Hida Observatory, ASP Conf. Ser. 437, Eds. J. R. Kuhn, S. V. Berdyugina, D. M. Harrington, S. Keil, H. Lin, T. Rimmele, J. Trujillo Bueno, 365-369.

Araki, M., **Takano, S.**, Koshikawa, H., Yamabe, N., Tsukiyama, K., Nakane, A., Okabayashi, T., Kunimatsu, A., Kuze, N.: 2011, A Search for Interstellar Carbon-Chain Alcohol HC_4OH in the Star Forming Region L1527, Int. Symp. on Molecular Spectroscopy, 66th meeting, abstract #EWF06.

Aretxaga, I., Wilson, G. W., Aguilar, E., Alberts, S., Scott, K. S., Scoville, N., Yun, M. S., Austermann, J., Downes, T. D., **Ezawa, H.**, Hatsukade, B., Hughes, D. H., **Kawabe, R.**, Kohno, K., **Oshima, T.**, Perera, T. A., Tamura, Y., Zeballos, M.: 2011, Plausible Boosting of Millimeter-Galaxies in the COSMOS Field by Intervening Large-Scale Structure, ASP Conf. Ser. 446, Eds. W. Wang, J. Lu, Z. Luo, Z. Yang, H. Hua, Z. Chen, 89-94.

Argudo, M., et al. including **Espada, D.**: 2011, A search for neighbours around isolated galaxies using the SDSS, Highlights of Spanish Astrophysics VI, 374.

Bae, H., **Yagi, M.**, Woo, J., Yoshida, M., Yoon, S.: 2011, On the Nature of LINERs A Clue from Keck/LRIS Observations, *Bulletin of the Korean Astronomical Society*, **36**(2), 61.2.

Cheoun, M. K., Ha, E., **Kajino, T.**: 2011, Neutrino-Nucleus Reactions for Nucleosynthesis, *J. Phys.: Conf. Ser.*, **312**, 42023.

Deguchi, S., **Koike, K.**, **Kuno, N.**, **Takahashi, S.**, Matsunaga, N., Nakashima, J.: 2011, Interaction between AGB Wind and Nova Outburst: The Case of V407 Cyg, a Symbiotic Star, ASP Conf. Ser. 445, Eds. F. Kerschbaum, T. Lebzelter, R. F. Wing, 319-320.

Fukagawa, M., Wisniewski, J. P., Hashimoto, J., Okamoto, Y., Grady, C. A., Muto, T., Inutsuka, S.-I., Hodapp, K. W., **Kudo, T.**, Momose, M., Shibai, H., **Tamura, M.**: 2011, High-contrast polarimetric imaging of the protoplanetary disk around AB Aurigae, Proc. IAU Symp. 276, Ed. A. Sozzetti.

Fukui, Y., Torii, K., Kudo, N., Yamamoto, H., **Kawamura, A.**, Machida, M., Takahashi, K., Nozawa, S., Matsumoto, R.: 2011, Molecular Loops in the Galactic Center, ASP Conf. Ser. 439, Eds. M. R. Morris, Q. D. Wang, F. Yuan, 61.

Gonzalez, A., **Fujii, Y.**, **Kaneko, K.**, **Uzawa, Y.**: 2011, Quasi-optical attenuators for ALMA band 10 receiver, Asia-Pacific Microwave Conference Proceedings (APMC), 2011, IEEE, 1997-1980.

Goto, M., **Usuda, T.**, Geballe, T. R., Indriolo, N., McCall, B. J., Oka, T.: 2011, Scrutiny of the Core of the Galactic Center by H_3^+ and Co: Gcirs 3 and Gcirs 1W, Int. Symp. on Molecular Spectroscopy, 66th meeting.

Gouda, N.: 2011, JASMINE, Scholarpedia, Ed. N. Zacharias, 6(10), 12021.

Hagino, M., **Hanaoka, Y.**, **Sakurai, T.**, Ichimoto, K.: 2011, Quantitative Comparison between the Polarization Data Taken with the Solar Flare Telescope and with the Hinode SOT Spectro-Polarimeter, ASP Conf. Ser. 437, Eds. J. R. Kuhn, S. V. Berdyugina, D. M. Harrington, S. Keil, H. Lin, T. Rimmele, J. Trujillo Bueno, 359-363.

Hanada, H., Ping, J., Funazaki, K., Kawano, N., Petrova, N., **Araki, H.**, **Tazawa, S.**, **Tsuruta, S.**, **Noda, H.**, **Asari, K.**, **Sasaki, S.**, Su, X., Satoh, A., Taniguchi, H., Kikuchi, M., Takahashi, H., Yamazaki, A., Murata, K., Iwata, T.: 2011, Development of a photographic zenith tube for observation of the lunar rotation and the deflection of the vertical, Proc. of IAG symp. on terrestrial gravimetry, Ed. V. G. Peshekhonov, 140-144.

Hanaoka, Y., **Sakurai, T.**, **Shinoda, K.**, **Noguchi, M.**, **Miyashita, M.**, **Fukuda, T.**, **Suzuki, I.**, **Hagino, M.**, **Arai, T.**, **Yamasaki, T.**, Takeyama, N.: 2011, Infrared Stokes Spectro-Polarimeter at the National Astronomical Observatory of Japan, ASP Conf. Ser. 437, Eds. J. R. Kuhn, S. V. Berdyugina, D. M. Harrington, S. Keil, H. Lin, T. Rimmele, J. Trujillo Bueno, 371-378.

Hanayama, H., Nakano, S., Asami, A., Hashimoto, N.: 2011, Comet 213P/Van Ness, Central Bureau Electronic Telegrams, Ed. D. W. E. Green, 2798,1.

Haruyama, J., Hara, S., Hioki, K., Iwasaki, A., **Morota, T.**, Ohtake, M., Matsunaga, T., **Araki, H.**, **Matsumoto, K.**, **Ishihara, Y.**, **Noda, H.**, **Sasaki, S.**, **Goossens, S.**, Iwata, T.: 2012, Lunar Global Digital Terrain Model Dataset Produced from SELENE (Kaguya) Terrain Camera Stereo Observations, 43rd Lunar and Planetary Science Conference, #1200.

Hatano, H., Kurita, M., Sato, S., **Nishiyama, S.**, IRSF/SIRIUS Group: 2011, Interstellar Polarization Efficiency toward the Galactic Center, Proc. IAU Symp. 280, Eds. J. Cernicharo, R. Bachiller.

Hibi, Y., **Matsuo, H.**, Ookawa, T., Nagata, H., Ikeda, H., Fujiwara, M.: 2011, "32-channel Multi-Chip-Module" The Cryogenic Readout System for Submillimeter/Terahertz Cameras, NRAO ISSTT Proceedings, Eds. C. Walker, C. Groppi, 95-99.

Hwang, N.: 2011, Origin of Extended Star Clusters, SCA Con. Ser., Eds. E. J. Alfaro Navarro, A. T. Gallego Calvente, M. R. Zapatero, 357-359.

Ishihara, Y., **Morota, T.**, Saruwatari, Y., Sawada, A., Hiramatsu, Y.: 2012, A Determination of Charactaristics of Impact Basins from "Kaguya" Geodetic Data, 43rd Lunar and Planetary Science Conference, #1723.

Jike, T., **Manabe, S.**, **Tamura, Y.**, **Shizugami, M.**: 2011, VERA Geodetic Activities, IVS Annual Report 2010, Eds. D. Beherend, K. D. Baver, 60-63.

Kajino, T.: 2011, Nucleosynthesis and Neutrinos, AIP Conf. Proc. 1355, 257-262.

Kanao, M., Maggi, A., **Ishihara, Y.**, Yamamoto, M. Y., Nawa, K., Yamada, A., Wilson, T., Himeno, T., Toyokuni, G., Tsuboi, S., Toho, Y., Anderson, K.: 2012, Interaction on Seismic Waves between Atmosphere - Ocean - Cryosphere and Geosphere in Polar Region, Seismic Waves -Research and Analysis-, Ed. M. Kanao, 1-20.

Kato, Y., Steiner, O., Steffen, M., **Suematsu, Y.**: 2011, Excitation of magneto-acoustic waves in network magnetic elements, Proc. IAU Symp. 273, Eds. D. P. Choudhary, K. G. Strassmeier, 442-445.

Katsukawa, Y., **Suematsu, Y.**, Shimizu, T., Ichimoto, K., Takeyama, N.: 2011, Focal plane instrument for the Solar UV-Vis-IR Telescope aboard SOLAR-C, Proc. of the SPIE, 8148, Eds. S. Fineschi, J. Fennelly, 81480E.

Kawabata, K. S., Nagae, O., Chiyonobu, S., Tanaka, H., Miyamoto, H., **Nakaya, H.**, Suzuki, M., **Kamata, Y.**, **Miyazaki, S.**, Hiragi, K., Yamanaka, M., Arai, A., **Yamashita, T.**, Uemura, M., Ohsugi, T., Isogai, M., Ishitobi, Y., Sato, S.: 2011, Wide-Field One-Shot Optical Polarimeter: HOWPol, ASP Conf. Ser. 449, 83.

Kiuchi, H., Kawanishi, T.: 2011, Photonic millimeter-wave/microwave signal generation and transmission techniques for a high-frequency Radio Interferometer and a very large anttena array, XXX URSI General Assembly and Scientific Symp. of Int. Union of Radio Science, 978-1-4244-6051-9/11/$26.00 © 2011 IEEE.

Komugi, S., Tosaki, T., Kohno, K., Tsukagoshi, T., Tamura, Y., **Miura, R.**, **Onodera, S.**, **Kuno, N.**, **Kawabe, R.**, **Nakanishi, K.**, **Sawada, T.**, **Ezawa, H.**, Wilson, G. W., Yun, M. S., Scott, K. S., Hughes, D. H., Aretxaga, I., Perera, T. A., Austermann, J. E., Tanaka, K., Muraoka, K., Egusa, F.: 2011, Cold Dust and its Heating Sources in M 33, Proc. IAU Symp. 277, Eds. C. Carignan, F. Combes, K. C. Freeman, 26-29.

Kudo, N., Torii, K., Machida, M., Takahashi, K., Nozawa, S., Yamamoto, H., Okuda, T., **Kawamura, A.**, **Mizuno, N.**, Onishi, T., Matsumoto, R., Fukui, Y.: 2011, Molecular Loops in the Galactic Center; The Physical Condition in the Whole Loops, ASP Conf. Ser. 439, Eds. M. R. Morris, Q. D. Wang, F. Yuan, 69.

Kuno, N., Tosaki, T., **Onodera, S.**, **Miura, R.**, Muraoka, K., **Komugi, S.**, **Sawada, T.**, **Nakanishi, K.**, Kohno, K., **Kaneko, H.**, **Hirota, A.**, **Arimoto, N.**, Nakanishi, H., **Kawabe, R.**: 2011, NRO Legacy Project: M33 all Disk Survey of Giant Molecular Clouds with NRO 45-m and ASTE 10-m telescopes, Proc. IAU Symp. 277, Eds. C. Carignan, F. Combes, K. C. Freeman, 67-70.

Kuroda, D., **Hanayama, H.**, **Miyaji, T.**, **Watanabe, J.**, **Yanagisawa, K.**, **Nagayama, S.**, Yoshida, M., Ohta, K., Kawai, N.: 2011, GRB 110402A: MITSuME okayama and ishigakijima optical upper limits, *GRB Coordinates Network, Circular Service*, 11873, 1.

Kuroda, D., **Hanayama, H.**, **Miyaji, T.**, **Watanabe, J.**, **Yanagisawa, K.**, **Nagayama, S.**, Yoshida, M., Ohta, K., Kawai, N.: 2011, GRB 110414A: MITSuME Ishigakijima Optical upper limits, *GRB Coordinates Network, Circular Service*, 11940, 1.

Kuroda, D., **Hanayama, H.**, **Miyaji, T.**, **Watanabe, J.**, **Yanagisawa, K.**, **Nagayama, S.**, Yoshida, M., Ohta, K., Kawai, N.: 2011, GRB 110422A: MITSuME Ishigakijima Optical Observation, *GRB Coordinates Network, Circular Service*, 11972, 1.

Kuroda, D., **Hanayama, H.**, **Miyaji, T.**, **Watanabe, J.**, **Yanagisawa, K.**, **Nagayama, S.**, Yoshida, M., Ohta, K., Kawai, N.: 2011, GRB 110709A: MITSuME Ishigakijima Optical upper limits, *GRB Coordinates Network, Circular Service*, 12139, 1.

Kuroda, D., **Hanayama, H.**, **Miyaji, T.**, **Watanabe, J.**, **Yanagisawa, K.**, **Nagayama, S.**, Yoshida, M., Ohta, K., Kawai, N.: 2011, GRB 110726A: MITSuME Ishigakijima Optical Observation, *GRB Coordinates Network, Circular Service*, 12204, 1.

Kuroda, D., **Hanayama, H.**, **Miyaji, T.**, **Watanabe, J.**, **Yanagisawa, K.**, **Nagayama, S.**, Yoshida, M., Ohta, K., Kawai, N.: 2011, GRB 110731A: MITSuME Ishigakijima Optical Upper Limits, *GRB Coordinates Network, Circular Service*, 12226, 1.

Kuroda, D., **Hanayama, H.**, **Miyaji, T.**, **Watanabe, J.**, **Yanagisawa, K.**, **Nagayama, S.**, Yoshida, M., Ohta, K., Kawai, N.: 2011, GRB 110801A: MITSuME Ishigakijima Optical Observation, *GRB Coordinates Network, Circular Service*, 12233, 1.

Kuroda, D., **Hanayama, H.**, **Miyaji, T.**, **Watanabe, J.**, **Yanagisawa, K.**, **Nagayama, S.**, Yoshida, M., Ohta, K., Kawai, N.: 2011, GRB 110801A: MITSuME Ishigakijima Optical Observation at 1 day after the burst, *GRB Coordinates Network, Circular Service*, 12240, 1.

Kuroda, D., **Hanayama, H.**, **Miyaji, T.**, **Watanabe, J.**, **Yanagisawa, K.**, **Nagayama, S.**, Yoshida, M., Ohta, K., Kawai, N.: 2011, GRB 110820A: MITSuME Ishigakijima Optical upper limits, *GRB Coordinates Network, Circular Service*, 12293, 1.

Kuroda, D., **Hanayama, H.**, **Miyaji, T.**, **Watanabe, J.**, **Yanagisawa, K.**, **Nagayama, S.**, Yoshida, M., Ohta, K., Kawai, N.: 2011, GRB 111029A: MITSuME Ishigakijima Optical upper limits, *GRB Coordinates Network, Circular Service*, 12511, 1.

Kuroda, D., **Hanayama, H.**, **Miyaji, T.**, **Watanabe, J.**, **Yanagisawa, K.**, **Nagayama, S.**, Yoshida, M., Ohta, K., Kawai, N.: 2012, GRB 120212A: MITSuME Ishigakijima Optical Observation, *GRB Coordinates Network, Circular Service*, 12947, 1.

Kuroda, D., **Hanayama, H.**, **Miyaji, T.**, **Watanabe, J.**, **Yanagisawa, K.**, **Nagayama, S.**, Yoshida, M., Ohta, K., Kawai, N.: 2012, GRB 120308A: MITSuME Ishigakijima Optical Upper Limits, *GRB Coordinates Network, Circular Service*, 13026, 1.

Kuroda, D., **Hanayama, H.**, **Miyaji, T.**, **Watanabe, J.**, **Yanagisawa, K.**, **Nagayama, S.**, Yoshida, M., Ohta, K., Kawai, N.: 2012, GRB 120326A: MITSuME Ishigakijima Optical Observation at 2 days afterthe burst, *GRB Coordinates Network, Circular Service*, 13170, 1.

Kuroda, D., **Hanayama, H.**, **Miyaji, T.**, **Watanabe, J.**, **Yanagisawa, K.**, **Nagayama, S.**, Yoshida, M., Ohta, K., Kawai, N.: 2012, GRB 120326A: MITSuME Ishigakijima Optical Observation at 3 days afterthe burst, *GRB Coordinates Network, Circular Service*, 13177, 1.

Kuroda, D., **Hanayama, H.**, **Miyaji, T.**, **Watanabe, J.**, **Yanagisawa, K.**, **Nagayama, S.**, Yoshida, M., Ohta, K., Kawai, N.: 2012, GRB 120327A: MITSuME Ishigakijima Optical Observation, *GRB Coordinates Network, Circular Service*, 13156, 1.

Kuroda, D., **Hanayama, H.**, **Miyaji, T.**, **Watanabe, J.**, **Yanagisawa, K.**, **Nagayama, S.**, Yoshida, M., Ohta, K., Kawai, N.: 2012, GRB 120327A: MITSuME Ishigakijima Optical Upper Limits at 1 day afterthe burst, *GRB Coordinates Network, Circular Service*, 13169, 1.

Kuroda, D., **Hanayama, H.**, **Miyaji, T.**, **Watanabe, J.**, **Yanagisawa, K.**, **Nagayama, S.**, Yoshida, M., Ohta, K., Kawai, N.: 2012, GRB 120328A: MITSuME Ishigakijima Optical Upper Limits, *GRB Coordinates Network, Circular Service*, 13171, 1.

Kuroda, D., **Hanayama, H.**, **Miyaji, T.**, **Watanabe, J.**, **Yanagisawa, K.**, Yoshida, M., Ohta, K., Kawai, N.: 2012, GRB 120326A: MITSuME Ishigakijima Optical Observation, *GRB Coordinates Network, Circular Service*, 13155, 1.

Kuroda, D., **Hanayama, H.**, **Yanagisawa, K.**, **Shimizu, Y.**, **Toda, H.**, **Miyaji, T.**, **Watanabe, J.**, **Nagayama, S.**, Yoshida, M., Ohta, K., Kawai, N.: 2011, GRB 110407A: MITSuME okayama and ishigakijima optical upper limits, *GRB Coordinates Network, Circular Service*, 11905, 1.

Kuroda, D., **Hanayama, H.**, **Yanagisawa, K.**, **Shimizu, Y.**, **Toda, H.**, **Miyaji, T.**, **Watanabe, J.**, **Nagayama, S.**, Yoshida, M., Ohta, K., Kawai, N.: 2011, GRB 110915A: MITSuME Okayama and Ishigakijima Optical upper limits, *GRB Coordinates Network, Circular Service*, 12344, 1.

Kuroda, D., **Hanayama, H.**, **Yanagisawa, K.**, **Shimizu, Y.**, **Toda, H.**, **Miyaji, T.**, **Watanabe, J.**, **Nagayama, S.**, Yoshida, M., Ohta, K., Kawai, N.: 2012, GRB 120211A: MITSuME Okayama and Ishigakijima Optical upper limits, *GRB Coordinates Network, Circular Service*, 12929, 1.

Kuroda, D., **Yanagisawa, K.**, **Shimizu, Y.**, **Toda, H.**, **Nagayama, S.**, Yoshida, M., Ohta, K., Kawai, N.: 2011, GRB 110414A: MITSuME Okayama Optical Upper Limits, *GRB Coordinates Network, Circular Service*, 11938, 1.

Kuroda, D., **Yanagisawa, K.**, **Shimizu, Y.**, **Toda, H.**, **Nagayama, S.**, Yoshida, M., Ohta, K., Kawai, N.: 2011, GRB 110530A: MITSuME Okayama Optical Observation, *GRB Coordinates Network, Circular Service*, 12053, 1.

Kuroda, D., **Yanagisawa, K.**, **Shimizu, Y.**, **Toda, H.**, **Nagayama, S.**, Yoshida, M., Ohta, K., Kawai, N.: 2011, GRB 111123A: MITSuME Okayama Optical upper limits, *GRB Coordinates Network, Circular Service*, 12591, 1.

Kuroda, D., **Yanagisawa, K.**, **Shimizu, Y.**, **Toda, H.**, **Nagayama, S.**, Yoshida, M., Ohta, K., Kawai, N.: 2011, GRB 111210A: MITSuME Okayama Optical upper limits, *GRB Coordinates Network, Circular Service*, 12659, 1.

Kuroda, D., **Yanagisawa, K.**, **Shimizu, Y.**, **Toda, H.**, **Nagayama, S.**, Yoshida, M., Ohta, K., Kawai, N.: 2012, GRB 120106A: MITSuME Okayama Optical upper limits, *GRB Coordinates Network, Circular Service*, 12814, 1.

Kuroda, D., **Yanagisawa, K.**, **Shimizu, Y.**, **Toda, H.**, **Nagayama, S.**, Yoshida, M., Ohta, K., Kawai, N.: 2012, GRB 120215A: MITSuME Okayama Optical upper limits, *GRB Coordinates Network, Circular Service*, 12960, 1.

Kuroda, D., **Yanagisawa, K.**, **Shimizu, Y.**, **Toda, H.**, **Nagayama, S.**, Yoshida, M., Ohta, K., Kawai, N.: 2012, GRB 120219A: MITSuME Okayama Optical upper limits, *GRB Coordinates Network, Circular Service*, 12969, 1.

Kuroda, D., **Yanagisawa, K.**, **Shimizu, Y.**, **Toda, H.**, **Nagayama, S.**, Yoshida, M., Ohta, K., Kawai, N.: 2012, GRB 120311B: MITSuME Okayama Optical upper limits, *GRB Coordinates Network, Circular Service*, 13046, 1.

Kuroda, D., **Yanagisawa, K.**, **Shimizu, Y.**, **Toda, H.**, **Nagayama, S.**, Yoshida, M., Ohta, K., Kawai, N.: 2012, GRB 120320A: MITSuME Okayama Optical upper limits, *GRB Coordinates Network, Circular Service*, 13082, 1.

Kuroda, D., **Yanagisawa, K.**, **Yoshida, M.**, **Shimizu, Y.**, **Nagayama, S.**, **Toda, H.**, Ohta, K., Yatsu, Y., Kawai, N.: 2011, The development of an automatic reduction system for Gamma-Ray Burst afterglow, Proc. of Telescopes from Afar Conf.

Kusakabe, M., **Kajino, T.**, Mathews, G. M.: 2011, SUSY-catalyzed big bang nucleosynthesis as a solution of lithium problems, *J. Phys.: Conf. Ser.*, **312**, 42012.

Kusakabe, N., **Tamura, M.**, **Kandori, R.**, **Kudo, T.**, **Hashimoto, J.**: 2011, Strategic Exploration of Exoplanets and Disks with Subaru: SEEDS, Proc. IAU Symp. 276, Ed. A. Sozzetti.

Lee, M. G., Lim, S., Park, H. S., Hwang, H. S., **Hwang, N.**: 2011, Wandering Globular Clusters: the First Dwarf Galaxies in the Universe?, EAS Publ. Ser., 48, Eds. M. Koleva, Ph. Prugniel, I. Vauglin, 243-248.

Li, J., Shen, Z.-Q., Miyazaki, A., Huang, L., Sault, R. J., **Miyoshi, M.**, Tsuboi, M., Tsutsumi, T.: 2011, Flaring Emission from Sagittarius A* at Millimeter Wavelengths, ASP Conf. Ser. 439, Eds. M. R. Morris, Q. D. Wang, F. Yuan, 319.

Maruyama, T., Yasutake, N., **Kajino, T.**, Cheoun, M. K., Ryu, C. Y.: 2011, Asymmetric Neutrino Reactions from Magnetized Proto-Neutron Stars in fully Relativistic Framework including Hyperons, AIP Conf. Proc. 1377, 389-391.

Matsuo, H., **Matsuo, T.**, Ohta, I. S.: 2011, A Study on Photon Counting Interferometry in Terahertz Frequencies, NRAO ISSTT Proceedings, Eds. C. Walker, C. Groppi, 62.

Mawet, D., et al. including **Nishikawa, J.**, **Tamura, M.**: 2011, Taking the vector vortex coronagraph to the next level for ground- and space-based exoplanet imaging instruments: review of technology developments in the USA, Japan, and Europe, Proc. of the SPIE, 8151, Ed. S. Stuart.

Mayama, S., **Tamura, M.**, Hanawa, T., Matsumoto, T., **Ishii, M.**, **Pyo, T.-S.**, **Suto, H.**, **Naoi, T.**, **Kudo, T.**, **Hashimoto, J.**, **Nishiyama, S.**, **Kuzuhara, M.**, Hayashi, M.: 2011, Direct imaging of bridged twin protoplanetary disks in a young multiple star, Proc. IAU Symp. 276, Ed. A. Sozzetti.

Miyoshi, M., et al. including **Furuya, R.-S.**, **Kawaguchi, N.**, **Nakajima, J.**, **Irimajiri, Y.**, **Koyama, Y.**: 2011, A First Black Hole Imager, Caravan-sub at Andes, ASP Conf. Ser. 439, Eds. M. R. Morris, Q. D. Wang, F. Yuan, 279-280.

Miyoshi, M., **Oyama, T.**, Shen, Z., **Takahashi, R.**, **Kato, Y.**: 2011, Oscillation Phenomena in Sagittarius A*, ASP Conf. Ser. 439, Eds. M. R. Morris, Q. D. Wang, F. Yuan, 336-339.

Miyoshi, M., **Oyama, T.**, Shen, Z.: 2011, VLBA Synthesis Imagings of SgrA* at 43 GHz, ASP Conf. Ser. 439, Eds. M. R. Morris, Q. D. Wang, F. Yuan, 386-388.

Miyoshi, M.: 2011, Slit-Modulation Imaging Method for Detecting Periodic Structural Change in SgrA*, ASP Conf. Ser. 439, Eds. M. R. Morris, Q. D. Wang, F. Yuan, 384.

Moritani, Y., Nogami, D., Okazaki, A. T., **Imada, A.**, **Kambe, E.**, Honda, S., Hashimoto, O., Ichikawa, K.: 2011, Optical spectroscopic observations of the Be/X-Ray binary A0535+262/V725 Tau during the giant outburst in 2009, Proc. IAU Symp. 272, Eds. C. Neiner, G. Wade, G. Meynet, G. Peters, 18-19.

Morota, T., **Ishihara, Y.**, **Sasaki, S.**, **Goossens, S.**, **Matsumoto, K.**, **Noda, H.**, **Araki, H.**, **Hanada, H.**, **Tazawa, S.**, **Kikuchi, F.**, **Ishikawa, T.**, **Tsuruta, S.**, Haruyama, J., Ohtake, M.: 2011, Lunar mare volcanism: lateral heterogeneity in eruptional activity and relationship with crustal structure, Proc. 44th ISAS Lunar. Planet. Symp., Abstract #44-07.

Nakajima, T., **Iwashita, H.**, **Miyazawa, C.**, **Yonezu, T.**, **Kuno, N.**, **Kawabe, R.**, Inoue, H., Sakai, T., Kohno, K., Koyano, M., Katase, T., Nishimura, A., Kimura, K., Ogawa, H., **Asayama, S.**, **Noguchi, T.**: 2011, Development of the Sideband-Separating (2SB) Receiver Systems for the NRO 45-m Millimeter Wave Telescope, Proc. of the 12th Workshop on Submillimeter-wave Receiver Technologies in Eastern Asia, 14.

Nakamura, K.: 2012, Construction of gauge-invariant variables for linear-order metric perturbations on general background spacetime, 21st Workshop on General Relativity and Gravitation in Japan, Eds. Y. Ito, T. Futamase, et al.

Narukage, N., et al. including **Tsuneta, S.**, **Bando, T.**, **Kano, R.**, **Kubo, M.**, **Ishikawa, R.**, **Hara, H.**, **Suematsu, Y.**, **Katsukawa, Y.**: 2011, Overview of Chromospheric Lyman-Alpha SpectroPolarimeter (CLASP), Proc. of the SPIE, 8148, Eds. S. Fineschi, J. Fennelly, 81480T.

Niino, Y.: 2011, High-Metallicity Host Galaxies and The Metallicity Dependence of Long Gamma-Ray Bursts, AIP Conf. Proc. 1358, Eds. J. E. McEnery, J. L. Racusin, N. Gehrels, 275-278.

Nishiyama, S., Hatano, H., **Tamura, M.**, Nagata, T.: 2011, Near-Infrared Polarimetry toward the Galactic Center - Magnetic Field Configuration in the Central One Degree Region, ASP Conf. Ser. 439, Eds. M. R. Morris, Q. D. Wang, F. Yuan.

Noda, H., Kunimori, H., **Araki, H.**, Fuse, T., **Hanada, H.**, **Katayama, M.**, Otsubo, T., **Sasaki, S.**, **Tazawa, S.**, **Tsuruta, S.**, Funazaki, K., Taniguchi, H., Murata, K.: 2012, Lunar Laser Ranging Experiment for SELENE-2, 43rd Lunar and Planetary Science Conference, #1855.

Oe, M., Onodera, Y., Murai, J.: 2011, Early survey report on ICT disaster recovery activities in the Great East Japan Earthquake, Int. Symp. on Disaster Simulation & Structural Safety in the Next Generation, 2011, 443-447.

Ohishi, M., Hanisch, R. J., Norris, R. P., Andernach, H., Bishop, M., Griffin, E., Kembhavi, A., Murphy, T., Pasian, F.: 2011, Commission 5: Documentation and Astronomical Data, Proc. IAU Symp., Ed. I. Corbet, 327-334.

Ohishi, M.: 2011, Impact to the radio astronomy by the interference caused by the solar power satellite systems, XXX URSI General Assembly and Scientific Symp. of Int. Union of Radio Science, 10.1109/URSIGASS.2011.6050557.

Ohishi, M.: 2011, IUCAF activity in 2008–2011, XXX URSI General Assembly and Scientific Symp. of Int. Union of Radio Science, 10.1109/URSIGASS.2011.6051246.

Oka, T., Geballe, T. R., Goto, M., **Usuda, T.**, Indriolo, N., McCall, B. J.: 2011, H_3^+ in Warm, Diffuse Gas of the Central Molecular Zone, ASP Conf. Ser. 439, Eds. M. R. Morris, Q. D. Wang, F. Yuan, 18.

Oka, T., Morong, C. P., Geballe, T. R., Indriolo, N., McCall, B. J., Goto, M., **Usuda, T.**: 2011, Warm and Diffuse Gas and High Ionization Rate Near the Galactic Center, Int. Symp. on Molecular Spectroscopy, 66th meeting.

Oka, T., Tanaka, K., Matsumura, S. Nagai, M., Kamegai, K., **Hasegawa, T.**: 2011, The ASTE Galactic Center CO J=3−2 Survey: Probing Shocked Molecular Gas in the CMZ, ASP Conf. Ser. 439, Eds. M. R. Morris, Q. D. Wang, F. Yuan, 3-12.

Oshima, A., et al.: 2011, Cosmic ray anisotropy observed by GRAPES-3 air shower array, 32nd Int. Cosmic Ray Conf., Eds. A. Oshima, et. al., Vol. 1, 109-112.

Pinfield, D. J., et al. including **Tamura, M.**: 2011, Understanding sub-stellar populations using wide-field infrared surveys, EPJ

Web of Conf., 16, Eds. E. L. Martin, J. Ge, W. Lin.

Saiki, K., Arai, T., **Araki, H.**, **Ishihara, Y.**, Ohtake, M., Karouji, Y., Kobayashi, N., Sugihara, T., Haruyama, J., Honda, C., Sato, H., Takeda, H.: 2011, SELENE-2 landing site research board activity report, Proc. 44th ISAS Lunar. Planet. Symp., Abstract #44-10.

Saito, M., Kitamura, Y., Momose, M., Tsukagoshi, T., **Kawabe, R.**: 2012, Aperture Synthesis Observations Toward The Protostellar Systems L1551 IRS 5 And Hl Tau: Rotation In The Infalling Envelope, AAS Meeting #219, #437.02.

Sakai, N., Sakai, T., **Hirota, T.**, Yamamoto, S.: 2011, Peculiar Carbon-Chain Chemistry in Low-Mass Star Forming Regions, EAS Publ. Ser., 52, Eds. M. Roellig, R. Simon, V. Ossenkopf, J. Stutzki, 235-238.

Sakao, T., Narukage, N., **Shimojo, M.**, **Tsuneta, S.**, **Suematsu, Y.**, **Miyazaki, S.**, Imada, S., Nishizuka, N., Watanabe, K., Dotani, T., DeLuca, E. E., Ishikawa, S.: 2011, Photon-counting soft x-ray telescope for the Solar-C mission, Proc. of the SPIE, 8148, Eds. S. Fineschi, J. Fennelly, 81480C.

Sasaki, S., **Goossens, S.**, **Ishihara, Y.**, **Araki, H.**, **Hanada, H.**, **Matsumoto, K.**, **Noda, H.**, **Kikuchi, F.**, Iwata, T.: 2012, Kaguya Selenodesy and the South Pole Aitken Basin, 43rd Lunar and Planetary Science Conference, #1838.

Sasaki, S., **Ishihara, Y.**, **Goossens, S.**, **Matsumoto, K.**, **Hanada, H.**, **Araki, H.**, **Noda, H.**, Iwata, T., Namiki, N.: 2011, The Shape and Interior Structure of the South Pole-Aitken Basin from KAGUYA Selenodesy Data, Proc. 44th ISAS Lunar. Planet. Symp., #10.

Sekiguchi, K.: 2012, WWDA Visit to Kazakhstan, IAU Information Bulletin, 109, 62-70.

Shibasaki, K., Narukage, N., Yoshimura, K.: 2011, Imaging Observations of Coronal Magnetic Field by Nobeyama Radioheliograph, Solar Polarization 6, Proc. of a conf. held in Maui, Hawaii, USA, Eds. J. R. Kuhn, D. M. Harrington, H. Lin, S. V. Berdyugina, J. Trujillo-Bueno, S. L. Keil, T. Rimmele, 433.

Shimajiri, Y., **Kawabe, R.**, Takakuwa, S., **Saito, M.**, Tsukagoshi, T., Momose, M., Ikeda, N., Akiyama, E., Austermann, J. E., **Ezawa, H.**, Fukue, K., **Hiramatsu, M.**, Hughes, D., Kitamura, Y., Kohno, K., **Kurono, Y.**, Acott, K. S., Wilson, G., Yoshida, A., Yun, M. S.: 2011, Star Formation in the Orion A Molecular Cloud, EAS Publ. Ser., 52, Eds. M. Roellig, R. Simon, V. Ossenkopf, J. Stutzki, 307-308.

Shimizu, T., **Tsuneta, S.**, **Hara, H.**, Ichimoto, K., Kusano, K., Sakao, T., **Sekii, T.**, **Suematsu, Y.**, **Watanabe, T.**: 2011, The SOLAR-C mission: current status, Proc. of the SPIE, 8148, Eds. S. Fineschi, J. Fennelly, 81480B.

Shimonishi, T., Onaka, T., Kato, D., Ita, Y., Sakon, I., **Kawamura, A.**, Kaneda, H.: 2011, Effect of Metallicity on the Chemical Properties of Ices around embedded Young Stellar Objects, Proc. IAU Symp. 280, Eds. J. Cernicharo, R. Bachiller, 339.

Shirasaki, Y., **Komiya, Y.**, **Ohishi, M.**, **Mizumoto. Y.**, Ishihara, Y., Yanaka, H., Tsutsumi, J., Hiyama, T., Nakamoto, H., Sakamoto, M.: 2011, Current Status of the Japanese Virtual Observatory Portal, ASP Conf. Proc. 442, Eds. I. N. Evans, A. Accomazzi, D. J. Mink, A. H. Rots, 591-594.

Sôma, M., Tanikawa, K.: 2011, Investigation of the Earth's Rotation using Ancient Chinese Occultation Records, Mapping the Oriental Sky, Proc. of the Seventh Int. Conf. on Oriental Astronomy (ICOA-7), Eds. T. Nakamura, W. Orchiston, M. Sôma, R. Strom, 64-66.

Sôma, M., Tanikawa, K.: 2011, Japanese astronomy in the 7th century, Highlighting the History of Astronomy in the Asia-Pcific Region, Proc. of the ICOA-6 Conf., Eds. W. Orchiston, T. Nakamura, R. Strom, 139-151.

Sotani, H., Kokkotas, K. D.: 2011, Non-axisymmetric Torsional Oscillations of Relativistic Stars, *J. Phys.: Conf. Ser.*, **314**, 12081.

Sotani, H.: 2011, Slowly Rotating Relativistic Stars in TeVeS, *J. Phys.: Conf. Ser.*, **314**, 12126.

Suematsu, Y., **Katsukawa, Y.**, Shimizu, T., Ichimoto, K., Horiuchi, T., Matsumoto, Y., Takeyama, N.: 2011, Short telescope design of 1.5-m aperture solar UV visible and IR telescope aboard Solar-C, Proc. of the SPIE, 8148, Eds. S. Fineschi, J. Fennelly, 81480D.

Suzuki, T., Mao, H., Honma, M., Yoshida, T., **Kajino, T.**, Otsuka, T.: 2011, Electron capture reactions and beta decays in stellar environments, AIP Conf. Proc. 1377, 28-32.

Suzuki, T., Yoshida, T., Honma, M., Mao, H., Otsuka, T., **Kajino, T.**: 2011, Gamow-Teller and First-Forbidden Transition Strengths in Astrophysical Processes, *J. Phys.: Conf. Ser.*, **312**, 72008.

Takanashi, N., **Hiramatsu, M.**: 2011, The TENPLA project: Communicating Astronomy with the Public in Japan, Proc. IAU Symp. 260, Eds. D. Valls-Gabaud, A. Boksenberg, 44-47.

Tanikawa, K., **Sôma, M.**: 2011, How were solar eclipses remembered when there were no astronomers?, Mapping the Oriental Sky, Proc. of the Seventh Int. Conf. on Oriental Astronomy (ICOA-7), Eds. T. Nakamura, W. Orchiston, M. Sôma, R. Strom, 67-69.

Tanikawa, K., Yamamoto, T., **Sôma, M.**: 2011, Solar Eclipses at Sunrise and Sunset in the Chunqiu Period, Highlighting the History of Astronomy in the Asia-Pcific Region, Proc. of the ICOA-6 Conf., Eds. W. Orchiston, T. Nakamura, R. Strom, 21-43.

Tholen, D. J., et al. including **Yagi, M.**, **Yoshida, F.**: 2011, Minor Planet Observations [568 Mauna Kea], *Minor Planet Circulars*, 7540.

Torii, K., Fukui, Y., Kudo, N., Yamamoto, H., **Kawamura, A.**, Machida, M., Takahashi, K., Nozawa, S., Matsumoto, R.: 2011, Molecular Loops in the Galactic Center: Detailed Observations of the Footpoint of the Loops, ASP Conf. Ser. 439, Eds. M. R. Morris, Q. D. Wang, F. Yuan, 71.

Tosaki, T., **Kuno, N.**, **Onodera, S.**, Miura, R., Muraoka, K., **Sawada, T.**, **Komugi, S.**, **Nakanishi, K.**, Kohno, K., **Kawabe, R.**, Nakanishi, H., Arimoto, N.: 2011, NRO Legacy Project: M 33 All Disk Survey of Giant Molecular Clouds (GMCs) with NRO-45m and ASTE-10m Telescope, EAS Publ. Ser., 52, Eds. M. Roellig, R. Simon, V. Ossenkopf, J. Stutzki, 125-128.

Tsujimoto, T., Bekki, K.: 2011, Diagnosis of the IMF in the Universe using C, N Abundances, ASP Conf. Ser. 445, Eds. F. Kerschbaum, T. Lebzelter, R. F. Wing, 549-550.

Uemoto, K., Ohtake, M., Haruyama, J., Matsunaga, T., Yokota, Y., Yamamoto, S., Nakamura, R., **Morota, T.**, Kobayashi, S., Iwata, T.: 2011, Geological structure of the lunar South Pole-Aitken basin based on data derived from SELENE, Proc. 44th ISAS Lunar. Planet. Symp., Abstract #44-12.

Ueta, T., **Izumiura, H.**, Yamamura, I., Matsunaga, N., Ita, Y., Matsuura, M., Nakada, Y., Fukushi, H., Mito, H., Tanabe, T., Hashimoto, O.: 2011, Extended Dust Shell of the Carbon Star U Hya Revealed by AKARI, ASP Conf. Ser. 445, Eds. F. Kerschbaum, T. Lebzelter, R. F. Wing, 627.

Vivian, U., Wang, Z., Sanders, D., Fazio, G., Chung, A., Petitpas, G., **Iono, D.**, Gao, Y., Kewley, L., Huang, J.-S., GOALS: 2011, High-Resolution Mapping of CO(3−2) in NGC 6240, ASP Conf. Ser. 446, Eds. W. Wang, J. Lu, Z. Luo, Z. Yang, H. Hua, Z. Chen, 97-102.

Watanabe, H., Narukage, N., **Kubo, M.**, **Ishikawa, R.**, **Bando, T.**, **Kano, R.**, **Tsuneta, S.**, Kobayashi, K., Ichimoto, K., Trujillo-Bueno, J.: 2011, Ly-alpha polarimeter design for CLASP rocket experiment, Proc. of the SPIE, 8148, Eds. S. Fineschi, J. Fennelly, 81480E.

Yamada, Y., Lammers, U., **Gouda, N.**: 2011, Application of Gaia Analysis Software AGIS to Nano-JASMINE, ASP Conf. Proc. 442, Eds. I. N. Evans, A. Accomazzi, D. J. Mink, A. H. Rots, 367-370.

Yamaguchi, T., Sugimura, M., Sakai, T., Sakai, N., **Takano, S.**, Hirano, N., Liu, S.-L., Nomura, H., Su, Y.-N., Takakuwa, S., Yamamoto, S.: 2011, Line Survey of L1157 B1 Shocked Region, EAS Publ. Ser., 52, Eds. M. Roellig, R. Simon, V. Ossenkopf, J. Stutzki, 311-312.

Yamamoto, S., Nakamura, R., Matsunaga, T., Ogawa, Y., **Ishihara, Y.**, **Morota, T.**, Hirata, N., Ohtake, M., Hiroi, T., Yokota, Y., Haruyama, J.: 2012, Global Distribution Trend of Purest Anorthosite on the Moon Revealed by SELENE Spectral Profiler, 43rd Lunar and Planetary Science Conference, #1356.

Yanagisawa, K., **Kuroda, D.**, **Shimizu, Y.**, **Okita, K.**, Yoshida, M., Ohta, K., Kawai, N.: 2011, GRB 110915A MITSuME Okayama j-band upper-limit, *GRB Coordinates Network, Circular Service*, 12345, 1.

Yanagisawa, K., **Kuroda, D.**, **Shimizu, Y.**, **Okita, K.**, Yoshida, M., Ohta, K., Kawai, N.: 2011, GRB 111210A: MITSuME Okayama J-band upper-limit, *GRB Coordinates Network, Circular Service*, 12655, 1.

Yanagisawa, K., **Kuroda, D.**, **Shimizu, Y.**, **Okita, K.**, Yoshida, M., Ohta, K., Kawai, N.: 2012, GRB 120106A: Mitsume okayama ks-band upper limit, *GRB Coordinates Network, Circular Service*, 12819, 1.

Yanagisawa, K., **Kuroda, D.**, **Shimizu, Y.**, Okita, K., Yoshida, M., Ohta, K., Kawai, N.: 2012, GRB 120211A: Mitsume okayama ks-band observation, *GRB Coordinates Network, Circular Service*, 12936, 1.

Yanagisawa, K., **Kuroda, D.**, **Shimizu, Y.**, **Okita, K.**, Yoshida, M., Ohta, K., Kawai, N.: 2012, GRB 120211A: Mitsume okayama ks-band upper limit, *GRB Coordinates Network, Circular Service*, 12923, 1.

Yanagisawa, K., **Kuroda, D.**, **Shimizu, Y.**, **Okita, K.**, Yoshida, M., Ohta, K., Kawai, N.: 2012, GRB 120212A: errata of subject in GCNC 12936, *GRB Coordinates Network, Circular Service*, 12938, 1.

Yasuda, N., **Okura, Y.**, **Takata, T.**, **Furusawa, H.**: 2011, A Method for Measuring Distortion in Wide-Field Imaging with High Order Polynomials, ASP Conf. Proc. 442, Eds. I. N. Evans, A. Accomazzi, D. J. Mink, A. H. Rots, 537-540.

Yokota, Y., Gwinner, K., Oberst, J., Haruyama, J., Matsunaga, T., **Morota, T.**, **Noda, H.**, **Araki, H.**, Ohtake, M., Yamamoto, S.: 2012, Lunar Surface Roughness at Baseline 0.15-100 km and the Impact History of the Highlands, 43rd Lunar and Planetary Science Conference, #2843.

Yoshida, F., **Yagi, M.**, Tomatic, A. U.: 2011, 2010 LQ68, *Minor Planet Electronic Circulars*.

Yung, B., Nakashima, J., Imai, H., **Deguchi, S.**, Diamond, P. J., Kwok, S.: 2011, High Velocity Precessing Jet from the Water Fountain IRAS 18286-0959 Revealed by VLBA Observations, AAS Meeting #218, #127.12.

Zamaninasab, M., Witzel, G., Eckart, A., Sabha, N., Dovciak, M., Karas, V., Schödel, R., García-Marín, M., Kunneriath, D., **Nishiyama, S.**, Straubmeier, C., Valencia-Schneider, M., Zensus, A.: 2011, Near Infrared Polarimetry as a Tool for Testing the Properties of Radiation from Sagittarius A*, ASP Conf. Ser. 439, Eds. M. R. Morris, Q. D. Wang, F. Yuan.

Zenitani, S., Hesse, M., Klimas, A.: 2011, Fluid and Magnetofluid Modeling of Relativistic Magnetic Reconnection, AIP Conf. Proc. 1366, Eds. V. Florinski, J. Heerikhuisen, G. P. Zank, D. L. Gallagher, 138-144.

Zhu, M., Papadopoulos, P. P., Xilouris, M., **Kuno, N.**, Lisenfeld, U.: 2011, Excess Submillimeter Emission in the Starburst Galaxy NGC 3310?, ASP Conf. Ser. 446, Eds. W. Wang, J. Lu, Z. Luo, Z. Yang, H. Hua, Z. Chen, 119-124.

5. Publications in English

Finoguenov, A., et al. including **Sekiguchi, K.**: 2012, SXDF X-ray groups and galaxy clusters, VizieR Online Data Catalog Vol. 740.

Nakamura, T., Orchiston, W., **Sôma, M.**, Strom, R.: 2011, Mapping the Oriental Sky, Proceedings of the Seventh International Conference on Oriental Astronomy (ICOA-7), NAOJ, Tokyo.

6. Conference Presentations

Agata, H.: 2011, “You are Galileo!” telescope workshop in Indnesia, APRIM2011, (Chiang Mai, Thailand, Jul. 25-29, 2011).

Agata, H.: 2011, Report of “You are Galileo!” telescope workshop, CAP2011, (Beijing, China, Oct. 10-14, 2011).

Agatsuma, K., **Chen, D.**: 2011, Folding PRC for bLCGT, 4th LCGT face to face meeting, (Kashiwa, Japan, Aug. 3-5, 2011).

Agatsuma, K., **Mori, T.**, Ballmer, S., Sakata, S., Nishida, E., **Kawamura, S.**: 2011, High accuracy measurement of the quantum efficiency using radiation pressure, 9th Edoardo Amaldi Conference on Gravitational Waves, (Cardiff, UK, Jul. 10-15, 2011).

Agatsuma, K., **Mori, T.**, Friedrich, D., Sakata, S., Ballmer, S., Miyakawa, O., Numata, K., **Kawamura, S.**: 2012, Radiation pressure noise measurement, 5th KAGRA face to face meeting, (Kashiwa, Japan, Feb. 2-4, 2012).

Akiyama, K.: 2011, Results of multi-epoch VERA observations of Sgr A* and future prospects for VERA+KVN, 1st VERA-KVN science working group, (Mitaka, Japan, Jun. 13-14, 2011).

Akiyama, K.: 2011, The results of multi-epoch VERA observations toward the galactic center, Sgr A*, AGN jet 2011, (Mitaka, Japan, Nov. 25, 2011).

Akutsu, T., **Chen, D.**, Ejiri, Y., Suzuki, R., Sato, S., Araya, A., Ando, M., **Tanaka, N.**, **Torii, Y.**, **Kawamura, S.**: 2011, Ground testing of inertial sensors for DECIGO Pathnder, 9th Edoardo Amaldi Conference on Gravitational Waves, (Cardiff, UK, Jul. 10-15, 2011).

Akutsu, T., DECIGO Working Group: 2011, DECIGO and DECIGO Pathfiner, Gravitational Wave Advanced Detector Workshop 2011, (Isola d'Elba, Italy, May 22-28, 2011).

Akutsu, T.: 2011, Status Report of Auxiliary Optics Subsystem, 4th LCGT face to face meeting, (Kashiwa, Japan, Aug. 3-5, 2011).

Akutsu, T.: 2012, Status Report of Auxiliary Optics, 5th KAGRA face to face meeting, (Kashiwa, Japan, Feb. 2-4, 2012).

Aoki, K., **Hara, H.**: 2011, A High-Velocity Motion of Active Region Loops Triggered by a 2011 Feb 18 Flare, The 5th Hinode Science Meeeting, (Boston, MA, USA, Oct. 11-15, 2011).

Aoki, K., **Iwata, I.**, **Hattoti, T.**: 2011, Mid-Infrared selected quasars in WISE Preliminary Data Release, Through the Infrared Looking Glass: A Dusty View of Galaxy and AGN Evolution, (Pasadena, CA, USA, Oct. 2-5, 2011).

Aoki, K.: 2011, Rest optical spectroscopy of FeLoBALs and LoBALs at intermideiate redshift, Narrow-line Seyfert1 galaxies and their place in the universe, (Milano, Italy, Apr. 4-6, 2011).

Aoki, W.: 2011, Extremely Metal-Poor Stars in the Milky Way Halo, 3rd Subaru Int. Conf., 1st NAOJ Symp., Galactic Archaeology: Near-Field Cosmology and the Formation of the Milky Way, (Shuzenji, Japan, Nov. 1-4, 2011).

Aoki, W.: 2011, Neutron-Capture Elements in Extremely Metal-Poor Stars, 11th Int. Symp. on Origin of Matter and Evolution of Galaxies, (Wako, Japan, Nov. 14-17, 2011).

Aoki, W.: 2011, The metallicity distribution of Sr-enhanced metal-poor stars, The Light Element Primary Process & the Origin of Lighter Heavy Elements, (GSI, Darmstadt, Germany, Oct. 10-12, 2011).

Aoki, W.: 2012, Li abundances in very metal-poor, main-sequence turn-off stars, Int. Workshop on Lithium in the Cosmos, (Paris, France, Feb, 27-29, 2012).

Araki, H., **Noda, H.**, **Hanada, H.**, **Katayama, M.**, **Sasaki, S.**, **Tazawa, S.**, **Tsuruta, S.**, Kunimori, H., Fuse, T., Otsubo, T., Funazaki, K., Sato, A., Taniguchi, H., Murata, K.: 2012, Research Activities in Japan for the Precise Measurement of the Lunar Rotation and Tide -LLR and ILOM-, Theory and Model For the New Generation of the Lunar Laser RANGING DATA; 3rd Work Shop, (ISSI, Bern, Switzerland, Mar. 23-25, 2012).

Araki, H., **Tazawa, S.**, **Noda, H.**, **Ishihara, Y.**, **Goossens, S.**, **Sasaki, S.**: 2012, The Status of Data Archive and Calibration/ Validation of LALT, The 6th KAGUYA (SELENE) Science Working Team Meeting (SWTM6), (Nagoya, Japan, Jan. 10-12, 2012).

Ariyoshi, S., Takahashi, K., **Noguchi, T.**, Koga, K., Furukawa, N., Otani, C.: 2011, Terahertz detector with transmission-line type superconducting tunnel junctions, Superconductivity Centennial Conf. (EUCAS-ISEC-ICMC 2011), (Hague, Netherlands, Sep. 18-23, 2011).

Black, C., Antiochos, S. K., Hesse, M., Karpen, J. T., DeVore, C. R., Kuznetsova, M. M., **Zenitani, S.**: 2011, Kinetic Simulations of Current-Sheet Formation and Reconnection at a Magnetic X Line, 53rd Annual Meeting of the APS Division of Plasma Physics, (Salt Lake City, UT, USA, Nov. 14-18, 2011).

Black, C., Antiochos, S. K., Hesse, M., Karpen, J. T., DeVore, C. R., **Zenitani, S.**, Kuznetsova, M. M.: 2011, Current-Sheet Formation and Reconnection at a Magnetic X Line in Particle-in-Cell Simulations, AGU Fall Meeting 2011, (San Francisco, CA, USA, Dec. 5-9, 2011).

Bowler, B. P., Liu, M. C., Shkolnik, E. L., **Tamura, M.**: 2012, A High-Contrast Adaptive Optics Imaging Search for Giant Planets Around Young M Dwarfs, AAS Meeting #219, (Austin, TX, USA, Jan. 8-12, 2012).

Carson, J., Thalmann, C., Janson, M., Kozakis, T., Wong, P., Goto, M., Henning, T., Brandner, W., Biller, B., Bonnefoy, M., Feldt, M., McElwain, M., **Kandori, R.**, **Tamura, M.**, SEEDS Team: 2012, A Subaru SEEDS Imaging Search for Extrasolar Planets Around Early-Type Stars, AAS Meeting #219, (Austin, TX, USA, Jan. 8-12, 2012).

Chen, D., **Akutsu, T.**, Ejiri, Y., Suzuki, R., **Ueda, A.**, **Torii, Y.**, **Tanaka, N.**, Araya, A., Sato, S., Ando, M., Gondo R., **Obuchi, Y.**, **Okada, N.**, **Kawamura, S.**, **Fujimoto, M.-K.**: 2011, Development of the inertial sensor for DECIGO Pathfinder, 9th Edoardo Amaldi Conference on Gravitational Waves, (Cardiff, UK, Jul. 10-15, 2011).

Eguchi, S., **Shirasaki, Y.**, **Komiya, Y.**, **Ohishi, M.**, **Mizumoto, Y.**, Ishihara, Y., Yanaka, H., Tsutsumi, J., Hiyama, T., Nakamoto, H., Sakamoto, M.: 2011, Improvement of Service Searching Algorithm in the JVO Portal Site, Astronomical Data Analysis Software and Systems XX, (Paris, France, Nov. 6-10, 2011).

Fukui, A., Homlan, M. J., **Narita, N.**, Sumi, T.: 2011, Frequency of Second Planet Occurrence in Mean Motion Resonances with Hot Jupiters, Exsteme Solar Systems II, (Jackson, WY, USA, Sep. 11-17, 2011).

Gonzalez, A., **Fujii, Y.**, **Kaneko, K.**, **Uzawa, Y.**: 2011, Quasi-optical attenuators for ALMA band 10 receiver, Asia-Pacific Microwave Conf. 2011 (APMC 2011), (Melbourne, Australia, Dec. 5-8, 2011).

Goossens, S., **Matsumoto, K.**, **Kikuchi, F.**, Liu, Q., **Hanada, H.**, Lemoine, F. G., Rowlands, D. D., Mazarico, E., **Ishihara, Y.**, **Noda, H.**, **Araki, H.**, Namiki, N., Iwata, T., **Sasaki, S.**: 2012, Improved high-resolution lunar gravity field model from SELENE and historical tracking data, The 6th KAGUYA (SELENE) Science Working Team Meeting (SWTM6), (Nagoya, Japan, Jan. 10-12, 2012).

Goossens, S., **Matsumoto, K.**, **Kikuchi, F.**, Liu, Q., **Hanada, H.**, Lemoine, F. G., Rowlands, D. D., **Ishihara, Y.**, **Noda, H.**, Namiki, N., Iwata, T., **Sasaki, S.**: 2011, Improved High-Resolution Lunar Gravity Field Model From SELENE and Historical Tracking Data, AGU Fall Meeting 2011, (San Francisco, CA, USA, Dec. 5-9, 2011).

Gouda, N., JASMINE working group: 2011, Infrared Space Astrometry Missions ~JASMINE missions~, 3rd Subaru Int. Conf., 1st NAOJ Symp., Galactic Archaeology: Near-Field Cosmology and the Formation of the Milky Way, (Shuzenji, Japan, Nov. 1-4, 2011).

Hada, K.: 2011, Measurement of the velocity field of the M87 jet with VERA/GENJI, AGN jet 2011, (Mitaka, Japan, Nov. 25, 2011).

Hada, K.: 2012, M87 observations, 2nd VERA-KVN science working group, (Seoul, Korea, Feb. 15-16, 2012).

Hanada, H., **Araki, H.**, **Tazawa, S.**, **Tsuruta, S.**, **Noda, H.**, **Asari, K.**, **Ishihara, Y.**, **Matsumoto, K.**, **Sasaki, S.**, Funazaki, K., Satoh, A., Taniguchi, H., Kato, H., Kikuchi, M., Murata, K., Itou, Y., Chiba, K., Wakamatsu, H., Petrova, N., Gusev, A., **Gouda, N.**, **Yano, T.**, Yamada, Y., **Niwa, Y.**, Ping, J., Kawano, N., Iwata, T., Heki, K.: 2011, Development of a Small Telescope for Observations of Lunar Rotation, ASTROKAZAN 2011, (Kazan, Russia, Aug. 22-30, 2011).

Hanada, H., **Tsuruta, S.**, **Araki, H.**, **Tazawa, S.**, **Asari, K.**, **Noda, H.**, **Ishihara, Y.**, **Matsumoto, K.**, **Sasaki, S.**, Funazaki, K., Satoh, A., Taniguchi, H., Kato, H., Kikuchi, M., Murata, K., Itou, Y., Chiba, K., Wakamatsu, H., **Gouda, N.**, **Yano, T.**, Yamada, Y., **Niwa, Y.**, Petrova, N., Gusev, A., Ping, J., Kawano, N., Iwata, T., Heki, K.: 2012, Development of a Small Digital Telescope for Observations of Lunar Rotation, The 6th KAGUYA (SELENE) Science Working Team Meeting (SWTM6), (Nagoya, Japan, Jan. 10-12, 2012).

Hanaoka, Y.: 2012, Long-Term Synoptic Observation of the Sun by the Solar Observatory of the NAOJ, The 2nd Nagoya Workshop on the Relationship between Solar Activity and Climate Changes, (Nagoya, Japan, Jan. 16-17, 2012).

Hara, C., **Kawabe, R.**, **Shimajiri, Y.**, **Saito, M.**, **Nakamura, F.**, Tsukagoshi, T., Wilner, D.: 2012, ASTE and SMA observations of B59 in the Pipe nebula; Evidence for disk-driven rotating molecular outflow from a protost, ALMA/NAASC 2012 Workshop: Outflows, Winds and Jets, (Charlottesville, Virginia, USA, Mar. 3-6, 2012).

Hara, H., **Watanabe, T.**, Harra, L. K., Culhane, J. L., Young, P. R.: 2011, Observed Features of Magnetic Reconnection in 2007 May 19 Flare, The 5th Hinode Science Meeeting, (Boston, MA, USA, Oct. 11-15, 2011).

Hara, H.: 2012, Photosphere -Corona Connection in Active-Region Plage, SDO-4/ IRIS/ Hinode Workshop, (Monterey, USA, Mar. 12-16, 2012).

Harada, Y., **Goossens, S.**, **Matsumoto, K.**, Yan, J., Ping, J.: 2012, The Tidal Response of the Moon, The 6th KAGUYA (SELENE) Science Working Team Meeting (SWTM6), (Nagoya, Japan, Jan. 10-12, 2012).

Hashimoto, J., **Tamura, M.**, Muto, T., SEEDS Project Team: 2011, Implications of Giant Planet Formation in the Protoplanetary Disk around AB Aurigae, Signposts of Planets Conf., (Goddard Space Flight Center, USA, Oct. 18-20, 2011).

Hashimoto, J., **Tamura, M.**, Muto, T., SEEDS Project Team: 2011, Initial Result of the Subaru SEEDS Project: Fine Structures of the Circumstellar Disk around AB Aur, Asia Oceania Geosciences Society 2011, (Taipei, Taiwan, Aug. 8-12, 2011).

Hayama, K., Niinuma, K., Oyama, T.: 2011, Proposal for multi-messenger observations of radio transients by Nasu and LIGO-Virgo, New Horizons in Time Domain Astronomy, (Oxford, UK, Sep. 19-23, 2011).

Hayama, K.: 2011, Multi-messenger observation using LCGT, 4th LCGT face to face meeting, (Kashiwa, Japan, Aug. 3-5, 2011).

Hayama, K.: 2012, Current status of Detector Characterization for KAGRA, 5th KAGRA face to face meeting, (Kashiwa, Japan, Feb. 2-4, 2012).

Hayano, Y., Akiyama, M., **Hattori, T.**, **Iwata, I.**, **Kodama, T.**, **Minowa, Y.**, Motohara, K., **Nishimura, T.**, **Ohashi, N.**, Ohno, Y., **Oya, S.**, **Shirahata, M.**, **Takami, H.**, **Takato, N.**, **Tamura, N.**, **Tanaka, I.**, **Terada, H.**, **Tomono, D.**, **Usuda, T.**: 2011, Next generation AO system of Subaru Telescope, 2nd Int. Conf. on Adaptive Optics for Extremely Large Telescopes, (Victoria, Canada, Sep. 25-30, 2011).

Hayano, Y., **Oya, S.**, **Hattori, M.**, **Minowa, Y.**, **Shirahata, M.**, **Terada, H.**, **Pyo, T.-S.**, **Takami, H.**, **Iye, M.**: 2011, AO188/LGS at Subaru Telescope, Mauna Kea AO meeting, (IfA Hilo, HI, USA, Sep. 14, 2011).

Hayashi, M.: 2011, Star formation activities in a cluster and its surrounding structure at $z=1.46$, Galaxy Formation 2011, (Durham, UK, Jul. 18-22, 2011).

Hayashi, T.: 2011, Rejuvenated young radio source J1159+011 as BAL quasar, 4th East Asia VLBI Workshop — Sciences and Technology by now and future, (Lijiang, China, Apr. 18-20, 2011).

Hayashi, T.: 2011, Young radio sources and BAL quasars, AGN jet 2011, (Mitaka, Japan, Nov. 25, 2011).

Hayashi, T.: 2011, Young Radio Sources Associated with Broad Absorption Line Quasars, Workshop on East-Asian collaboration for SKA, (Daejeon, Korea, Nov. 30-Dec. 2, 2011).

Hibi, Y., **Matsuo, H.**, Ikeda, H., Fujiwara, M.: 2011, 32-ch multi-chip module with GaAs-JFET cryo-ASICs, 12th Workshop on Submillimeter-Wave Receiver Technologies in Eastern Asia, (Seoul, Korea, Dec. 5-6, 2011).

Hibi, Y., **Matsuo, H.**, Ikeda, H., Fujiwara, M.: 2011, The Cryogenic Multi-Channel Readout System for Submillimeter/Terahertz Cameras, 14th Int. Workshop on Low Temperature Detectors, (Heidelberg, Germany, Aug. 1-5, 2011).

Hibi, Y., **Matsuo, H.**, Ookawa, T., Nagata, H., Ikeda, H., Fujiwara, M.: 2011, "32-channel Multi-Chip-Module" The Cryogenic Readout System for Submillimeter/Terahertz Cameras, 22nd Int. Symp. on Space Terahertz Technology, (Tucson, AZ, USA, Apr. 26-28, 2011).

Higuchi, A., Kokubo, E., **Ito, T.**: 2012, Radial transport of small solar system bodies - from 10^0 AU to 10^5 AU -, MISASA IV Solar System Exploration and New Geosciences -Perspective for the Next Decade-, (Tottori, Japan, Feb. 24-26, 2012).

Hirota, T.: 2011, Observational Studies on Star-formation with VERA, Ishigaki International Workshop "Formation of Stars & Planets 2011(FSP2011)", (Ishigaki, Okinawa, Japan, Oct. 3-7, 2011).

Hirota, T.: 2011, Review of "VERA nearby SFRs project", 1st VERA-KVN science working group, (Mitaka, Japan, Jun. 13-14, 2011).

Hirota, T.: 2012, Proposal of SFRs studies with VERA+KVN, 2nd VERA-KVN science working group, (Seoul, Korea, Feb. 15-16, 2012).

Hirota, T.: 2012, Status report of SFRs sub-WG, 2nd VERA-KVN science working group, (Seoul, Korea, Feb. 15-16, 2012).

Hirota, T.: 2012, VERA observations of the H_2O maser burst in Orion KL, IAU Symp. 287, "Cosmic Masers - from OH to H0", (Stellenbosch, South Africa, Jan. 30-Feb. 3, 2012).

Honma, M.: 2011, Maser astrometry and East-Asian VLBI, 11th Asian-Pacific Regional IAU Meeting, (Chiang Mai, Thailand, Jul. 26-29, 2011).

Honma, M.: 2011, mm/sub-mm VLBI, AGN jet 2011, (Mitaka, Japan, Nov. 25, 2011).

Honma, M.: 2011, VLBI astrometry with VERA+KVN, 1st VERA-KVN science working group, (Mitaka, Japan, Jun. 13-14, 2011).

Honma, M.: 2012, EHT and Chandra Sgr A* campaign, 2nd VERA-KVN science working group, (Seoul, Korea, Feb. 15-16, 2012).

Honma, M.: 2012, Maser astrometry with VERA and Galactic structure, IAU Symp. 287, "Cosmic Masers - from OH to H0", (Stellenbosch, South Africa, Jan. 30-Feb. 3, 2012).

Hori, Y., Ikoma, M.: 2011, Gas Giant Formation with Small Cores Triggered by Envelope Pollution by Icy Planetesimals, Extreme Solar Systems II, (Moran, WY, USA, Sep. 11-17, 2011).

Hori, Y., Kokubo, E., Oshino, S., Ida, S.: 2011, Formation and Diversity of Planetary Systems around M-dwarfs: Toward the Next-Generation Observations, The 1st Kepler Science Conf., (NASA Ames Research Park, USA, Dec. 5-9, 2011).

Hwang, N.: 2011, Origin of Extended Star Clusters: New Archaeological Tracers of Galaxy Evolution?, 3rd Subaru Int. Conf., 1st NAOJ Symp., Galactic Archaeology: Near-Field Cosmology and the Formation of the Milky Way, (Shuzenji, Japan, Nov. 1-4, 2011).

Hwang, N.: 2011, The Nature of Extended Star Clusters in the Dwarf Galaxy NGC 6822, Stellar Clusters & Associations: A RIA Workshop on Gaia, (Granada, Spain, May 23-27, 2011).

Ichimoto, K., **Suematsu, Y.**, **Katsukawa, Y.**, Shimizu, T., SUVIT Team: 2011, Science objective and design concept of the Large Aperture Solar UV Visible and IR Observing Telescope for Solar-C Mission, 2nd ATST-EAST Workshop in Solar Physics, (Washington, DC, USA, Oct. 9-11, 2011).

Iguchi, S.: 2011, ALMA and Key Technologies for Future Large Single Dishes, Large Aperture Millimeter/Submillimeter Telescopes in the ALMA Era, (Osaka, Japan, Sep. 12-13, 2011).

Iguchi, S.: 2011, ALMA Status and Development Policy, ALMA EA Development Workshop 2011, (Mitaka, Japan, Sep. 8, 2011).

Iguchi, S.: 2011, ALMA Status, Science Operation, and EA Science activities, The 5th East Asian Core Observatories Association Meeting, (Kyoto, Japan, Nov. 7-8, 2011).

Iguchi, S.: 2011, Very Close Binary Black Hole in a Giant Elliptical Galaxy 3C 66B and its Black Hole Merger, Gravitational Wave Astrophysics, Binary Supermassive Black Holes, and Galaxy Mergers, (Lijiang, Yunnan, China, Aug. 1-5, 2011).

Iguchi, S.: 2012, A Very Close Binary Black Hole in a Giant Elliptical Galaxy 3C 66B and its Black Hole Merger, AAS Meeting #219, (Austin, TX, USA, Jan. 8-12, 2012).

Ikoma, M., **Hori, Y.**: 2011, Accumulation of Hydrogen-rich Atmospheres of Nebular Orgins on Short-Period Super-Earths: Implications for Kepler-11 Systems, The 1st Kepler Science Conf., (NASA Ames Research Park, USA, Dec. 5-9, 2011).

Imada, S., **Hara, H.**, **Watanabe, T.**, Shimizu, T., Harra, L. K.: 2011, Imaging Spectroscopic Observation of Filament Eruptions by Hinode/EIS Flare Hunting Study, The 5th Hinode Science Meeeting, (Boston, MA, USA, Oct. 11-15, 2011).

Imamura, T., Iwata, T., Yamamoto, Z., Mochizuki, N., **Kono, Y.**, **Matsumoto, K.**, Liu, Q., **Noda, H.**, **Hanada, H.**, Oyama, K., Futaana, Y., Nabatov, A., Saitou, A., Ando, H.: 2012, The status of data archive and calibration/validation of RS, The 6th KAGUYA (SELENE) Science Working Team Meeting (SWTM6), (Nagoya, Japan, Jan. 10-12, 2012).

Imanishi, M., Nakagawa, T., Ohyama, Y., **Shirahata, M.**, Onaka, T.: 2012, AKARI IRC systematic infrared spectroscopy of luminous infrared galaxies, The 2nd AKARI Conf., Legacy of AKARI: A Panoramic View of the Dusty Universe, (Jeji, Korea, Feb. 27-29, 2012).

Ishigaki, M., Chiba, M., **Aoki, W.**: 2011, Chemical abundance analyses of the kinematically selected thick disk/halo stars, 3rd Subaru Int. Conf., 1st NAOJ Symp., Galactic Archaeology: Near-Field Cosmology and the Formation of the Milky Way, (Shuzenji, Japan, Nov. 1-4, 2011).

Ishihara, Y., Hiramatsu, Y., Yamamoto, M., Furumoto, M., Fujita, K.: 2011, Infrasound and Seismic Observation of Hayabusa Reentry as An Artificial Meteorite Fall, AGU Fall Meeting 2011, (San Francisco, CA, USA, Dec. 5-9, 2011).

Ishihara, Y., Hiramatsu, Y., Yamamoto, M., Furumoto, M., Fujita, K.: 2012, Infrasound and Seismic Observation of Hayabusa Reentry as An Artificial Meteorite Fall, MISASA IV Solar System Exploration and New Geosciences -Perspective for the Next Decade-, (Tottori, Japan, Feb. 24-26, 2012).

Ishikawa, R.: 2011, Properties of transient horizontal magnetic fields; their implication to the origin of quiet-Sun magnetism, The 5th Hinode Science Meeeting, (Boston, MA, USA, Oct. 11-15, 2011).

Ishikawa, R.: 2011, Properties of Transient Horizontal Magnetic Fields and Their Implication to the Origin of the Quiet-Sun Magnetism, Asia Oceania Geosciences Society 2011, (Taipei, Taiwan, Aug. 8-12, 2011).

Ishisaki, Y., Henmi, K., Akamatsu, H., Enoki, T., Ohashi, T., Hoshino, A., Shinozaki, K., **Matsuo, H.**, **Okada, N.**, **Oshima, T.**: 2011, Development of active gas-gap heat switch for double-stage adiabatic demagnetization refrigerator, 14th Int. Workshop on Low Temperature Detectors, (Heidelberg, Germany, Aug. 1-5, 2011).

Ishitsu, N.: 2011, Dust Settling in Turbulent Protoplanetary Disks, Ishigaki International Workshop "Formation of Stars & Planets 2011 (FSP2011)", (Ishigaki, Okinawa, Japan, Oct. 3-7, 2011).

Ito, T., Higuchi, A.: 2011, Dynamical evolution of the Oort cloud new comets, Asia-Oceania Geoscience Society 8th Annual Meeting, (Taipei, Taiwan, Aug. 8-12, 2011).

Ito, T.: 2012, Asymmetric cratering on the Moon and its implication to a hidden NEA population, 3rd Maidanak Observatory Users Meeting, (Mitaka, Japan, Jan. 30-Feb. 1, 2012).

Iwata, I., Yamada, T., WISH Working Group: 2011, Our WISH: Feeding z>10 Targets to ELTs, Feeding the Giants: ELTs in the era of Surveys, (Ischia, Italy, Aug. 29-Sep. 2, 2011).

Iwata, T., **Matsumoto, K.**, **Ishihara, Y.**, **Kikuchi, F.**, **Harada, Y.**, **Sasaki, S.**: 2011, Measurements of Martian rotational variations by space geodetic techniques, 28th Int. Symp. on Space Technology and Science (28th ISTS), (Okinawa, Japan, Jun. 5-12, 2011).

Iwata, T., **Matsumoto, K.**, **Ishihara, Y.**, **Kikuchi, F.**, **Harada, Y.**, **Sasaki, S.**: 2011, A study of Mars' rotation measurements using four-way Doppler and inverse VLBI methods, EPSC-DPS Joint Meeting 2011, (Nantes, France, Oct. 2-7, 2011).

Iwata, T., **Matsumoto, K.**, **Ishihara, Y.**, **Kikuchi, F.**, **Harada, Y.**, **Sasaki, S.**: 2011, A study on the four-way Doppler measurements and inverse VLBI observations for Mars rotation, European Geosciences Union General Assembly 2011, (Vienna, Austria, Apr. 3-8, 2011).

Iwata, T., **Matsumoto, K.**, **Ishihara, Y.**, **Kikuchi, F.**, **Harada, Y.**, **Sasaki, S.**: 2011, A study on the Four-way Doppler Measurements and Inverse VLBI Observations for Mars' Rotation, Asia Oceania Geosciences Society 2011, (Taipei, Taiwan, Aug. 8-12, 2011).

Iye, M.: 2011, From the early universe to the formation of galaxies, German-Japan Round Table: From the Early Universe to the Evolution of Life, (Heiderberg, Germary, Dec. 1-3, 2011).

Izumiura, H., Kambe, E., Kuroda, D., Yanagisawa, K., Fukui, A., Shimizu, Y., Okita, K., Koyano, H., Sakamoto, A.: 2011, Refurbishing the 188cm reflector for exoplanet studies, Workshop on Astronomy with Precise Radial Velocity - Exoplanet Search and Asteroseismology, (Seoul, Korea, Sep. 26-28, 2011).

Izumiura, H., Ueta, T., Yamamura, I., Nakada, Y., Matsunaga, N., Ita, Y., Matsuura, M., Fukushi, H., Mito, H., Tanabe, T., Sorahana, T., Hashimoto, O., Arimatsu, K., Onaka, T.: 2012, AKARI observations of cool evolved stars, The 2nd AKARI Conf., Legacy of AKARI: A Panoramic View of the Dusty Universe, (Jeji, Korea, Feb. 27-29, 2012).

Jayawardhana, R., Muzic, K., Scholz, A., Geers, V., **Tamura, M.**: 2011, Substellar Objects in Nearby Young Clusters (SONYC): Latest Results, AAS Meeting #218, (Boston, USA, May 22-26, 2011).

Jike, T., **Manabe, S.**, **Tamura, Y.**, **Shizugaki, M.**: 2012, Movement of the 2011 off the Pacific coast of Tohoku Earthquake detected by VERA geophysical observations, 6th IVS General Meeting, (Spain, Madrid, Mar. 4-9, 2012).

Kajino, T.: 2011, Big-Bang Models, 6th European Physical Society Summer School of on Experimental Nuclear Astrophysics, (Catania, Italy, Sep. 18-27, 2011).

Kajino, T.: 2011, Cosmology and the Formation of Elements in the Early Universe, 2nd Multidisciplinary Science Forum, (Kalamazoo, MI, USA, Oct. 27-28, 2011).

Kajino, T.: 2011, Neutrinos in Cosmology, Astronomy and Astrophysics, Korean Physical Society, Annual meeting, (Daejon, Korea, Apr. 13-15, 2011).

Kajino, T.: 2011, Nuclear Weak Interactions, Supernova Nucleosynthesis and Neutrino Oscillation, Rutherford Centennial Conf. on Nuclear Physics, (Manchester, UK, Aug. 24-29, 2011).

Kajino, T.: 2011, R-Process in Gamma-Ray Bursts, Int. Workshop on Physics of Rare-Ring, (Wako, Japan, Nov. 10-12, 2011).

Kajino, T.: 2011, Supernova Neutrino-process Nucleosynthesis and Implications in Neutrino Oscillation, 3rd Subaru Int. Conf., 1st NAOJ Symp., Galactic Archaeology: Near-Field Cosmology and the Formation of the Milky Way, (Shuzenji, Japan, Nov. 1-4, 2011).

Kajino, T.: 2011, Supernova Nucleosynthesis and Neutrino Oscillation, 19th Particles and Nuclei International Conference (PANIC) , (MIT, Boston, USA, Jul. 25-30, 2011).

Kajino, T.: 2012, Quest for Particle Astrophysics Solution to Lithium Problems, Int. Workshop on Lithium in the Cosmos, (Paris, France, Feb, 27-29, 2012).

Kameya, O.: 2011, Pulsar Study using SKA, Workshop on East-Asian collaboration for SKA, (Daejeon, Korea, Nov. 30-Dec. 2, 2011).

Kameya, O.: 2012, Short commet on pulsar observations, 2nd VERA-KVN science working group, (Seoul, Korea, Feb. 15-16, 2012).

Kaneko, H., **Kuno, N.**, **Iono, D.**, Tamura, Y., Tosaki, T., **Nakanishi, K.**, **Sawada, T.**: 2011, Molecular Gas Properties and Star Formation in Interacting Galaxies, Galaxy Mergers In An Evolving Universe, (Hualien, Taiwan, Oct. 23-28, 2011).

Kano, R., Narukage, N., **Ishikawa, R.**, **Kubo, M.**, **Katsukawa, Y.**, **Suematsu, Y.**, **Hara, H.**, **Bando, T.**, **Tsuneta, S.**, Watanabe, H., Ichimoto, K., **Kubo, M.**, Song, D., Kobayashi, K., Trujillo Bueno, J.: 2011, Instrument for the Chromospheric Lyman-Alpha SpectroPolarimeter (CLASP) program, The 5th Hinode Science Meeeting, (Boston, MA, USA, Oct. 11-15, 2011).

Kano, R., **Tsuneta, S.**, Ueda, K.: 2011, What determines coronal-loop temperature?, The 5th Hinode Science Meeeting, (Boston, MA, USA, Oct. 11-15, 2011).

Kato, Y., Carlsson, M., Hansteen, V., Steiner, O.: 2011, Propagation of Slow-Modes through the Transition Region in Network Magnetic Elements, The 5th Hinode Science Meeeting, (Boston, MA, USA, Oct. 11-15, 2011).

Kato, Y.: 2012, Generation of shock waves traveling from the photosphere to the transition region within network magnetic elements, SDO-4/ IRIS/ Hinode Workshop, (Monterey, USA, Mar. 12-16, 2012).

Katsukawa, Y., Hinode SOT Team: 2011, Magnetic Field Diagnostics with the HINODE Spectro-Polarimeter, AGU Fall Meeting 2011, (San Francisco, CA, USA, Dec. 5-9, 2011).

Katsukawa, Y., **Orozco Suarez, D.**: 2011, Power spectra of the solar surface convection and implication to local dynamo, The 5th Hinode Science Meeeting, (Boston, MA, USA, Oct. 11-15, 2011).

Katsukawa, Y., **Suematsu, Y.**, Shimizu, T., Ichimoto, K., Takeyama, N.: 2011, Focal Plane Instrument for the Solar UV-Vis-IR Telescope aboard SOLAR-C, SPIE Optics + Photonics, (San Diego, CA, USA, Aug. 21-25, 2011).

Katsukawa, Y., **Suematsu, Y.**, **Tsuneta, S.**, Ichimoto, K., Shimizu, T.: 2011, Modeling and verification of the diffraction-limited visible light telescope aboard the solar observing satellite HINODE, Symp. on Integrated Modeling of Complex Optomechanical Systems, (Kiruna, Sweden, Aug. 15-17, 2011).

Katsukawa, Y.: 2011, Spacecraft overview, Solar-C Meeting, (Boston, MA, USA, Oct. 16, 2011).

Kawaguchi, N.: 2011, Earthquake damage on Mizusawa VLBI Observatory and Operation Plan in 2011, 4th East Asia VLBI Workshop — Sciences and Technology by now and future, (Lijiang, China, Apr. 18-20, 2011).

Kikuchi, F., **Matsumoto, K.**, **Hanada, H.**, **Tsuruta, S.**, **Asari, K.**, **Kono, Y.**, **Yamada, R.**, **Ishihara, Y.**, **Sasaki, S.**, Iwata, T., Iijima, Y., Ogawa, K., Kamata, S., **Goossens, S.**: 2012, Recent status of SELENE-2/VLBI instrument, The 6th KAGUYA (SELENE) Science Working Team Meeting (SWTM6), (Nagoya, Japan, Jan. 10-12, 2012).

Kim, M. K.: 2011, Dimensional Kinematics of H_2O and SiO Masers in OrionKL, 4th East Asia VLBI Workshop — Sciences and Technology by now and future, (Lijiang, China, Apr. 18-20, 2011).

Kim, M. K.: 2011, The origin of outflows in Orion-KL, 1st VERA-KVN science working group, (Mitaka, Japan, Jun. 13-14, 2011).

Kim, M. K.: 2012, 3-Dimensional Kinematics of water/SiO Masers in Orion-KL, IAU Symp. 287, "Cosmic Masers - from OH to H0", (Stellenbosch, South Africa, Jan. 30-Feb. 3, 2012).

Kim, M. K.: 2012, Water/SiO masers in Orion-KL, 2nd VERA-KVN science working group, (Seoul, Korea, Feb. 15-16, 2012).

Kim, S., Bain, H. M., **Shibasaki, K.**: 2011, Hot Flare Plasma Observed by Nobeyama Radioheliograph, RHESSI, and AIA/SDO, LWS/SDO Workshop "Many Spectra of Solar Activity", (Tahoe, CA, USA, May 1-5, 2011).

Kim, S., Bain, H. M., **Shibasaki, K.**: 2011, Microwave Emission of Supra-Arcade Structure Associated with M1.6 Limb Flare, 11th Asian-Pacific Regional IAU Meeting, (Chiang Mai, Thailand, Jul. 26-29, 2011).

Kim, S., Bain, H. M., **Shibasaki, K.**: 2011, Multi-wavelength Observations of Supra-Arcade Structure associated with M1.6 Limb Flare, Japan-Korea Space Weather Workshop 2011: Current Status and Prospect of Space Weather Modeling and Obervation, (Daejeon, Korea, Sep. 29- Oct. 1, 2011).

Kim, S., Bain, H. M., **Shibasaki, K.**: 2011, Multi-wavelength Observations of Supra-Arcade Structure associated with M1.6 Limb Flare, 12th RHESSI Workshop and High Energy Solar Physics Symp., (Nanjing, China, Oct. 17-21, 2011).

Kim, S., Bain, H. M., **Shibasaki, K.**: 2011, Multi-wavelength Observations of Supra-Arcade Structure associated with M1.6 Limb Flare, AGU Fall Meeting 2011, (San Francisco, CA, USA, Dec. 4-9, 2011).

Kino, M.: 2011, AGN jet Science with KVN+VERA, AGN jet 2011, (Mitaka, Japan, Nov. 25, 2011).

Kino, M.: 2011, Where is the gamma-ray emission region in AGNs? Monthly monitoring of M87, 1st VERA-KVN science working group, (Mitaka, Japan, Jun. 13-14, 2011).

Kino, M.: 2012, Initial report on AGN observations with VERA+KVN: Overview, 2nd VERA-KVN science working group, (Seoul, Korea, Feb. 15-16, 2012).

Kiuchi, H., Kawanishi, T.: 2011, Photonic millimeter-wave/microwave signal generation and transmission techniques for a high-frequency Radio Interferometer and a very large anttena array, XXX URSI General Assembly and Scientific Symp. of Int. Union of Radio Science, (Istanbul, Turkey, Aug. 13-20, 2011).

Kiuchi, H.: 2011, Artificial calibration source on the ALMA high-site, ALMA EA Development Workshop 2011, (Mitaka, Japan, Sep. 8, 2011).

Kiuchi, H.: 2011, Photonic LO signal generation and transmission techniques, ALMA EA Development Workshop 2011, (Mitaka, Japan, Sep. 8, 2011).

Kobayashi, H.: 2011, Japanese VLBI activities and East Asian VLBI Network, Advances in Asia and Oceania Toward Very Long Baseline Interferometry in the Age of the Square Kilometre Array, (Perth, Australia, May 4-6, 2011).

Kobayashi, H.: 2011, Japanese VLBI activities and East Asian VLBI Network, Postgraduate Bursary Conf. Project 2011 Postgraduate Bursary Conf., (Stellenbosch, South Africa, Nov. 21-25, 2011).

Kobayashi, H.: 2011, Status and future of EAVN, 4th East Asia VLBI Workshop — Sciences and Technology by now and future, (Lijiang, China, Apr. 18-20, 2011).

Kobayashi, K., et al. including **Tsuneta, S.**, **Hara, H.**, **Ishikawa, R.**, **Kano, R.**, **Katsukawa, Y.**, **Kubo, M.**, **Suematsu, Y.**: 2011, The Chromospheric Lyman-Alpha Spectro Polarimeter (CLASP), The 5th Hinode Science Meeeting, (Boston, MA, USA, Oct. 11-15, 2011).

Kobayashi, M. A. R.: 2011, A Model Prediction to the Nature of High-z Lyman-Alpha Emitters, Galaxy Formation 2011, (Durham, UK, Jul. 18-22, 2011).

Kodama, T.: 2011, Mahalo-Subaru: Mapping Star Formation at the Peak Epoch of Galaxuy Formation, Galaxy Formation 2011, (Durham, UK, Jul. 18-22, 2011).

Kokubo, E.: 2011, The Final Stage of Terrestrial Planet Formation, The 1st Kepler Science Conf., (NASA Ames Research Park, USA, Dec. 5-9, 2011).

Kokubo, E.: 2012, Formation of Terrestrial Planets: The Basic Dynamical Model, MISASA IV Solar System Exploration and New Geosciences -Perspective for the Next Decade-, (Tottori, Japan, Feb. 24-26, 2012).

Komiya, Y., **Eguchi, S.**, **Shirasaki, Y.**, **Ohishi, M.**, **Mizumoto, Y.**, Ishihara, Y., Yanaka, H., Tsutsumi, J., Hiyama, T., Nakamoto, H., Sakamoto, M.: 2011, VO Crawler: a crawling system for Virtual Observatory services, Astronomical Data Analysis Software and Systems XX, (Paris, France, Nov. 6-10, 2011).

Komiya, Y., **Suda, T.**, Yamada, S., Fujimoto, M. Y.: 2011, Hierarchical Chemical Evolution and R-process Elements of EMP Stars, 3rd Subaru Int. Conf., Galactic Archaeology, (Shuzenji, Kyoto, Japan, Nov. 6-10, 2011).

Kotake, K.: 2011, 3D simulations of core-collapse supernovae with spectral neutrino transport, Coconuts meeting 2011, (Meudon observatory, Paris, Nov. 17, 2011).

Kotake, K.: 2011, Multidimensional supernova simulations with a concentration of equation of state, Int. symp. of symmetry energy, (Massachusetts, USA, Jun. 17-19, 2011).

Kotake, K.: 2011, Multimessenger from core-collapse supernovae: multidimensionality as a key to bridge theory and observation, Multi-messenger probe into nuclear physics, (Washington, USA, Jul. 16, 2011).

Kotake, K.: 2011, Numerical recipes in microphysics to energize core-collapse supernovae, Microphysics in Computational Relativistic Astrophysics, (Perimeter institute, Ontario, Canada, Jun. 20, 2011).

Kotake, K.: 2012, 3D vs. GR: which one will help the onset of neutrino-driven explosions, 16th Workshop on "Nuclear Astrophysics", (Ringberg, Germany, Mar. 30, 2012).

Kotake, K.: 2012, Cutting-edge issues in core-collapse supernova modeling, Formations of compact objects: from the cradle to the grave, (Tokyo, Japan, Mar. 8, 2012).

Kotake, K.: 2012, Cutting-edge issues in the theory of core-collapse supernovae, IAU Symp. 279, "Death of Massive Stars:

Supernovae and Gamma-Ray Bursts", (Nikko, Japan, Mar. 12-16, 2012).

Koyama, Y., **Kodama, T.**, **Hayashi, M.**, **Tadaki, K.**, **Nakata, F.**, **Tanaka, I.**, **Shimasaku K.**, **Okamura, S.**: 2011, Red Star Forming Galaxies in Distant Cluster Outskirts A key population for understanding environmental effects at $z<1$, Galaxy Formation 2011, (Durham, UK, Jul. 18-22, 2011).

Kroug, M., **Gonzales, A.**, **Kuroiwa, K.**, **Miyachi, A.**, **Uzawa, Y.**, Makise, K., Wang, Z.: 2011, Resonances in Superconducting Circuits at THz Frequencies, Superconductivity Centennial Conf. (EUCAS-ISEC-ICMC 2011), (Hague, Netherlands, Sept. 18-23, 2011).

Kroug, M., **Uzawa, Y.**: 2011, Plans for an SIS Based Heterodyne Receiver above 1 THz, 12th Workshop on Submillimeter-Wave Receiver Technologies in Eastern Asia, (Seoul, Korea, Dec. 5-6, 2011).

Kubo, M., **Sekii, T.**, Gizon, L.: 2011, Comparing Photospheric Magnetic Fields and Subsurface Flows in the Quiet Sun, The 5th Hinode Science Meeeting, (Boston, MA, USA, Oct. 11-15, 2011).

Kurosaki, K., Ikoma, M., **Hori, Y.**: 2011, Thermal Evolution and Mass Loss of Water-rich Super-Earths, The 1st Kepler Science Conf., (NASA Ames Research Park, USA, Dec. 5-9, 2011).

Leisawitz, D., et al. including **Matsuo, H.**: 2011, Is Space-based Interferometry Dead?, AAS Meeting #218, (Boston, USA, May 22-26, 2011).

Masuda, S., Goto, T., **Shimojo, M.**, Kawate, T.: 2011, An extremely microwave-rich flare observed with Nobeyama Radio Heliograph, AGU Fall Meeting 2011, (San Francisco, CA, USA, Dec. 4-9, 2011).

Matsumoto, K., **Kikuchi, F.**, Iwata, T., **Kono, Y.**, **Tsuruta, S.**, **Hanada, H.**, **Goossens, S.**, **Ishihara, Y.**, Kamata, S., **Sasaki, S.**: 2011, VLBI mission proposed for SELENE-2 and its contribution to constrain the lunar internal structure, AGU Fall Meeting 2011, (San Francisco, CA, USA, Dec. 5-9, 2011).

Matsumoto, K., **Kikuchi, F.**, Iwata, T., **Kono, Y.**, **Tsuruta, S.**, **Hanada, H.**, **Goossens, S.**, **Ishihara, Y.**, Kamata, S., **Sasaki, S.**: 2011, VLBI radio sources on a lander and an orbiter for study of lunar internal structure proposed for SELENE-2 mission, ASTROKAZAN 2011, (Kazan, Russia, Aug. 22-30, 2011).

Matsumoto, K., **Kikuchi, F.**, Iwata, T., **Kono, Y.**, **Tsuruta, S.**, **Hanada, H.**, **Goossens, S.**, **Ishihara, Y.**, Kamata, S., **Sasaki, S.**: 2011, VLBI radio sources on a lander and an orbiter for study of lunar internal structure proposed for SELENE-2 mission, European Geosciences Union General Assembly 2011, (Vienna, Austria, Apr. 3-8, 2011).

Matsumoto, K., **Kikuchi, F.**, Iwata, T., **Kono, Y.**, **Tsuruta, S.**, **Hanada, H.**, **Goossens, S.**, **Ishihara, Y.**, Kamata, S., **Sasaki, S.**: 2012, VLBI mission proposed for SELENE-2 and its contribution to constrain the lunar internal structure, The 6th KAGUYA (SELENE) Science Working Team Meeting (SWTM6), (Nagoya, Japan, Jan. 10-12, 2012).

Matsumoto, N., **Honma, M.**, Isono, Y., Fujisawa, K.: 2011, Astrometry observations of 6.7 GHz methanol maser sources with VERA/JVN, Star Formation through Spectroimaging at High Angular Resolution, (Taipei, Taiwan, Jun. 20-24, 2011).

Matsumoto, N.: 2011, Astrometry Observation of 6.7 GHz Methanol Maser Sources with JVN/VERA, 4th East Asia VLBI Workshop — Sciences and Technology by now and future, (Lijiang, China, Apr. 18-20, 2011).

Matsumoto, N.: 2011, Investigation of 3D Galactic Gas Dynamics with 6.7 GHz Methanol Masers Sources, Workshop on East-Asian collaboration for SKA, (Daejeon, Korea, Nov. 30-Dec. 2, 2011).

Matsumoto, N.: 2011, Proper motion measurements of sources around the galactic bar structure, 1st VERA-KVN science working group, (Mitaka, Japan, Jun. 13-14, 2011).

Matsumoto, N.: 2012, Investigation of 3-D galactic dynamics with masers, 2nd VERA-KVN science working group, (Seoul, Korea, Feb. 15-16, 2012).

Matsumoto, N.: 2012, The bar effect in the galactic gas motions traced by 6.7 GHz methanol maser sources with VERA, IAU Symp. 287, "Cosmic Masers - from OH to H0", (Stellenbosch, South Africa, Jan. 30-Feb. 3, 2012).

Matsuo, H., **Hibi, Y.**, **Matsuo, T.**, Ohta, I. S., Kawada, M.: 2011, Technical Challenges in Photon Counting Terahertz Interferometry (PCTI), 12th Workshop on Submillimeter-Wave Receiver Technologies in Eastern Asia, (Seoul, Korea, Dec. 5-6, 2011).

Matsuo, H., Kosaka, A., Arai, T., Tanaka, M.: 2012, Far-Infrared Spectroscopic Study of Interstellar Material around Eta Carinae, The 2nd AKARI Conf., Legacy of AKARI: A Panoramic View of the Dusty Universe, (Jeji, Korea, Feb. 27-29, 2012).

Matsuo, H., **Matsuo, T.**, Ohta, I. S.: 2011, A Study on Photon Counting Interferometry in Terahertz Frequencies, 22nd Int. Symp. on Space Terahertz Technology, (Tucson, AZ, USA, Apr. 26-28, 2011).

Matsuo, H., Shi, S.-C.: 2011, High-Angular Resolution Terahertz Astronomy from Dome A, SCAR Astronomy and Astrophysics from Antarctica 2011, (Sydney, Australia, Jun. 29-Jul. 1, 2011).

Matsuo, H.: 2011, Requirements on photon counting detectors in terahertz frequencies, 14th Int. Workshop on Low Temperature Detectors, (Heidelberg, Germany, Aug. 1-5, 2011).

Mauersberger, R., et al. including **Asayama, S.**, **Kamazaki, T.**, **Komugi, S.**, **Sawada, T.**, **Tachihara, K.**: 2011, Commissioning and Science Verification of ALMA, IAU symp. 280, "The Molecular Universe", (Toledo, Spain, May 30-Jun. 3, 2011).

Min, C. H.: 2011, Orbital determination for R Aquarii, 1st VERA-KVN science working group, (Mitaka, Japan, Jun. 13-14, 2011).

Miyazaki, S.: 2011, Hyper Suprime-Cam, First eROSITA Int. Conf., (Garmisch-Partenkirchen, Germany, Oct. 17-20, 2011).

Miyazaki, S.: 2011, Hyper Suprime-Cam, Very Wide Field Surveys in Light of the Astro2010, (STScI, MD, USA, Jun. 13-16, 2011).

Miyoshi, M., Shen, Z.-Q., **Oyama, T.**, Takahashi, R., **Kato, Y.**: 2011, Oscillation Phenomena in the Disk around the Massive Black Hole Sagittarius A*, 21st Workshop on General Relativity and Gravitation (JGRG21), (Sendai, Japan, Sep. 26-29, 2011).

Miyoshi, M.: 2011, ALMA EA Development WorkShop 2011, ALMA EA Development Workshop 2011, (Mitaka, Japan, Sep. 8, 2011).

Mizuno, N.: 2011, The CO View of the Milky Way by NANTEN, IAU Symp. 284 "The Spectral Energy Distribution of the Galaxies", (Preston, UK, Sep. 5-9, 2011).

Mori, T., **Agatsuma, K.**, Ballmer, S., Sakata, S., Miyakawa, O., Numata, K., **Kawamura, S.**, Mio, N.: 2011, Control of motions of a suspended mirror through radiation pressure in a high-power optical cavity, 9th Edoardo Amaldi Conference on

Gravitational Waves, (Cardiff, UK, Jul. 10-15, 2011).

Mori, T., **Agatsuma, K.**, Ballmer, S., Sakata, S., Miyakawa, O., Numata, K., **Kawamura, S.**, Mio, N.: 2011, Ponderomotive squeezing experiment for gravitational wave detectors, Gravity and quantum information workshop, (Seoul, Korea, Aug. 29-30, 2011).

Nagai, H., et al.: 2012, Status report of GENJI, KVN-VERA Science Workshop 2012, (Yonsei University, Korea, Feb. 14-16, 2012).

Nagai, H.: 2011, Current status of GENJI projects and future prospects for VERA+KVN, 1st VERA-KVN science working group, (Mitaka, Japan, Jun. 13-14, 2011).

Nagai, H.: 2011, Preliminary Cycle 1 Capability of ALMA & Short Comments for Jet Science, AGN jet 2011, (Mitaka, Japan, Nov. 25, 2011).

Nagai, H.: 2012, GENJI status report, 2nd VERA-KVN science working group, (Seoul, Korea, Feb. 15-16, 2012).

Nagashima, K., Zhao, J., Duvall, Jr. T., Kosovichev, A. G., Parchevsky, K., **Sekii, T.**: 2011, Time-distance helioseismology analyses of multi-wavelength datasets obtained with Hinode/ SOT and SDO/HMI, The 5th Hinode Science Meeeting, (Boston, MA, USA, Oct. 11-15, 2011).

Nagayama, T.: 2011, Astrometry of Galactic Star-Forming Regions ON1 and ON2N with VERA: Estimation of Angular Velocity of Galactic Rotation at the Sun, 11th Asian-Pacific Regional IAU Meeting, (Chiang Mai, Thailand, Jul. 26-29, 2011).

Nagayama, T.: 2012, Astrometry of Galactic star-forming regions ON1 and ON2N with VERA, IAU Symp. 287, "Cosmic Masers - from OH to H0", (Stellenbosch, South Africa, Jan. 30-Feb. 3, 2012).

Nagayama, T.: 2012, Reports from Astrometry sub WG, 2nd VERA-KVN science working group, (Seoul, Korea, Feb. 15-16, 2012).

Nakajima, T., **Iwashita, H.**, **Miyazawa, C.**, **Yonezu, T.**, **Kuno, N.**, **Kawabe, R.**, Inoue, H., Sakai, T., Kohno, K., Koyano, M., Katase, T., Nishimura, A., Kimura, K., Ogawa, H., **Asayama, S.**, **Noguchi, T.**: 2011, Development of the Sideband-Separating (2SB) Receiver Systems for the NRO 45-m Millimeter Wave Telescope, 12th Workshop on Submillimeter-Wave Receiver Technologies in Eastern Asia, (Seoul, Korea, Dec. 5-6, 2011).

Nakajima, T., Sakai, T., Kimura, K., **Iwashita, H.**, **Miyazawa, C.**, Katase, T., Koyano, M., Inoue, H., **Kuno, N.**, **Kawabe, R.**, Ogawa, H., **Asayama, S.**, **Noguchi, T.**: 2011, Development of a New Multi-Beam Array 2SB Receiver and the Measurment System of Image Rejection Ratio for 2SB Mixer, ALMA EA Development Workshop 2011, (Mitaka, Japan, Sep. 8, 2011).

Nakajima, T., Sakai, T., Kimura, K., Nishimura, A., Katase, T., Koyano, M., Inoue, H., **Iwashita, H.**, **Miyazawa, C.**, **Kuno, N.**, **Kawabe, R.**, Ogawa, H., Kohno, K., **Asayama, S.**, **Tamura, T.**, **Noguchi, T.**: 2011, 100-GHz Band Sideband-Separating (2SB) Receivers for the NRO 45-m Telescope, Large Aperture Millimeter/Submillimeter Telescopes in the ALMA Era, (Osaka, Japan, Sep. 12-13, 2011).

Nakajima, T., **Takano, S.**, Kohno, K., Inoue, H., the line survey team: 2011, Line Survey Project of External Galaxies with NRO 45-m Telescope, IAU symp. 280, "The Molecular Universe", (Toledo, Spain, May 30-Jun. 3, 2011).

Nakajima, T.: 2011, Imaging of Molecular Abundances toward Active Galactic Nucleus, IAU symp. 280, "The Molecular Universe", (Toledo, Spain, May 30-Jun. 3, 2011).

Nakamura, F.: 2012, A Burst of Molecular Outflows From the Serpens South Protocluster, ALMA/NAASC 2012 Workshop: Outflows, Winds and Jets, (Charlottesville, Virginia, USA, Mar. 3-6, 2012).

Nakamura, K., Harikae, S., **Kajino, T.**, Mathews, G. J.: 2011, Long Gamma-ray Burst as a Production Site of R-process Elements, 11th Int. Symp. on Origin of Matter and Evolution of Galaxies, (Wako, Japan, Nov. 14-17, 2011).

Nakamura, K., Hayakawa, T., **Kajino, T.**, Chiba, S., Iwamoto, N., Cheoun, M.-K., Mathews, G. J.: 2011, Radioactivities from Supernovae and Its Application to Cosmochronology, 3rd Subaru Int. Conf., 1st NAOJ Symp., Galactic Archaeology: Near-Field Cosmology and the Formation of the Milky Way, (Shuzenji, Japan, Nov. 1-4, 2011).

Nakamura, K., **Kajino, T.**, Hayakawa, T., Chiba, S., Iwamoto, N., Cheoun, M.-K., Mathews, G. J.: 2011, Radioactive Niobium-92 Production via Neutrino-induced Nucleosynthesis, 11th Int. Symp. on Origin of Matter and Evolution of Galaxies, (Wako, Japan, Nov. 14-17, 2011).

Nakamura, K., **Takiwaki, T.**, **Kotake, K.**, Nishimura, N.: 2011, Supernova Shock Revival by Nuclear Reactions, 11th Int. Symp. on Origin of Matter and Evolution of Galaxies, (Wako, Japan, Nov. 14-17, 2011).

Nakamura, K.: 2011, Construction of gauge-invariant variables for linear-order metric perturbations on general background spacetime, 21st Workshop on General Relativity and Gravitation (JGRG21), (Sendai, Japan, Sep. 26-29, 2011).

Narita, N.: 2011, Subaru Observations of Spin-Orbit Angles and Outer Massive Bodies, Exploring Strange New Worlds: From Giant Planets to Super Earths, (High Country Conference Center, AZ, USA, May 2-6, 2011).

Narita, N., SEEDS/RV team: 2011, Companion Candidates around Transiting Planetary Systems: SEEDS First/Second Year Results, Extreme Solar Systems II, (Wyoming, USA, Sep. 11-17, 2011).

Narita, N.: 2011, Status of RV Sub-Category, SEEDS 2nd General Workshop, (Heidelberg, Germany, Oct. 10-12, 2011).

Narita, N.: 2012, High Frequency of Candidate Companions around Planetary Systems with High Obliquity, Subaru Users Meeting 2011, (Mitaka, Japan, Feb. 28-Mar. 1, 2012).

Narita, N.: 2012, JHKs Simultaneous Transit Photometry of GJ1214b, Exoclimes 2012 The Diversity of Planetary Atmospheres, (Aspen Center for Physics, USA, Jan. 15-20, 2012).

Narukage, N., Sakao, T., **Kano, R.**, **Shimojo, M.**: 2011, Diagnostics of coronal temperature based on the calibration result of X-Ray Telescope and further calibration, The 5th Hinode Science Meeeting, (Boston, MA, USA, Oct. 11-15, 2011).

Naruse, M., **Sekimoto, Y.**, **Miyachi, A.**, **Uzawa, Y.**, **Nitta, T.**, **Karatsu, K.**, **Sekine, M.**, **Noguchi, T.**: 2011, The properties of MKID made of crystal Al films and amorphous-Al films, 4th Microresonator Workshop, (Grnoble, France, Jul. 26-27, 2011).

Naruse, M., **Sekimoto, Y.**, **Miyachi, A.**, **Uzawa, Y.**, **Nitta, T.**, **Noguchi, T.**: 2011, Development of Crystal Al MKIDs by Molecular Beam Epitaxy, 14th Int. Workshop on Low Temperature Detectors, (Heidelberg, Germany, Aug. 1-5, 2011)

Niino, Y.: 2011, Revisiting Metallicity of Long GRB Host Galaxies: the Chemical Inhomogeneities in Galaxies, "Chemical Evolution of GRB Host Galaxies", (Sexten, Italy, Jul. 18-22, 2011).

Niino, Y.: 2012, Revisiting Metallicity of Long GRB Host Galaxies: the Chemical Inhomogeneities in Galaxies, IAU Symp. 279, "Death of Massive Stars: Supernovae and Gamma-Ray Bursts", (Nikko, Japan, Mar. 12-16. 2012).

Nishizawa, A., **Nakamura, K.**, **Fujimoto, M.-K.**: 2012, Weak measurement for gravitational wave detectors, 5th KAGRA face to face meeting, (Kashiwa, Japan, Feb. 2-4, 2012).

Nitta, T., **Naruse, M.**, **Sekimoto, Y.**, **Matsuo, H.**, **Noguchi, T.**, **Uzawa, Y.**, **Mitsui, K.**, **Okada, N.**, **Karatsu, K.**, **Sekine, M.**, Seta, M., Nakai, N.: 2011, Development of silicon lens array for MKID camera, 4th Workshop on the Physics and Applications of Superconducting Microresonators, (Grenoble, France, Jul. 28-29, 2011).

Niwa, Y., **Kobayashi, Y.**, **Gouda, N.**, **Yano, T.**, Yamada, Y., Hatsutori, Y.: 2011, Performance Evaluation of Nano-JASMINE Telescope Flight Model, 28th Int. Symp. on Space Technology and Science (28th ISTS), (Okinawa, Japan, Jun. 5-12, 2011).

Noda, H., Kunimori, H., **Araki, H.**, Funazaki, K., Fuse, T., **Hanada, H.**, **Katayama, M.**, Murata, K., **Morota, T.**, Otsubo, T., **Sasaki, S.**, Taniguchi, H., **Tazawa, S.**, **Tsuruta, S.**: 2011, Lunar Laser Ranging Experiment in Japanese Lunar Lander SELENE-2, ASTROKAZAN 2011, (Kazan, Russia, Aug. 22-30, 2011).

Noda, H., Kunimori, H., **Araki, H.**, Funazaki, K., Fuse, T., **Hanada, H.**, **Katayama, M.**, Murata, K., Otsubo, T., **Sasaki, S.**, Taniguchi, H., **Tazawa, S.**, **Tsuruta, S.**: 2012, Development status of the Lunar Laser Ranging Experiment for SELENE-2, The 6th KAGUYA (SELENE) Science Working Team Meeting (SWTM6), (Nagoya, Japan, Jan. 10-12, 2012).

Noda, H., Kunimori, H., **Araki, H.**, Funazaki, K., Fuse, T., **Hanada, H.**, **Katayama, M.**, Otsubo, T., **Sasaki, S.**, Taniguchi, H., **Tazawa, S.**, **Tsuruta, S.**: 2011, Lunar Laser Ranging experiment in Japanese lunar lander SELENE-2, 4th annual NASA Lunar Science Forum, (Ames/NASA, USA, Jul. 19-21, 2011).

Noda, H., Kunimori, H., **Araki, H.**, Fuse, T., **Hanada, H.**, **Katayama, M.**, Otsubo, T., **Sasaki, S.**, **Tazawa, S.**, **Tsuruta, S.**, Funazaki, K., Taniguchi, H., Murata, K.: 2011, Lunar Laser Ranging Experiment for SELENE-2, 43rd Lunar and Planetary Science Conference, (Woodlands, TX, USA, Mar. 19-23, 2012).

Noda, H., Kunimori, H., **Araki, H.**, Fuse, T., **Hanada, H.**, **Katayama, M.**, Otsubo, T., **Sasaki, S.**, **Tazawa, S.**, **Tsuruta, S.**: 2011, Lunar Laser Ranging Experiment in SELENE-2, Asia Oceania Geosciences Society 2011, (Taipei, Taiwan, Aug. 8-12, 2011).

Noguchi, T., **Naruse, M.**, **Sekimoto, Y.**: 2011, RF conductivity and surface impedance of a superconductor taking into account the complex superconducting gap energy, Superconductivity Centennial Conf. (EUCAS-ISEC-ICMC 2011), (Hague, Netherlands, Sep. 18-23, 2011)

Noguchi, T., **Naruse, M.**, **Sekimoto, Y.**: 2011, Surface Resistance of a Superconductor Taking into Account the Quasiparticle States Inside the Energy Gap, 12th Workshop on Submillimeter-Wave Receiver Technologies in Eastern Asia, (Seoul, Korea, Dec. 5-6, 2011).

Noguchi, T.: 2011, Rf conductivity of a superconductor taking into account the complex Superconducting gap energy, East Asia Symp. on Superconductor Electronics (EASSE 2011), (Yamagata, Japan, Oct. 27-29, 2011).

Noguchi, T.: 2012, Surface resistance of a NbN film accounting for the broadening of the qp DOS, 2nd Superconducting Nitride Detector Workshop, (Pasadena, CA, USA, Feb. 21-22, 2012).

Oe, M., Onodera, Y., Murai, J.: 2011, Early survey report on ICT disaster recovery activities in the Great East Japan Earthquake, Int. Symp. Disaster Simulation & Structural Safety in the Next Generation, 2011, (Kobe, Japan, Sep. 17-18, 2011).

Ohishi, M.: 2011, Case Study – PLT Impacts on Radio Astronomy, ITU Forum on compatibility between Power Line Telecommunication systems and Radiocommunication Services, (Geneva, Switzerland, May 27, 2011).

Ohishi, M.: 2011, Data Discovery in and Science Results by means of Vos, JSPS-DST Asia Academic Seminar, CPS 8th Int. School of Planetary Sciences, Challenges in Astronomy: Observational Advances, (Minamiawaji, Hyogo, Japan, Sep. 26-Oct. 1, 2011).

Ohishi, M.: 2011, Impact to the Astronomy by Interference caused by the Solar Power Satellite Systems, XXX URSI General Assembly and Scientific Symp. of Int. Union of Radio Science, (Istanbul, Turkey, Aug. 13-20, 2011).

Ohishi, M.: 2011, IUCAF Activity Report between 2008 and 2011, XXX URSI General Assembly and Scientific Symp. of Int. Union of Radio Science, (Istanbul, Turkey, Aug. 13-20, 2011).

Ohishi, M.: 2011, IUCAF and its activities within ITU-R, XXX URSI General Assembly and Scientific Symp. of Int. Union of Radio Science, (Istanbul, Turkey, Aug. 13-20, 2011).

Ohishi, M.: 2011, Search for Large Molecules and Spectral Line Surveys, 11th Asian-Pacific Regional IAU Meeting, (Chiang Mai, Thailand, Jul. 26-29, 2011).

Ohishi, M.: 2012, Towards Life in the Universe, Sokendai Asian Winter School "Basics and Frontiers in Molecular Science", (Okazaki, Aichi, Japan, Jan. 10-13, 2012).

Ohsuga, K.: 2011, Radiation-HD/MHD simulations, Black Hole Slim Disk Workshop, (Warsaw, Poland, Jul. 1-8, 2011).

Ohsuga, K.: 2011, Radiation-MHD simulations of black hole accretion flows and outflows, AGN Winds in Charleston, (Charleston, SC, USA, Oct. 15-18, 2011).

Ohtake, M., Mastunaga, T., Takeda, H., Yokota, Y., Yamamoto, S., Morota, T., **Ishihara, Y.**, Ogawa, Y., Hirori, T., Nakamura, R., Haruyama, J.: 2011, Compositional trend within the lunar highland crust, EPSC-DPS Joint Meeting 2011, (Nantes, France, Oct. 2-7, 2011).

Okada, T., et al. including **Arai, T.**: 2012, Thermal Infrared Imager TIR on Hayabusa 2 to Investigate Physical Properties of C-Class Near-Earth Asteroid 1999JU3, 43rd Lunar and Planetary Science Conference, (Woodlands, TX, USA, Mar. 19-23, 2012).

Okamoto, T. J., De Pontieu, B.: 2011, Propagating waves along spicules, The 5th Hinode Science Meeeting, (Boston, MA, USA, Oct. 11-15, 2011).

Okamoto, T. J., De Pontieu, B.: 2012, Propagating waves along spicules, SDO-4/ IRIS/ Hinode Workshop, (Monterey, USA, Mar. 12-16, 2012).

Okita, K., Ohtani, H., **Yoshida, F.**, **Ito, T.**: 2012, Assemble and Test of New CCD Camera System for Kiev 60 cm Telescope, 3rd Maidanak Observatory Users Meeting, (Mitaka, Japan, Jan. 31-Feb. 1, 2012).

Oshima, A.: 2011, Cosmic ray anisotropy observed by GRAPES-3 air shower array, 32nd Int. Cosmic Ray Conf., (Beijing, China, Aug. 11-18, 2011).

Oshima, A.: 2011, Estimation of 3D structures of cosmic-ray low density region behind shock waves associated with solar flares, 32nd Int. Cosmic Ray Conf., (Beijing, China, Aug. 11-18, 2011).

Oshima, A.: 2011, Rigidity dependence of the solar-wind-effect on cosmic-ray intensities associated with Solar activity, 32nd Int. Cosmic Ray Conf., (Beijing, China, Aug. 11-18, 2011).

Oshima, A.: 2012, Contamination of radioactive caesium in soil in the campus of NAOJ Mitaka, 3rd Maidanak Observatory Users Meeting, (Mitaka, Japan, Jan. 30-Feb. 1, 2012).

Otsubo, T., Kunimori, H., **Noda, H.**, **Hanada, H.**, **Araki, H.**, **Katayama, M.**: 2011, Optical design for next-generation single-reflector LLR targets, AGU Fall Meeting 2011, (San Francisco, CA, USA, Dec. 5-9, 2011).

Otsubo, T., **Noda, H.**, **Araki, H.**, Kunimori, H., **Hanada, H.**: 2011, Simulation of optical response for next-generation single-reflector LLR targets: Asymmetric dihedral angle offsets, 17th Int. Workshop on Laser Ranging, (Bad Kötzting, Germany, May 16-20, 2011).

Otsuji, K., Kitai, R., Ichimoto, K., Shibata, K.: 2011, Statistical Study on the Nature of Solar Flux Emergence, The 5th Hinode Science Meeeting, (Boston, MA, USA, Oct. 11-15, 2011).

Oyama, T.: 2011, Astrometric observations toward the galactic center region, 1st VERA-KVN science working group, (Mitaka, Japan, Jun. 13-14, 2011).

Oyama, T.: 2012, Astrometric observations of maser sources in the galactic center region with VERA and VLBA, IAU Symp. 287, "Cosmic Masers - from OH to H0", (Stellenbosch, South Africa, Jan. 30-Feb. 3, 2012).

Parthasarathy, M.: 2011, Chemical Composition of UV-Bright Stars in Globular Clusters, 3rd Subaru Int. Conf., 1st NAOJ Symp., Galactic Archaeology: Near-Field Cosmology and the Formation of the Milky Way, (Shuzenji, Japan, Nov. 1-4, 2011).

Reznikova, V., **Shibasaki, K.**, Nakariakov, V., Sych, R.: 2011, Three-minutes oscillations over sunspot umbra observed with SDO and NoRH, 13th European solar Physics Meeting, (Rhodes, Greece, Sep. 12-16, 2011).

Reznikova, V., **Shibasaki, K.**, Nakariakov, V., Sych, R.: 2011, Three-minutes oscillations over sunspot: SDO and NoRH data analysis, LWS/SDO Workshop "Many Spectra of Solar Activity", (Tahoe, CA, USA, May 1-5, 2011).

Reznikova, V., **Shibasaki, K.**, Nakariakov, V., Sych, R.: 2011, Three-minutes oscillations over sunspot: SDO/AIA and NoRH data analysis, 11th Asian-Pacific Regional IAU Meeting, (Chiang Mai, Thailand, Jul. 26-29, 2011).

Reznikova, V., **Shibasaki, K.**: 2011, The slow magnetoacoustic mode in the flaring loop, 11th Asian-Pacific Regional IAU Meeting, (Chiang Mai, Thailand, Jul. 26-29, 2011).

Saiki, K., Arai, T., **Araki, H.**, **Ishihara, Y.**, Ohtake, M., Karouji, Y., Kobayashi, N., Sugihara, T., Haruyama, J., Honda, C., Sato, H., Takeda, H.: 2011, Landing Site Evaluation for the Nest Lunar Exploration Project: SELENE-2, AGU Fall Meeting 2011, (San Francisco, CA, USA, Dec. 5-9, 2011).

Saiki, K., Arai, T., **Araki, H.**, **Ishihara, Y.**, Ohtake, M., Karouji, Y., Kobayashi, N., Sugihara, T., Haruyama, J., Honda, C., Sato, H., Takeda, H.: 2012, Report on Landing Site Evaluation for the Next Lunar Exploration Project: SELENE-2, The 6th KAGUYA (SELENE) Science Working Team Meeting (SWTM6), (Nagoya, Japan, Jan. 10-12, 2012).

Saito, M., Kitamura, Y., Momose, M., Tsukagoshi, T., **Kawabe, R.**: 2012, Aperture Synthesis Observations Toward The Protostellar Systems L1551 Irs 5 And Hl Tau: Rotation In The Infalling Envelope, AAS Meeting #219, (Austin, TX, USA, Jan. 8-12, 2012).

Saito, M.: 2011, ALMA Antenna, XXX URSI General Assembly and Scientific Symp. of Int. Union of Radio Science, (Istanbul, Turkey, Aug. 13-20, 2011).

Sakai, N.: 2012, Galactic Outer Rotation Curve with VERA+KVN, 2nd VERA-KVN science working group, (Seoul, Korea, Feb. 15-16, 2012).

Sakai, N.: 2012, Mass distribution of the Galaxy using H_2O maser with VERA, IAU Symp. 287, "Cosmic Masers - from OH to H0", (Stellenbosch, South Africa, Jan. 30-Feb. 3, 2012).

Sakurai, T.: 2012, Magnetic Helicity as a Probe of Magnetic Flux-Tube Dynamics in the Solar Interior, Plasma Astrophysics: Acquired Knowledge and Future Perspectives, (Leuven, Belgium, Feb. 22-24, 2012).

Sasaki, S., **Araki, H.**, **Hanada, H.**, Iwata, T., Namiki, N., **Matsumoto, K.**, **Noda, H.**, **Ishihara, Y.**, **Goossens, S.**, **Kikuchi, F.**, Kawano, N., **Tazawa, S.**, **Tsuruta, S.**, **Asari, K.**, **Ishikawa, T.**, **Morota, T.**, Liu, Q., Harada, Y.: 2011, The First Precise Gravity and Topography of the Global Moon by KAGUYA (SELENE), Astro Kazan 2011, (Kazan, Russia, Aug. 22-30, 2011).

Sasaki, S., **Araki, H.**, **Goossens, S.**, **Hanada, H.**, **Ishihara, Y.**, **Kikuchi, F.**, **Matsumoto, K.**, **Noda, H.**, **Kawano, N.**, **Kono, Y.**, **Yamada, R.**, Iwata, T., Namiki, N., Kunimori, H., Funazaki, K.: 2012, Selenodesy from KAGUYA to SELENE-2, MISASA IV Solar System Exploration and New Geosciences -Perspective for the Next Decade-, (Tottori, Japan, Feb. 24-26, 2012).

Sasaki, S., Fujimoto, M., Takashima, T., Yano, H., Kasaba, Y., Kimura, J., Takahashi, Y., Tsuda, Y., Funase, R., Mori, O.: 2011, The Jupiter Magnetospheric Orbiter and the Trojan Asteroid Explorer in EJSM (Europa Jupiter System Mission), 28th Int. Symp. on Space Technology and Science (28th ISTS), (Okinawa, Japan, Jun. 5-12, 2011).

Sasaki, S., Fujimoto, M., Yano, H., Takashima, T., Kasaba, Y., Takahashi, Y., Kimura, J., Funase, R., Mori, O., Tsuda, Y., Campagnola, S., Kawakatsu, Y.: 2011, Japanese mission plan for Jupiter system: The Jupiter magnetospheric orbiter and the Trojan asteroid explorer, EPSC-DPS Joint Meeting 2011, (Nantes, France, Oct. 2-7, 2011).

Sasaki, S., **Goossens, S.**, **Ishihara, Y.**, **Araki, H.**, **Hanada, H.**, **Matsumoto, K.**, **Noda, H.**, **Kikuchi, F.**, Iwata, T.: 2012, KAGUYA Selenodesy and the South Pole Aitken basin, 43rd Lunar and Planetary Science Conference, (Woodlands, TX, USA, Mar. 19-23, 2012).

Sasaki, S., **Hanada, H.**, **Noda, H.**, **Kikuchi, F.**, **Araki, H.**, **Matsumoto, K.**, Iwata, T., **Goossens, S.**, Kunimori, H., Ootsubo, T.: 2011, Lunar gravity and rotation measurements by Japanese lunar landing missions, 28th Int. Symp. on Space Technology and Science (28th ISTS), (Okinawa, Japan, Jun. 5-12, 2011).

Sasaki, S., Hiroi, T., Yokota, Y., Matsunaga, T.: 2011, Possible Variation of Space Weathering Degree on Mercury: Lessons from the Moon, Asia Oceania Geosciences Society 2011, (Taipei, Taiwan, Aug. 8-12, 2011).

Sasaki, S., Hiroi, T.: 2011, Difference of Space Weathering Degree of Asteroids: Lessons from Itokawa, 28th Int. Symp. on Space Technology and Science (28th ISTS), (Okinawa, Japan, Jun. 5-12, 2011).

Sasaki, S., Hiroi, T.: 2011, Space weathering of Itokawa, a small rubble pile asteroid, EPSC-DPS Joint Meeting 2011, (Nantes, France, Oct. 2-7, 2011).

Sasaki, S., **Ishihara, Y.**, **Araki, H.**, **Matsumoto, K.**, **Goossens, S.**, **Hanada, H.**, Ohtake, M., Iwata, T.: 2011, Structure of the South Pole Aitken basin from KAGUYA selenodesy data, 28th Int. Symp. on Space Technology and Science (28th ISTS), (Okinawa, Japan, Jun. 5-12, 2011).

Sasaki, S., **Ishihara, Y.**, **Araki, H.**, **Noda, H.**, **Goossens, S.**, Namiki, N., Iwata, T., **Hanada, H.**, **Matsumoto, K.**, SELENE Topography/Gravity Team Group.: 2011, The first precise global gravity and topography of the Moon by KAGUYA (SELENE), 28th Int. Symp. on Space Technology and Science (28th ISTS), (Okinawa, Japan, Jun. 5-12, 2011).

Sasaki, S., **Ishihara, Y.**, **Araki, H.**, **Noda, H.**, **Hanada, H.**, **Matsumoto, K.**, **Goossens, S.**, **Kikuchi, F.**, Iwata, T., Namiki, N.: 2011, The First Accurate Global Gravity and Topography of the MOON by KAGUYA (SELENE) and Implication for Lunar Basin Evolution, Asia Oceania Geosciences Society 2011, (Taipei, Taiwan, Aug. 8-12, 2011).

Sasaki, S., **Ishihara, Y.**, **Goossens, S.**, **Matsumoto, K.**, **Araki, H.**, **Hanada, H.**, **Kikuchi, F.**, **Noda, H.**, Iwata, T., Ohtake, M.: 2011, Structure of lunar crust from KAGUYA selenodesy data, EPSC-DPS Joint Meeting 2011, (Nantes, France, Oct. 2-7, 2011).

Sasaki, S., **Noda, H.**, **Kikuchi, F.**, Kumimori, H., **Araki, H.**, **Matsumoto, K.**, **Goossens, S.**, **Ishihara, Y.**, **Hanada, H.**, Otsubo, H., Iwata, T.: 2011, Lunar rotation and gravity measurements by SELENE-2 and future landers, EPSC-DPS Joint Meeting 2011, (Nantes, France, Oct. 2-7, 2011).

Sasaki, S.: 2011, Science of Mercury Dust Monitor, BepiColombo Science Working Group Meeting, (Ishikawa, Japan, Sep. 8-10, 2012).

Sasaki, S.: 2012, KAGUYA and Beyond: Summary of Selenodesy Results and Future Plans, Int. Symp. on Lunar and Planetary Science 2012, (Macau, China, Mar. 26-27, 2012).

Sasaki, S.: 2012, State of the core and lower mantle should constrain the lunar origin, The 6th KAGUYA (SELENE) Science Working Team Meeting (SWTM6), (Nagoya, Japan, Jan. 10-12, 2012).

Sasaki, T., Yao, Y., Yoshida, M., **Ohshima, N.**, **Mikami, Y.**, **Okada, N.**, **Koyanao, H.**, **Sekiguchi, K.**, Liu, L., Li, L.: 2011, A China-Japan Collaborative Site Survey in west Tibet Sky clearness at Oma, Tibet, 11th Asian-Pacific Regional IAU Meeting, (Chiang Mai, Thailand, Jul. 26-29, 2011).

Sawada-Satoh, S.: 2011, Amplitude Calibration of the KVN+VERA Array, 4th East Asia VLBI Workshop — Sciences and Technology by now and future, (Lijiang, China, Apr. 18-20, 2011).

Sawada-Satoh, S.: 2011, Early Phase Observations of the KVN+VERA Joint Array, 11th Asian-Pacific Regional IAU Meeting, (Chiang Mai, Thailand, Jul. 26-29, 2011).

Sawada-Satoh, S.: 2011, Molecular absorption lines as new tracers in circumnuclear region, 1st VERA-KVN science working group, (Mitaka, Japan, Jun. 13-14, 2011).

Sawada-Satoh, S.: 2011, Recent results of VERA, KVN/TRAO Users Meeting, (Busan, Korea, Aug. 25-26, 2011).

Sawada-Satoh, S.: 2012, Internal Proper Motion of 6.7 GHz Methanol Masers in Ultra Compact HII Region S269, IAU Symp. 287, "Cosmic Masers - from OH to H0", (Stellenbosch, South Africa, Jan. 30-Feb. 3, 2012).

Sawada-Satoh, S.: 2012, Search for Molecular Absorptions on Acrive Galactic Nuclei, 2nd VERA-KVN science working group, (Seoul, Korea, Feb. 15-16, 2012).

Sekiguchi, K.: 2011, Astronomy: "Then", "Now" and "Future", The 5th Annual Int. Workshop on Applications of Remote Sensing and Space Science in Mongolia, (Ulaanbaatar, Mongolia, Jun. 6-7, 2011).

Sekiguchi, K.: 2011, Collaboration in Astronomy between Egypt and Japan, 2nd Middle-East and Africa Regional IAU Meeting, (Cape Town, South Africa, Apr. 10-15, 2011).

Shibasaki, K.: 2011, Diamagnetic and Non-linear Nature of Plasma as a Cause of Solar Activities, PROM2011 Workshop "Prominence Research: Observations and Models", (Pasadena, CA, USA, Dec. 13-15, 2011).

Shibasaki, K.: 2011, Measurements of Total Radio Flux from the Sun for Sixty Years, The first ICSU World Data system Conference "Global Data for Global Science", (Kyoto, Japan, Sep. 3-6, 2011).

Shibasaki, K.: 2011, Radio Imaging Observations of Solar Activity Cycle and Its Anomaly, AGU Fall Meeting 2011, (San Francisco, CA, USA, Dec. 4-9, 2011).

Shibasaki, K.: 2011, Radio Imaging Observations of Solar Activity Cycle and Its Anomaly, The 2nd Nagoya Workshop on the Relationship between Solar Activity and Climate Changes, (Nagoya, Japan, Jan. 16-17, 2012).

Shibata, K. M.: 2012, VERA status, 2nd VERA-KVN science working group, (Seoul, Korea, Feb. 15-16, 2012).

Shimizu, T., Ichimoto, K., **Suematsu, Y.**: 2011, Precursor of sunspot penumbral formation discovered with Hinode SOT observations, The 5th Hinode Science Meeeting, (Boston, MA, USA, Oct. 11-15, 2011).

Shimojo, M., **ALMA project**: 2012, Millimeter/sub-millimeter wave observations for chromospheric science, SDO-4/ IRIS/ Hinode Workshop, (Monterey, USA, Mar. 12-16, 2012).

Shimojo, M., **Tsuneta, S.**, Shiota, D., Itoh, H.: 2011, The Solar Polar Region Observed with Hinode, Sun-360: Stereo-4, SDO-2, SOHO-25 Workshop, (Kiel, Germany, Jul. 25-29, 2011).

Shimojo, M.: 2011, Acceleration & Heating in Prominence Eruption Observed in Radio & EUV, Japan-Korea Space Weather Workshop 2011: Current Status and Prospect of Space Weather Modeling and Obervation, (Daejeon, Korea, Sep. 29-Oct. 1, 2011).

Shimojo, M.: 2011, The Solar polar field from Hinode, Sun-360: Stereo-4, SDO-2, SOHO-25 Workshop, (Kiel, Germany, Jul. 25-29, 2011).

Shiota, D., **Tsuneta, S.**, **Orozco Suarez, D.**, **Shimojo, M.**, **Sako, N.**: 2011, Yearly Variation of Magnetic Field in the Polar Regions

Observed with Hinode, The 5th Hinode Science Meeeting, (Boston, MA, USA, Oct. 11-15, 2011).

Shirasaki, Y., **Komiya, Y.**, **Ohishi, M.**, **Mizumoto, Y.**, Ishihara, Y., Tsutsumi, J., Hiyama, T., Nakamoto, H., Sakamoto, M.: 2011, Current status of VO compliant data service in Japanese Virtual Observatory, ADASS XXI Conference, (Paris, France, Nov. 6-10, 2011).

Shirasaki, Y., **Tanaka, M.**, **Ohishi, M.**, **Mizumoto, Y.**, Yasuda, N., Takata, T.: 2011, AGN and Galaxy Clustering at z = 0.3 to 3.0 measured by using the Japanese Virtual Observatory, Galaxy Formation 2011, (Durham, UK, Jul. 18-22, 2011).

Shum, C, K., Fok, H, S., Yi, Y., Dai, C., **Araki, H.**, **Matsumoto, K.**, **Sasaki, S.**, Bâki Iz, H., Ding, X., Ping, J.: 2012, Improved Lunar Topography Model Using Laser Altimetry from Multiple Orbiters!, The 6th KAGUYA (SELENE) Science Working Team Meeting (SWTM6), (Nagoya, Japan, Jan. 10-12, 2012).

Sôma, M., **Tanikawa, K.**: 2011, Determination of ΔT and Lunar Tidal Acceleration from Ancient Eclipses and Occultations, StephensonFest, (Durham, UK, Apr. 13-16, 2011).

Sotani, H., Yasutake, N., Maruyama, T., Tatsumi, T.: 2011, Signatures of hadron-quark mixed phase in gravitational waves, 20th Stellar Pulsation Conf. Series, (Granada, Spain, Sep. 5-9, 2011).

Sotani, H.: 2011, Constraints on Pasta Structure of Neutron Stars, 20th Stellar Pulsation Conf. Series, (Granada, Spain, Sep. 5-9, 2011).

Sotani, H.: 2011, Effect of Pasta Phase on Oscillations in Neutron Stars, 21st Workshop on General Relativity and Gravitation (JGRG21), (Sendai, Japan, Sep. 26-29, 2011).

Sotani, H.: 2011, Imprint of Alternative Theories, Numerical Relativity and High Energy Physics, (Madeira, Portugal, Aug. 31-Sep. 3, 2011).

Sotani, H.: 2011, Probing the Pasta Structure of Neutron Stars, Frontier Issues in Physics of Exotic Nuclei (YKIS2011), (Kyoto, Japan, Oct. 11-15, 2011).

Sotani, H.: 2011, Nonuniform nuclear structures and QPOs in giant flares, 11th Int. Symp. on Origin of Matter and Evolution of Galaxies, (Wako, Japan, Nov. 14-17, 2011).

Sotani, H.: 2011, Probing nuclear properties via asteroseismology in neutron stars, YITP-KoRIA Workshop on Nuclear Symmetry Energy, (Kyoto, Japan, Nov. 10-12, 2011).

Suda, T., Hirschi, R., Fujimoto, M. Y.: 2010, Triple-alpha Reaction Rates Constrained by Stellar Evolution Models, 11th Int. Symp. on Origin of Matter and Evolution of Galaxies, (Wako, Japan, Nov. 14-17, 2011).

Suda, T., Yamada, S., Katsuta, Y., **Komiya, Y.**, Fujimoto, M. Y.: 2010, Star Formation History of Our Galaxy Explored with AGB Star Evolution Models, 3rd Subaru Int. Conf., 1st NAOJ Symp., Galactic Archaeology: Near-Field Cosmology and the Formation of the Milky Way, (Shuzenji, Japan, Nov. 1-4, 2011).

Suematsu, Y., **Sano, I.**, Ueno, S.: Integral Field Spectroscopy of the Sun with Microlens Array and Liquid Crystal Retarders, AGU Fall Meeting 2011, (San Francisco, CA, USA, Dec. 5-9, 2011).

Suematsu, Y., Yatini, C. Y.: 2011, Study of Short-Term Sunspot Motion toward Flare Onset Prediction, AGU Fall Meeting 2011, (San Francisco, CA, USA, Dec. 5-7, 2011).

Suematsu, Y., Yatini, C. Y.: 2011, Study of Sunspot Proper Motion toward Flare Onset Prediction, Asia Oceania Geosciences Society 2011, (Taipei, Taiwan, Aug. 8-12, 2011).

Suematsu, Y.: 2011, Study of Small-Scale Chromospheric Plasmoid Ejections with Improved Hinode Ca II H Filtergrams, The 5th Hinode Science Meeeting, (Boston, MA, USA, Oct. 11-15, 2011).

Suematsu, Y.: Instrument Design of Large Aperture Solar UV Visible and IR Observing Telescope for SOLAR-C Mission, 2nd ATST-EAST Workshop in Solar Physics, (Washington, DC, USA, Oct. 9-11, 2011).

Tachihara, K., **Saigo, K.**, **Higuchi, A.**, Inoue, T., Inutsuka, S.: 2012, Small Scale Structures as Units of Dynamical Multi-Phase Interstellar Medium, AAS Meeting #219, (Austin, TX, USA, Jan. 8-12, 2012).

Takahashi, H. R., **Ohsuga, K.**: 2011, Magnetic Energy Release in Relativistic Plasma, IAU Symp. 279, "Death of Massive Stars: Supernovae and Gamma-Ray Bursts", (Nikko, Japan, Mar. 12-16. 2012).

Takahashi, H. R.: 2012, Numerical Study of Relativistic Magnetic Reconnection with R3MHD Codes, Int. Workshop on Particles and Radiation from Cosmic Accelerators (CA2012), (Chiba, Japan, Feb. 20-22, 2012).

Takahashi, R.: 2011, Vibration Isolation, 4th LCGT face to face meeting, (Kashiwa, Japan, Aug. 3-5, 2011).

Takahashi, R.: 2012, Seismic Attenuation System (SAS) for LCGT, 1st Korea-Japan Workshop on LCGT, (Souel, Korea, Jan. 12-13, 2012).

Takahashi, R.: 2012, Vibration Isolation, 5th KAGRA face to face meeting, (Kashiwa, Japan, Feb. 2-4, 2012).

Takano, S., et al. including **Hirota, T.**, **Nakajima, T.**, **Ohishi, M.**, **Umemoto, T.**: 2011, Nobeyama 45m telescope legacy project: Line survey, IAU symp. 280, "The Molecular Universe", (Toledo, Spain, May 30-Jun. 3, 2011).

Takeda, Y.: 2011, Application of Iodine-Cell Technique to High-Precision Radia-Velocity Studies of the Solar Disk, Workshop on Astronomy with Precise Radial Velocity - Exoplanet Search and Asteroseismology, (Seoul, Korea, Sep. 25-28, 2011).

Takiwaki, T.: 2012, Three-dimensional Hydrodynamic Core-Collapse Supernova Simulations for an 11.2 M_S Star with Spectral Neutrino Transport, 11th Int. Symp. on Origin of Matter and Evolution of Galaxies, (Wako, Japan, Nov. 14-17, 2011).

Takiwaki, T.: 2012, Three-dimensional simulations of core-collapse supernovae, Nuclear, Particle and Astrophysics Seminar, (Basel, Switzerland, Mar. 22, 2012).

Takiwaki, T.: 2012, Three-dimensional simulations of core-collapse supernovae, Formations of compact objects: from the cradle to the grave, (Tokyo, Japan, Mar. 8, 2012).

Takiwaki, T.: 2012, Three-dimensional simulations of core-collapse supernovae, 16th Workshop on "Nuclear Astrophysics", (Ringberg, Germany, Mar. 30, 2012).

Tamura, M., SEEDS team: 2011, Direct imaging of exoplanets and their formation sites with Subaru, "Germany-Japan Round Table", (Heidelberg, Germany, Dec. 1-3, 2011).

Tamura, M., SEEDS team: 2011, Early Result from SEEDS and The Subaru's Next Step, Exploring Strange New Worlds: From Giant Planets to Super Earths, (High Country Conference Center, AZ, USA, May 2-6, 2011).

Tamura, M., SEEDS team: 2011, SEEDS Overview, SEEDS 2nd General Workshop, (Heidelberg, Germany, Oct. 10-12, 2011).

Tamura, M., SEEDS team: 2011, Strategic Explorations of Exoplanets and Disks with Subaru and its next step, Ishigaki International Workshop "Formation of Stars & Planets 2011 (FSP2011)", (Ishigaki, Okinawa, Japan, Oct. 3-7, 2011).

Tamura, M., SEEDS team: 2012, SEEDS Status, Subaru Users Meeting 2011, (Mitaka, Japan, Feb. 28-Mar. 1, 2012).

Tamura, Y.: 2012, Monitoring of coordinates and estimation of wet zenith delay at VERA stations by GPS, 2nd VERA-KVN science working group, (Seoul, Korea, Feb. 15-16, 2012).

Tanaka, M.: 2012, Spectropolarimetry of Type Ibc Supernovae, IAU Symp. 279, "Death of Massive Stars: Supernovae and Gamma-Ray Bursts", (Nikko, Japan, Mar. 12-16. 2012).

Tazawa, S., **Noda, H.**, **Araki, H.**, **Ishihara, Y.**, Kawano, N., **Sasaki, S.**: 2011, Behavior of return pulse intensity data obtained by the laser altimeter onboard KAGUYA, 28th Int. Symp. on Space Technology and Science (28th ISTS), (Okinawa, Japan, Jun. 5-12, 2011).

Terai, T., Itoh, Y., Jewitt, D.: 2011, Photometric Observations for the Brightness Variations on the Irregular Satellites of Uranus and Neptune, Asia Oceania Geosciences Society 2011, (Taipei, Taiwan, Aug. 8-12, 2011).

Tomida, K., Machida, M. N., **Saigo, K.**, **Tomisaka, K.**, Matsumoto, T.: 2011, Exposed Long-lifetime First core: Star formation in very low-mass molecular cloud cores, Formation and Early Evolution of Very Low Mass Stars and Brown Dwarfs, (ESO Garching, Germany, Oct. 11-14, 2011)

Tomida, K., **Tomisaka, K.**, **Kawabe, R.**, **Saigo, K.**, Machida, M. N., Matsumoto, T., **Hori, Y.**: 2011, RMHD simulations of protostellar collapse, Ishigaki International Workshop "Formation of Stars & Planets 2011 (FSP2011)", (Ishigaki, Okinawa, Japan, Oct. 3-7, 2011).

Toyokuni, G., **Ishihara, Y.**, Takenaka, H.: 2011, Global seismic waveform modeling in the whole Mars -a preliminary study-, EPSC-DPS Joint Meeting 2011, (Nantes, France, Oct. 2-7, 2011).

Tsujimoto, T.: 2011, Galactic Chemical Evolution in the context of the recently revealed SN Ia delay time distribution, IAU Symp. 281, "Binary Paths to the Explosions of Type Ia Supernovae", (Padova, Italy, Jul. 4-8, 2011).

Tsujimoto, T.: 2012, The IMF variation and short-delayed SNe Ia in the context of Galactic chemical evolution, The Chemical Evolution of the Milky Way, (Sesto, Italy, Jan. 23-27, 2012).

Tsukamoto, Y., Machida, N. M.: 2011, The formation and evolution processes of circum stellar disk, Ishigaki International Workshop "Formation of Stars & Planets 2011 (FSP2011)", (Ishigaki, Okinawa, Japan, Oct. 3-7, 2011).

Tsuneta, S., **Solar-C Working Group**: 2011, Solar-C mission with Solar-D on the horizon, The 5th Hinode Science Meeeting, (Boston, MA, USA, Oct. 11-15, 2011).

Tsuneta, S., Ueda, K., Reardon, K., Cauzzi, G., **Ishikawa, R.**: 2011, Evidence of magnetic heating of chromosphere, The 5th Hinode Science Meeeting, (Boston, MA, USA, Oct. 11-15, 2011).

Tsuneta, S.: 2011, Solar-C status and Science Goals overview, Solar-C Meeting, (Boston, MA, USA, Oct. 16, 2011).

Umemoto, T., **Saito, M.**, **Nakanishi, K.**, **Kuno, N.**, Tsuboi, M.: 2011, Radio Flare at Millimeter-wavelengths from Young Stellar Objects, Star Formation through Spectroimaging at High Angular Resolution, (Taipei, Taiwan, Jun. 20-24, 2011).

Urakawa, S., Okumrua, S., Nishiyama, K., Sakamoto, T., Takahashi, N., Abe, S., Ishiguro, M., Kitazato, K., **Kuroda, D.**, Hasegawa, S., Ohta, K., Kawai, N., **Shimizu, Y.**, **Nagayama, S.**, **Yanagisawa, K.**, Yoshida, M., Yoshikawa, M.: 2011, Photometric Observations of 107P/4015Wilson-Harrington, Asia Oceania Geosciences Society 2011, (Taipei, Taiwan, Aug. 8-12, 2011).

Urakawa, S., Okumrua, S., Nishiyama, K., Sakamoto, T., Takahashi, N., Abe, S., Ishiguro, M., Kitazato, K., **Kuroda, D.**, Hasegawa, S., Ohta, K., Kawai, N., **Shimizu, Y.**, **Nagayama, S.**, **Yanagisawa, K.**, Yoshida, M., Yoshikawa, M.: 2011, Photometric Observations of 107P/Wilson-Harrington, EPSC-DPS Joint Meeting 2011, (Nantes, France, Oct. 2-7, 2011).

Usuda, T., **Arimoto, N.**: 2011, Status and Future view of Subaru Telescope, Keck Science Meeting, (Pasadena, CA, USA, Sep. 23-24, 2011).

Uzawa, Y., Saito, S., **Kuroiwa, K.**, **Kroug, M.**, **Fujii, Y.**, Takeda, M., Makise, K., Wang, Z., Hosako, I.: 2011, Direct Observation of Superconducting Gap Broadening in a Niobium Nitride film by Terahertz Time Domain Spectroscopy, Superconductivity Centennial Conf. (EUCAS-ISEC-ICMC 2011), (Hague, Netherlands, Sep. 18-23, 2011)

Uzawa, Y.: 2011, Current status and future development of Band 10 cartridge, EA ALMA development workshop, (Mitaka, Tokyo, Japan, Sep. 8, 2011).

Uzawa, Y.: 2011, Heterodyne receivers for submm and THz bands, Large Aperture Millimeter/Submillimeter Telescopes in the ALMA Era, (Osaka, Japan, Sep. 12-13, 2011).

Wada, T., **Takata, J.**, **Shibata, S.**: 2011, Particle Simulation for the Axisymmetric Pulsar Magnetosphere, 2nd Fermi Asian Network (FAN) Workshop, (Hsinchu, Taiwan, Aug. 1-5, 2011).

Wada, T.: 2012, A Particle Simulation for the Axisymmetric Pulsar Magnetosphere, Int. Workshop on Particles and Radiation from Cosmic Accelerators (CA2012), (Chiba, Japan, Feb. 20-22, 2012).

Watanabe, T., **Hara, H.**, Imada, S., Watanabe, K., Shimizu, T.: 2011, High-Temperature & High-Speed Downflows in an Impulsive Flare of 2011 March 12, The 5th Hinode Science Meeeting, (Boston, MA, USA, Oct. 11-15, 2011).

Watanabe, T., Sterling, A. C., Harra, L. K., **Hara, H.**: 2011, Small Loop-loop Interaction in the Initial Phases of A C9.7 Flare, Sun-360: Stereo-4, SDO-2, SOHO-25 Workshop, (Kiel, Germany, Jul. 25-29, 2011).

Wisniewski, J. P., Fukagawa, M., Goto, M., Grady, C., **Hashimoto, J.**, Henning, T., Hodapp, K., Honda, M., Janson, M., **Kudo, T.**, Thalmann, C., Whitney, B., **Tamura, M.**, SEEDS Team: 2012, SEEDS Polarimetric Differential Imaging of LkCa 15, AAS Meeting #219, (Austin, TX, USA, Jan. 8-12, 2012).

Yagi, M.: 2012, Crosstalk in Suprime-Cam, Subaru Users Meeting 2011, (Mitaka, Japan, Feb. 28-Mar. 1, 2012).

Yamada, R., Shiraishi, H., Kobayashi, N., Takeuchi, N., Murakami, H., Tanaka, S., Okamoto, T., Ishihara, Y., Hayakawa, M., Hayakawa, H., Garcia, R., Lognonne, P.: 2012, Exploration of the Materials in Lunar Deep Region using the Seismological Method, MISASA IV Solar System Exploration and New

Geosciences -Perspective for the Next Decade-, (Tottori, Japan, Feb. 24-26, 2012).

Yamada, R., Yamamoto, Y., Nakamura, Y., Kuwamura, J.: 2012, A New Retrieval System of Apollo Lunar Seismic Data with Data Correction, 43rd Lunar and Planetary Science Conference, (Woodlands, TX, USA, Mar. 19-23, 2012).

Yamada, Y., **Hara, T.**, Yoshioka, S., **Kobayashi, Y.**, **Gouda, N.**, Miyashita, H., Hatsutori, Y., Lammers, U., Michalik, D.: 2011, Nano-JASMINE data analysis and publication, Astronomical Data Analysis Software and Systems XX, (Paris, France, Nov. 6-10, 2011).

Yao, Y., Wang, Y., Liu, L., Zhou, Y., Li, L., **Sasaki, T.**, Yoshida, M., **Ohshima, N.**, **Mikami, Y.**, **Sekiguchi, K.**: 2011, The NAOC Ali Observatory, Tibet, 11th Asian-Pacific Regional IAU Meeting, (Chiang Mai, Thailand, Jul. 26-29, 2011).

Yasui, C., Kobayashi, N., Tokunaga, A. T., **Saito, M.**: 2011, The Lifetime of Protoplanetary Disks Surrounding Intermediate-mass stars, AAS Meeting #219, (Austin, TX, USA, Jan. 8-12, 2012).

Zenitani, S., Hesse, M., Klimas, A., Black, C., Kuznetsov, M.: 2011, The electron-frame dissipation measure in collisionless magnetic reconnection, AGU Fall Meeting 2011, (San Francisco, CA, USA, Dec. 3-7, 2011).

Annual Report of the National Astronomical Observatory of Japan

Volume 14 Fiscal 2011